Fabrication and assessment of self-healing performance in CFRP composites to maintain structural Integrity

Submitted in partial fulfilment of the requirements of the degree of

DOCTOR OF PHILOSOPHY

in

MECHANICAL ENGINEERING

By

RAJ KUMAR PITTALA

(Roll No: 717127)

Supervisor

Dr. B. SATISH BEN

(Associate Professor)

Department of Mechanical Engineering

National Institute of Technology Warangal,

Warangal -506004, Telangana, India

February 2022

Dedicated to my wife

NATIONAL INSTITUTE OF TECHNOLOGY WARANGAL (T.S.) INDIA 506 004

Certificate

This is to certify that the thesis entitled "**Fabrication and assessment of self-healing performance in CFRP composites to maintain structural Integrity**"**,** being submitted by **Mr. Raj Kumar Pittala** for the award of the degree of Doctor of Philosophy in Mechanical Engineering, is the record of bonafide research work carried out under my supervision. The thesis has fulfilled the requirements according to the regulations of this Institute and has reached the standards for submission. The results embodied in the thesis have not been submitted to any other University or Institute for the award of any degree.

Dr. B. Satish Ben
Research Supervisor
Associate Professor
Department of Mechanical Engineering

Date:

Place: Warangal

NATIONAL INSTITUTE OF TECHNOLOGY
WARANGAL (T.S.) INDIA 506 004

Declaration

This is to certify that the work presented in the thesis entitled **"Fabrication and assessment of self-healing performance in CFRP composites to maintain structural Integrity",** is a bonafide work done by me under the supervision of Dr. B. Satish Ben and was not submitted elsewhere for the award of any degree.

I declare that this written submission represents my idea in my own words and where other's ideas or words have not been included. I have adequately cited and referenced the original sources. I also declare that I have adhered to all principles of academic honesty and integrity and have not misinterpreted or fabricated or falsified any idea/data/fact/source in my submission. I understand that any violation of the above will be a cause for disciplinary action by the Institute and can also evoke penal action from the sources which have thus not been properly cited or from whom proper permission has not taken when needed.

(Mr. Raj Kumar Pittala)

Date: Research Scholar

Place: Warangal (Roll No.717127)

Acknowledgement

It gives me immense pleasure to express my deep sense of gratitude and thanks to my beloved supervisor **Dr. B. Satish Ben**, Associate Professor, Department of Mechanical Engineering, National Institute of Technology Warangal, for his invaluable guidance, support and suggestions. His knowledge, and suggestions, and discussions helped me to become a capable researcher. He has shown me the interesting side of this wonderful potential research area. His encouragement helped me to overcome the difficulties encountered in my research as well in my life also. I am highly indebted to him for his expertise while sharing his knowledge, understanding, encouragement and patience.

I wish to express my sincere thanks to **Prof. N.V. Ramana Rao**, Director, NIT Warangal for his official support and encouragement. I am very much thankful to **Prof. A. Kumar**, Head, Dept. of Mechanical Engineering for his constant encouragement, support and cooperation. I also express my sincere thanks to **Prof. N. Selvaraj** and **Prof. P. Bangaru Babu**, former Heads, Dept. of Mechanical Engineering for their constant encouragement, suggestions, support and cooperation.

I take this privilege to thank all my Doctoral Scrutiny Committee members, **Prof. K. V. Sai Srinadh**, Professor, Department of Mechanical Engineering, **Prof. A. Kumar**, Professor, Department of Mechanical Engineering and **Dr. P. Syam Prasad,** Associate Professor, Department of physics for their detailed review, constructive suggestions and excellent advice during the progress of this research work.

I am highly indebted to **Prof. V. Suresh Babu,** Design Section Head, Department of Mechanical Engineering for his valuable comments and guidance during semester presentations.

I am very much thankful to **Dr. G. Raghavendra** and **Dr. Syed Ismail,** Assistant Professors Department of Mechanical Engineering and **Prof. R. N. Rao,** Professor Department of Mechanical Engineering, for their guidance during course of project.

I would like to place on record my thanks to all the faculty and staff of Mechanical Engineering Department, NIT Warangal for the knowledge they have imparted to me.

I would like to express my sincere gratitude to **Science and Engineering Research Board (SERB)** New Delhi, INDIA, for providing the financial assistance during the course of current research work. [**Project No: ECR/2017/000238** sanctioned under ECR scheme]

I am thankful to my student colleagues **Dr. Syam Kumar Chokka, Mr. Dhanaraju, Mr. Niranjan Prasad, Mr. K. Naresh, Mr. MVNV Satyanarayana, Mr. K. Nagu, Dr. Manoj Panchal**, **Dr. Om Prakash, Mr. M. Kamesh, Mr. D. Venkata Ramana**, **Mr. Rakesh Kanakam** for the technical discussions that we had during my course work and research work. I would also like to thank my fellow research scholars from other departments, **Mr. Vidish, Dr. K. Bharath, Mr. Akshay, Mr. Jayaram and Dr. Mohan Babu**. A very special thanks to my dear fellow batch mates, **Dr. K. Lokesh, Mr. Mahesh Pallikonda, Mr. M. Nitin, Mr. S. Rakesh, Mr. M. Sateesh Kumar** and all my well-wishers who were always there to support and encourage me.

A very special thanks to **Osmania University, Hyderabad** and **Centre for Automation & Instrumentation** (**CAI**)-NIT Warangal, for providing the technical assistance to carry out some of the characterization analysis involved in my research work.

Words cannot express how grateful I am to my parents (my father **Mr. Durgaiah Pittala**, my mother **Mrs. Komala)** for all of the sacrifices that they have made for my growth. Your prayers for me were what I am today. Finally, I render my respect to all my family members (my wife **Mrs. Sri Sailaja,** my son **Mr. Aarush Pranav** and my brother **Mr. Thirupathi Pittala**) for giving me moral support and inspiration. They have motivated and helped me in my life. Also, I take this opportunity to thank all my relatives, friends and well-wishers who are part of this journey directly and indirectly.

Last but not the least; I want to express my deepest gratitude to God Almighty for giving me such a fulfilling life with the blessings of whom I believe nothing is impossible.

Raj Kumar Pittala

Abstract

Synthetic materials like polymers, fibre reinforced polymer (FRP) composites have been widely used in various fields such as automotive, aerospace, marine and construction industries due to their attractive properties such as high stiffness to weight ratio, corrosion resistance and tailorable properties. In addition, these composites also offer multifunctionality due to their inherent structure. Since degradation, damage and failure are natural consequences of materials application, eventually during service conditions, polymer composites also experience mechanical damages and thus induce micro and nano cracks deep within the structure. Some of these micro cracks are invisible, difficult to identify and repair manually. If these micro cracks not repaired intime will lead to further propagation and finally causes for catastrophic failure of the component. Hence there is a need to develop new class of materials which can detect and offer onsite damage repair without human intervention. Biologically inspired systems such as self-healing materials addresses above issues and offer crack type independent repair strategies. Thus, these smart healing systems also offer delayed catastrophic failure and therefore enhanced service life of the component, improved reliability and durability of the structures.

The present study aim to achieve self-healing in epoxy composite and carbon fibre reinforced polymer composites. Separately encapsulated epoxy resin, amine hardener microcapsules were chosen as the healing agents and dual capsules reinforced self-healing system is considered to evaluate the healing performance. Firstly, Diglycidylether of bisphenol A (DGEBA) based epoxy resins (LY556,CY230), Triethylenetetramine (TETA) based amine hardener (HY951) were encapsulated in a thermoplastic Polymethylmethacrylate (PMMA) shell material using oil in water (o/w) solvent evaporation method. Effect of different process parameters such as surfactant type and concentration, processing temperature, solvent evaporation rate, type of agitator and agitation speed on the surface morphology of the developed capsules were investigated. Based on the results, It is recommended that slow solvent evaporation rates and 40˚C processing temperature are ideal to synthesis epoxy, hardener encapsulated PMMA microcapsules. Effect of core to shell (c/s) ratio and the effect of healing agents viscosity on the encapsulation of epoxy capsules were investigated. Encapsulation of healing agent in the PMMA shell was confirmed by FTIR, NMR and TGA analyses. It was found that the developed capsules have atleast 3 months storage stability at room temperature and observed that the weight loss percentage of the capsules increased with the increase in c/s ratio.

In order to assess self-healing performance of epoxy composite, dual capsules were reinforced into the epoxy matrix and fabricated the tensile, flexural and tapered double cantilever beam (TDCB) samples. Mode I fracture test was conducted on the TDCB specimens and the healing efficiency was evaluated based on the healed samples ability to regain its initial fracture toughness. It is observed that the healing efficiency increases with the increase in microcapsules concentration. The tensile strength, flexural strength and Charpy impact strength of the capsules reinforced epoxy composite decreased with the increase in capsules concentration. To study the effect of healing agents viscosity on the mechanical and self-healing performance of epoxy composite, (LY556+HY951) capsules combination and (CY230+HY951) capsules combinations were chosen and investigated for tensile strength and fracture toughness. From the investigation it is noticed that (CY230+HY951) capsules combination showed more healing efficiency and less % reduction in mechanical performance. Finally, 7.5 wt% of (CY230+HY951) capsules combination, 5 wt% SDS surfactant, 40˚C temperature, 2:1 c/s ratio CY230 epoxy capsules and 4:1 c/s ratio HY951 hardener capsules were suggested as an ideal parameter to produce dual capsules incorporated self-healing epoxy composite. The maximum healing efficiency obtained with these parameters is 71.35%.

Dual capsules reinforced carbon fibre epoxy composite was fabricated by employing 0.5:0.5 weight fraction of matrix, carbon fibre and 5, 10 and 15 wt% of epoxy and hardener microcapsules. Matrix cracking and delamination damages were induced in the capsules reinforced CFRP composite flexural specimens and the healing efficiency is evaluated based on the flexural strength recovery for those damages. Effect of induced damages (matrix cracking and delamination) on the flexural strength of CFRP composite was studied and observed that 21.73% and 29.32% reduction in flexural strength was noticed for 5 wt% capsules reinforced CFRP composite. Effect of capsules wt%, healing temperature and pressure on the healing performance of CFRP composite was investigated and recommended that 15 wt% capsules concentration,80˚C healing temperature and 1 bar pressure are an ideal conditions to fabricate and heal the capsules reinforced CFRP composite.

The load bearing capacity of the developed capsules was numerically analysed using Hertzian contact model and found that for same shell thickness, smaller diameter capsules break easily than the larger diameter capsules. Effect of capsule diameter and the shell thickness on the capsules failure strength was investigated. The stress distribution at the crack front was analysed using TDCB specimen and Mode I fracture test. It is observed that the maximum principal stress developed at the pure epoxy sample crack front is 28 MPa.

Table of Contents

List of Figures

List of Tables

List of Abbreviations

ASTM	American Society for Testing and Materials
CFRP	Carbon Fibre Reinforced Polymer
CY230	DGEBA based epoxy resin of viscosity 1.3 - 2 Pa.s at 25˚C
DCM	Dichloromethane
DCPD	Dicyclopentadiene
DGEBA	Diglycidylether of bisphenol-A
DTA	Differential Thermal Analysis
FTIR	Fourier Transform Infrared Spectroscopy
HY951	TETA based amine hardener of viscosity 0.01 - 0.022 Pa.s at 25˚C
IET	Impulse Excitation Technique
LY556	DGEBA based epoxy resin of viscosity 10 - 12 Pa.s at 25˚C
MF	Melamine Formaldehyde
NMR	Nuclear Magnetic Resonance spectroscopy
PMMA	Polymethylmethacrylate
PVA	Poly Vinyl Alcohol
RT	Room Temperature
SDS	Sodium Dodecyl Sulfate
SEM	Scanning Electron Microscope
TDCB	Tapered Double Cantilever Beam
TETA	Triethylenetetramine
TGA	Thermogravimetric Analysis
UF	Urea Formaldehyde
UTM	Universal Testing Machine

Chapter 1

Introduction

1.1 Motivation

Materials play an important role in designing the components and thus becomes crucial to achieve desired functionality of the structure. Based on the application, selection of material varies from metals to polymers and to composite materials. Over the past decades materials are designed in such a way that they should have good strength and reliability. No matter how well the materials are designed and processed, cracking is the essential issue that need to be solved. The existence of the cracks in the materials is almost unavoidable as micro cracks initiates either during material processing stage or during service conditions. Thus, the paradigm of damage prevention forced scientists and engineers to use extra material and over design the component to address the issue of cracking. However, still there is a need to work on damage management and to develop damage resistant and reliable materials.

Thermosetting polymers and fibre reinforced polymer composites are receiving tremendous interest from the research community due to their numerous structural advantages such as high strength to weight ratio, good corrosion resistance and tailorable properties and found applications in various fields such as automotive, aerospace, marine and construction industries. Epoxy is one of the most used thermosetting polymers in various structural applications due to its good mechanical strength. However, due to inherent brittle nature epoxy thermosets are highly susceptible to micro cracks. During service conditions, polymeric structures experience damage due to external mechanical loads, thermal loads and any other environmental factors and thus induces micro, nano cracks deep within the structure. In such cases, if developed microcrack not repaired intime will extends to macro crack and finally lead to catastrophic failure of the component and may cause for severe property loss or even human death. But unfortunately, some of these microcracks are invisible, difficult to identify and repair manually. Hence there is a requirement to develop new class of materials which can address the microcracking problem and offer self sensing and self repair strategies to prevent further damage and recover materials original properties such as strength, stiffness and fracture toughness automatically.

Fibre reinforced polymer composites also experience certain failures such as matrix micro cracking, fibre-matrix debonding and impact damages during their running conditions. In general, these damages initiates at micro level and propagates further till serious damage and finally causes for catastrophic failure of the structure. These catastrophic failures show significant impact on the repair, maintenance and rehabilitation of the structure and causes

social and economic losses. Therefore, it is very much required to address the problem at microlevel itself and thus to prevent the serious damage from happening.

Self-healing materials, which have the ability to heal the damage automatically and recover their original properties are the best solution to address aforementioned issues. These self-healing materials offers onsite damage repair and eliminates consideration of mode of damage in repair strategy. Indeed, these self-healing systems are not entirely new, they existed in almost all living organisms since many years. Examples of self-healing systems are growth of tissue in cuts, wounds and bone remodelling when it is fractured. Inspired by nature, many efforts have been made to develop the self-healing materials to recover their properties without causing any adverse effects on the structure. The self-healing in biological systems generally happens in three stages (i) blood clotting (ii) cell proliferation and (iii) remodelling of the skin [1]. Analogous to the biological systems, the self-healing in synthetic materials system also happens in three stages i.e., triggering, transportation and remodelling through chemical reactions. In the first stage, damage will initiate and interacts with the healing material, in the second stage corresponding healing agents will be supplied to the crack surface and finally in the third stage healing happens through the curing reaction or polymerization reaction between the released healing agents. Thus, these smart healing systems offer enhanced service life of the component, improved reliability and durability of the structures.

1.2 Applications

The main aim of the self-healing approach is to reduce the damage, restore the performance and enhance the service life of the structure. Based on these aspects, self-healing polymers and polymer composites are finding applications in various fields such as coating or painting industries, construction industries, electronics industries, aerospace applications and medical applications. Self-healing polymers have been widely used in coating industries to protect metallic surfaces from corrosion. Most of the metal industries are employing autonomous corrosion control techniques to protect various metals from corrosion and thus to enhance the coating performance. Autonomous corrosion control can be achieved by embedding the corrosion inhibitors and adhesion promotors in the matrix of polymeric coatings and restoring the protective layer properties in the damaged coating area [2]. Though structural components like aircraft wings and frames are designed to withstand harsh environmental conditions, thermal loadings and UV radiation, at a point of time in service period, experience micro voids and micro cracks due to unforeseen conditions. These defects if not addressed within time

reduces the structural integrity and lead to premature failure of the component. By encapsulating the healing agents either in fragile walls or in vascular networks and embedding them into composite matrix material, autonomous healing of the damage can be achieved.

Hydrogel is a three dimensional structure that contains high water content and has application in the mimicking of the soft tissues due to its tunable structure. Over the decade self-healing hydrogels are finding applications in tissue engineering due to their good rheological behavior and ability to intrinsically heal the damage. Injectable self-healing hydrogels have found applications in the cell therapy, tumour therapy and wound healing [3]. Similarly, conductive hydrogels have been used in tissue engineering to mimic cardiac muscles and nerves. In construction industries, concrete has been the building block for so many years due to its high compressive strength, fire resistance and low cost. But due to relatively low tensile strength, design errors, inadequate selection of materials and other environmental factors concrete vulnerable to micro cracking. These cracks acts as a host for other foreign constituents like chlorine, sulphur and carbonate and causes for deterioration of concrete and thus the structure. One of the best way to arrest concrete deterioration is to control or repair the micro cracks in their initial stages itself. Recently, self-healing of cementitious constituents gained interest from academia as well as industries due to their ability to extend the life the structure. By incorporating the suitable healing agents into the concrete self-healing can be achieved.

Self-healing techniques are progressively finding applications in various fields. The global self-healing materials market survey conducted by Grandview research [4] portrayed that self-healing materials market size was $291.4 M in 2018 and expected to grow at a CAGR of 46.1% for a period of 2019-2025. Increased demand for energy efficient construction solutions and requirement for self-healing polymers and fibre reinforced composites expected to drive the growth. The survey even forecasted that polymers and fibre reinforced composites grow at a CAGR of 46.4% from 2019-2025 and major contributors for this growth will be construction, automotive, transportation and energy generation industries.

1.3 Microencapsulation

Microencapsulation is a process in which solid, liquid or gaseous ingredients as core martials are wrapped by another polymeric material as shell material for the purpose of protecting core material from the surrounding environment. In simple terms, microencapsulation is a process of enveloping the core material in a fragile walled shell material. The output product of the

microencapsulation process is known as microcapsule and its diameter ranges from micrometer to nanometer. The morphology of the microcapsules greatly depends on the physicochemical properties of the chosen core material, shell material and encapsulation technique adopted. Based on the surface morphology of the microcapsules they can be classified as monocore, polycore, multiwall and matrix type capsules. In monocore capsules only single core material will be encapsulated in a single shell material and known as core/shell type capsules. In polycore capsules different types of core materials will be encapsulated in a single shell material and in multiwall capsules single core material will be encapsulated in two or more shell materials. In matrix type capsules core material will be integrated with the matrix of shell material. The features such as controlled release of core material and huge surface area made polymer capsules to have applications in different fields. According to the core material encapsulated, microcapsules have applications in cosmetic field, textile industry, drug delivery applications, anticorrosion paints, thermal energy storage and self-healing materials.

The selection of microcapsule synthesis method greatly depends on the type of core material and shell material and their physicochemical properties. Microencapsulation techniques are broadly classified as physical methods and chemical methods. In Physical methods the starting materials are polymers and no chemical reactions involves and during synthesis only shape fabrication takes place. Whereas in chemical methods the starting materials are monomers and during synthesis chemical reactions takes place along with microcapsules formation [5]. Physical methods include solvent evaporation/extraction, coacervation, spray drying, co-extrusion, layer by layer deposition and fluidized bed coating. Chemical methods include suspension polymerization, emulsion polymerization and interfacial polymerization.

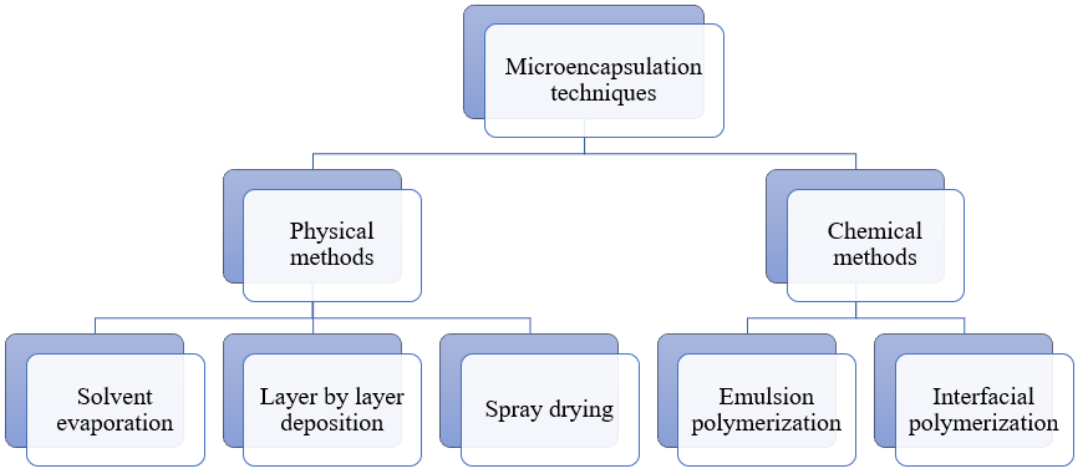

Figure 1.1: Classifications of microencapsulation techniques

1.4 Fibre reinforced polymer composites

Composite material is a structural material that consists of two or more combined constituents at macroscopic scale that do not dissolve in each other. The constituent materials have chemically distinct phases and significantly different properties. Generally, composites are statistically homogeneous at macroscopic scale and heterogenous at microscopic scale. Because of inherent nature of the composite, it gives better properties than the properties of the individual constituents. The characteristics such as light in weight, high strength/weight ratio, excellent toughness, better wear resistance and good fatigue life made composites to have different kinds of applications in various industries.

The basic constituents involved in the composite material are matrix and reinforcement. Based on the type of matrix material used composites are classified as polymer matrix, metal matrix and ceramic matrix composites. Similarly, based on the form of reinforcement used they have been classified as fibre reinforced and particulate reinforced composites. Polymer composites further classified as thermosetting and thermoplastic polymer composites and fibre reinforced composites further classified as unidirectional and bidirectional continuous fibre composites. The major function of the reinforcement is to carry the loads, contribute to desired properties and transfer the strength to matrix phase. The matrix constituent takes care of holding fibres together, protecting fibres from environment, distributing loads evenly among fibres and providing good surface finish to product.

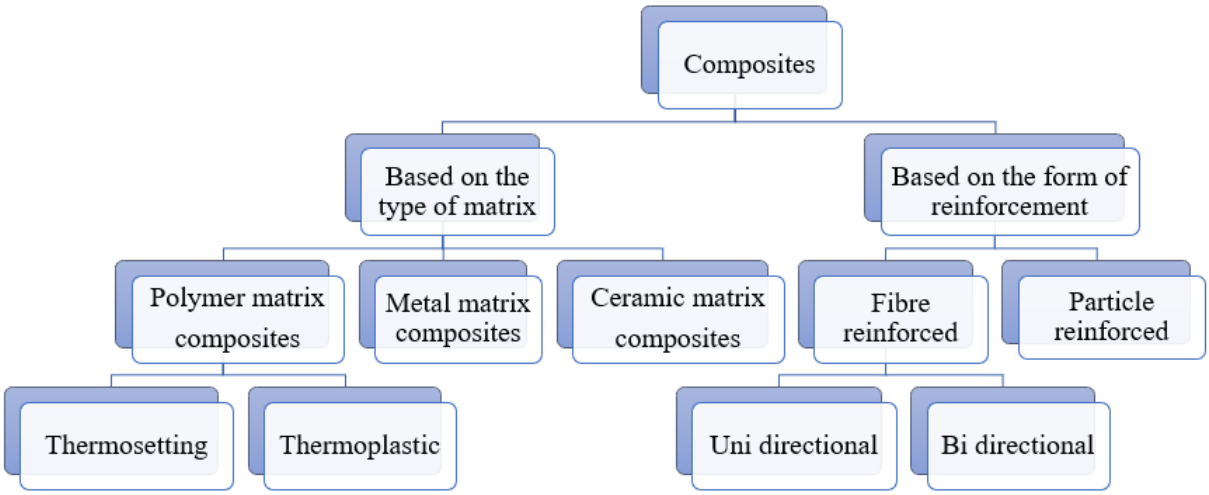

Figure 1.2: Classifications of composites

1.5 Structure of the Thesis

The outline of the thesis is organized as follows.

Chapter 1: In this chapter, motivation behind the current research work and the applications of the work are explained. Different terms related to current work have been introduced and discussed.

Chapter 2: Provides brief literature review on the common types of damages in polymer composites and different self-healing mechanisms with major focus on the capsules reinforced self-healing system. Solvent evaporation microencapsulation technique, mechanical and self-healing performance of capsules reinforced epoxy composites have been discussed.

Chapter 3: This chapter deals with the materials and synthesis procedures involved in the development of self-healing microcapsules and discusses the effect of different process parameters on the microcapsules surface morphology. The characterization techniques used to analyse the developed microcapsules have been presented. A brief discussion on the characterization procedures and the equations used to find different properties have been discussed.

Chapter 4: This chapter describes the fabrication of dual capsules reinforced self-healing epoxy composite and discusses the effect of capsules addition on the mechanical performance of epoxy composite. The influence of microcapsules core material viscosity on the mechanical and self-healing performance of the epoxy composite has been presented.

Chapter 5: Discusses the effect of microcapsules concentration on the flexural strength and self-healing efficiency of carbon fibre reinforced epoxy composite. Brief discussion on the damping characterization of capsules reinforced CFRP and pure epoxy composites have been presented.

Chapter 6: This chapter represents the numerical analysis on the load bearing capacity of the developed microcapsules and the evaluation of stress distribution at the pure epoxy crack front.

Chapter 7: Discusses the overall conclusions of the study and presents the scope for future works.

Chapter 2

Literature Review

This chapter describes the basic knowledge related to self-healing materials and the past research conducted by various researchers on the self-healing performance evaluation of thermosetting polymer composites. In particular, this chapter focuses on the capsules based self-healing approach and briefs the methods used to quantify the healing efficiency.

2.1 Various damages in polymer composites

The rapid growth of aerospace industry encouraged many researchers to develop lightweight materials and thus to reduce the operational cost. Composites are one of the best lightweight materials and have an ability to provide tailorable properties. They can be strong in one direction and at the same time can be flexible enough in another direction. Light weight design of aircraft frames and fuselage with enhanced mechanical properties can improve the fuel efficiency, increased running hours, increased payload and thus can reduce the operating cost[6]. Carbon fibre reinforced polymer (CFRP) and glass fibre reinforced polymer (GFRP) are most of the common composites used in aircraft structures. CFRP and GFRP have higher specific strength, better corrosion resistance and good fatigue life than most of the metals, for ex, CFRP has minimum yield strength around 550 MPa while its density is only one fifth of steel and three fifth of aluminium [7]. Because of these structural advantages, composites are replacing most of the metals and occupied 50% of the aircraft materials share.

Despite having many structural advantages, their functionality is restricted due to presence of some damages. These damages may happen either in processing stage or during running conditions. Figure 2.1 shows the common damages that can present in the polymer composites. Three types of damages i.e., matrix microcracking, delamination and fibre breakage are the most common dominating damages.

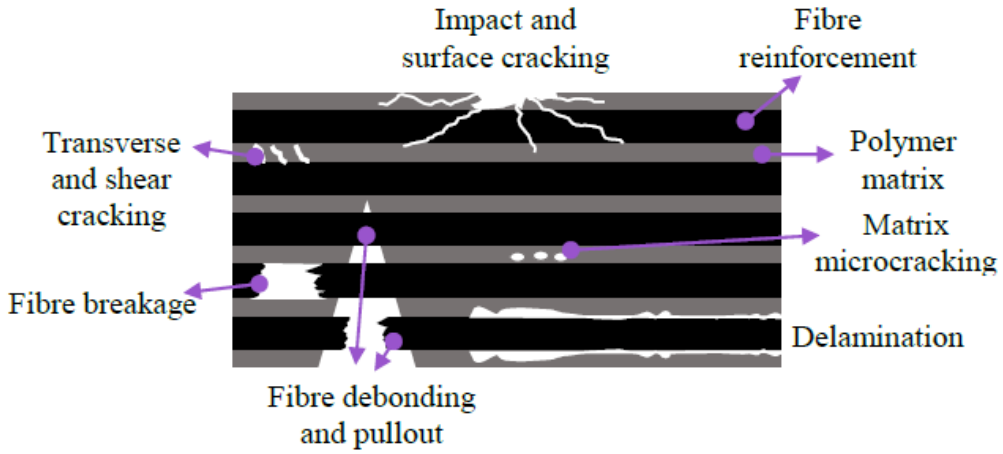

Figure 2.1 Various damages in polymer composites [8]

Matrix microcracking and delamination damages mainly depend on the type of matrix material and its mechanical and adhesion properties. Most of the common matrix material chosen in thermosetting polymer composites is epoxy. The characteristics such as better adhesion capabilities, lower shrinkage and superior mechanical properties made epoxy as the best matrix material for polymer composites. Fibre breakage mostly happens during service period due to application of excessive loads. Compared to GFRP, CFRP takes more load and less susceptible to fibre breakage and thus provides better service life. The damages due to lightning strike and bird strike also sometimes become severe and results in loss of mechanical property. Gharghabi et al. [9] simulated the lightning strike damages in polymer composites and concluded that the flow of current causes irreversible damages and loss in material properties which cannot be identified easily by examining the composite.

Since past decade, lots of structural health monitoring (SHM) techniques were developed to identify the different damages present in the polymer composites. Among different SHM techniques, Guided wave based Lamb wave techniques are mostly preferred due to their ability to identify small size defects, larger area under inspection and low attenuation [10]. Wave field imaging is another SHM technique which is used to identify the damages in complex structures. RAPID (Reconstruction Algorithm for the Probabilistic Inspection of Defects) [11] and WEAM (window energy arrival method) [12] are the some other SHM techniques which uses algorithms to identify the damage locations. All these SHM techniques need baseline data to compare with the real time data that is obtained from sensors. Generally, baseline data will be collected by conducting various experiments. But testing the structure in its all possible service conditions is almost impossible and hence still there is a requirement for better damage identification mechanism.

There are only few conventional methods available to repair the damages in polymer composites. Hot plate welding [13], adhesive bonding based composite patches [14] and resin injection [15] are the few techniques that have been used to repair the composite damages. However, these repair strategies have few limitations; hot plate welding is a slow process and weld zone will be always the weakest area. In composite patches repair method, patches sustainability, toughness, hydro-thermal consequences and optimal patch form are major concerns [14]. If the crack is not accessible for repair then the resin injection repair strategy cannot be employed. Selection of repair method greatly depends on the type of damage and damage location. Though all the available repair methods can overhaul the structures, the ideal repair strategy should offer quick action, onsite damage repair and should eliminate the chance

of removing component for repair process. The above mentioned repair methods require human intervention and observation of damage during repair. Thus, these repair methods are time consuming, costly and ineffective to repair micro cracks that are developed deep within the structures [16]. Hence extensive efforts have been made by various researchers to improve the structural integrity, halt the failure and extend the service life of the component by employing concepts like self-healing, self-lubricate and self-cleaning. The self-healing materials have the capability of automatic damage detection and self repair the damage. Inspired by autonomic healing processes in biological systems, continuous efforts have been made by scientists to incorporate these self-healing concepts in structural applications of the polymer composites.

2.2 Self-healing materials and types of self-healing techniques

Self-healing materials are synthetically developed smart materials that have an ability to repair the micro cracks developed in the structures without any human intervention. Autonomous healing, biomimetic healing, self mending and self repair are the synonym terms used to describe the characteristics of self-healing materials. Biology provides an abundance of self-healing examples; for example, the cut or wound on the skin automatically triggers the repair process and remodelling of the skin will takes place within a day or week based on the size and type of damage. The Self-healing process in biological systems can be briefly understood through three stages: inflammatory response, cell proliferation and matrix remodelling [1]. Figure 2.2 depicts the three stages involved in the biological as well as the synthetic self-healing systems. Analogous to biological systems, the self-healing in synthetic routes also can be achieved in triggering, transportation and chemical repair stages. In both the cases the initial response is triggered by injury.

As part of the healing, in both the cases the first step takes place immediately after the Injury and causes for blood clotting in biological route and actuation in synthetic route. The second step in the synthetic route involves transportation of released healing agents to the crack surface and happens at a rapid rate whereas in the biological route the second step takes time to react and happens at a little lower speed than the synthetic route. Based on the type of damage to be healed, the matrix remodelling stage of biological route requires time from weeks to months. Time required for the synthetic route third stage greatly depends on the rate of healing and the type of healing mechanism employed.

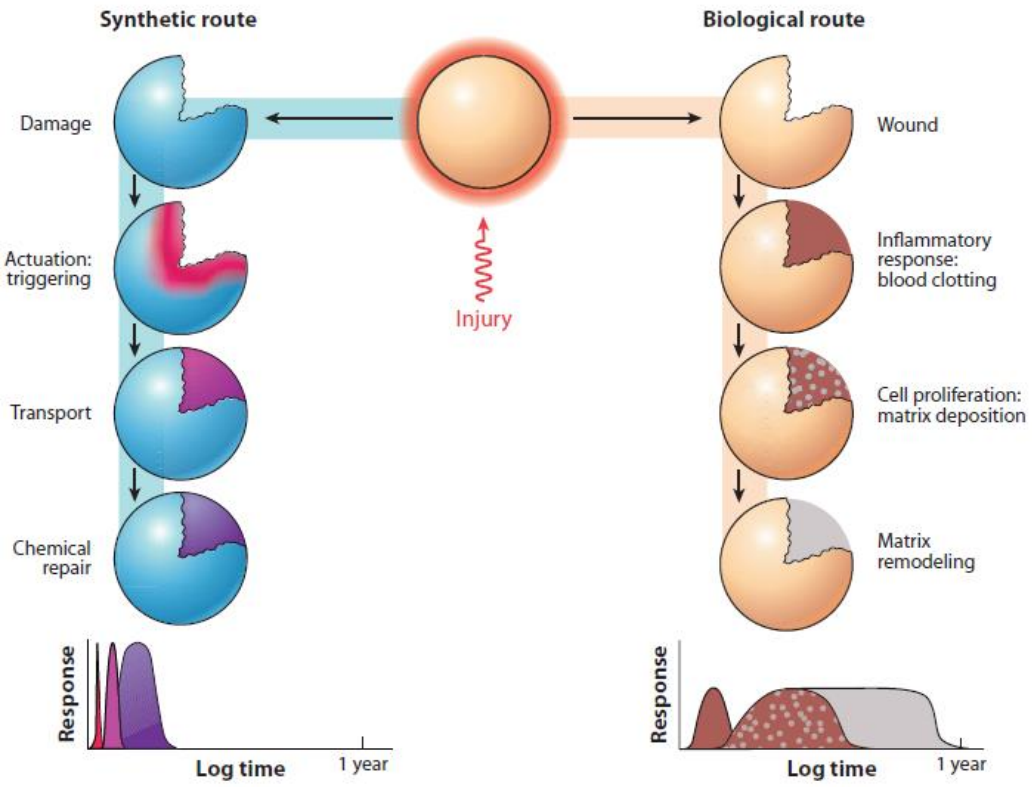

Figure 2.2 Schematic representation of self healing in biological and synthetic routes [1]

There are several approaches available to synthesize the self-healing materials. Based on the type of healing mechanism and nature of healing, self-healing materials are broadly classified as extrinsic and intrinsic approaches. In extrinsic approaches propagating crack itself acts as stimulus and the response will be autonomic repair of the crack without any human intervention whereas in intrinsic approaches any of the external stimulus such heat, pressure or light are necessary to initiate the crack repair. Henceforth extrinsic approaches are known as autonomous healing methods and intrinsic approaches are known as non-autonomous healing methods. Figure 2.3 depicts different types of extrinsic and intrinsic approaches available. Extrinsic approaches include microencapsulation [17,18] hollow fibre [19,20] and microvascular networks [21,22] and intrinsic approaches include Diels Alder-retro Diels Alder (DA-rDA) based healing [23,24], supramolecular interactions with hydrogen bonds [25,26] and Ionomeric interactions [27,28].

In capsules based approach, healing agent is encapsulated in a shell material and dispersed into the polymer matrix. Whenever the embedded capsules encounter the crack, capsules subject to rupture and releases the healant into the crack plane and undergoes polymerization reaction to heal the cracked surface. Similarly in hollow fibre and vascular networks to achieve self-healing, healing agents are encapsulated in materials like hollow glass

fibres and integrate with the material to be healed. In intrinsic approaches, self-healing can be achieved by means of the inherent capability of reversibility of bonding of polymer matrix. But external stimulus such as heat, pressure, electrical current, photochemical effect or light need to be applied on the polymer to initiate the healing process.

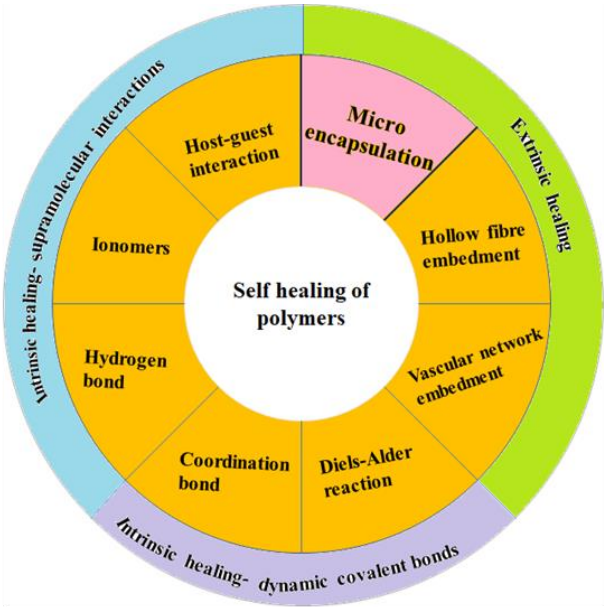

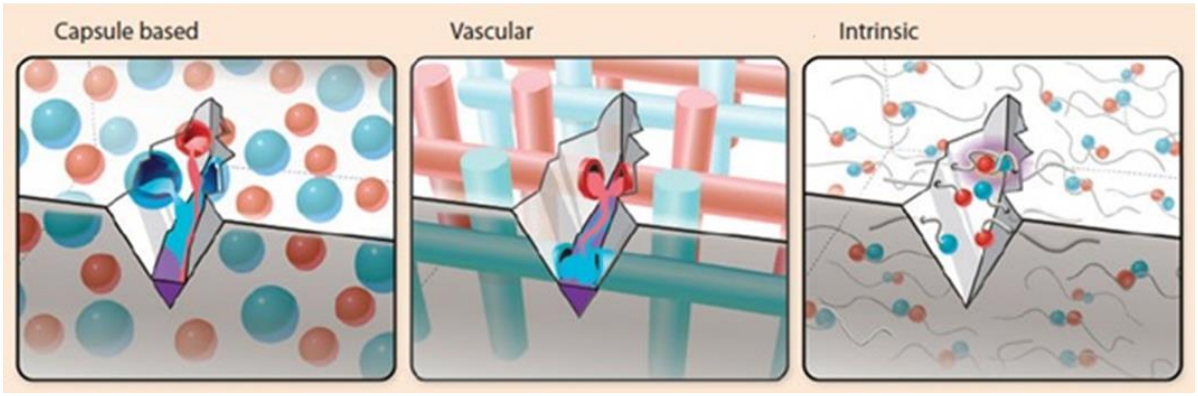

Figure 2.3 Types and classification of extrinsic and Intrinsic self-healing approaches [1]

2.2.1 Capsules based self-healing approach

One of the most effective and promising self-healing approach is capsules based healing method. The concept of capsules based self-healing was first introduced by White et al. [29,30] and shown in Figure 2.4. In this study, dicyclopentadiene (DCPD) was used as healing agent and encapsulated in poly urea formaldehyde (PUF) shell material. Whenever the crack encounters the DCPD capsules, healing agent releases from the capsules and reacts with Grubb's catalyst to heal the crack by polymerization reaction. Through this approach, self-healing can be achieved by embedding either microcapsule containing single healing agent-catalyst or dual capsules containing different healing agents in the host material. Numerous

studies have been conducted on the encapsulation of different healing agents such as 5-ethylidene-2-norbornene (ENB) [31], Isocyanates [32], polydimethylsiloxane [33], paraffin[34] and epoxy [35] to evaluate the self-healing behavior. Caruso et al. [36] investigated the self-healing performance of epoxy system by encapsulating the chlorobenzene solvent in PUF shell material. When the damage induces, capsules will break and releases the solvent to crack surface. Released solvent acts as wetting agent and causes host material to swell and then to reptation & interlocking of the chains across the crack surface.

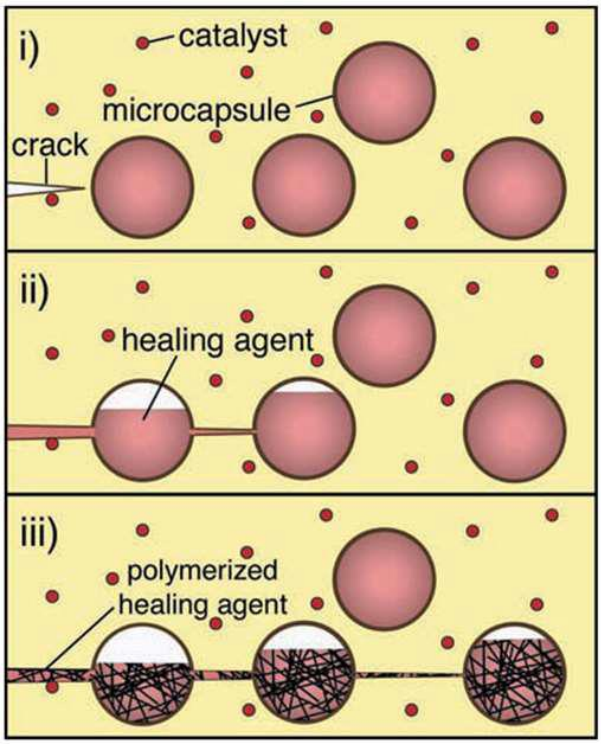

Figure 2.4 Capsules based self-healing approach (i) formation of crack in matrix material (ii) releasing of healing agent to the crack plane (iii) polymerization and curing of the crack [29]

2.2.2 Vascular network based self-healing approach

The idea of vascular network based healing system is inspired from the arteries of human body. Three types of vascular networks 1D, 2D and 3D are developed with the primary aim of multiple healing. 1D vascular network systems are known as hollow fibre based healing systems. Similar to capsules, in 1D network approach healing agent will be encapsulated in hollow tubes through capillary action, surface pores or vacuum assistance [37]. After filling the healing agent open end will be sealed and tubes will be integrated with the polymer matrix to achieve self-healing functionality. For the first time Dry et al. [38] implemented this hollow fibre healing approach to heal the cracks in concrete. Trask et al. [20,39] worked on the optimization of hollow fibres production process and produced optimal hollow glass fibres in

the range of 30 - 100 μm with hollowness around 65%. Size of the hollow fibres, distribution of the fibres throughout the matrix material and effect on mechanical properties are the main limitations associated with this process.

The basic difference between 1D network and 3D network systems is the later one will be designed with interconnected vascular structure and earlier one will be designed with discrete hollow tubes. Because of interconnected networks vascular healing approaches are capable of continuously supply healing agent to the damage site till it cures. Laser micromachining, fugitive inks, soft lithography and 3D printing technologies are some of the available methods to fabricate vascular structures [40]. After fabrication healing agent will be injected into the vascular structure using syringe or pump [41]. Toohey et al. [21,42] developed 3D vascular networks based on direct ink writing technique and used Grubb's catalyst and DCPD as the healing agents. They achieved good healing efficiencies up to 7 healing cycles. Later Hansen et al. [43] modified the design and incorporated the catalyst and monomer in two isolated vascular networks and achieved good healing performance up to 30 healing cycles. Patrick et al. [44] further modified the design and achieved the healing efficiency of ~ 100%.

Though vascular network self-healing approach is capable of multiple healings there are lot of challenges need to be addressed for successful implementation. First of all, the design of vascular network is very complex and difficult to fabricate and integrate with the host material. The scaling up of designed structure also a major issue for implementation. Similar to microencapsulation approach, this method also requires healing agents quantity equals to their stoichiometric ratio and they should be inactive until the damage occurs [45]. Since vascular approach is an interconnected networks system, keeping the healing agents inactive until the damage occurs is a challenging task. The direct contact of healing agents with host polymer matrix restricted this approach to have applications in various fields [46]. The release and mixing of healing agents at the damage site also a challenging task. To have perfect healing, it is necessary to optimize vascular tube diameter, healing agents flow properties and capillary forces. Injecting healing agents into the vascular structure is a big task; at present manual pumping systems are used to refill the healing agents into the vascular networks. But to achieve autonomous healing, it is required to design automatic refilling of the healing agents into the vascular networks. The loss of healing agents during refilling and also during healing process need to be controlled for better healing efficiencies. All these challenges need to be addressed before implementing this healing approach in various applications.

2.2.3 Intrinsic self-healing approach

Unlike microcapsule and vascular self-healing approaches, in intrinsic approaches there is no need to pre embed the healing agents into the polymer matrix, whereas in this approach healing is achieved by hidden healing functionality of host polymer with the help of macromolecular reactions. The hidden healing functionality will be activated by external stimulus such as heat or light. Intrinsic approaches are broadly classified as healing techniques based on dynamic covalent bonds and healing techniques based on non-dynamic covalent bonds (based on supramolecular interactions). Chen et al. [47] first developed the remendable polymers based on dynamic covalent bonds with the help of external heating. As the healing takes place through macromolecular reactions, it is necessary to maintain required chemicals at nanometer scale to have reversible bonding and thus to initiate the healing process. It is always necessary to bring back damaged parts into contact and maintain that intact to achieve self-healing functionality. Intrinsic self-healing approach also can be used to achieve multiple healings. Type of external stimulus applied, chain mobility and entanglement, reversible polymerization capabilities, supramolecular interactions such as hydrogen bonds and ionomeric reactions are some of the factors that influence the healing efficiency [1]. However, this approach has few limitations such as it can heal only microscale and small scale damaged areas [48]. Cordier et al. [49] for the first time investigated the room temperature healing in elastomers (rubber) based on hydrogen bonds remendability.

Dynamic covalent bond based cycloaddition reactions are used by researchers [50,51] to achieve self-healing in various polymers like epoxy, polyamide and polyacrylate. Cycloaddition is a reversible covalent reaction where unsaturated molecules join together and forms a ring [52]. Diels-Alder (DA) reversible reactions uses diene and dienophile as the pre cursors and achieve remending of polymers through [4+2] cycloaddition reaction. Here 4, 2 indicates the number of electrons supplied by diene and dienophile to initiate the healing process. In this approach, at elevated temperatures the bond between diene and dienophile will break and at lower temperatures the reversible reaction occurs and forms the bond and heals the crack. Park et al. [53] used electric resistive heating and DA reversible reactions to heal the delamination damages in bis-maleimide tetra furan based polymer composite.

Self-healing through noncovalent bonds are obtained with the help of various supramolecular interactions such as hydrogen bond, ionomeric interactions, π-π stacking sequence and host-guest interactions. By applying the mechanical force, the weaker supramolecular bonds disassociates and due to dynamic chemistry of noncovalent bonds self-

healing takes place [54]. Guadagno et al. [55] utilized hydrogen bonds to develop epoxy based self-healing nano composites and proved that the developed composites have both better mechanical and self-healing properties. In π-π stacking sequence healing approach, π-electron deficient groups and π- electron rich groups are utilized to achieve self-healing by thermal activation. Burattini et al. [56] used π- electron deficient di-imide groups and π- electron rich pyrenyl groups to achieve self-healing in elastomers.

2.3 Capsules based self-healing in epoxy composites

Epoxy based thermosetting polymers have applications in the transportation sector, energy generation industries and automotive sectors due to its high strength to weight ratio and good corrosion resistance. But they are susceptible to microcracks because of their inherent brittle nature. In the recent years, various self-healing approaches were applied on the epoxy composites to arrest the crack growth and to extend the life of the component by healing the damage autonomously. Wool et al. [57,58] studied the theory of crack healing in polymers and explained the healing process in five steps; surface rearrangement, surface approach, wetting of the surface, low level diffusion between surfaces and high level diffusion, randomization.

Brown et al. [59] used DCPD microcapsules and Grubbs catalyst to evaluate the self-healing performance in the epoxy composite and obtained healing efficiencies around 63%. Grubbs catalyst has melting temperature around 153°C and its reactivity decreases with the exposure to oxygen and moisture [60]. To overcome these limitations Kamphaus et al. [61] used Tungsten chloride (WCl_6) whose melting temperature is around 275°C as the catalyst to achieve self-healing in epoxy composite. However, weak stability of catalyst, necessity of uniform and close proximity dispersion of capsules and catalyst hindered the application of single component capsule system to assess self-healing performance [62].

As an alternate to the capsule-catalyst approach, dual healing agents encapsulated in two separate capsules approach is used to achieve self-healing in polymer composites. The dual component microcapsules system has not been fully explored yet because of developed capsules integration difficulties and encapsulation of suitable curing agent to the polymerizable component. Jin et al. [63] used epoxy resin- amine hardener based dual component microcapsules system to achieve self-healing in thermoset epoxy resin. In epoxy resin and amine hardener dual component microcapsules system one component consists of epoxy resin microcapsules and the other component consists of corresponding curing agent microcapsules. Figure 2.5 represents the schematic view of epoxy-hardener dual component system. Whenever

the micro crack encounters the capsules, they subject to rupture and healing occurs through the chemical reaction of stoichiometric ratio of epoxy and hardener. Based on the healing capabilities of the system, either the crack can be fully healed or partially healed. Similarly, whenever other crack ruptures the capsules of other areas, same process continues and heals the crack to re-establish the structural integrity.

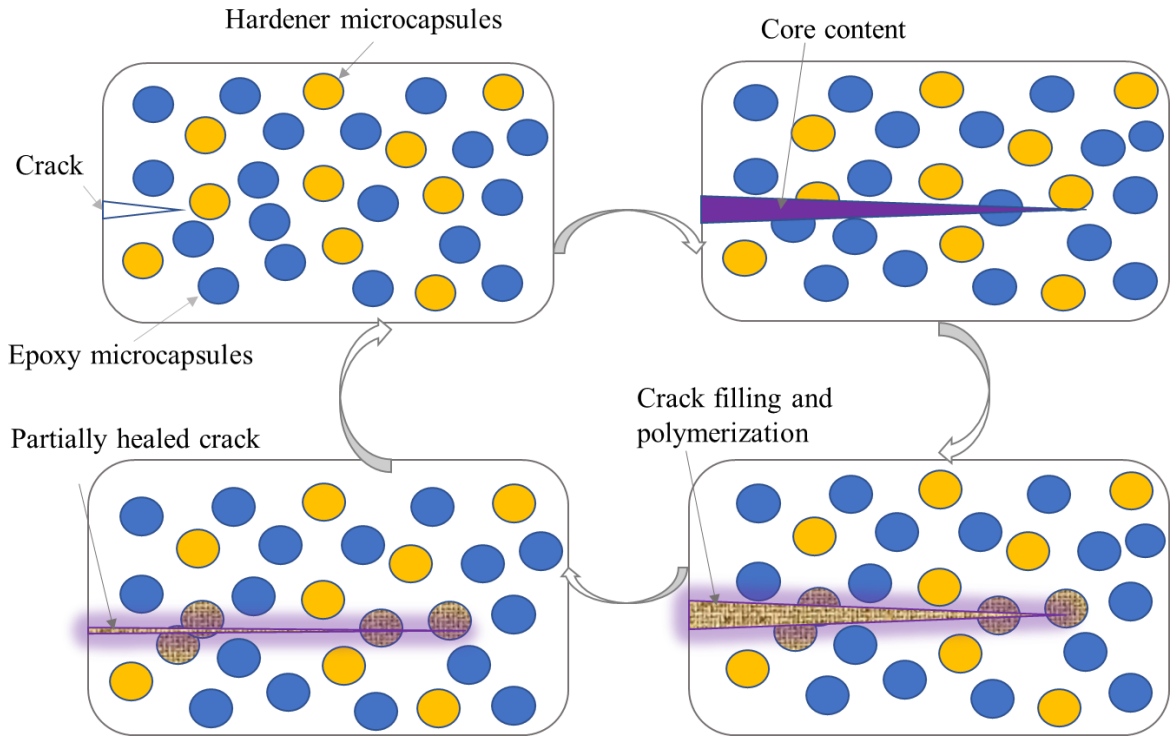

Figure 2.5 Schematic representation of dual capsules incorporated self-healing system

The crack healing capability of the system depends on the uniform distribution of the capsules in the base epoxy matrix and the ability of the capsules to break and deliver the healing agent to the crack surface. Li et al. [64] developed epoxy resin, polyetheramine encapsulated two types of separate microcapsules and studied their influence on the self-healing performance of the epoxy matrix. They evaluated the self-healing performance based on specimen's ability to regain its initial fracture toughness and achieved maximum healing efficiency of 84.5% with 15 wt% capsules concentration. Yuan et al. [65] synthesized epoxy resin, mercaptan encapsulated melamine formaldehyde capsules and studied their influence on the mechanical properties of the polymer matrix. Ahangaran et al. [66] developed epoxy resin, mercaptan encapsulated PMMA microcapsules and studied the fracture toughness, self-healing performance of the system. They concluded that the fracture toughness and self-healing efficiency increase with the increase in capsules content and reported the maximum healing efficiency of 80% with 10 wt% microcapsules concentration.

2.3.1 Synthesis of microcapsules through solvent evaporation method

The healing agent should remain inactive until the damage occurs in the material. Thus, the prime function of the microencapsulation technique is to protect heling agent from the surrounding environment. Solvent evaporation method is one of the techniques available to encapsulate healing agent and thus to synthesize the microcapsules. In this method, shell material is first dissolved in solvents like dichloromethane and then core material also dissolves in it. This mix is then added dropwise to solution having emulsifier to produce microdroplets. With the time, solvent evaporates from the emulsion and produces hardened, free flowing microcapsules. However, there are other methods such as interfacial polymerization, in situ polymerization and spray drying are available to produce capsules. But due to no requirement of emulsion pH control, ability to produce similar size range microcapsules, no washing and filtering difficulties, solvent evaporation method is preferred over other methods.

Developed capsules should be strong enough to remain intact during fabrication and fragile enough to break whenever the crack encounters it. Donnell et al. [67] reviewed the preparation of microspheres through solvent evaporation method and addressed the different challenges in encapsulating hydrophilic compounds. Ming Li et al. [68] reviewed the microencapsulation by solvent evaporation method and suggested the choice of materials, encapsulation procedure and optimized process parameters. The synthesis of microcapsules with solvent evaporation method is simple, straight forward and quicker. Zhao et al. [69] used solvent evaporation method to encapsulate different type of hydrophobic healing agents in polyvinyl formaldehyde, polylactic acid and polymethylmethacrylate.

Based on the type of core material i.e., hydrophilic or hydrophobic, the method of solvent evaporation is chosen. For encapsulating hydrophobic or poorly water soluble healing agents, oil in water (o/w) solvent evaporation method is frequently used. Figure 2.6 depicts the steps involved in the o/w solvent evaporation method. The major steps involved in this process are (i) dissolving core material and shell material in the solvent (ii) dropwise addition of oil phase to water phase (iii) solvent evaporation from the emulsion (iv) recovery and drying of microcapsules. If the chosen healing agent is hydrophilic or not soluble in the dichloromethane then other methods such as water in oil in water (w/o/w), o/w co-solvent, o/w dispersion methods are used. The encapsulation efficiency and physical properties of the microcapsules depends on the method of encapsulation, type of healing agent and process parameters applied during synthesis.

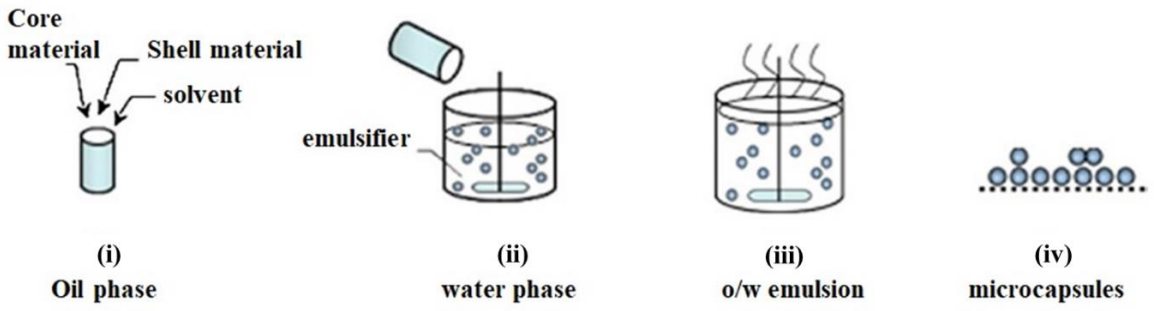

Figure 2.6 Schematic representation of o/w solvent evaporation method

2.3.2 Factors influencing the properties of microcapsules

The microcapsules features such as core content, yield, capsule size and shell thickness, surface morphology and encapsulation efficiency are affected by process parameters such as operating temperature, type and concentration of emulsifier, viscosity of oil phase, type of agitator and agitation rate [70,71]. Temperature is one of the important factors that influence the size and morphology of capsules. At higher temperatures because of shorter reaction time rough and bigger size capsules form whereas at lower temperatures smaller and smooth surface capsules form. In order to find optimal temperature ranges, Yuan et al. [72] studied the effect of heating rates on the PUF microcapsules. They concluded that with increase in heating rates bigger and rougher capsules formed and stated that when heating rate increases the rate of polymerization shoots up and causes for more UF shell material to deposit on the capsules surface.

The size and shell thickness of the capsules are most important features as these features control the amount of healing agent encapsulated and thus the healing efficiency of the composite. Agitation rate affects both surface morphology and average size of the capsules. Various studies on the microcapsules synthesis proved that with the increase in agitation rate average microcapsule size reduces and vice versa. Brown et al. [30] developed microcapsules with 10 - 1000 nm by applying agitation rates in the range of 200 - 2000 rpm and reported that agitation rate and average microcapsules have linear relationship in log-log scale. Type and amount of emulsifier/surfactant used is another factor that influences the size and thickness of the capsules. Ting et al. [73] studied the size of PUF microcapsules by varying surfactant wt% from 0.5 to 5 wt% and obtained smaller size, unevenly distributed microcapsules with 5 wt% surfactant concentration. Good dispersion stability of surfactant is required to achieve effective interfacial tensile forces between oil and water phases and this stability influences by type and concentration of surfactant. Sodium dodecyl sulfate (SDS), sodium dodecyl benzene sulfonate (SDBS), poly vinyl alcohol (PVA), gum Arabic (GA) and gelatin are few surfactants

generally used to synthesis microcapsules. Even though same surfactant is used to encapsulate different core materials, the results will be different because of nature of core materials, chemical reactions during synthesis and method of encapsulation [74].

Viscosity of oil phase which in turn influences by core and shell material concentration, amount of solvent, surfactant wt%, processing temperature and viscosity of core material affects the size of microcapsules. If the oil phase viscosity is comparatively less, lower shear forces are enough to break the droplets. The amount of shear forces required depends on the ratio of oil phase viscosity to water phase viscosity. The size of the microcapsules increases with the increase in oil to water phase viscosity ratio. Ahangaran et al. [75] encapsulated two different healing agents having different viscosities with same method and found that the healing agent having lower viscosity had produced narrow size distribution and lower capsules size than the healing agent having the higher viscosity.

2.3.3 Microcapsules characterization techniques

Characterization techniques are inevitable to monitor the self-healing process and examine the healing agents encapsulation in a shell material. The characterization techniques such as Optical, Scanning Electron and Transmission Electron Microscopes (OM, SEM,TEM), Fourier Transform Infrared spectroscopy (FTIR), Nuclear Magnetic Resonance spectroscopy (NMR), Thermogravimetric analysis (TGA), Differential Thermal analysis (DTA), Atomic Force Microscope (AFM), ultrasonics and Raman spectroscopy are most commonly used techniques to monitor self-healing process as well as to characterize the core material encapsulation.

Microscopy techniques generally used to monitor the three dimensional structure, size, and formation of the capsules. Optical microscopy was most widely used to monitor the formation of microcapsules immediately after the process. SEM was used to observe the inside and outside surface morphologies of the microcapsules, fracture surfaces of capsules incorporated composites, capsules distribution and to examine the healed and unhealed areas. Li et al. [76] used SEM technique to monitor the self-healing process in cementitious materials. In this study they used epoxy resin adhesive encapsulated polystyrene-divinylbenzene microcapsules as the healing materials and evaluated the cement paste healing capability in terms of its ability to restore mechanical properties. TEM was mostly used to examine the nano inclusions in the epoxy composite and also to observe the nano capsules surface morphologies. In the self-healing paintings/coatings TEM was used to examine the presence of core material in the nano capsules and the fracture surface of nano capsules reinforced epoxy coating system.

FTIR is a technique used to monitor the chemical bonds (functional groups) present in the microcapsules based on their molecular interactions. This technique was mostly used in capsules based healing system, intrinsic healing systems, autonomous corrosion systems and hydrogels to monitor the healing functionality and chemical reactions during healing process. In the study conducted by Araya-Hermosilla et al. [77] FTIR was used to examine the cycloaddition reaction in DA-rDA based reversible self mending thermosets. In this study they varied the molar ratio between furan and maleimide groups to observe the intensity of bond and thus observed the formation of DA reaction. In another study conducted by Garcia et al.[78] FTIR was employed to confirm the hydrolysis of silyl ester healing agent which later incorporated into self-healing anticorrosive coating system. Through FTIR technique they confirmed hydrolysis reaction and proved silyl ester ability to act as hydrophobic protective layer in self-healing coatings.

NMR technique uses nuclear magnetic resonance phenomenon to examine the chemical structure of the product, interactions between core and shell material, state of chemical reactions and formation of self-healing system. Zhu et al. [79] used NMR technique in capsules reinforced epoxy system to check the polymerization reaction after the microcapsules rupture. They confirmed the formation of polymerization reaction and thus confirmed the encapsulation of healing agent in a shell material. Raman spectroscopy is another technique to monitor the functional groups and chemical reactions involved in the self-healing system. TGA and DTA analyses were generally used to study the thermal stability of microcapsules and the healing agents. Zhang et al. [80] investigated the amine loaded hollow glass bubbles and epoxy capsules for their thermal stability and amount of healing agent encapsulated using TGA. They reported the thermal decomposition of capsules in the range of room temperature to 600˚C and represented the weight loss % at each stage.

AFM is generally used to evaluate the self-healing performance of the systems in terms of time, temperature and local mobility of the atoms. Brancart et al. [81] evaluated the healing performance of reversible polymer networks based self-healing coatings using AFM. They developed nano scratches using nanolithography technique and investigated the self-healing coatings ability to heal the nano scratches. Ultrasonics, being a non-destructive testing is used to monitor the progression of self-healing process. C.W. In et al. [82] used diffused ultrasonics to monitor the self-healing of cracks in concrete. Ultrasonics were applied on the fractured surfaces of tensile specimens and self-healing behavior was monitored using ultrasonics diffusivity and arrival time of maximum energy.

2.4 Modelling of microcapsules

Understanding the mechanical properties of microcapsules helps to prevent the damage of capsules during processing, maintain long term stability and realize the triggered release of core material. Two different category techniques have been developed to investigate the mechanical properties of microcapsules and can be found in Table 2.1.

Table 2.1 Techniques to investigate mechanical properties of microcapsules

characterization techniques based on bulk microcapsules	**characterization techniques based on single microcapsule**
• Compression between plates • Osmotic pressure test • Shear breakage of capsules in turbine reactor	• Atomic force microscopy • Micromanipulation • Nano indentation • Texture analyser

The main limitations associated with bulk capsules characterization techniques are they neglect the effect of capsule size and shell thickness and won't provide mechanical properties of individual capsules. Hence it is important to employ the single capsule characterization techniques to understand the mechanical properties of individual capsules. However, it is difficult to synthesize the capsules with controlled diameter, shell thickness and same surface roughness. Examining each parameter effect on the mechanical strength of microcapsule is a laborious process and time taking. Hence few researchers [83–86] in their studies tried to model the microcapsules to evaluate its mechanical properties, rupture force and rupture stress.

Mercade´-Prieto et al. [85] investigated the failure behavior of elastic, elastic-perfectly plastic melamine formaldehyde (MF) microcapsules by FEM and micromanipulation techniques. They have modelled the microcapsules to determine the failure stress, failure strain and reported as 350 MPa, 0.48 respectively. Core material was modelled as 2 node linear hydrostatic fluid and shell material treated as 4 node axisymmetric solid object.

X. Pan et al. [86] synthesized the perfume oil encapsulated PMMA microcapsules and investigated their mechanical properties using FEM. Based on the ratio of shell thickness to capsule radius they divided the capsules as thin shell and thick shell capsules and evaluated the rupture forces using force-displacement graphs obtained from FEM and micromanipulation techniques. For both thin and thick shell capsules, elastic modulus and rupture stress found to be independent of reaction time.

2.5 Mechanical properties of capsules reinforced composites

In order to implement self-healing materials in real time applications, it is important to understand the effect of healing agents addition on the virgin properties of the host polymer matrix and on the composite. The polymer matrix properties such as fracture toughness, strength, stiffness, elastic modulus and glass transition temperatures need to be understood for the practical implementation of self-healing technology.

2.5.1 Pure epoxy composite

In most of the self-healing composites, because of its structural properties epoxy is chosen as the polymer matrix. It is so common that the addition of any foreign fillers into the base material causes either decrement or increment in its original properties. Typically, in self-healing materials also the healing agents such as microcapsules, hollow glass fibres and vascular networks alter the base material properties. Dynamic Mechanical Analyzer (DMA) is generally used to study the change in physical properties such as glass transition temperature, coefficient of thermal expansion and viscoelastic properties. Tensile test, flexural test, impact test and mode I fracture tests are conducted to investigate the mechanical properties of healing agents added epoxy composites.

In the study conducted by Brown et al. [87] they investigated the effect of UF microcapsules filled with DCPD healing agent on the fracture toughness, tensile strength and tensile modulus. They reported that the fracture toughness increases with the increase in capsules concentration up to critical peak load and then decreases. But in the studies conducted by Kamphaus et al. [61] they reported that the addition of capsules has no effect or minimal effect on the fracture toughness of epoxy and the study conducted by Yin et al. [88] reported the decrease in fracture toughness at 5 wt% and 20 wt% capsules concentration. However, they reported that the decrease in toughness may be due to matrix dissolved catalyst concentration and interplay between matrix and microcapsules. Yuan et al. [65] studied the effect of epoxy/mercaptan capsules addition on the mechanical performance of epoxy composites and reported that with increase in capsules concentration both tensile strength and tensile modulus decreases. Rectangular shaped and dog bone shaped specimens are used to evaluate the mechanical performance. In the studies conducted by Li et al. [64] they investigated stress-strain relations, ultimate tensile strength and Youngs modulus and compared with neat epoxy to understand the effect of capsules addition on the epoxy composite.

Tripathi et al. [89] studied the effect of microcapsules shell material on the mechanical properties of the epoxy composite and reported that irrespective of the shell material tensile strength and tensile modulus decreases with the increase in capsules concentration. Similarly, Kosarli et al. [90] investigated the effect of capsule size on the fracture toughness of the epoxy and concluded that the capsule size is inversely proportional to the reduction in mechanical properties.

Caruso et al. [36,91] investigated the effect of chlorobenzene solvent encapsulated UF capsules to heal the epoxy system. They investigated the fracture toughness of the epoxy system using TDCB specimen and found that with the increase in solvent capsules concentration the maximum fracture peak load increases. The same group also studied the effect of phenyl acetate (PA), ethyl phenylacetate (EPA) solvents encapsulated UF capsules addition on the maximum peak load of capsules reinforced epoxy composite. They concluded that both the solvent capsules had a positive effect on the fracture toughness of the composite and showed increasing trend with the increase in capsules concentration.

2.5.2 Fibre reinforced epoxy composite

CFRP and GFRP are the most commonly used FRP composites in the structural applications. The method of integration of healing agents into the matrix material, quality of integration and the bonding between healing agents and matrix material affect the mechanical properties of matrix material and thus the mechanical performance of overall composite. Zhang et al. [92] investigated the effect of microcapsules addition on the glass fibre reinforced nylon composites and found that percentage reduction in mechanical properties increased with the increase in capsules concentration. Conversely, in the studies conducted by Coppola et al. [93] they reported that the addition of healing agents had insignificant or no effect on the in plane tensile strength and modulus properties of woven glass fibre epoxy composites. Barbero et al.[94] investigated the influence of DCPD capsules and solid Grubbs catalyst on the tensile strength, shear strength and modulus of glass fibre reinforced epoxy composite. They observed that both the modulus, tensile and shear strength decreased with the increase in capsules concentration.

In order to employ high fibre volume fractions and to study effect of capsules size on the interlaminar fracture toughness, Ghazali et al. [95] used vacuum assisted resin infusion technique to fabricate dual capsules reinforced carbon fibre epoxy composite and found that both smaller diameter capsules and larger diameter capsules had detrimental effect on the fracture toughness. Ebrahimnezhad et al. [96] investigated the tensile and interlaminar shear

properties of UF capsules and imidazole catalyst reinforced glass fibre epoxy composites and found that both tensile strength and interlaminar shear strength of the composite decreased with the increase in capsules concentration. In another study conducted by Xiao et al. [97] they investigated the effect of epoxy loaded capsules and boron trifluoride diethyl etherate catalyst addition on the impact strength and flexural strength of sisal fibres reinforced epoxy composite. They concluded that at lower wt% of capsules and catalyst combination, the variation in impact and flexural performance is less and the reduction in mechanical performance increases with the increase in capsules and catalyst concentration.

2.6 Self-healing efficiency of capsules reinforced composites

Self-healing performance of the composites are generally measured in qualitative and quantitative terms. For qualitative evaluation different microscopes such as optical microscope, SEM and confocal lase microscopes are generally used. Quantitative healing performance is measured based on the ability of the system to recover material original or virgin properties. In both the assessments, the main aim of the self-healing approach is to recover the damage and extend the service life of the component by restricting the crack growth. Different material properties such as fracture toughness, strength and stiffness are used to quantify the healing efficiency. For convenience, researchers made the definition of healing efficiency common to any material property of interest and defined as.

$$\eta = \frac{f_{healed} - f_{damaged}}{f_{virgin} - f_{damaged}} \qquad \text{Eq. 2.1}$$

where f - property of interest

Which material property has to be chosen to define the healing efficiency may depends on the virgin material properties, healing mechanism and the desired failure mode. For example, healing efficiency measurement based on the fracture toughness requires mode I fracture crack opening which is very similar to the micro crack growth phenomenon that occurs in the real time applications [37]. Healing efficiency based on tear strength or strain energy is a better choice for evaluating the elastomers healing efficiency. Recovery of impact or flexural properties after the damage is a better metrics for evaluating the fibre reinforced composites healing efficiency. Flexural and impact loadings induce micro cracking, delamination and fibre-matrix debonding failure damages and hence evaluating the healing efficiency based on those damages recovery is a best choice for fibre reinforced polymer composites.

2.6.1 Self-healing of pure epoxy

Epoxy resin based polymer composites have been receiving attention from the research community to develop thermosetting polymer based self-healing composites. Damage can happen anywhere in the structure in the form of crack due to different loading conditions and type of application. Several healing efficiency evaluation methods have been proposed based on the type of damage recovery to assess the healing performance of epoxy composites. Damage in epoxy composites often involves some form of fracture and hence to have structural applications it is necessary to evaluate the self-healing performance of the composite based on the fracture toughness recovery.

2.6.1.1 Healing performance based on fracture toughness recovery

Quasi static fracture tests are commonly used to design the self-healing systems based on the fracture toughness recovery. There are different mechanical techniques such as compact tension (CT), double cantilever beam (DCB), tapered double cantilever beam (TDCB), width tapered double cantilever beam (WTDCB), single edge notch bending (SENB), double cleavage drilled compression (DCDC), three point bending and four point bending are available to measure the fracture toughness. But to evaluate mode I fracture toughness, DCB and TDCB are the most commonly preferred techniques due to controlled and predicted crack propagation. Furthermore, with these geometries smaller damage volumes can be induced and all the fracture parameters can be measured. The damage volume induced generally depends on the type of geometry employed and the loads applied during testing. The micro cracking that happens in the real time applications can be simulated exactly using TDCB geometry proposed by White et al. [29]. In addition to crack propagation along the centreline of the specimen TDCB geometry also offers the crack length independent fracture toughness measurement. Since it is difficult to measure healed sample crack length in most of the studies researchers employed TDCB geometry to evaluate the healing performance.

For mode I quasi static fracture tests, as the fracture resistance of the damaged state becomes zero the self-healing efficiency is defined as the ratio of healed and virgin sample fracture toughness and can be evaluated by Eq. 2.2.

$$\eta = \frac{K_{IC}\, healed}{K_{IC}\, Virgin} \qquad \text{Eq.2.2}$$

Where K_{IC} healed and K_{IC} virgin are the fracture toughness of healed and virgin specimens respectively.

Brown et al. [59] investigated the self-healing performance of epoxy composite based on its ability to recover initial fracture toughness. In this study they employed TDCB geometry and DCPD filled UF microcapsules, Grubbs catalyst to achieve self-healing of the crack. They studied the effect of healing time, catalyst concentration and capsules concentration on the healing performance and found the optimized parameters at 10 hr healing time, 2.5 wt% catalyst and 10 wt% microcapsules concentration and achieved healing efficiency of 90%. The schematic of TDCB geometry used in their study is shown in Figure 2.7.

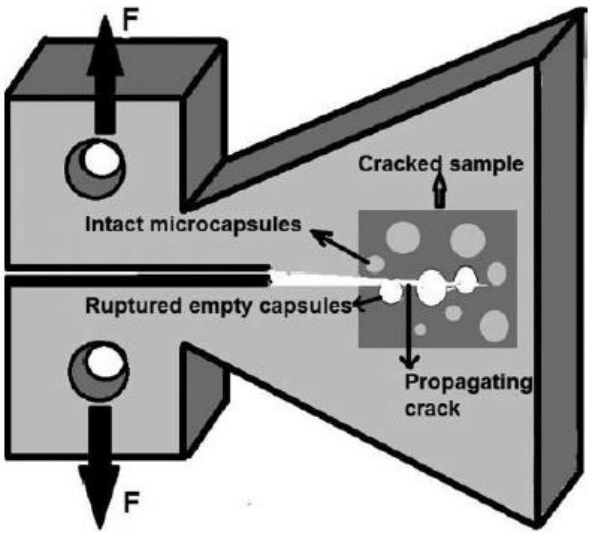

Figure 2.7 Schematic representation of TDCB geometry [59]

Subsequent studies [87,98,99] on self-healing of epoxy composites employed same geometry and studied the effect of capsule size and damage volumes on the fracture toughness and healing performance. Ahangaran et al. [66] investigated the effect of diluted epoxy capsules and mercaptan capsules on the self-healing performance of epoxy composites by a measure of fracture toughness recovery. They also employed TDCB geometry to measure fracture toughness and found that fracture toughness of virgin epoxy increases with the increase in capsules concentration and found to be optimum at 15 wt% capsules concentration.

As an alternative to TDCB geometry Jin et al. [100] employed WTDCB geometry (which also provides crack length independent fracture toughness measurement) to evaluate the healing performance of steel adherents bonded self-healing epoxy adhesive system using quasi static fracture test. They reported 56% of original fracture toughness recovery at room temperature healing and 24 hours (hrs) healing time.

2.6.2 Self-healing of fibre reinforced epoxy composite

Since composite materials are made up of different materials they behave differently for different thermomechanical loadings. But having structural integrity and maintaining it is important to have applications as structural materials. In self-healing systems, structural integrity of the components can be achieved by recovering the virgin or original mechanical properties. As a consequence, it is important to assess the self-healing efficiency based on the mechanical properties recovery. The properties such as fracture toughness, impact strength, ultimate tensile strength, compressive and bending strength and fatigue resistance are used to evaluate the healing performance.

2.6.2.1 Healing performance based on mode I damage assessment

Compared to capsules reinforced epoxy composite, fabrication of capsules reinforced glass/carbon fibre epoxy composite is difficult as it involves incorporation of microcapsules onto dry fibre reinforcement. Most of the studies [101–104] employed hand layup technique and low fibre volume fractions to fabricate capsules reinforced glass/carbon fibre epoxy composite. Kessler et al. [101] employed WTDCB specimen to calculate the interlaminar fracture toughness and created the delamination damage in the central layers of DCPD capsules reinforced carbon fibre epoxy composite to assess the healing performance. 20 wt% of DCPD capsules and 5 wt% Grubbs catalyst were used as healing agents and incorporated in the central region of laminate and examined the healing performance by evaluating the fracture toughness recovery. They observed that at room temperature healing 45% of fracture toughness was recovered and upon elevating the healing temperature to 80˚C achieved the maximum healing efficiency of 80%.

T. Yin et al. [103] investigated the delamination damage recovery in woven glass fibre reinforced epoxy composite by employing DCB specimen and by conducting mode I damage fracture test. Epoxy loaded UF microcapsules and latent hardener catalyst were used as healing materials and studied their influence on the tensile properties, interlaminar fracture toughness and healing efficiency. They reported maximum healing efficiency of 70% with 30 wt% epoxy capsules and 2 wt% catalyst.

Bolimowski et al. [105] examined the autonomic healing in unidirectional carbon fibre reinforced epoxy composite by employing epoxy resin-imidazole chemistry. Mode I fracture tests were conducted to evaluate the recovery in fracture toughness and observed that the self-healing efficiency is strongly dependent on the distribution pattern and capsules concentration.

2.6.2.2 Healing performance based on other mechanical properties recovery

In few studies [106–109] recovery in compressive strength after impact, ultimate tensile strength, interlaminar shear strength and flexural strength are used as the parameters to evaluate the self-healing performance in fibre reinforced epoxy composites. Yuan et al. [106] fabricated the woven glass fibre reinforced epoxy composite by embedding diluted epoxy and mercaptan capsules and evaluated the healing performance based on the recovery of compressive strength after impact and rate of damage area reduction. Impact energy of 1.5 J to 5.5 J were applied on the composite and observed that the rate of damage area recovery decreased with the increase in applied impact energy. The rate of reduction in damage area is proportional to capsules concentration and size of the capsules and obtained maximum healing efficiency when the lateral pressure is applied.

Sanada et al. [109] investigated the self-healing of interfacial debonding in unidirectional carbon fibre reinforced epoxy composites by embedding the DCPD microcapsules and Grubbs catalyst. To create interfacial debonding they have tested the composite in a directional normal to fibres orientation and evaluated the healing performance by calculating the tensile strength ratio of healed and virgin samples. Maximum healing efficiency of 19% and 14% are obtained for FRP composite and neat epoxy, respectively. They concluded from the study that the reinforcement of fibres in epoxy causes modification of stress state around the microcapsules.

2.7 Research gaps & Objectives

After conducting a thorough literature review on the past available studies pertaining to self-healing of epoxy and fibre reinforced polymer composites, the following gaps were identified.

- Most of the polymer composites self-healing performance evaluated embedding either microcapsule containing single healing agent- catalyst or dual capsules containing epoxy-mercaptan healing agents. Very few studies reported self-healing performance using TDCB model and employing epoxy-amine hardener microcapsules.
- Even though synthesis of epoxy resin capsules reported in few works, none of the works studied the influence of epoxy resin healing agent viscosity on the encapsulation, surface morphologies, core content percentage and self-healing performance.
- Effect of surfactant type and its concentration on the surface morphology, core content and yield of capsules were reported in very few studies, and it needs further investigation.

- Studies pertaining to epoxy resin-amine hardener capsules embedded epoxy composites to evaluate the effect of microcapsules concentration on the mechanical and self-healing performance of composite are very few.
- Matrix cracking and delamination damages are very predominant in CFRP composite structures. But very few studies reported the self-healing of CFRP composites based on those damages recovery and there is a need to crosscheck the reliability of the results.
- Stiffness is one of the important parameters to evaluate structural integrity of the components, but no study available on the self-healing performance of CFRP composites based on stiffness recovery and also no literature found on the damping characterization of self-healing CFRP composites.
- To design epoxy based self-healing system it is important to know the load bearing capacity of capsules. Thus, numerical analysis of microcapsules load bearing capacity and the stress distribution at the pure epoxy crack front need to be investigated more.

In order to address above said research gaps, the following objectives are outlined for the current research work.

1. Development of self-healing microcapsules and process parameters optimization of healing agent filled PMMA microcapsules.
2. Integration of optimized dual microcapsules with matrix material and evaluating the mechanical performance and quantitative self-healing efficiency.
3. Self-healing performance evaluation and damping characterization of dual capsules reinforced carbon fibre epoxy composites.
4. Numerical investigation on microcapsules load bearing capacity and the evaluation of stress distribution at the pure epoxy crack front.

Integration of above objectives towards the main aim of the work can be seen in Figure 2.8. On the whole the current research work is intended at fabrication of dual capsules reinforced epoxy, CFRP composites and assessment of self-healing performance of those composites.

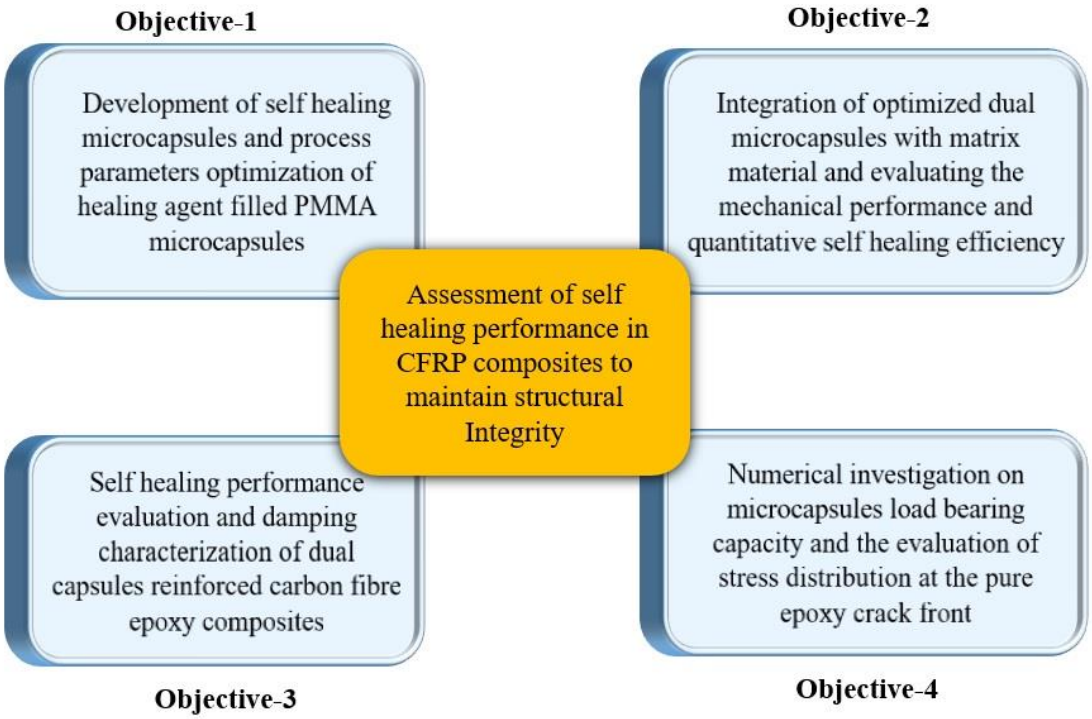

Figure 2.8 Integration of the objectives

2.8 Work plan

The following work plan is followed to accomplish the main aim of the work.

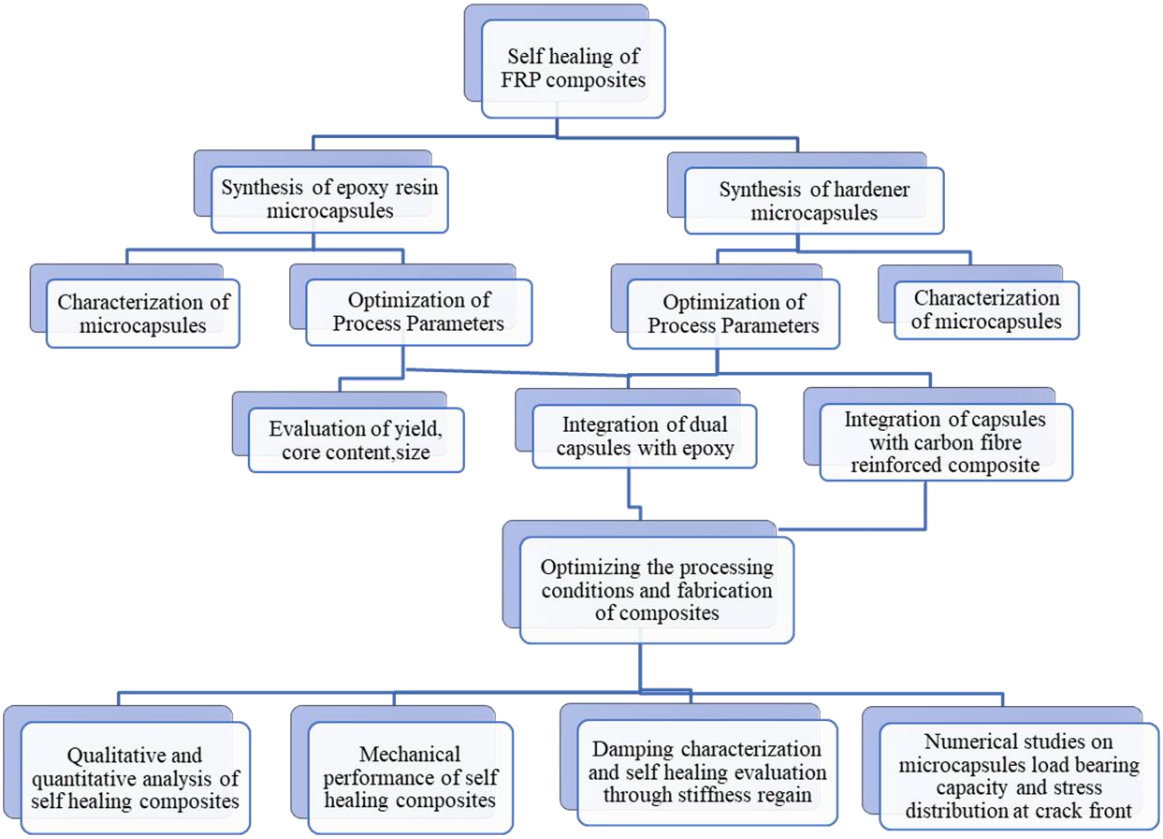

Figure 2.9 Work plan

Chapter 3

Synthesis and process parameters optimization of self-healing microcapsules

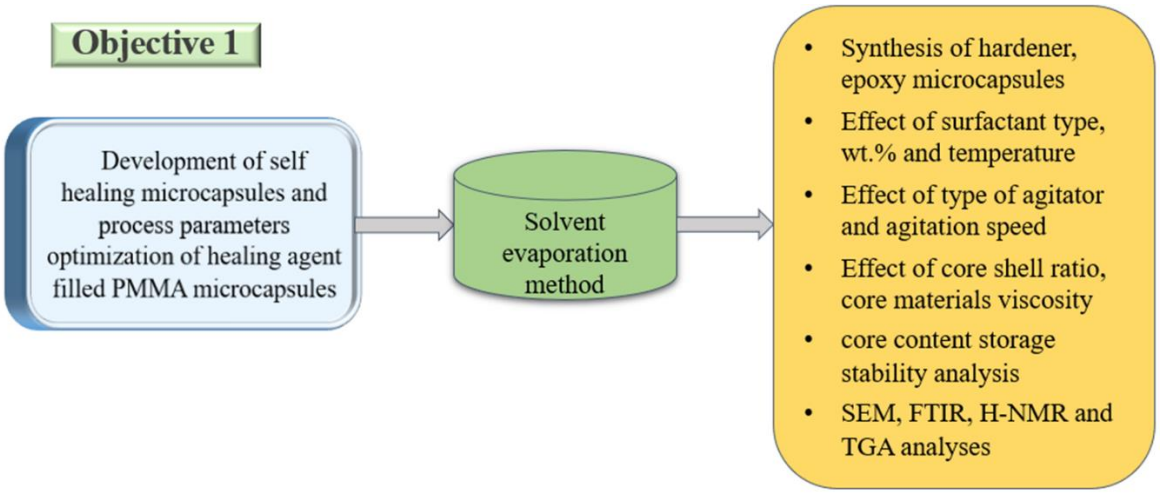

This chapter discusses the encapsulation of epoxy resin, amine hardener as two separate healing agents into PMMA shell material. Process parameters that affect the encapsulation of healing agents were discussed and optimized for an ideal conditions. This chapter also briefs about different characterization techniques used to confirm the encapsulation of healing agents in the shell material.

3.1 Introduction

The main objectives of the self-healing materials are to offer autonomic repair of invisible microcracks, enhanced service life of the component, improved reliability and durability of the structures. While several strategies were investigated, one of the most versatile and successful method to achieve self-healing is encapsulating the healing agent in a fragile walled shell material and integrating those microcapsules with polymer matrix. In the event of the crack, microcapsules rupture and fill the crack plane through capillary action and undergoes polymerization reaction to re-establish the structural integrity of the component.

In the microencapsulation approach, self-healing can be achieved either due to chemical reaction between single capsule-catalyst combination or due to curing reaction between released healing agents from two different capsules. However, catalyst characteristics such as weak stability, low melting temperature and reduction in reactivity when exposed to moisture hindered the applications of single capsule-catalyst self-healing approach. To overcome these limitations many authors [63,65,66] suggested dual component microcapsules self-healing system. Numerous studies [17,110] have been conducted on the encapsulation of different healing agents to evaluate the self-healing performance and reported that the selected core material should have an attribute of easy release during damage event. Epoxy resin and amine hardener are well well-known for their room temperature curability, good flowability, better adhesion capabilities and rapid solidification. Hence, in the present study epoxy resin and amine hardener are chosen as healing agents and dual component capsules system is considered as self-healing approach. In epoxy resin and amine hardener dual component microcapsules system one component consists of epoxy resin microcapsules and the other component consists of corresponding curing agent (amine hardener) microcapsules. Whenever the approaching crack interacts and rupture the capsules, the core content inside the capsules flows into the crack surface and polymerizes through curing reaction of stoichiometric amount of epoxy and hardener.

The selected healing agents can be encapsulated in polymer shells such as urea formaldehyde, melamine formaldehyde and polymethyl methacrylate (PMMA). Since one of the chosen healing agents i.e., amine hardener is highly active at room temperature, a polymeric shell material which does not react adversely with healing agents is needed for encapsulation. PMMA, which does not create any adverse reactions with either epoxy resin or amine hardener is selected as the shell material for the present study. PMMA has biocompatibility, high chemical stability, good mechanical properties and good adhesion capability with host polymer matrix [111]. PMMA is strong enough to intact during fabrication, brittle enough to rupture and release healing agent when the crack intervene the capsules.

In order to get better self-healing performance through epoxy resin, amine hardener capsules combination, it is necessary to have capsules with similar surface morphologies, same geometrical shape and narrow differences in the size range. There are few methods such as in situ polymerization [112], solvent evaporation [68] and interfacial polymerization [113] are available to encapsulate various healing agents. Since solvent evaporation method does not have any PH control requirement, no washing and filtering difficulties it is selected as the microencapsulation method for the present study. Sharma et al. [114] investigated the synthesis of epoxy resin encapsulated PMMA microcapsules and optimized the different process parameters to prepare such microcapsules.

To encapsulate healing agent through solvent evaporation method it requires an emulsifying agent (surfactant) which can create homogeneous emulsion during synthesis. Surfactants such as poly vinyl alcohol (PVA), sodium dodecyl sulfate (SDS), sodium dodecyl benzene sulfonate (SDBS) and cetrimonium bromide (CTAB) are generally used to create homogeneous emulsion systems. But the selected surfactant should have an ability of encapsulating the healing agent with less required quantity and also should produce undamaged capsules with good surface morphologies. Since PVA and SDS surfactants satisfies above conditions they were chosen as the surfactants for the present study.

Surface morphology plays a critical role in evaluating the capsules adhesion capability with the host polymer matrix. Capsules size distribution, core content and shell thickness are other important parameters that decide the self-healing performance. To address one of the research gaps, in this chapter the effect of surfactant type and its concentration on the capsules surface morphology, core content and size distribution are discussed. Effect of different process parameters on the encapsulation of healing agents is also elaborated.

3.2 Materials and Methods

Different materials used in the synthesis of microcapsules and the synthesis procedures of epoxy resin, amine hardener microcapsules are discussed in this section.

3.2.1 Materials

Diglycidylether of bisphenol-A based epoxy resins (LY556,CY230) and Triethylenetetramine based amine hardener (HY951) were chosen as the healing agents and obtained from composites tomorrow, Vadodara, India. LY556 epoxy and HY951 hardener were also used to fabricate host polymer matrix. PMMA with average molecular weight of 5,50,000 was chosen as the shell material and PVA, SDS were used as surfactants. The solvents methanol and dichloromethane (DCM) were purchased from Finar chemicals, India. Grade 93 Whatman filter paper (pore size 10 µm) was used for capsules filtration. Analytical grade reagents were used without any additional purification and Deionized (DI) water was used throughout the study. Table 3.1 indicates the list of materials used in the present study and Table 3.2 indicates the key data specifications of epoxy resins and amine hardener obtained from standard data sheets. Figure 3.1 shows the chemical structures of the materials used in the study.

Table 3.1 List of materials used in the current study

Material	Purpose	Purchased from	Remarks
DGEBA based epoxy resin	Epoxy capsules core material	Composites Tomorrow, Vadodara, India	Araldite® LY556 (Trade name)
TETA based amine hardener	Hardener capsules core material	Composites Tomorrow, Vadodara, India	Aradur® HY951 (Trade name)
PMMA	Shell material	Alfa Aesar, Mumbai, India	Average M_w 5,50,000
PVA	Surfactant	Sigma-Aldrich, Germany	Average M_w 1,25,000
SDS	Surfactant	Sisco Research Laboratories, India	AR grade
DCM, methanol ethanol	Solvent	Finar chemicals Ltd, Mumbai, India	AR grade
Whatman filter paper of grade 93	Filtration	Sigma-Aldrich, USA	Pore size 10 µm

Table 3.2 Key data specifications of epoxy resin and amine hardener

Material	Visual appearance	Density (g/cc)	Viscosity (Pa.s) at 25°C	Epoxy content (eq/kg)	Storage life (in years)
LY 556	clear, viscous liquid	1.15 - 1.20	10 - 12	5.30 - 5.45	3
CY230	clear, viscous liquid	1.1 - 1.2	1.3 - 2	4.20 - 4.35	2
HY951	clear liquid	0.98	0.01 - 0.02	NA	1

Material	Chemical structure
DGEBA	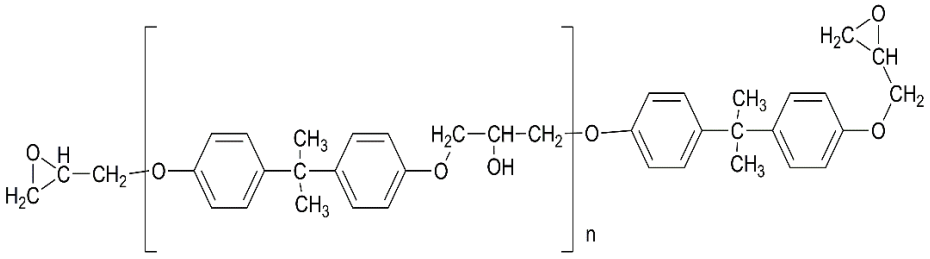
TETA	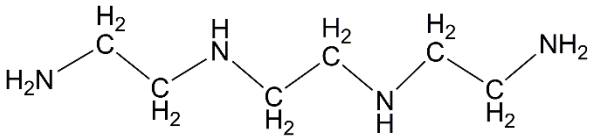
PMMA	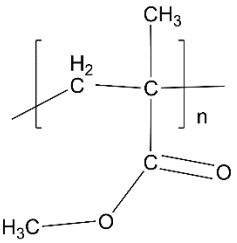
PVA	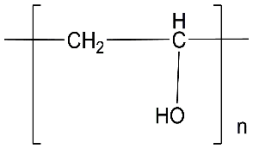
SDS	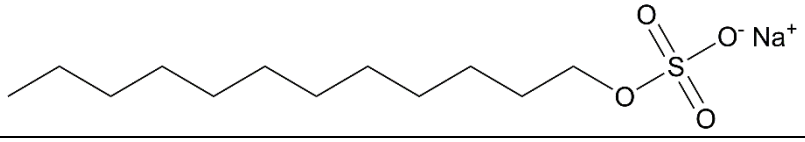

Figure 3.1 Representative chemical structures of materials used in the study

3.2.2 Synthesis of epoxy resin microcapsules

Both LY556 and CY230 epoxy resin microcapsules were synthesized using oil in water (o/w) solvent evaporation method and shown in Figure 3.2. To synthesis LY556 capsules, 1 g LY556 and 1 g PMMA were taken and dissolved in 30 ml DCM to prepare oil phase. Next, in a separate beaker 5 wt% SDS surfactant was dissolved in 250 ml DI water to prepare water phase. After ensuring both core and shell materials were well dissolved in DCM, oil phase was added to 70 ml water phase in a dropwise manner over a period of 15 - 20 min at room temperature, 400 rpm stirring speed and allowed to rotate for 45 min using overhead stirrer. The resultant emulsion was poured into remaining 180 ml water phase at 400 rpm, 40˚C and rotated for another 100 min. Over this duration DCM was allowed to evaporate and produce epoxy resin encapsulated PMMA microcapsules. Synthesized capsules were allowed to cool to room temperature (RT) and filtered. Sieved capsules were washed with DI water, methanol and dried in an open atmosphere for 48 hrs. CY230 epoxy microcapsules were also synthesized in the same way as LY556 capsules synthesized. The only difference between LY556 capsules synthesis and CY230 capsules synthesis was CY230 capsules were found to be optimum at 2:1 core to shell (c/s) ratio whereas LY556 capsules were found to be optimum at 1:1 c/s ratio.

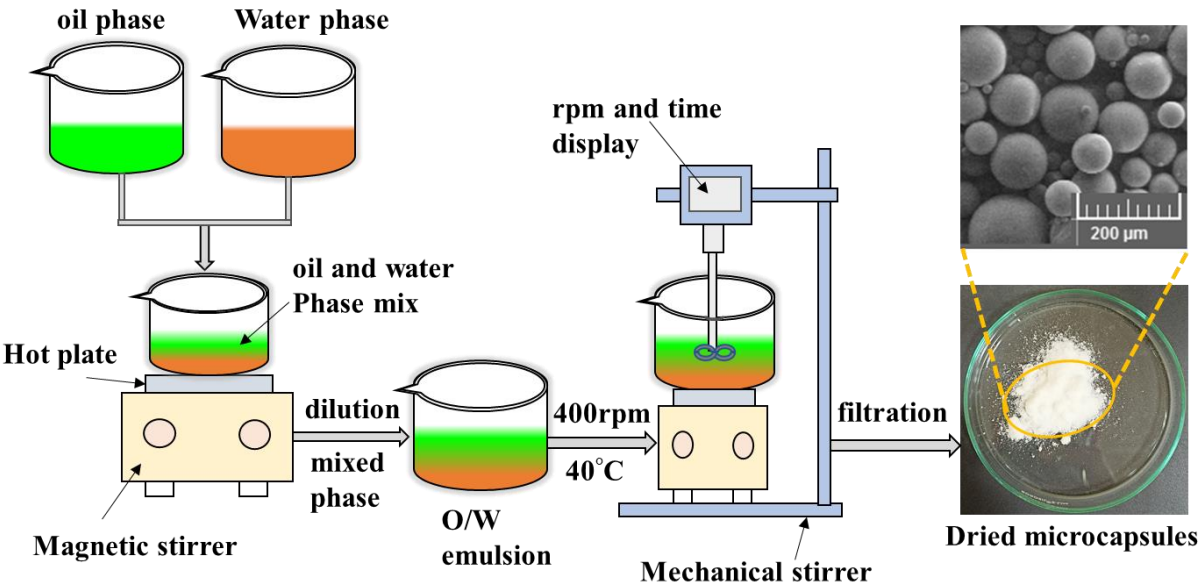

Figure 3.2 Synthesis of epoxy resin microcapsules through solvent evaporation method

3.2.3 Synthesis of amine hardener microcapsules

The amine hardener (HY951) encapsulated PMMA microcapsules were also synthesized using solvent evaporation method in the similar way as epoxy microcapsules. Figure 3.3 shows the schematic description of hardener encapsulated PMMA microcapsules synthesis. The main difference in synthesizing hardener and epoxy capsules is that, in hardener capsules optimized c/s ratio, stirring speeds were observed as 4:1, 500 rpm and in LY556 epoxy capsules those values were noted as 1:1 and 400 rpm respectively. To synthesize HY951 hardener capsules, oil phase was prepared by blending 4 g HY951 and 1 g PMMA in 30 ml DCM and water phase was prepared by blending PVA surfactant in DI water. Oil phase was added to 70 ml water phase under stirring speed of 500 rpm and allowed to rotate for 30min. The resultant mixed phase solution was diluted with remaining 180 ml water phase and allowed to rotate at 500 rpm, 40°C temperature for 100 min. Complete evaporation of DCM from o/w phase results in the formation of hardened microcapsules. Finally, synthesized microcapsules were filtered, washed and permitted to dry for 48 hrs at RT. Figure 3.4 shows the schematic view of epoxy resin and amine hardener containing PMMA microcapsules.

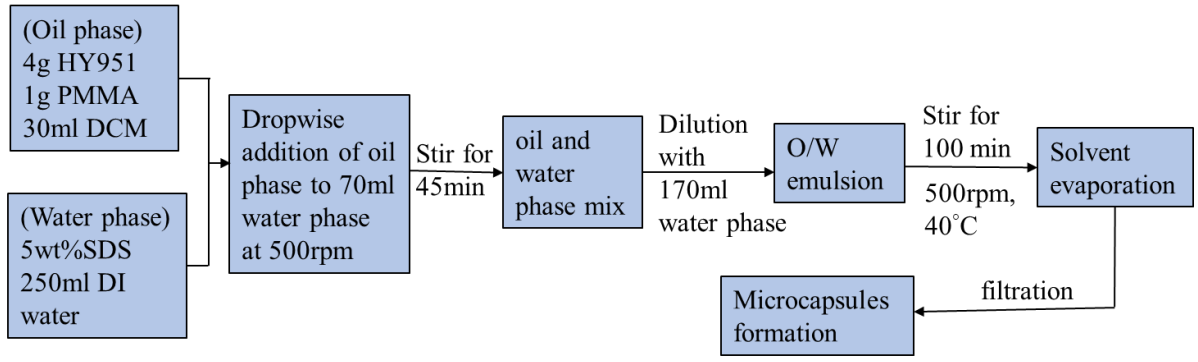

Figure 3.3 Schematic representation of synthesis of amine hardener microcapsules

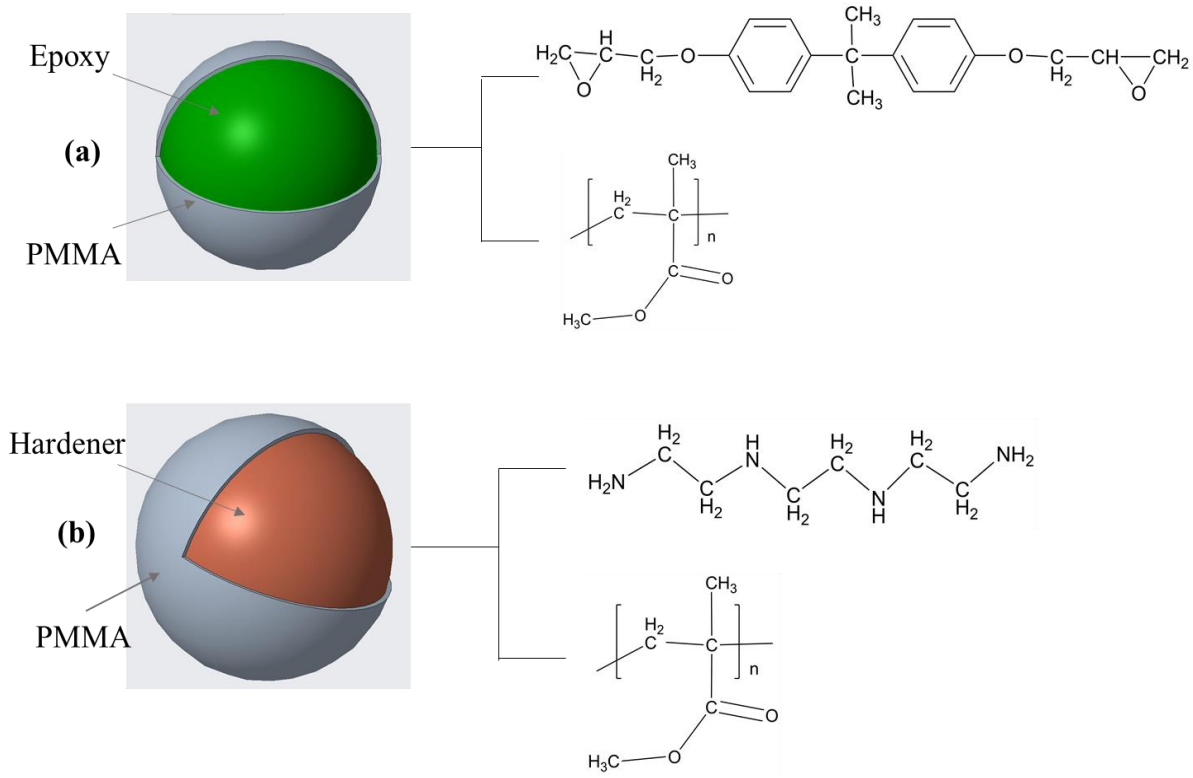

Figure 3.4 Schematic view of (a) epoxy and (b) hardener containing PMMA microcapsules.

3.3 Characterization of microcapsules

Different characterization techniques used to investigate the average capsule size, core content, chemical structure and thermal analysis of microcapsules are discussed in this section.

3.3.1 Surface morphology and average capsule size

Surface morphology of the capsules is one of the important aspects to be investigated to achieve better self-healing performance. In order to find microcapsules average size, shell thickness and surface morphology TESCAN Vega 3 scanning electron microscope (SEM) was used. Before inspection, capsules were glued to conductive carbon tape and gold sputtered to avoid charging of the capsules during examination and to get better image clarity. The images were taken at a working depth of 10 - 11 mm and 10 kV voltage. Average capsule size was measured using Image J software by considering at least five SEM images per sample. To measure average shell thickness at least three SEM images were considered.

SEM uses high energy electrons to scan the surface of the specimen and produces various signals due to interaction between electrons and atoms of the specimen. Respective detectors detect these signals and produces scan images which contains information such as surface morphology and composition.

3.3.2 Core content and yield

The core content percentage of the developed capsules was assessed using solvent extraction method. Initially, accurately measured microcapsules ($W_{capsule}$) were heated to 130˚C using hot plate and then crushed to fine powder using mortar and pestle. To the crushed capsules 10ml of methanol was added and rotated for 30 min using magnetic stirrer followed by filtration with 10 µm pore size filter paper. Later, the collected residue (W_{shell}) in filter paper was allowed to dry at RT for 48 hrs and weighed until the constant weight was obtained. All the developed capsules i.e., LY556 capsules, CY230 capsules and HY951 capsules core content was measured by following above procedure and according to Eq. 3.1.

$$W_{core} = (1 - \frac{W_{Shell}}{W_{capsule}})\ X\ 100\,\% \qquad \text{Eq.3.1}$$

The yield percentage of the developed microcapsules was determined by the ratio of microcapsules weight ($W_{capsule}$) to the weight of raw materials supplied to synthesize those microcapsules i.e., weight core material (W_{core}) and weight of shell material (W_{shell}).

$$Yield = (\frac{W_{capsule}}{W_{core} + W_{shell}})\ X\ 100\,\% \qquad \text{Eq.3.2}$$

The healing agent storage stability of the developed capsules was measured by storing them at room temperature for a period of 3 months and then by calculating the weight loss %.

3.3.3 Molecular architecture analysis

The molecular architecture and the functional groups present in the capsules were examined using Bruker Alpha II Fourier transform Infrared spectrometer (FTIR) in the wavenumber range of 4000 cm^{-1} – 400 cm^{-1} with 2 cm^{-1} resolution . Microcapsules were crushed to fine powder and then blended with potassium bromide (Kbr) powder to make the pellets. The FTIR spectra was observed in the transmittance mode.

To verify the healing agent encapsulation and to cross check exact functional groups present in the capsules, Bruker Avance III HD 400 Nuclear magnetic resonance (NMR) spectrometer was used. For all the samples ^{1}H NMR spin echo technique, deuterated chloroform ($CDCl_3$) solvent was used and tetramethyl silane (TMS) was considered as the reference compound. For complete solubility of microcapsules in $CDCl_3$, the mix was rotated for 30 min and filtered. The soluble fraction was considered for the study.

3.3.4 Thermal stability analysis

To have high temperature applications it is important to understand the degradation behavior of microcapsules due to temperature effect. The thermal decomposition behavior of microcapsules can be assessed using thermogravimetric analysis (TGA). In this analysis, weight loss of the capsules measured as a function of temperature.

Differential thermal analysis (DTA) is another technique used to study the decomposition, melting, oxidation and crystallization of the sample. In this technique, sample under investigation and inert reference sample undergo same heat flow during analysis and the temperature difference between them is monitored to understand endothermic or exothermic reactions happened in the sample.

In the present study thermal stability of the microcapsules was examined using STA 2500 Regulus NETZSCH TG-DTA analyser at a heating rate of 10˚C/min under argon environment. The stability of the capsules was verified within the temperature range of 25˚C to 600˚C at a gas flow rate of 60 ml/min. Analysis was performed by taking 10 - 15 mg of microcapsules into sample crucible and keeping reference crucible empty.

3.4 Results and Discussion

This section deals with the effect of different process parameters on the surface morphology, size distribution, core content and yield of epoxy, hardener microcapsules and discusses the techniques used to confirm the encapsulation of epoxy resin, amine hardener in PMMA shell.

3.4.1 Hardener capsules synthesized with PVA surfactant

The process parameters such as processing temperature, surfactant type and its concentration, type of agitator and agitation speed, core to shell ratio, viscosity of core material, ratio of oil phase to water phase and solubility of core and shell material in the solvent affect the surface morphology of microcapsules. As surfactant type and its concentration most affect the synthesis of microcapsules [114], in this study along with other parameters the influence of PVA and SDS as surfactants are investigated. In particular, in this section the effect of PVA surfactant on the surface morphology, average size and core content of the hardener microcapsules is discussed.

3.4.1.1 Effect of processing temperature on the surface morphology of capsules

Since the solvent (DCM) has a boiling temperature of 39˚C, the effect of processing temperature on the surface morphology of capsules is studied in the range of 35˚C to 50°C. The

temperatures in the range of 35˚C - 40˚C are considered as slow solvent evaporation rates and temperatures in the range of 45˚C - 50˚C are considered as fast solvent evaporation rates. Figure 3.5 illustrates that by varying processing temperature, surface morphology of capsules varies from rough surface to formation of dimples. Normally, core material encapsulates within the shell material and becomes hard during the solvent evaporation [68]. Thus, slower solvent evaporation rates allow the resultant oil-in water emulsion to react and form capsules and also provide time for the formed capsules to become hard, whereas faster evaporation rates causes formation of dimpled capsules because of quick evaporation of solvent. Even though dimpled capsules have applications in self-healing ,their usage can be limited due to core material leakage and improper adhesion with the matrix material. From the results, it is concluded that reaction temperatures in the range of 35˚C - 45˚C are preferred due to the preferred surface morphology. Since 40˚C temperature is close to solvent boiling temperature and microcapsules processed at 40˚C have better rough surface, it is recommended as the optimum processing temperature.

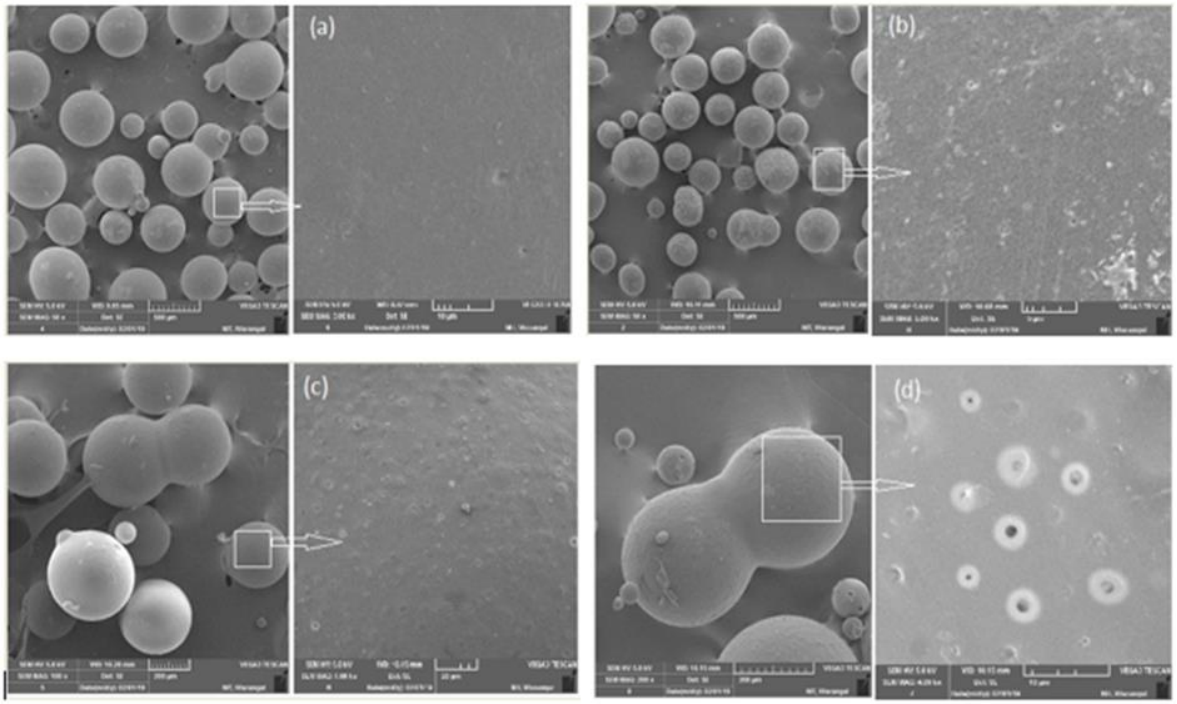

Figure 3.5 Surface morphology of hardener microcapsules processed at different processing temperatures (a) 35˚C (b) 40˚C (c) 45˚C (d) 50˚C

3.4.1.2 Effect of surfactant concentration on the surface morphology of capsules

The influence of PVA as a surfactant on the surface morphology of PMMA microcapsules was examined according to one parameter at a time approach by keeping core to shell ratio at 4:1, process temperature at 40˚C and stirring speed at 500 rpm. It can be noted from the Figure 3.6

that all the capsules synthesized at 0.5, 1, 2 and 3 wt% surfactant concentrations are spherical in shape and have rough surface finish. It can also be observed that some of the capsules have acorn shape with rough surface and some of the capsules got agglomerated. The formation of acorn shaped capsules can be attributed to partial encapsulation of core material in the polymeric shell [115]. It can be observed from Figure 3.6(a) that the agglomeration of capsules is due to insufficient emulsifier concentration and lump formation on the surface is due to unreacted shell material and improper solvent evaporation. Figure 3.6(b) - (d) confirms that agglomerated and lumped capsules also have rough surface morphologies. Since rough surface morphology, uniform and un agglomerated capsules distribution are required for better adhesion between capsules and matrix, 1 wt% PVA capsules which satisfied both the requirements, suggested as the optimum capsules to consider in the further studies.

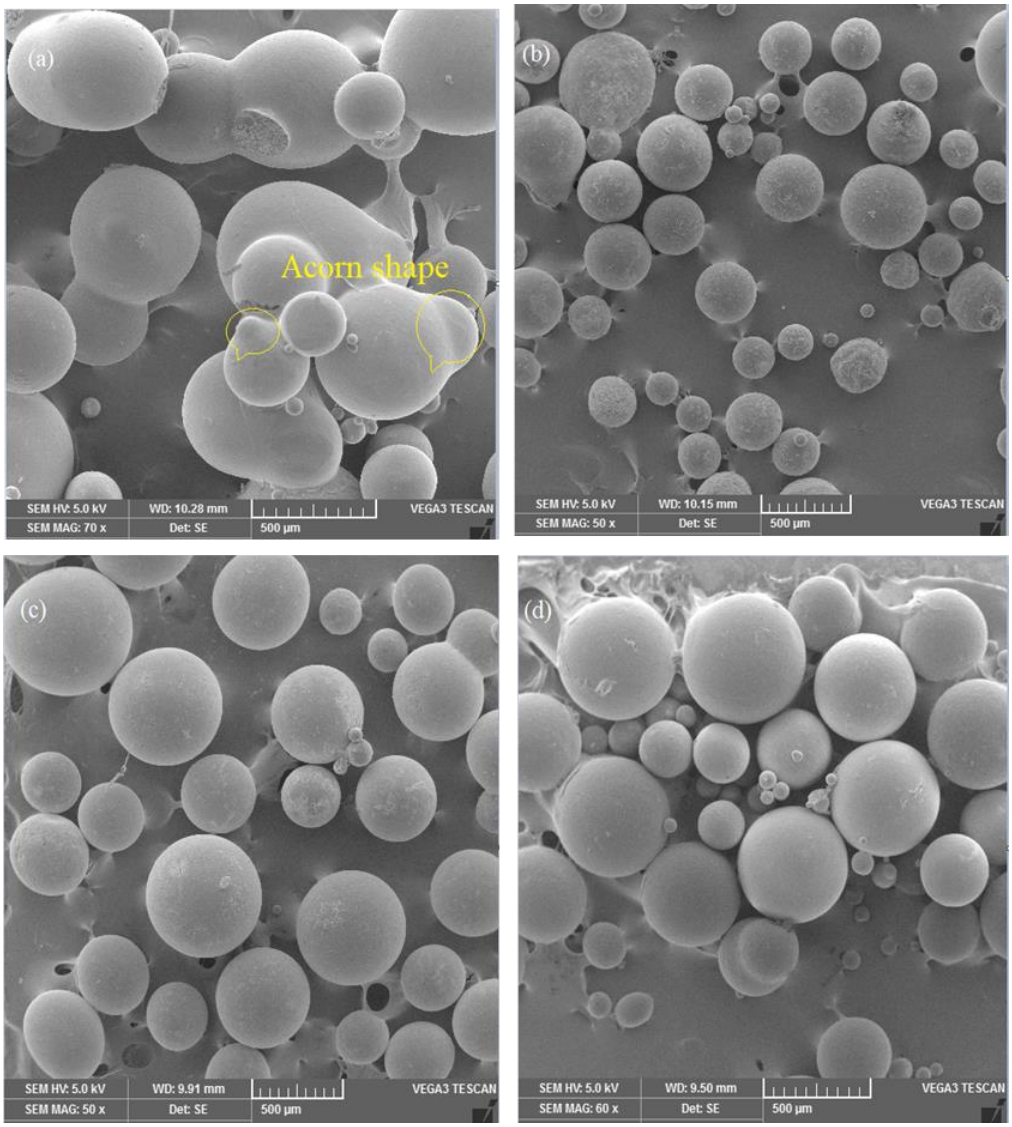

Figure 3.6 Surface morphology of microcapsules prepared at different surfactant weight % (a) 0.5 wt% (b) 1 wt% (c) 2 wt% (d) 3 wt%

3.4.1.3 Effect of surfactant wt% on the average size and size distribution of capsules

The effect of surfactant wt% on the microcapsules average size and size distribution is as shown in Figure 3.7. The average microcapsule size is determined by providing SEM images as input to Image J software. A wide range of size distribution is noted in all the cases though the range of size distribution is narrowed with the increase in surfactant wt%. The increased PVA adsorption at oil water interface reduces the water surface tension and causes for the formation of narrow size distribution capsules. The standard deviation (SD) of 1 wt% surfactant capsules is less compared to other surfactant wt% capsules which in turn indicates that most of the capsules size is close to average size of the capsule population. The differences in SD can be attributed to balance between resulting shear forces and interfacial tension forces. It is evidenced from Figure 3.7 that with the increase in surfactant concentration, average microcapsule size decreases. The average size decreased from 231.2 µm to 197 µm (~15% decrease) with the increase in surfactant (PVA) wt% from 0.5 to 3. The decrease in average capsule size is owing to reduction in interfacial tension between oil and water interface in the resultant system.

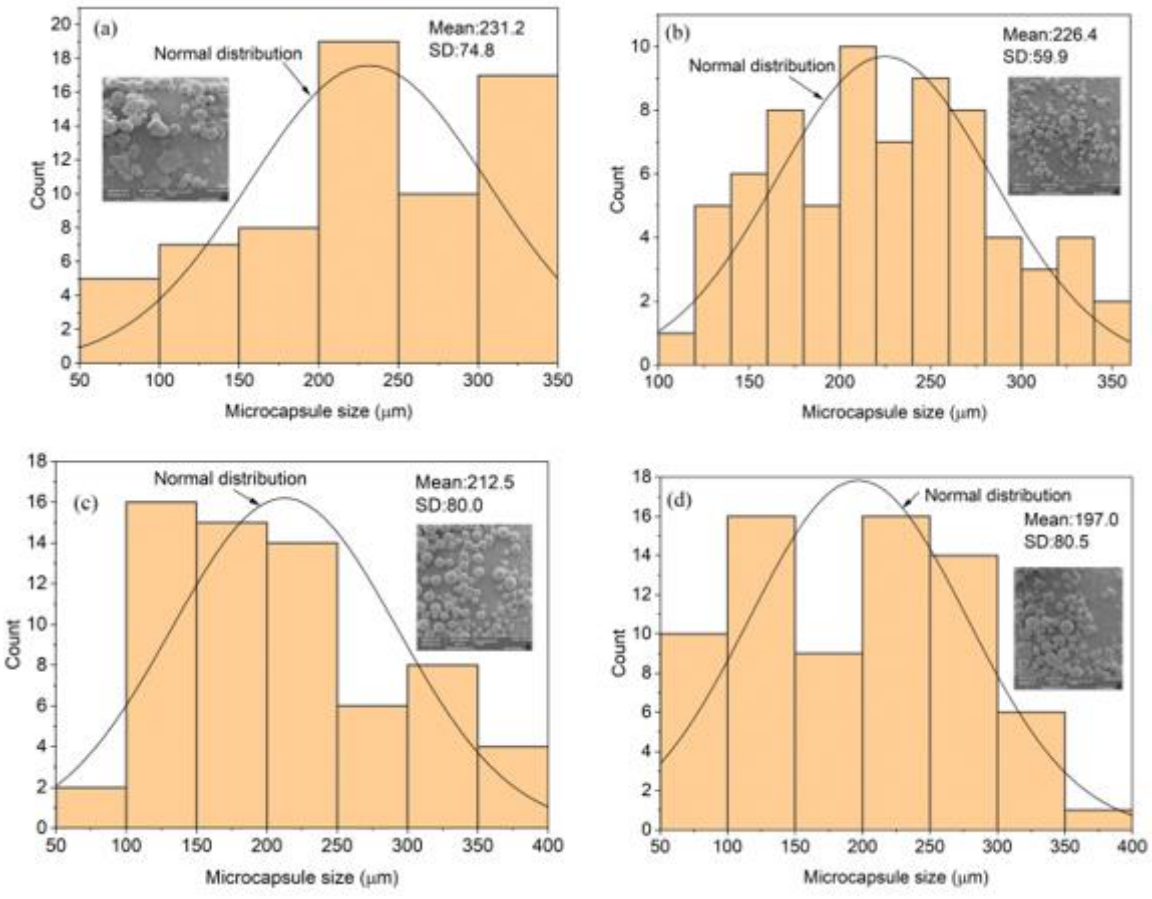

Figure 3.7 Average size and size distribution of hardener capsules synthesized at (a) 0.5% (b) 1% (c) 2% (d) 3% surfactant wt%

3.4.1.4 Effect of surfactant wt% on the core content of hardener capsules

Table 3.3 illustrates the variation in core content with the variation in surfactant wt% from 0.5 to 4. The amount of core content present inside the capsules increased gradually up to 2 wt% surfactant and then showed a slight increase trend from 2 to 4 wt%. Since < 5% increase in core content is observed by varying the surfactant wt% from 3 to 4, other studies in this work are restricted to 3 wt% surfactant concentration only. Q. Li et al. [116] observed a similar trend by varying the surfactant wt%. The increase in core content with the increase in PVA wt% can be ascribed to decrease in the shell thickness of microcapsules and presence of more number of smaller capsules.

Table 3.3 Core content of the microcapsules synthesized at different surfactant wt%

Surfactant wt%	Core content (%)	% Increase
0.5	10.2	--
1	11.9	16.66
2	13.4	12.60
3	14.4	7.46
4	15.1	4.86

3.4.1.5 Effect of surfactant wt% on the shell thickness of hardener microcapsules

Figure 3.8 shows the shell thicknesses of 0.5 wt% and 3 wt% PVA microcapsules processed at 500 rpm, 4:1 core to shell ratio and 40˚C processing temperature. From the available literature, it is noted that the shell thickness required for self-healing capsules should lie in the range of 11.2 - 19.04 µm [116]. It is observed from Figure 3.8 that the shell thickness for low surfactant concentration (0.5 wt%) and high surfactant concentration (3 wt%) is within acceptable range and far better. Since low and high surfactant wt% capsules shell thicknesses lie within the range, the shell thickness for other two surfactant wt% also lies within the acceptable range. Thus, from the results, it is confirmed that as prepared microcapsules will break when crack intervene and hence can have direct applications as self-healing materials. It is further confirmed from the Figure 3.8(b) that hardener was successfully encapsulated within PMMA shell wall with a shell thickness of 3.26 µm. The variation in the shell thicknesses can be ascribed to equilibrium between fluid flow shear forces and interfacial tensile forces during the synthesis of microcapsules.

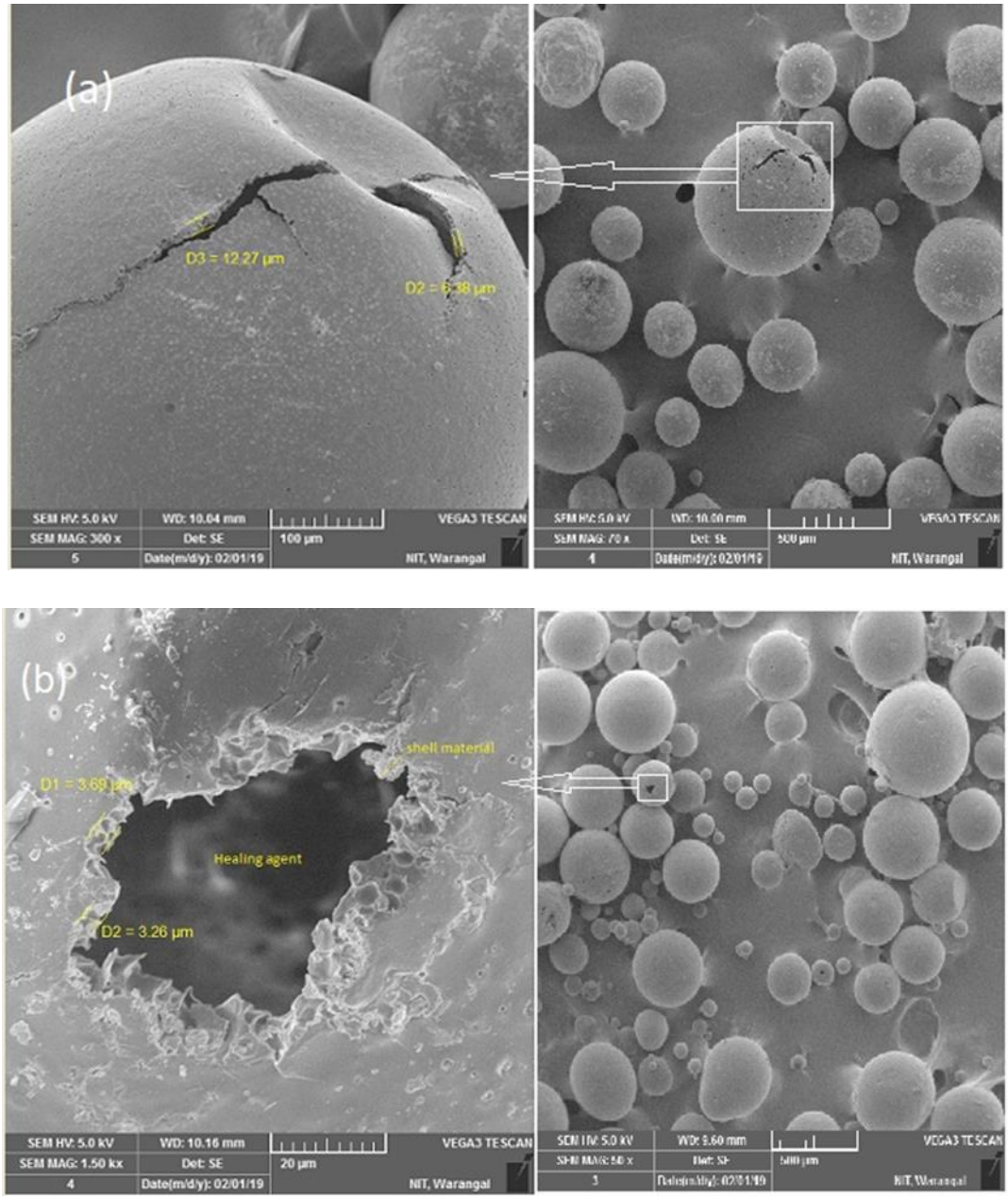

Figure 3.8 Shell thickness of (a) 0.5 wt% and (b) 3 wt% surfactant concentration capsules

3.4.1.6 Effect of agitator and agitation speed on the hardener microcapsules

To study the influence of agitation speed on the surface morphology and average size of the capsules 400 rpm, 500 rpm and 800 rpm were employed to synthesis capsules. It is observed from the results that with the increase in rpm average size of the capsules decreased. At high rpm shear forces dominate the interfacial tensile forces and easily breaks the droplets to produce smaller size capsules. Though average capsule size reduced few broken microcapsules were observed at 800 rpm. Since the microcapsules processed at 500 rpm have intact surface morphologies and narrow size distribution, it is suggested as an optimum rpm to consider in the further studies.

In order to study the effect of agitator, two types of agitators i.e., magnetic stirrer and overhead mechanical stirrer were considered and rotated at 500 rpm during capsules synthesis. All other process parameters were kept same for both the agitators during rotation. With 1 wt% PVA surfactant and 40˚C processing temperature magnetic stirrer and mechanical stirrer produced an average capsule size of 226.4 µm and 190.6 µm respectively. Due to increased shear forces and uniform distribution of emulsion, mechanical stirrer produced smaller size and uniformly distributed microcapsules. Hence in the further studies to synthesis hardener capsules, mechanical stirrer with 500 rpm is employed.

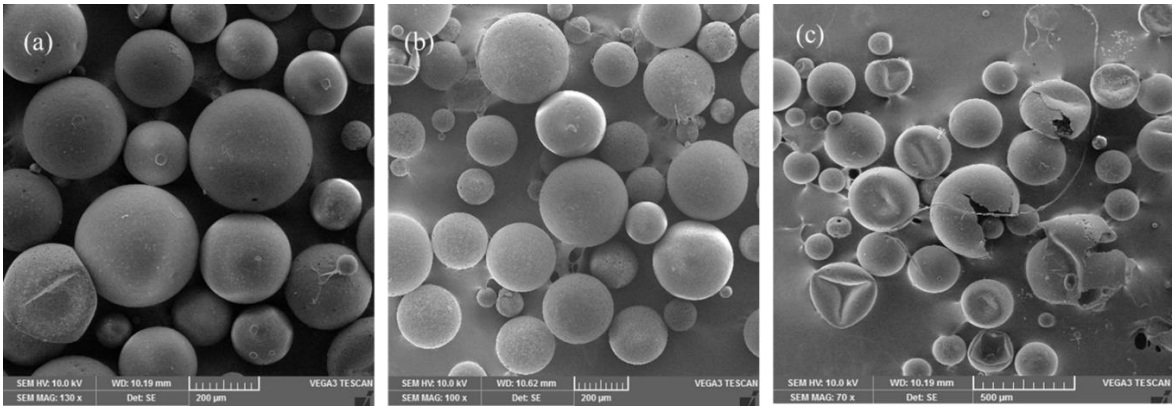

Figure 3.9 Effect of agitation speed on the average size and surface morphology of hardener microcapsules (a) 400 rpm (b) 500 rpm and (c) 800 rpm

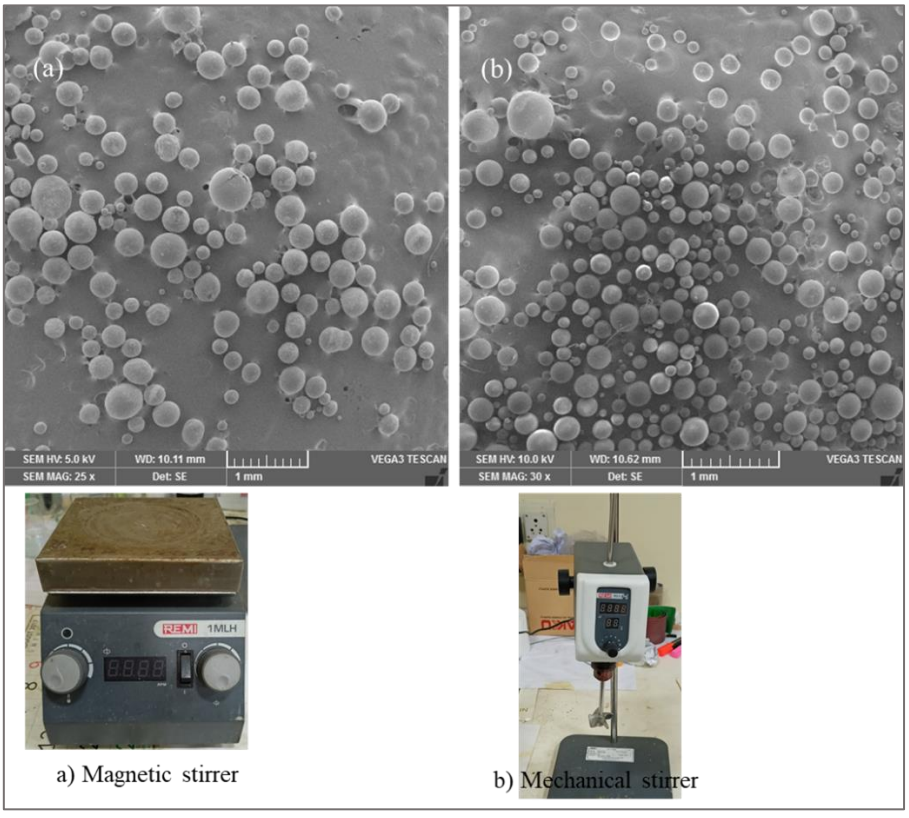

Figure 3.10 Effect of agitator on the average size of hardener microcapsules

3.4.2 Hardener capsules synthesized with SDS surfactant

To investigate the effect of surfactant type on the synthesis of hardener microcapsules one non-ionic surfactant (PVA) and another cationic surfactant (SDS) were considered. This section discusses the effect of SDS on the surface morphology, size distribution, shell thickness and core content of hardener capsules. The effect of PVA on the synthesis of hardener capsules is discussed in the previous section i.e., 3.4.1.

3.4.2.1 Surface morphology and size distribution of hardener microcapsules

Figure 3.11 illustrates the surface morphology of HY951 hardener microcapsules synthesized using SDS as surfactant and by employing optimal conditions as explained in the section 3.4.1. It can be noticed from the results that all most all hardener capsules have spherical geometry. It can be seen from Figure 3.11(a) that few hardener capsules have shrunk and collapsed. The partial encapsulation of healing agent in the PMMA shell prompts formation of fragile microcapsules [63]. As a result, improper handling during filtering, drying and even during SEM inspection causes collapse and shrinkage of few capsules.

Figure 3.11(b) demonstrates the size distribution and number of capsules considered at each size range to calculate average capsule size. From the observation it is noted that capsules were synthesized in the size range of 31 to 117 μm and average size is measured as 63.31 μm. Due to higher shear rates and more energy transfer, in the vicinity of propeller blades smaller diameter capsules were formed and away from the propeller i.e., around periphery of glass beaker, larger diameter capsules were formed.

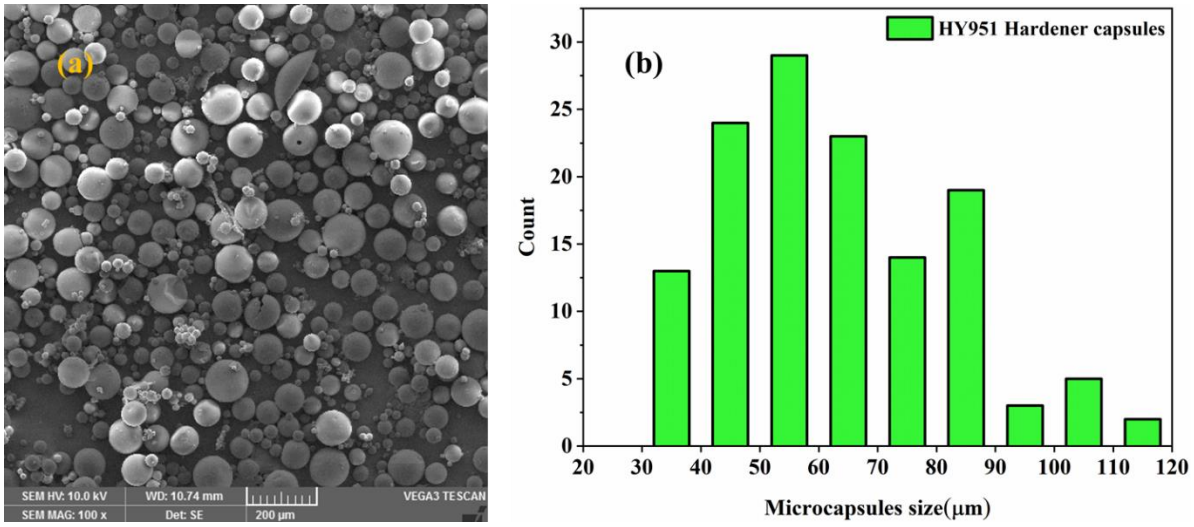

Figure 3.11 Effect of SDS on the (a) surface morphology (b) size distribution of hardener microcapsules

3.4.2.2 Core content and yield analysis of hardener microcapsules

Core content and yield percentages of hardener microcapsules were calculated based on their initial and final weights. From the surface morphology of hardener capsules, it is noticed that amine hardener is partially encapsulated in the PMMA shell and hence as a result few hardener capsules were shrunk and ruptured. Thus, this phenomenon affirms less core content and yield values of hardener microcapsules.

In brief, Table 3.4 indicates the effect of surfactant type on the synthesis of hardener microcapsules. Hardener capsules synthesized with SDS surfactant reported reduced average capsule size, shell thickness and increased core content % than the capsules synthesized with PVA. This phenomenon can be attributed to difference in functioning of surfactant, difference in interfacial tensile force and interactions among surfactant, core material and shell material.

Table 3.4 Effect of surfactant type on the synthesis of hardener microcapsules

Parameter	PVA surfactant	SDS surfactant
Avg. size (µm)	190.60	63.31
Avg. shell thickness (µm)	3.47	1.70
Core content (%)	11.90	28.93
Yield (%)	25.75	22.35
Optimum surfactant wt%	1wt%	5wt%

3.4.2.3 Effect of core to shell ratio on the synthesis of hardener microcapsules

From the section 3.4.2.1, it is noticed that the hardener capsules synthesized at higher c/s (4:1) ratio ensured all the requisite conditions. Since core content is proportional to c/s ratio, effect of lower c/s ratios on the surface morphology of hardener microcapsules were not investigated. Increased rupture and shrinkage hardener capsules were observed with 5:1 c/s ratio.

From the section 3.4.1 and 3.4.2 results, it can be concluded that the hardener capsules synthesized with SDS surfactant have better properties than the capsules synthesized with PVA surfactant and hence it is suggested as an ideal surfactant to synthesize hardener microcapsules. Ratio of oil phase to water phase found to be optimum at 1:7 to 1:9 and solubility of core and shell material is best with DCM solvent. The other optimized process parameters are 40˚C processing temperature, 500 rpm, 4:1 c/s ratio and 5 wt% SDS.

3.4.3 Process parameters optimization of epoxy microcapsules

Similar to hardener microcapsules synthesis, all the process parameters involved in the synthesis of epoxy microcapsules were also investigated for optimized conditions. It was found that epoxy capsules also optimized at 40˚C processing temperature, 5 wt% SDS but at 400 rpm. To avoid the repeatability those results are not discussed here. To study the effect of surfactant type on the synthesis of epoxy capsules both PVA and SDS were investigated and found that PVA didn't help to produce any microcapsules. It instead formed a gel type layer during the synthesis. This phenomenon is attributed to different chemical structure of surfactant, core and shell materials and the reactions among them. Hence in this section only the effect of SDS on the epoxy microcapsules synthesis is discussed.

In order to assess the influence of epoxy resin healing agent viscosity on the encapsulation and self-healing performance, two types of epoxy resins (LY556, CY230) of respective viscosities 10 - 12 Pa.s, 1.3 - 2 Pa.s were chosen and encapsulated in PMMA. All the features of microcapsules were investigated for both LY556 and CY230 epoxy capsules and discussed in this section.

3.4.3.1 Effect of core to shell ratio on the synthesis of epoxy microcapsules

Figure 3.12 shows the surface morphology of LY556 epoxy capsules synthesized at 5 wt% SDS, 40˚C processing temperature and 400 rpm stirring speed. It can be observed from the results that all the microcapsules have spherical shape and agglomeration increased with the increase in c/s ratio. Agglomeration of capsules can be attributed to insufficient surfactant concentration, stirring speeds and faster solvent evaporation rates. For encapsulation of high c/s ratios, due to increased viscosity of organic phase, higher stirring speeds and higher surfactant concentrations were needed. But in this study, surfactant concentration and stirring speeds were kept constant to study the influence of c/s ratio on the capsules encapsulation. Since the microcapsules synthesized at 1:1 c/s ratio satisfied all the required conditions such as un agglomeration, spherical shape and good amount of core content, it is suggested as an optimal condition to synthesize LY556 capsules at the aforesaid process parameters.

CY230 epoxy capsules also synthesized at aforesaid conditions by varying c/s ratios. It can be noticed from the Figure 3.13 that formation of acorn shaped capsules increased with the increase in c/s ratio from 2:1 to 4:1. This phenomenon is due to incomplete encapsulation of healing agent, improper solvent evaporation rates and variation in the shear forces around the

agitator blades. Since capsules with 2:1 c/s ratio satisfied un agglomeration and good amount of yield, core content it is recommended as an ideal ratio to produce CY230 epoxy capsules.

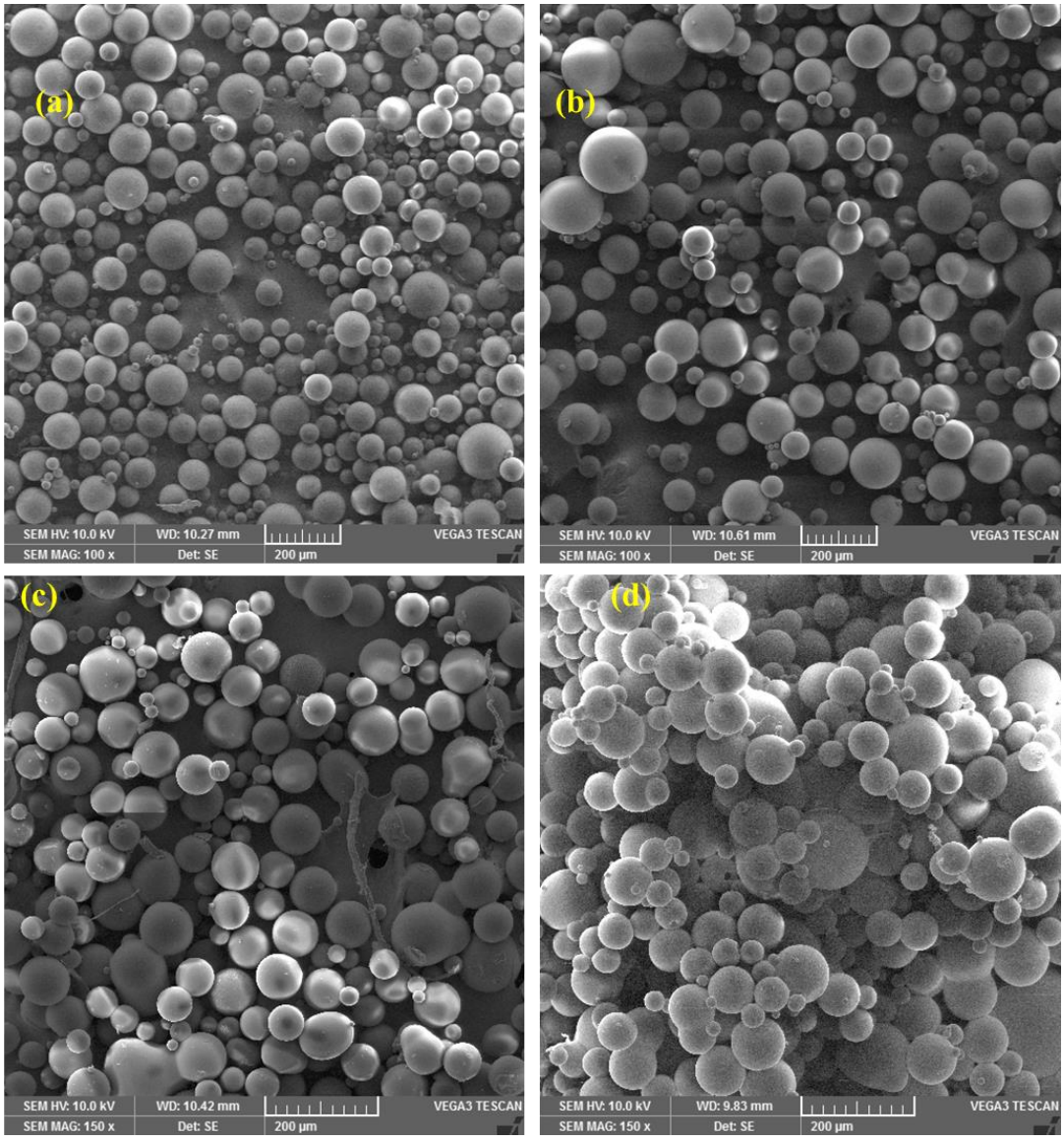

Figure 3.12 Effect of c/s ratio on the morphology of LY556 capsules: (a) 1:1 (b) 2:1 (c) 3:1 (d) 4:1

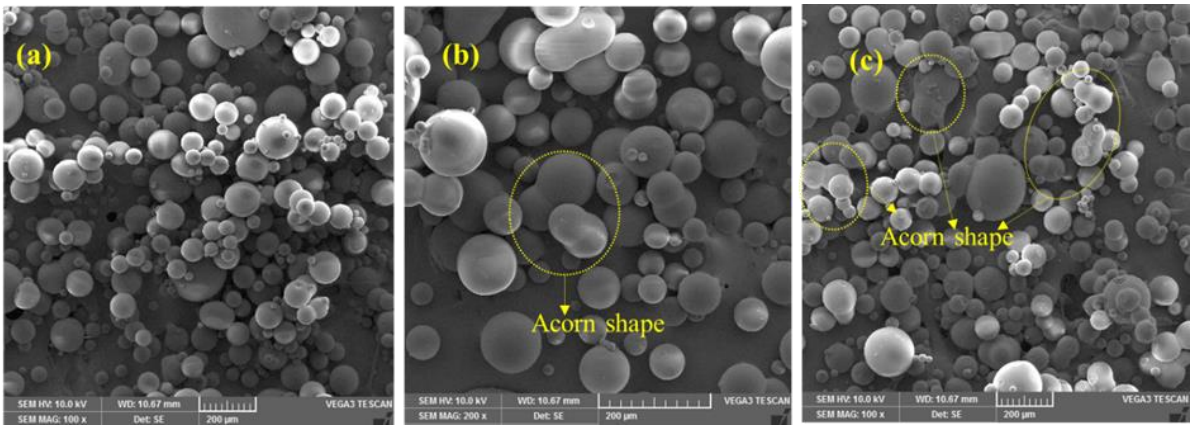

Figure 3.13 Effect of c/s ratio on the morphology of CY230 capsules: (a) 2:1 (b) 3:1 (c) 4:1

3.4.3.2 Surface morphology and size distribution of epoxy microcapsules

Similar surface features and narrow size distributions of microcapsules promote uniform distribution in the self-healing system and thus causes for better healing efficiencies. Figure 3.14 shows the surface morphology of LY556 and CY230 epoxy microcapsules synthesized at optimal conditions. It is observed that two types of epoxy capsules have spherical geometry and good surface morphologies. It can be noticed from the results that few capsules surface is attached with other small capsules. This phenomenon can be attributed to presence of unreacted shell material and wet surface on the capsule. The presence of wet surface even after the drying can be because of improper solvent evaporation. Healing agent leakage from the capsules during handling and filtering also can cause sticking of small capsules to other capsules surface. Compared to LY556 capsules CY230 capsules have more smaller capsules sticked to other capsule surface. This may be due to increased core content or improper solvent evaporation during drying.

LY556 and CY230 epoxy capsules were synthesized in the respective size range of 27 to 112 µm, 27 to 115 µm and average size is measured as 61.58 µm, 67.64 µm respectively. The variation in the size of the capsules can be attributed to variation of fluid flow around the agitator [35]. In the vicinity of the agitator blades due to higher shear forces smaller diameter capsules were formed and around the periphery of the beaker due to comparatively lower shear forces larger diameter capsules were formed. Individually each capsule type had wide range of size distribution but both the capsules have similar size distribution which is the essential criteria to get uniform distribution. The characteristics such as similar surface morphology, same spherical geometry and same size range promote easy rupture of both epoxy, hardener capsules and thereby heals the crack surface by the curing reaction between released healants.

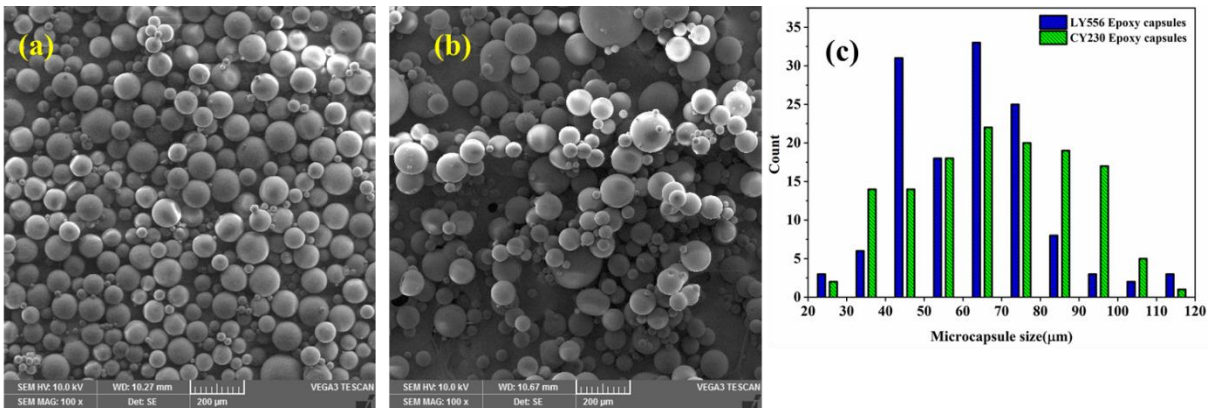

Figure 3.14 Surface morphology of (a) LY556 capsules (b) CY230 capsules (c) size distribution of both LY556 and CY230 epoxy microcapsules

3.4.3.3 Average shell thickness, core content and yield of the epoxy microcapsules

Capsules with lower shell thickness values break easily than the capsules with higher shell thickness and thus helps for enhanced self-healing performance. Figure 3.15 indicates the shell thickness of LY556 and CY230 epoxy capsules. For each capsule type, shell thickness is measured on the minimum of three capsules and the average value is considered for reporting. The average shell thickness of the LY556 and CY230 capsules observed as 2.47 µm and 1.64 µm respectively. It can be observed that both the capsules have similar range of shell thickness and within the acceptable range of shell thicknesses that are reported in the previous studies[117]. The smaller difference in the capsules shell thickness is due to difference in o/w emulsion chemical reactions, difference in c/s ratios and difference in core materials viscosity.

Core content and yield of the microcapsules were calculated as discussed in the section 3.3.2. Table 3.5 shows the core content and yield percentages of both the microcapsules. Even though same temperature and same surfactant type was used to synthesize capsules, the difference in the core content and yield percentages of the capsules can be attributed to difference in c/s ratios, difference in core materials viscosity and balance between shear forces and interfacial tensile forces.

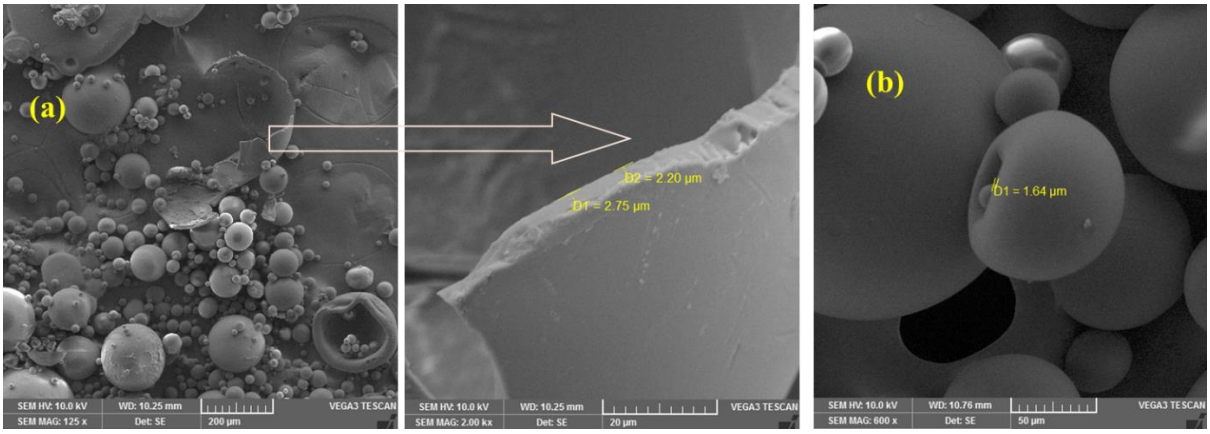

Figure 3.15 Average shell thickness of (a) LY556 epoxy capsules (b) CY230 epoxy capsules

Table 3.5 Average shell thickness, core content and yield of the epoxy microcapsules

Parameter	LY556 capsules	CY230 capsules
Average size (µm)	61.58	67.64
Average shell thickness (µm)	2.47	1.64
Yield (%)	57.85	53.33
Core content (%)	56.64	59.08

3.4.4 Healing agent storage stability analysis of epoxy, hardener capsules

To examine the developed microcapsules healing agent storage stability, three types of capsules were taken and stored at room temperature for a period of three months. Figure 3.16 shows the weight loss % of the LY556, CY230 and HY951 capsules after three months of storage. It is observed that weight loss % increased with the increase in c/s ratio. This phenomenon can be due to thin shell walls and external surface morphologies of developed capsules. Since all the three types of capsules have negligible weight losses, it can be concluded from this study that the developed capsules have at least three months of storage life at room temperature.

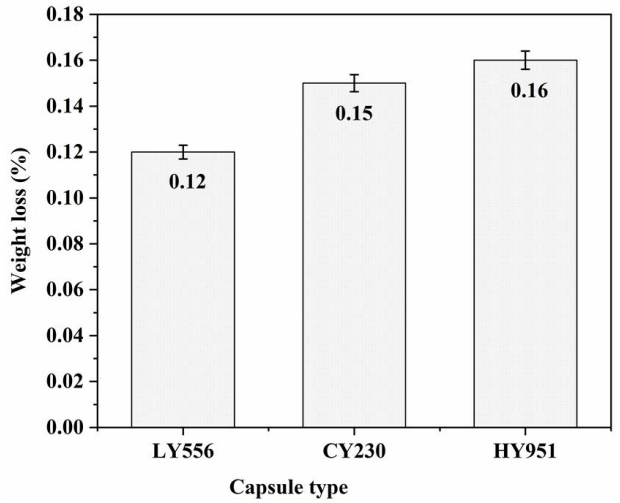

Figure 3.16 Healing agent storage stability of epoxy and hardener microcapsules

3.4.5 Molecular architecture analysis of epoxy and hardener microcapsules

To verify the molecular architecture and functional groups present in the microcapsules FTIR and NMR analyses are used. Both of these techniques verifies the encapsulation of healing agent in the shell material by examining the functional groups present in the capsules.

3.4.5.1 FTIR analysis of epoxy and hardener microcapsules

The chemical structure and functional groups present in the pure PMMA, LY556 capsules, CY230 capsules and pure epoxy resin liquid were examined with FTIR spectrometer and shown in Figure 3.17. The different functional groups present in the respective materials can be identified by the presence of peak at corresponding wavenumber. The absorption bands at 2945 cm^{-1} and 2845 cm^{-1} show the -CH_2 asymmetric and symmetric stretching vibrations of pure PMMA. The strong peak at 1732 cm^{-1} represents the presence of C=O_{str} vibration. Table 3.6 indicates the functional groups present in the LY556 capsules and CY230 capsules. It can be noticed from Figure 3.17 and Table 3.6 that both shell material and pure epoxy liquid

functional groups were present in both types of epoxy capsules. Thus, this study confirms the encapsulation of epoxy resin in both LY556 capsules and CY230 capsules.

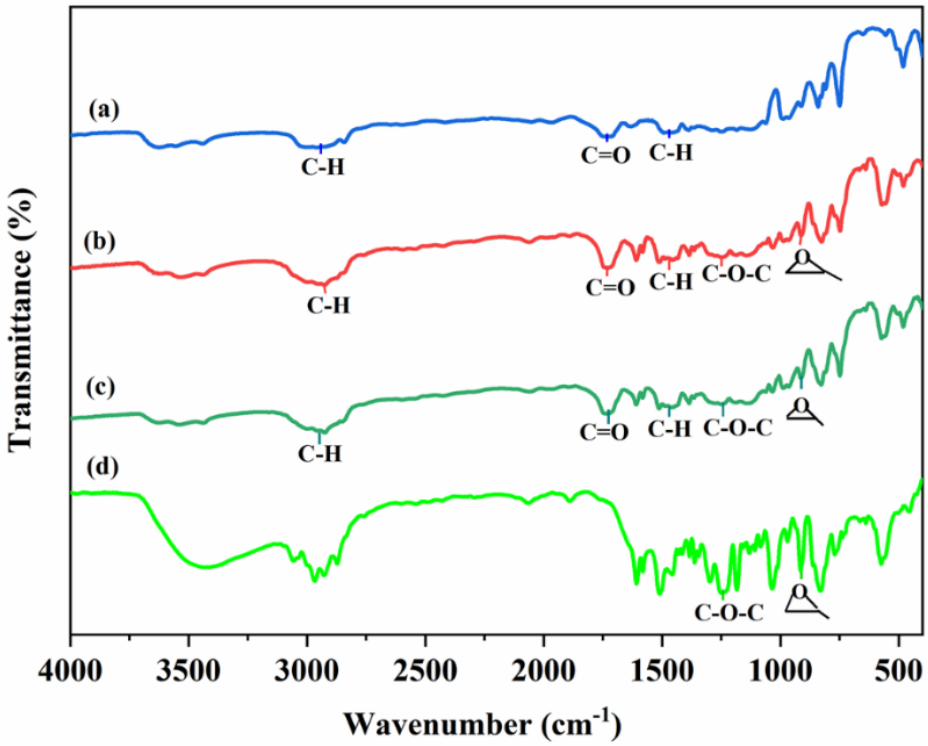

Figure 3.17 FTIR spectrum of (a) pure PMMA (b) LY556 microcapsules (c) CY230 microcapsules (d) pure epoxy liquid

Table 3.6 Functional groups present in the LY556 and CY230 epoxy microcapsules

Wavenumber (cm^{-1})	**Peak**	**Intensity**
2945	$-CH_2$ asymmetric ($C-H_{str}$) vibration of alkane group	medium
2845	$-CH_2$ symmetric ($C-H_{str}$) vibration of alkane group	medium
1732	$C=O_{str}$ vibration	strong
1475	$C-H_{bend}$ vibration of methyl group	medium
1388	$-CH_3$ bending vibration of alkane group	medium
1186	$C-O_{str}$ vibration of ether group	strong
1243	$C-O-C_{str}$ vibration of ether group	strong
914	epoxide ring, $C=O_{str}$ and $-CH_2$ asymmetric, symmetric stretching vibrations	strong

The functional groups present in the pure amine hardener liquid and HY951 hardener capsules were shown in Figure 3.18. The major absorption peaks seen in the hardener capsules

were indicated in Table 3.7. Since FTIR spectrum of hardener capsule contain all the peaks of hardener liquid and PMMA, it is confirmed that the amine hardener is successfully encapsulated in HY951 capsules.

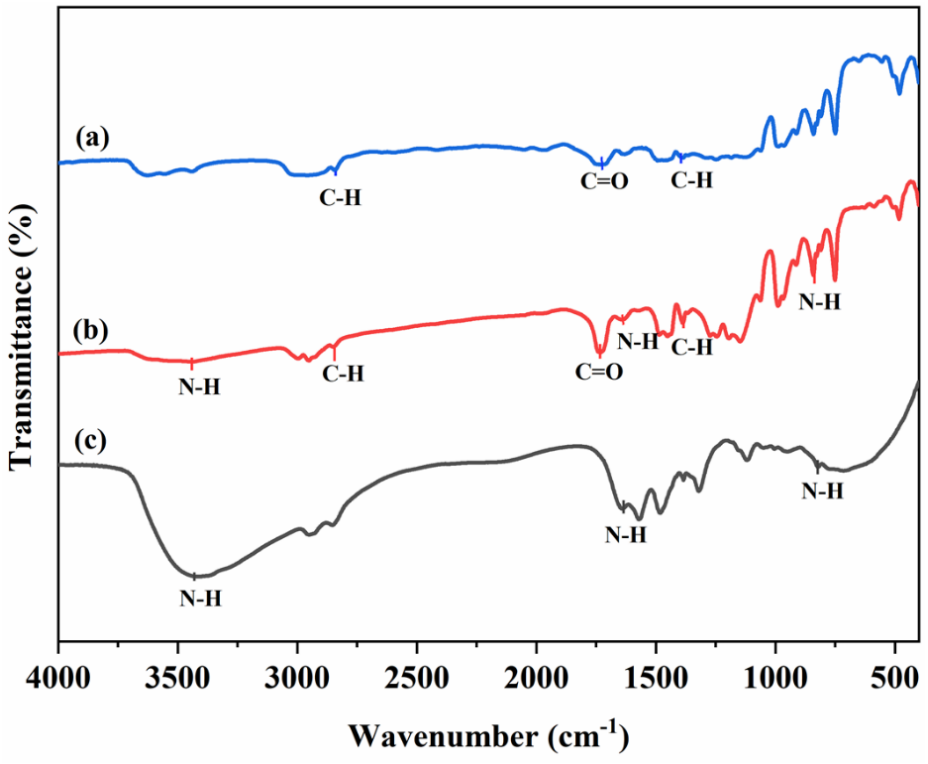

Figure 3.18 FTIR spectrum of (a) pure PMMA (b) HY951 capsules (c) amine hardener liquid

Table 3.7 Functional groups present in the HY951 hardener microcapsules

Wavenumber (cm^{-1})	**Peak**	**Intensity**
2845	$-CH_2$ symmetric stretching vibration of alkane group	medium
1732	$C=O_{str}$ vibration	strong
1475	$C-H_{bend}$ vibration of methyl group	medium
1186	$C-O_{str}$ vibration of ether group	strong
3432	$N-H_{str}$ vibration of primary amine	medium
1632	$N-H_{bend}$ vibration of primary amine	medium
842	$N-H_{bend}$ vibration of primary amine	Strong

3.4.5.2 ^{1}H NMR analysis of epoxy and hardener microcapsules

In order to cross verify the encapsulation of LY556 epoxy,CY230 epoxy and HY951 hardener in the PMMA shell ^{1}H NMR analysis was done and the spectrum was shown in Figure 3.19. Approximate chemical shifts and corresponding type of proton observed in the epoxy capsules and hardener capsules were shown in Table 3.8 and Table 3.9 respectively. All the key peaks related to core and shell material were detected in the epoxy capsules, hardener capsules and thus this study confirms the successful encapsulation of epoxy, hardener in the PMMA.

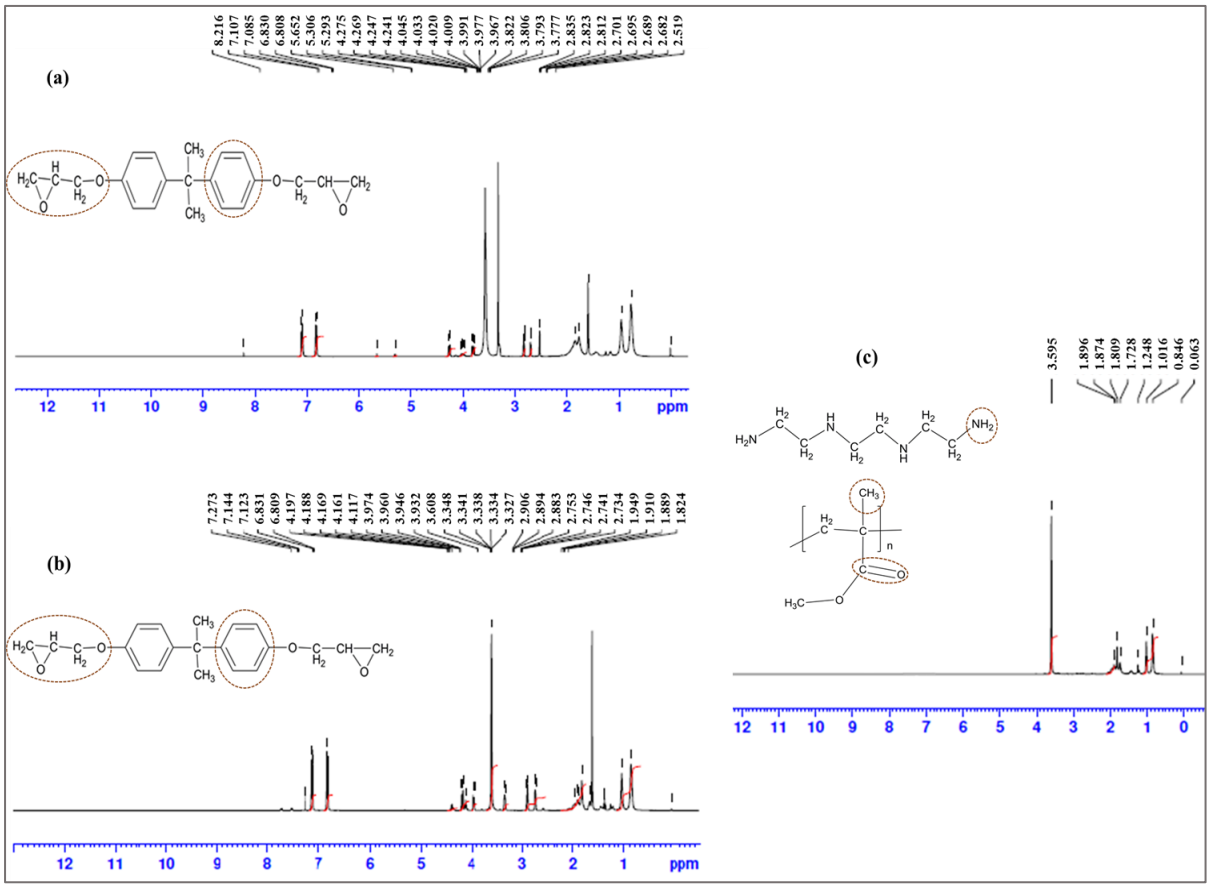

Figure 3.19 ^{1}H NMR analysis of (a) LY556 epoxy capsules (b) CY230 epoxy capsules (c) HY951 hardener microcapsules

Table 3.8 ^{1}H NMR analysis of LY556 and CY230 epoxy microcapsules

Approximate chemical shift(ppm)	Type of proton
0.8-1.0	methyl group of PMMA
1.8-1.9	protons present next to C=C
2.5-2.8	carbonyl group of PMMA
3.3-4.2	ether group of epoxy resin
5.2-5.7	internal alkene group of epoxy resin
6.8-8.2	benzene ring protons of epoxy resin

Table 3.9 ^{1}H NMR analysis of HY951 hardener capsules

Approximate chemical shift(ppm)	Type of proton
0.84,1.01	methyl group of PMMA
1.24	methylene group proton
1.72,1.80,1.87,1.89	amine group protons of hardener
3.59	amine group proton

3.4.6 Thermal stability analysis of epoxy and hardener microcapsules

Typical TGA and DTA curves of epoxy and hardener microcapsules are shown in Figure 3.20. It can be noticed that pristine PMMA has two step decomposition pattern and both epoxy, hardener microcapsules have three step decomposition patterns. As explained in the Table 3.10, for PMMA, the first step decomposition is observed from room temperature (RT) to 220˚C and can be ascribed to removal of residual water. The second step decomposition which is due to degradation of PMMA is observed in the range of 220˚C to 410˚C.

For HY951 hardener microcapsules, 5.61% weight loss is observed in the range of 140˚C - 220˚C which corresponds to loss of residual water content and hardener present in the microcapsules. The second step decomposition occurred in between 220°C - 330˚C due to deprivation of PMMA and hardener. The weight loss that occurred in the range of 330°C - 440˚C is due to deprivation of PMMA alone.

The first step decomposition of LY556 epoxy microcapsules is noticed in the temperature range of 220˚C - 330˚C and can be attributed to degradation of shell material. The second step and third step decompositions are observed in the temperature range of 330˚C - 420˚C, 420˚C - 480˚C which can be ascribed to degradation of PMMA and epoxy, degradation of epoxy in the capsules respectively. Similarly, for CY230 capsules also the first step decay is due to deprivation of PMMA. The second and third steps are due to deprivation of PMMA and epoxy resin, epoxy core material respectively. The degradation occurred in hardener capsules from RT to 140˚C and in epoxy capsules from RT to 220˚C can be attributed to removal of moisture content present on the surface of microcapsules. Neat hardener and neat epoxy had single step decomposition patterns in 95˚C - 240˚C and 270˚C - 450˚C temperature ranges respectively [118].

It can be observed from Table 3.10 that the healing agents decomposition temperature shifted slightly higher than neat healing agents decomposition temperature. Hence from this study it can be confirmed that amine hardener and epoxy were successfully encapsulated in

PMMA. It is also observed from the TGA analysis of capsules that at temperatures > 400˚C, LY556 epoxy capsules have greater thermal stability than both CY230 and HY951 hardener capsules. The increasing thermal stability order of the capsules can be noted as LY556 > CY230 > HY951. This stability order can be ascribed to existence of more thermally stable networks in the epoxy healing agent.

Table 3.10 TGA analysis of epoxy, hardener encapsulated PMMA capsules

Material	Step	Start Temperature (°C)	End Temperature (°C)	weight loss (%)
PMMA	I	27	220	5.66
	II	220	410	91.47
Hardener capsules	I	140	220	5.61
	II	220	330	13.63
	III	330	440	78.62
LY556 capsules	I	220	330	17.68
	II	330	420	75.24
	III	420	480	4.03
CY230 capsules	I	200	320	20.15
	II	320	420	72.50
	III	420	500	4.26

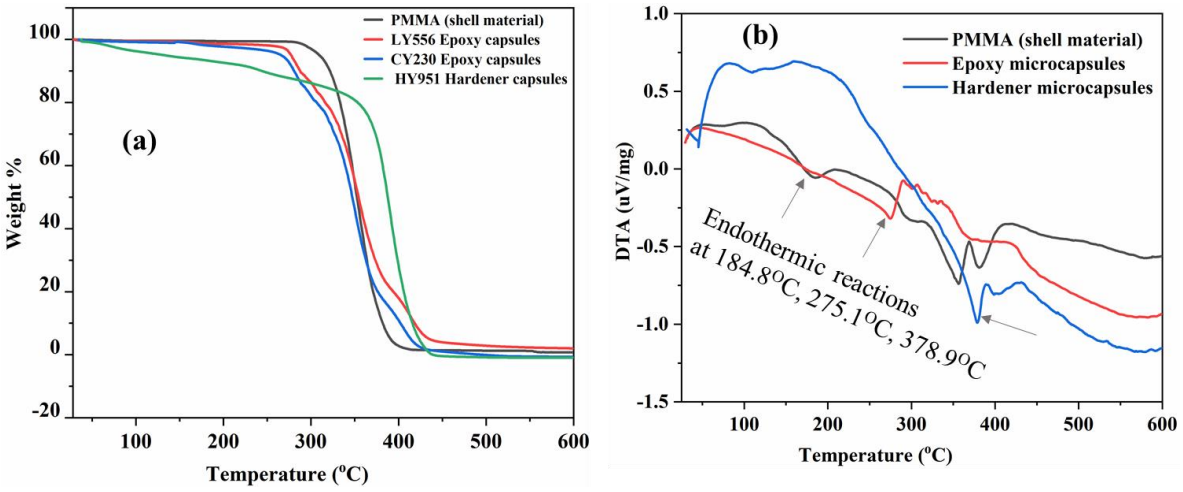

Figure 3.20 (a) TGA (b) DTA curves of PMMA, epoxy and hardener microcapsules

Three major endothermic reactions can be noticed in the Figure 3.20(b) at 184.8˚C, 275.1˚C and 378.9˚C for PMMA, LY556 epoxy microcapsules and HY951 hardener

microcapsules respectively. These endothermic reactions are due to melting of PMMA in corresponding materials at respective temperatures. This phenomenon is in accord with the earlier discussed TGA results of PMMA and micro capsules. Hence, from this study the degradation temperatures of PMMA in epoxy and hardener microcapsules can be evaluated.

3.5 conclusions

Two types of epoxy resins (LY556, CY230) and HY951 amine hardener encapsulated PMMA microcapsules were synthesized using solvent evaporation method and investigated for process parameters optimization. The effect of PVA and SDS surfactants and their concentration on the surface morphology, core content, yield, size distribution and shell thickness are investigated. The following conclusions can be drawn from the present study.

- Effect of processing temperature on the synthesis of microcapsules was investigated and 40˚C is suggested as an ideal temperature for processing.
- HY951 amine hardener encapsulated PMMA microcapsules were synthesized with both PVA and SDS surfactants and found that most of the capsules were spherical in shape with rough surface morphologies.
- HY951 hardener capsules synthesized with SDS surfactant have better properties than the capsules synthesized with PVA surfactant and hence SDS surfactant is suggested as an ideal surfactant to synthesize hardener microcapsules.
- Synthesis of epoxy resin microcapsules were investigated with both PVA and SDS surfactants and found that PVA didn't help to produce microcapsules. SDS surfactant produced most intact and good surface morphology microcapsules.
- The shell thickness of both epoxy resins and amine hardener capsules are within the optimal range and thus can have direct application as self-healing materials.
- Average capsule size, core content and yield percentages of microcapsules were slightly influenced by surfactant type, concentration and found to be optimal with 5 wt% SDS surfactant for both types of epoxy resin and amine hardener microcapsules.
- Effect of agitator and agitation speed on the average capsule size were investigated and found to be optimum at 400 rpm, 500 rpm with overhead mechanical stirrer for epoxy resin microcapsules and amine hardener microcapsules respectively.

- Optimized process parameters to synthesize amine hardener microcapsules are 40˚C processing temperature, 4:1 core to shell ratio, 500 rpm, ratio of oil phase to water phase in between 1:7 to 1:9 and 5 wt% SDS surfactant concentration.
- Optimized process parameters to synthesize epoxy resin microcapsules are 40˚C processing temperature, 400 rpm, 5 wt% SDS surfactant concentration and 1:1 core to shell ratio for LY556 capsules and 2:1 for CY230 capsules.
- The average capsule size of the LY556 epoxy, CY230 epoxy and HY951 hardener microcapsules synthesized at optimum conditions were measured as 61.58 µm, 67.64 µm and 63.31 µm respectively.
- SEM, FTIR, ^{1}H NMR and TGA analyses confirmed the successful encapsulation of LY556 epoxy resin, CY230 epoxy resin and HY951 hardener in the PMMA.
- TGA analysis of pure PMMA demonstrated two step thermal degradation pattern and all three types of capsules demonstrated three step degradation patterns.

Chapter 4

Self-healing performance and mechanical behavior of capsules reinforced thermosetting polymer

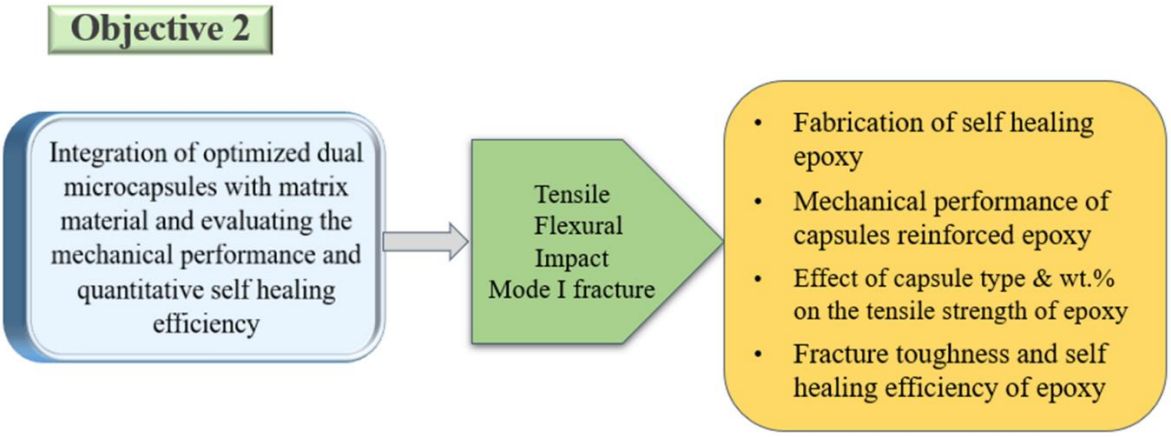

This chapter discusses the effect of microcapsules addition on the tensile, flexural and Charpy impact strength of pure epoxy. Effect of capsule type and their concentration on the self-healing performance of capsules reinforced epoxy are presented.

4.1 Introduction

Thermosetting polymers such as epoxy resins have been widely employed in polymer composites, coatings and adhesives due to their better mechanical and adhesive properties. Epoxy resins have other advantages such as low shrinkage during curing, adjustable curing range, better resistance to chemicals and solvents, good electrical properties, high strength and better adhesion between fibres and matrix. Despite having many structural properties, epoxy resins usage is restricted in the few fields due to their brittleness and sensitivity to micro cracking [119]. Various studies [120–122] have been conducted on the epoxy resins to improve their flexibility and fracture toughness by inserting the thermoplastic fillers, rubber particles and modifying the monomer with the additives. However, during service conditions, the microcracks developed in the structure propagates further and thus leads to catastrophic failure of the component. In order to address such issues and re-establish the structural integrity of micro and nano cracked polymer composites, few authors [62,74,123] suggested the use of self-healing materials technology.

These self-healing polymers offer crack independent autonomic repair strategies and thus extends the service life and reliability of the components. Self-healing of polymeric materials can be achieved through two approaches namely extrinsic and intrinsic. One of the extrinsic approaches i.e., capsule based self-healing system repairs the micro cracks without human intervention by employing the microcapsules containing healing agents into the base material. Based on the type of capsules and number of components used in the system, these capsule based systems are classified as catalyst-capsule, single component containing solvent capsules and dual component capsules self-healing system.

The self-healing performance of the both catalyst-capsule system and single component solvent capsules system depend on the functionality and reactivity of the polymer matrix. In the catalyst-capsule system polymerization of the crack surface occurs by the chemical reaction between released healing agent and the catalyst. But the catalyst reactivity decreases when exposed to oxygen and moisture ambience and cannot be used at higher temperatures. Whereas in single component capsule system, polymerization depends on the reactivity of hardener premixed with polymer matrix. To overcome these limitations and to take advantage of matrix

functionality independent healing strategy many authors [124–126] suggested dual component microcapsules self-healing system. This system also offers minimal change in host polymer matrix inherent properties.

In dual component capsules system, one component consists of polymerizable monomer capsules and the other component consists of corresponding curing agent capsules and healing occurs by the curing reaction between the released healing agents. The major challenge in the dual component capsules system is to find and encapsulate curing agent corresponding to polymerizable component. Epoxy resin/amine hardener and epoxy resin/mercaptan are the most commonly used dual capsules component systems. Jin et al. [63] developed epoxy monomer, aliphatic polyamine encapsulated urea formaldehyde microcapsules and incorporated them into polymer matrix to investigate the self-healing performance. Healing efficiency was evaluated based on the mode I fracture toughness recovery and achieved 91% of healing efficiency with 7 wt% amine capsules and 10.5 wt% epoxy capsules.

Yuan et al. [125] investigated the factors influencing the self-healing performance of epoxy composite by employing epoxy/mercaptan capsules system. High activity of mercaptan and low viscosity of epoxy influences the healing rate and healing efficiency. It was noticed that the healing efficiency increases with the increase in capsules concentration and found full recovery of damage at 20 wt% capsules combination. They suggested an optimal capsules weight ratio of 1 - 1.25 to achieve better healing efficiencies.

In order to have structural applications, it is important to understand the effect of microcapsules addition on the mechanical properties of epoxy matrix. Qi Li et al. [64] investigated the effect of epoxy resin and polyetheramine capsules addition into epoxy composite and reported that the addition of capsules up to 5 wt% increased the tensile strength and later decreased with the increase in capsules concentration till 20 wt%. Good interfacial bonding between microcapsules and host polymer matrix improves the self-healing performance and reduces the percentage reduction in mechanical properties [90]. Zhang et al.[126] investigated the self-healing of epoxy matrix by reinforcing the epoxy-amine micro containers and achieved highest healing efficiency of 62% for a healing time of 24 hrs at 50˚C with 12 - 15 wt% microcapsules. They reported that the addition of capsules to pure epoxy increases the fracture toughness, decreases the tensile strength and tensile modulus.

In the present study epoxy resin, amine hardener encapsulated PMMA microcapsules and dual component capsules system were employed to evaluate the effect of capsules addition on the tensile, flexural and impact strength of epoxy matrix. The effect of epoxy resin healing agent viscosity on the mechanical performance and self-healing efficiency is studied by employing the combination of different epoxy microcapsules and same hardener microcapsules in the base polymer matrix.

4.2 Materials and Methods

Different types of microcapsules used to fabricate the capsules reinforced epoxy composite and the method of fabrication are discussed in this section.

4.2.1. Materials

As discussed in the chapter 3, two types of epoxy resins (LY556, CY230) of respective viscosities 10 - 12 Pa.s, 1.3 - 2 Pa.s and amine hardener (HY951) of viscosity 0.01 - 0.02 Pa.s were chosen as healing agents and encapsulated in a thermoplastic PMMA shell.

LY556 microcapsules synthesized at 400 rpm, 1:1 c/s ratio, 40˚C processing temperature, 5 wt% SDS surfactant and CY230 microcapsules synthesized at 400 rpm, 2:1 c/s ratio, 40˚C processing temperature, 5 wt% SDS surfactant were chosen as epoxy microcapsules. HY951 microcapsules synthesized at 500 rpm, 4:1 c/s ratio, 40˚C processing temperature, 5 wt% SDS surfactant were chosen as hardener microcapsules.

Epoxy resin/amine hardener microcapsules dual component self-healing system is chosen to investigate the mechanical and self-healing performance of the epoxy composite. LY556 epoxy and CY230 epoxy microcapsules with respective average diameter of 61.58 µm, 67.64 µm and HY951 hardener microcapsules with average diameter of 63.31 µm were used in this study. LY556 epoxy resin and HY951 amine hardener were also used to fabricate base epoxy composite.

4.2.2 Fabrication of dual capsules reinforced self-healing epoxy composite

In order to fabricate epoxy based self-healing system, initially base material's (LY556) viscosity was reduced by heating at 60˚C for 15 minutes using hot plate. This reduction in viscosity causes agitator shear forces to overcome viscous forces and thus helps in proper distribution of microcapsules in the base material. Required amount of each microcapsule type was calculated by considering an optimum weight ratio of 1:1 epoxy resin, amine hardener microcapsules. Then, both epoxy and hardener microcapsules were weighed precisely using

Aczet CG203L weighing balance and added to viscosity reduced epoxy matrix in 2.5, 5, 7.5 and 10 wt% of specimen weight. Later, the mix was rotated using Remi 1 MLH magnetic stirrer at 400 rpm for 20 min to ensure both the microcapsules were uniformly distributed in the epoxy matrix. Afterwards, dual capsules reinforced epoxy resin was allowed to degas at 250 mm of Hg for 5 min using vacuum desiccator to remove entrapped air bubbles. Rotary vane vacuum pump of ¼ HP power and 1.5 CFM flow rate was used in the desiccator setup. Then, to the above mix stoichiometric amount (10 wt% of epoxy) of hardener was added and again rotated for 5 min using magnetic stirrer. Thereafter the final mix was once again allowed to degas at room temperature for 3 min and poured in to the silicon rubber moulds to get desired specimens. Both (LY556+HY951) capsules and (CY230+HY951) capsules incorporated self healing epoxy composites were fabricated by following above said procedure. Figure 4.1 indicates schematic representation of fabrication of dual capsules reinforced self-healing epoxy

Pure epoxy specimens i.e specimens without addition of any microcapsules were fabricated by mixing 100 parts of LY556, 12 parts of HY951 and degassing it for 5 min. Both self healing and pure epoxy specimens were cured at room temperature for 24 hrs.Tensile specimen, flexural specimen, Charpy impact specimen and TDCB specimens (mode I fracture test specimens) were fabricated as per ASTM D638 Type V, ASTM D790 and ASTM D6110 and ISO 25217 respectively. Figure 4.2 indicates dimensions (in mm) of tensile, flexural and Charpy impact specimens used in the present study.

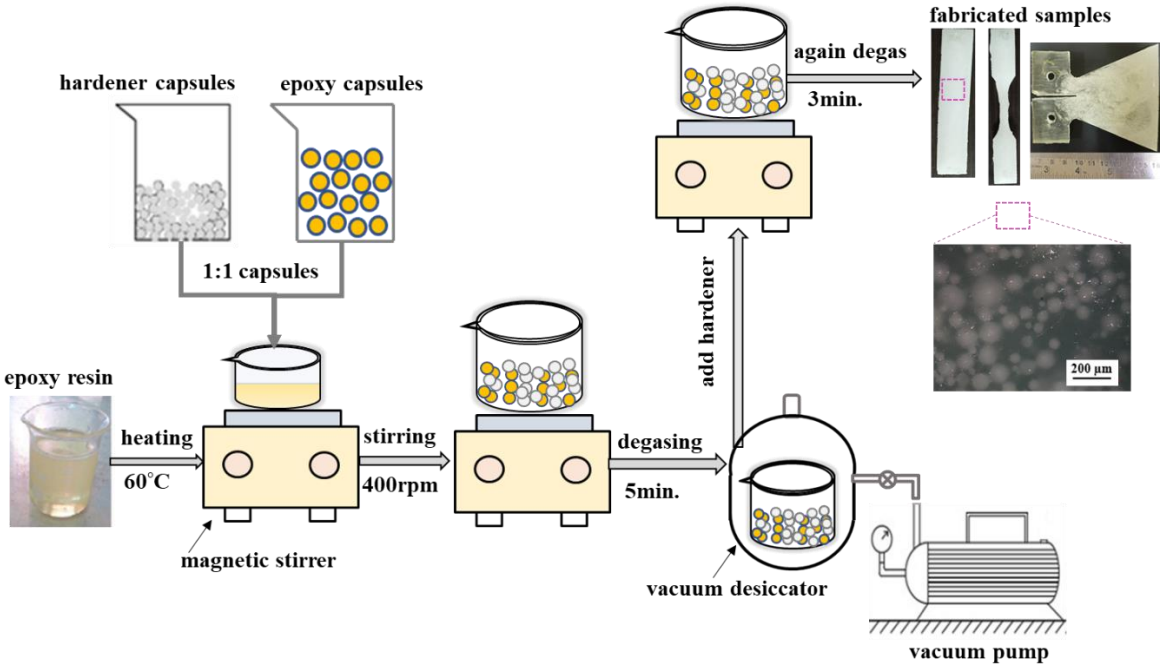

Figure 4.1 Schematic representation of fabrication of dual capsules reinforced self-healing epoxy composite

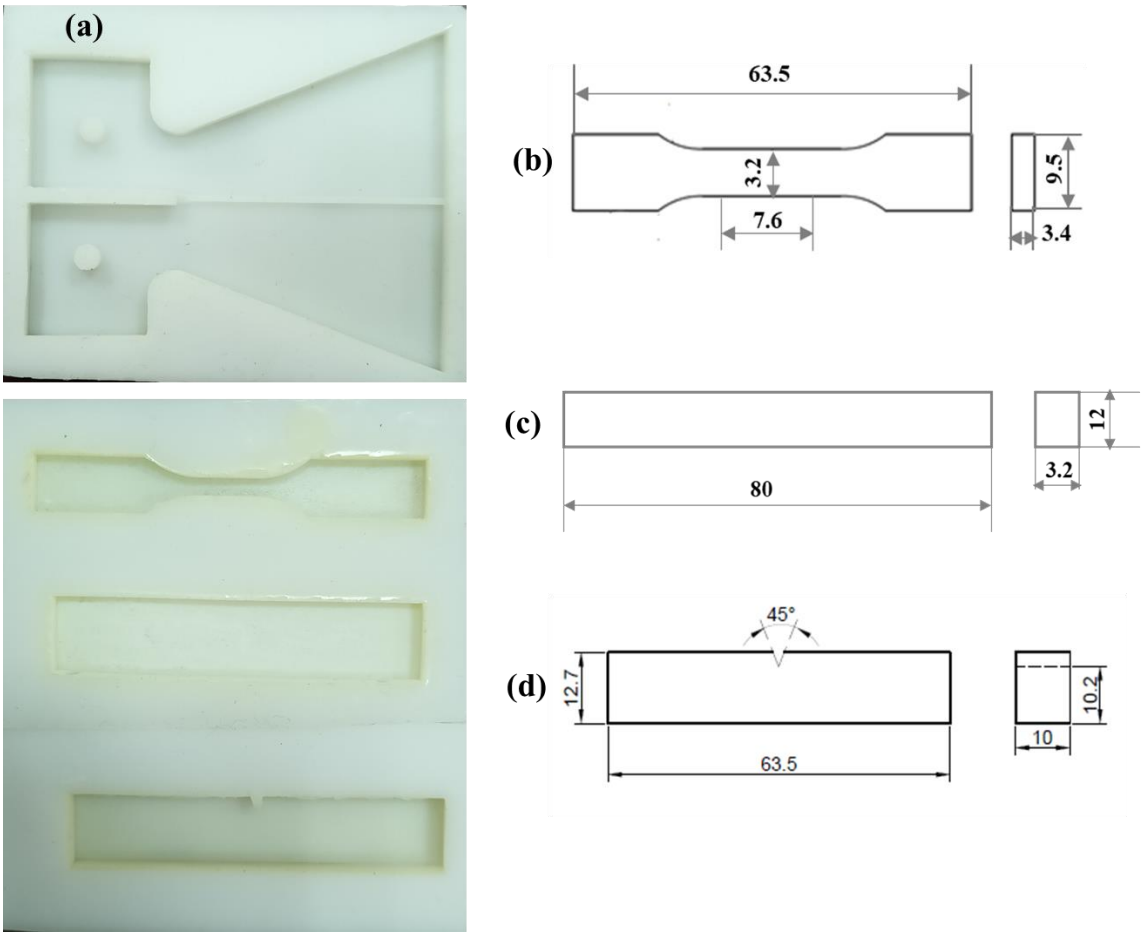

Figure 4.2 (a) TDCB, tensile, flexural and impact silicon rubber moulds used in the study Dimensions of (b) tensile specimen (c) flexural specimen and (d) Charpy impact specimen

4.2.3 Calculations of amount of capsules required

The amount of microcapsules mass required to fabricate each specimen is calculated using rule of mixture of composites. According to rule of mixure, volume of the composite is equals to the summation of volume of the filler materials and volume of matrix material.

By considering full volume of the composite is filled only with base epoxy i.e. LY556, then

Volume of the flexural specimen = 80 X 12 X 3.2 = 3072 mm^3 = 3.072 cc

Mass of the flexural specimen matrix = 1.16 X 3.072 = 3.563 g (epoxy density = 1.16 g/cc)

Mass of the epoxy = 0.91 X 3.563 = 3.242 g

Mass of the hardener = 0.09 X 3.563 = 0.320 g

For 2.5 wt% of capsules, mass of capsules = (2.5/100) X 3.242 = 0.081 g

By considering 1:1 capsules weight ratio, required mass of each capsule = 0.081/2 = 0.0405 g

Required mass of each capsule type for other specimens also calculated by following the above said procedure and can be found in the Table 4.1.

Table 4.1 Required mass of each capsule to fabricate self-healing epoxy composites

Capsules wt%	Required mass of each capsule (g)			
	Tensile specimen	Flexural specimen	Charpy specimen	TDCB specimen
2.5	0.031	0.040	0.091	0.275
5	0.062	0.081	0.183	0.550
7.5	0.093	0.121	0.274	0.825
10	0.124	0.161	0.366	1.100

4.3 Mechanical behavior and self-healing characterization

This section deals with the characterization techniques used to evaluate the effect of microcapsules concentration on the mechanical properties and self-healing performance of the epoxy matrix. The self-healing performance of the epoxy system evaluated both qualitatively and quantitatively using optical 3D microscope and mode I fracture test using TDCB specimen respectively.

4.3.1 Mechanical behavior characterization

To study the mechanical behaviour of capsules incorporated self-healing epoxy composites and pure epoxy specimens, tensile test was conducted by employing Advance Equipments (AE) 30kN universal testing machine (UTM) at a crosshead speed of 0.5 mm/min and 1 kN load cell. Two different self-healing systems i.e., (LY556+HY951) capsules, (CY230+HY951) capsules reinforced composite systems were evaluated in terms of tensile strength, tensile modulus and compared for mechanical performance. For each result, three indistinguishable samples were tested and the average value was considered for reporting.

Flexural strength of the capsules reinforced epoxy composite was evaluated by using AE30kN UTM three point bend flexural setup. 1 kN load cell, 56 mm span and 0.5 mm/min crosshead speed were applied during the testing. For each result, three identical samples were tested and the average value considered for reporting. Flexural strength of the specimen calculated according to Eq. 4.1.

$$Flexural \quad Strength = \frac{3PL}{2bd^2} \qquad \text{Eq.4.1}$$

Where P- applied load in N; L- span distance between two supports in mm; b- width of the specimen in mm and d- thickness of the specimen in mm.

Impact strength of the composite was evaluated by employing Charpy impact test equipment (Make: EIE Instruments Pvt. Ltd, India) of 300 J capacity and according to Eq. 4.2. For each result, three identical samples were tested and the average value considered for plotting.

$$impact\ Strength = \frac{impact\ energy}{(width - notch\ depth)\ X\ Thickness} \qquad \text{Eq. 4.2}$$

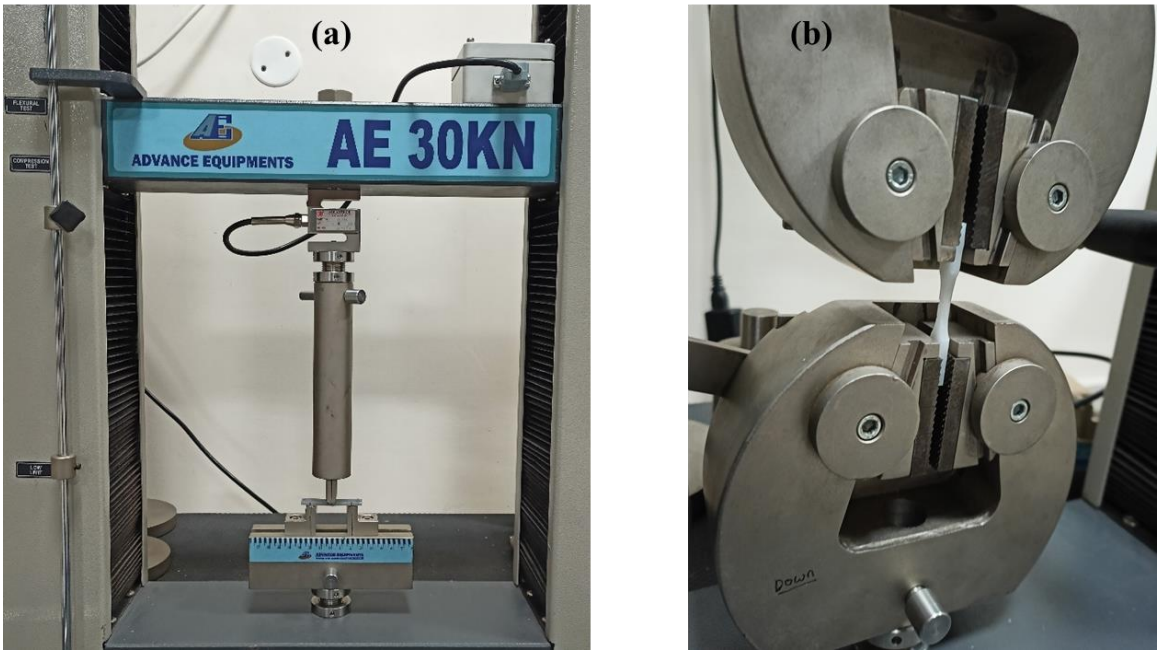

Figure 4.3 (a) AE30kN UTM flexural specimen holder (b) Tensile specimen sample holder

4.3.2 Assessment of self-healing performance

Qualitative and quantitative methods used to investigate the self-healing performance of epoxy system are discussed in this section.

4.3.2.1 Qualitative self-healing performance assessment

A qualitative study on the self-healing capability of the microcapsules integrated composite specimen was conducted using Huvitz 3D optical microscope. To study the self-healing behaviour of the specimen, an artificial pre crack was created by tapping with sterile surgical blade. In this state, the cracked surfaces were kept in contact with each other and allowed to self-heal at room temperature for a healing time of 24 hrs. Later, the healed specimen was

examined under the microscope to confirm the ruptured microcapsules and released healing agents. Figure 4.4(a) shows the 3D optical microscope used in the study.

Figure 4.4 (a) Huvitz 3D optical microscope (b) TDCB specimen during mode I fracture test

4.3.2.2 Quantitative self-healing performance assessment

In order to assess the self-healing performance of dual capsules impregnated epoxy composite, (LY556+HY951) capsules reinforced, (CY230+HY951) capsules reinforced TDCB specimens were prepared and assessed for fracture toughness according to the procedure reported by White et al. [29]. TDCB specimen was fabricated with rectangular central groove and 45˚ side grooves to ensure crack growth along the centre line of the specimen. As shown in Figure 4.4(b), the capsules were incorporated in the middle rectangular portion of the TDCB specimen. In order to find the fracture toughness of the virgin sample (i.e., a sample without any prior damage) pre crack was created at the end of the central groove and then tested for failure using AE 30kN UTM at a load cell of 1 kN and crosshead speed of 0.5 mm/min. To calculate the fracture toughness of healed samples, capsules reinforced TDCB specimens were loaded and tested till the crack propagates to 20 - 40 mm as shown in Figure 4.5(a). Since critical load and fracture toughness are independent of crack length within 20 - 40 mm of crack length [127,128], after reaching that crack length range, cracked samples were unloaded and kept in the TDCB silicon moulds for 24 hrs to self-heal at RT. Finally, the healed samples were again tested under same loading conditions till failure and assessed for self-healing efficiency. For each result, three indistinguishable samples were tested and an average value was considered for reporting.

Self-healing efficiency (η) is defined as the fracture toughness (K_{IC}) ratio of healed sample to virgin sample [129]. It can be determined using Eq. 4.3.

$$\eta = \frac{K_{IC}healed}{K_{IC}Virgin} = \frac{P_C healed}{P_C Virgin} \qquad \text{Eq.4.3}$$

Where P_C is critical fracture load in N

As suggested by Brown et al. [127], crack length independent fracture toughness can be calculated using Eq. 4.4.

$$K_{IC} = 2\,P_C \frac{\sqrt{m}}{\beta} \qquad \text{Eq. 4.4}$$

Where m, β are geometric terms of TDCB geometry

Eq. 4.4 can be modified as $K_{IC} = \sqrt{G_{IC}\,E} = 2\,P_C\sqrt{\frac{m}{b_n\,b}} = \alpha\,P_C$ Eq.4.5

Where b_n, b are the crack width and specimen width respectively, G_{IC} is strain energy release rate, E is Young's modulus of the epoxy and is a constant.

For the Figure 4.5(a) TDCB geometry, b and b_n values are 6.25, 2.5 mm respectively. The value of m depends on the crack length (a), specimen height (h(a)) and as investigated by Brown et al. [130], the value of β and m can be defined as

$$\begin{aligned} \beta &= b^{0.61}\,b_n^{\,0.39} \\ m &= 0.6\ mm^{-1} \\ \alpha &= 11.2\times10^{3}\,m^{-3/2} \end{aligned} \qquad \text{Eq. 4.6}$$

Thus, substituting all the values in the Eq. 4.5, the fracture toughness can be evaluated as

$$K_{IC} = 11.2\times10^{-3}\,P_C \quad MPam^{1/2} \qquad \text{Eq.4.7}$$

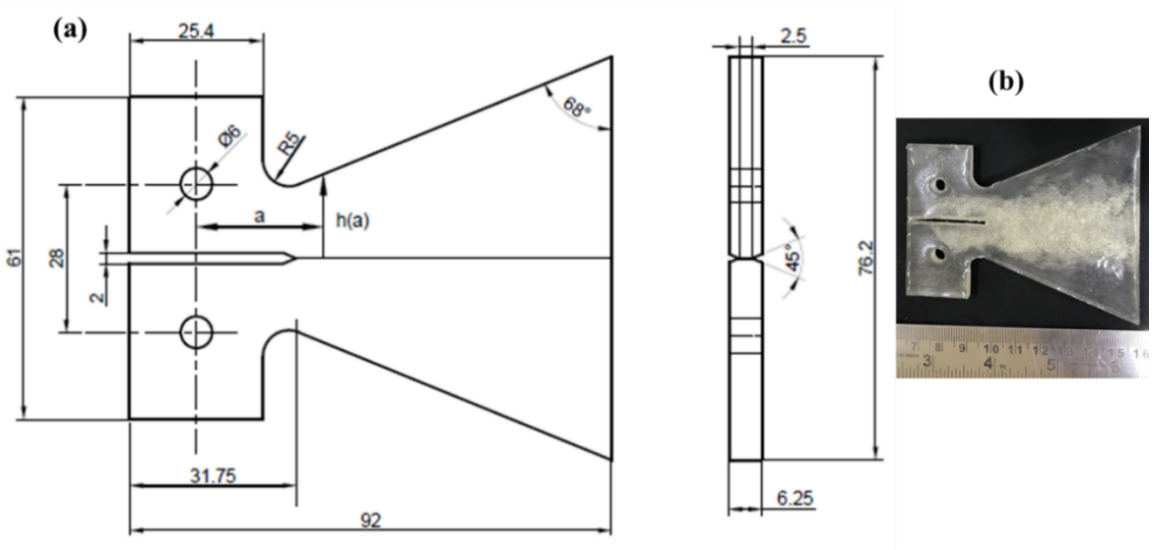

Figure 4.5 (a) Geometric dimensions of TDCB specimen in mm (b) Dual capsules reinforced TDCB epoxy specimen

4.4 Results and Discussion

Effect of capsule type and their concentration on the mechanical properties and self-healing performance of capsules reinforced epoxy are discussed in this section.

4.4.1 Thermal analysis of dual capsules reinforced self-healing epoxy

Thermal analysis of the capsules reinforced epoxy composite was done to understand the effect of capsules addition on the curing temperature of pure epoxy and to study the thermal stability of composite at the elevated temperatures. For this purpose, TG-DTA analysis was conducted on the pure epoxy and dual capsules incorporated epoxy composite. Figure 4.6 shows the TGA and DTA curves of different wt% (LY556+HY951) capsules reinforced epoxy composite. It is observed from the TGA results that the addition of capsules slightly affected the thermal stability of pure epoxy and found to decrease with the increase in capsules wt%. For a weight loss of 100 to 97 %, the thermal stability of pure epoxy decreased from 280˚C to 160˚C with an addition of 5 wt% epoxy and hardener microcapsules. This phenomenon can be due to presence of moisture content or due to more number of hollow capsules. But other wt% capsules reinforced composite have less weight loss compared to 5 wt% capsules reinforced epoxy. Hence from this study it can be suggested that the capsules reinforced composites can have applications till 200˚C.

It can be observed from the Figure 4.6(b) that pure epoxy has exothermic peak at a temperature of 355.1˚C and all other capsules impregnated epoxy composite specimens have similar exothermic peaks at a narrow temperature range of 334.2˚C - 343.2˚C. Thus, this study

confirms that the addition of capsules to pure epoxy composite does not affect the curing process appreciably.

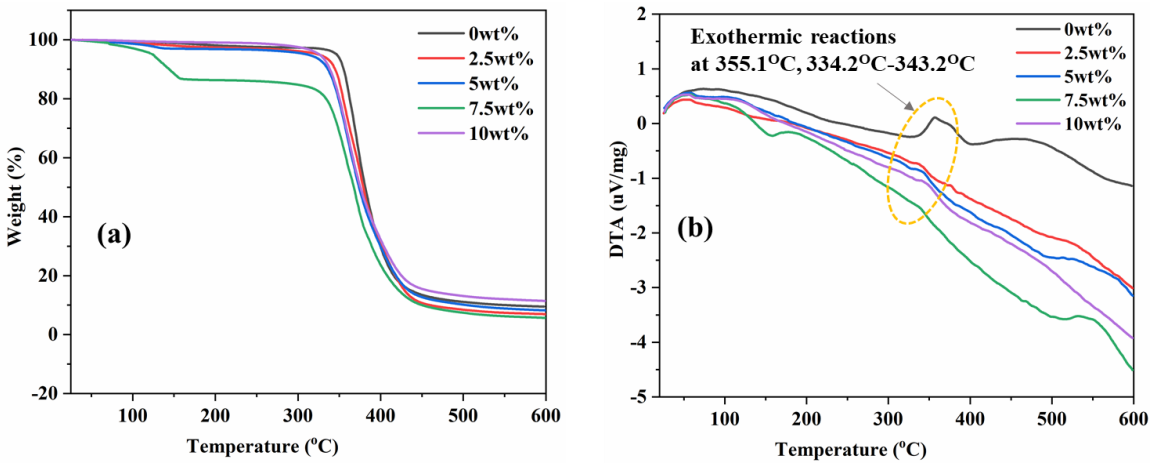

Figure 4.6 (a) TGA (b) DTA curves of pure epoxy and capsules reinforced epoxy composite

4.4.2 Chemical composition analysis of capsules reinforced epoxy composite

In order to cross verify the presence of epoxy microcapsules and hardener microcapsules in the composite and to study the chemical composition of composite FTIR analysis was done. Figure 4.7 shows the FTIR spectrum of crushed fracture surface of (LY556+HY951) capsules reinforced epoxy composite tested as discussed in the section 4.3.1. The major absorption peaks present in the epoxy composite were shown in Table 4.2. In the FTIR spectrum of epoxy composite, presence of major peaks of both epoxy, hardener microcapsules indicate successful incorporation of capsules into epoxy matrix. With the increase in capsules concentration, the increase in peaks intensity is noticed. This phenomenon can be attributed to increase in the healing agent content with the increase in capsules concentration.

Table 4.2 Functional groups present in the capsules reinforced epoxy composite

Wavenumber (cm^{-1})	Peak	Bond
1732	$C=O_{str}$ vibration	$C=O_{str}$
1480	C-H bending vibration which confirms presence of methyl group	C-H bend
1370	$-CH_3$ bending vibration	C-H bend
1274	$C-O-C_{str}$ vibration of ether group	$C-O-C_{str}$
900	Presence of epoxide ring along with $C=O_{str}$ and $-CH_2$ asymmetric, symmetric stretching vibrations	
1197		
1632	N-H bending vibration of primary amine	N-H bend
1093	$C-O-C_{str}$ vibration	$C-O-C_{str}$
783	N-H wagging (bending) vibration of primary amine	N-H bend

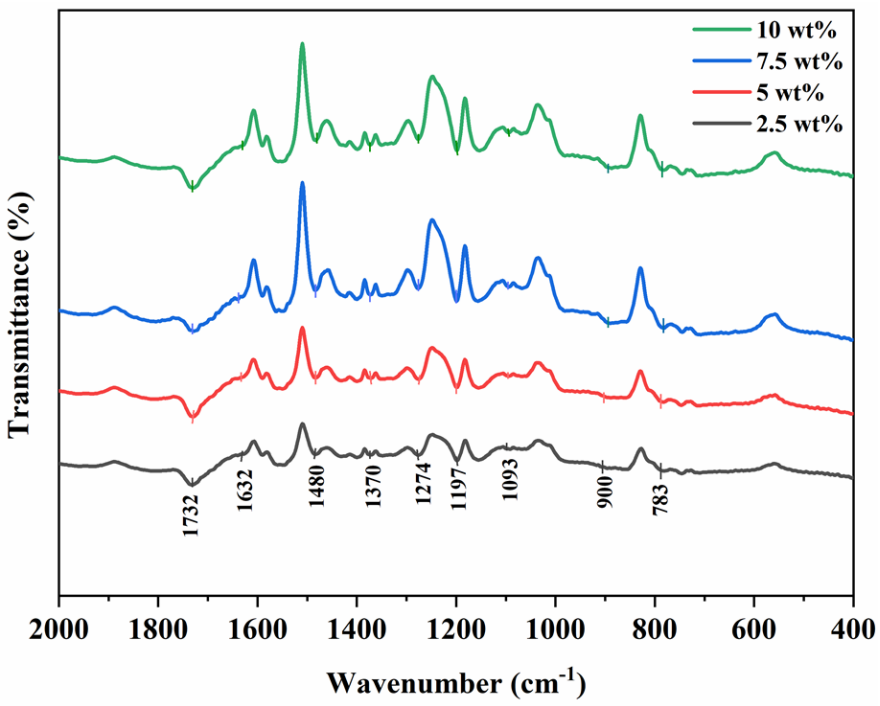

Figure 4.7 FTIR spectrum of epoxy and hardener capsules incorporated epoxy composite

4.4.3 Mechanical properties of dual capsules reinforced epoxy composite

Since polymeric structures subject to different types of mechanical loadings during service conditions, it is necessary to study the influence of capsules concentration on the mechanical properties of pure epoxy. Tensile test, flexural test and Charpy impact test were conducted on the different wt% (LY556+HY951) capsules reinforced epoxy composite.

4.4.3.1 Tensile strength of dual capsules reinforced self-healing epoxy composite

Figure 4.8(a) shows the typical stress-strain curves of capsules reinforced epoxy composite as a function of microcapsules concentration. It can be observed from the stress- strain curves that with the increase in capsules concentration both the tensile stress and tensile strain decreases. Reduction in tensile strain can be due to possible restriction of chain mobility of epoxy network under applied loads.

Effect of microcapsules concentration on the tensile strength and tensile modulus of epoxy composite is as shown in Figure 4.8(b). It can be noted from the results that with the increase in capsules concentration both the tensile strength and tensile modulus decreases. With the addition of 2.5 wt% capsules to base epoxy, the tensile strength and tensile modulus of composite reduced 18.06 % and 7.61 % respectively. Effect of capsules concentration on the % reduction in the tensile strength and tensile modulus of composite can be clearly understood

from the Table 4.3. Yuan et al. [65] also reported the decreasing trend in tensile strength and tensile modulus with the increase in epoxy/mercaptan capsules concentration.

The reduction in tensile strength of the composite can be mainly attributed to two factors. Generally, in the epoxy composite, microcapsules act as fillers and thus generates stress concentration sites, which in turn causes reduction in the tensile strength of the composite. The weaker interfacial adhesion between epoxy matrix and capsules shell material also causes reduction in the mechanical properties. The decrease in tensile modulus with the increase in capsules concentration can be ascribed to incorporation of low modulus thermoplastic polymer (PMMA) shell capsules into relatively high modulus thermosetting epoxy polymer. The shell thickness of microcapsules also affects the increasing or decreasing trend of tensile modulus. The weaker interfacial area between epoxy matrix and shell material may cause slippage of micro capsule surface during loading and thus in turn causes for the reduction in the tensile modulus.

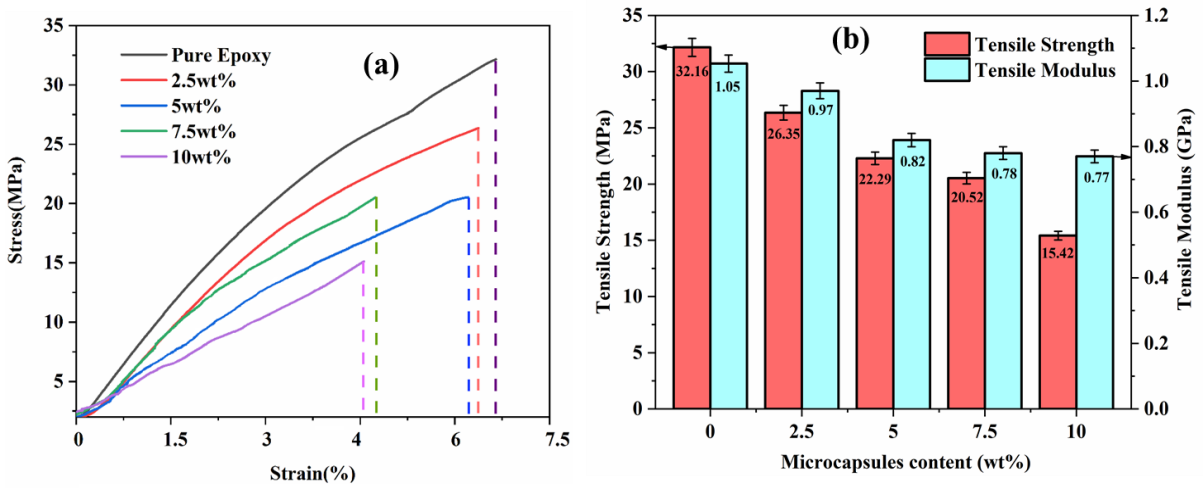

Figure 4.8 (a) Typical stress-strain curves (b) Tensile strength and Tensile modulus of dual capsules reinforced epoxy composite

Table 4.3 Tensile strength and Tensile modulus of dual capsules reinforced epoxy composite

Capsules concentration (wt%)	Tensile strength (MPa)	% reduction in Tensile strength	Tensile Modulus (GPa)	% reduction in Tensile modulus
0	32.16	--	1.05	--
2.5	26.35	18.06	0.97	7.61
5	22.29	30.69	0.82	21.90
7.5	20.52	36.19	0.78	25.71
10	15.42	52.05	0.77	26.67

4.4.3.2 Flexural strength of dual capsules reinforced self-healing epoxy composite

Figure 4.9 shows the effect of microcapsules concentration on the flexural strength of capsules reinforced epoxy composite. Flexural strength of the composite initially increased and then decreased with the increase in capsules concentration. The increase in flexural strength can be due to increase in toughness of the epoxy due to addition of capsules. Tripathi et al. [89] also observed the increase in flexural strength with epoxy encapsulated melamine formaldehyde and urea formaldehyde microcapsules. As explained in the section 4.4.3.1, the decrease in flexural strength can be due to stress concentration effect and weaker interfacial adhesion between epoxy matrix and microcapsules. The percentage increase or decrease in the flexural strength can be observed from the Table 4.4.

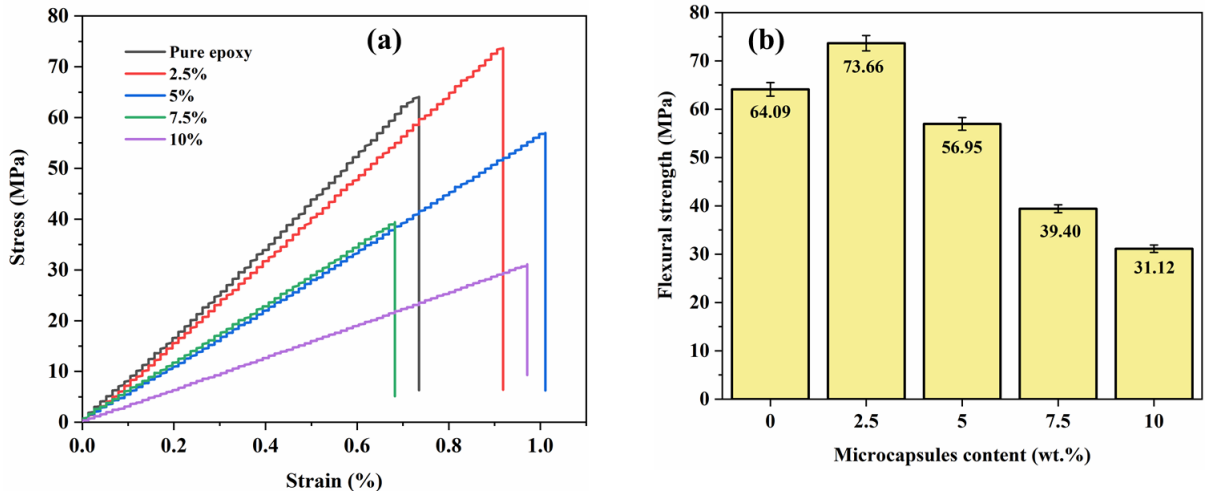

Figure 4.9 (a) Flexural test stress-strain curves (b) Flexural strength of dual capsules reinforced epoxy composite

Table 4.4 Flexural and Charpy impact strength of dual capsules reinforced epoxy composite

Capsules concentration (wt%)	Flexural strength (MPa)	%increase/decrease in Flexural strength	Charpy impact strength (kJ/m^2)	% reduction in impact strength
0	64.09	--	22.54	--
2.5	73.66	14.93	18.62	17.39
5	56.95	11.14	16.67	26.04
7.5	39.40	38.52	15.68	30.43
10	31.12	51.44	13.72	39.13

4.4.3.3 Charpy impact strength of dual capsules reinforced self-healing epoxy composite

As evident from Figure 4.10, it can be noticed that the Charpy impact strength of capsules reinforced epoxy composite decreases with the increase in capsules concentration. During the damage event, crack propagates through PMMA microcapsules and causes for failure of the specimen. Charpy impact strength of pure epoxy composite decreased from 22.54 kJ/m^2 to 13.72 kJ/m^2 with the addition of 10 wt% epoxy and hardener microcapsules. The percentage reduction in impact strength of the composite with the increase in capsules concentration can be noticed from Table 4.4. Similar decreasing trend of impact strength was reported in the earlier studies [131] by incorporating the UF microcapsules into the epoxy composite. The value of strain rate applied also affects the impact strength of the composite. Slower strain rate offers specimen enough time to respond to applied load while the relatively faster strain rate cannot.

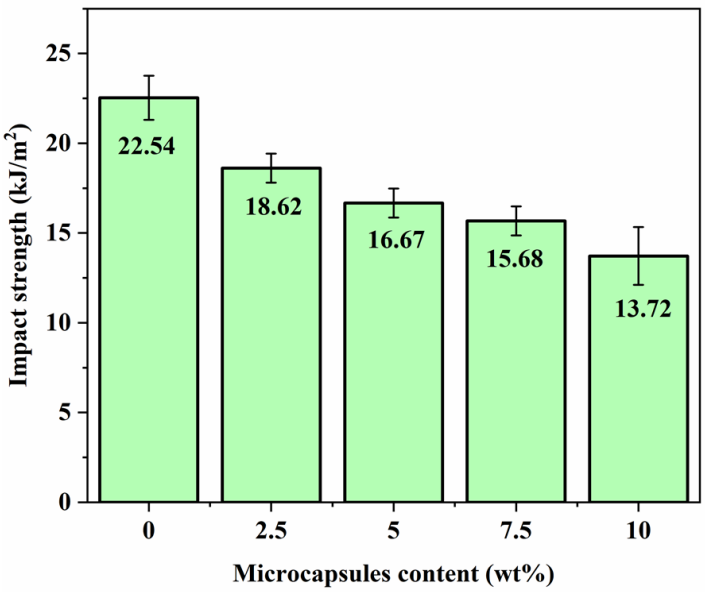

Figure 4.10 Charpy impact strength of dual capsules reinforced epoxy composite

Figure 4.11 shows the 5 wt% epoxy and hardener capsules reinforced epoxy composite fracture surface cross section . It can be observed from the SEM image that the PMMA microcapsules have good adhesion bonding with the base epoxy matrix. The broken microcapsule and crack tails can be noted from the fractured surface of the composite. Hence, from this observation it can be concluded that the majority of reduction in mechanical performance may be not due to weaker interfacial adhesion between epoxy and microcapsules.

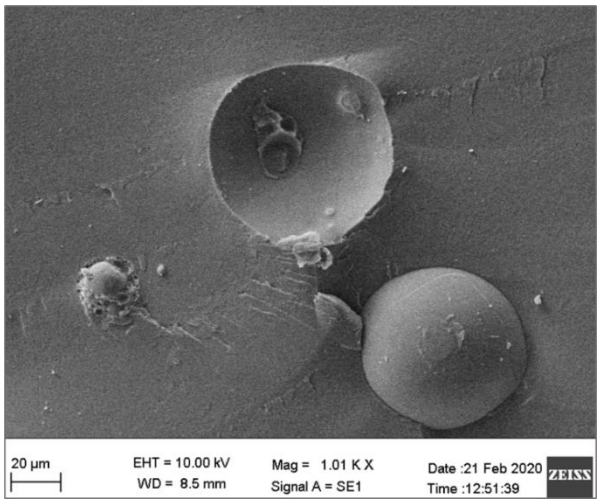

Figure 4.11 SEM image of 5 wt% capsules reinforced epoxy composite cross section

4.4.4 Effect of capsule type & wt% on the tensile strength of self-healing epoxy composite

In order to evaluate the influence of epoxy microcapsules core material viscosity on the tensile strength of self-healing epoxy composite, two types of composites i.e., (LY556+HY951) microcapsules and (CY230+HY951) microcapsules reinforced epoxy composites were fabricated and investigated for tensile strength and tensile modulus. Figure 4.12 shows the typical stress-strain curves of both the composites. It is observed that the tensile stress and tensile strain of the both the composites decreases with the increase in capsules wt% content. The decrease in tensile strain is due to possible restraint of chain movement of epoxy network under subjected loads.

As evident from Figure 4.13, tensile strength of the base epoxy decreased from 32.16 MPa to 15.42 MPa with the addition of 10 wt% LY556+HY951 capsules and from 32.16 MPa to 19.92 MPa with the addition of 10 wt% CY230+HY951 capsules. The difference in percentage reduction in tensile strength can be due to difference in synthesized capsules size and the adhesion between epoxy and microcapsules surface. Table 4.5 and Table 4.6 indicate the effect of capsules type and their wt% on the tensile strength and tensile modulus of base

epoxy. The tensile modulus of the composite was determined from the slope of stress-strain graphs at strain values lower than 1%. The tensile modulus of the base epoxy decreased from 1.05 GPa to 0.77 GPa, 1.05 GPa to 0.93 GPa with the addition of 10 wt% LY556+HY951 capsules and CY230+HY951 capsules respectively. Since the percentage reduction in both the tensile strength and tensile modulus is less with CY230+HY951 capsules combination it is suggested as an ideal combination to get better mechanical properties. The decrease in the tensile strength and tensile modulus with the increase in UF and MF capsules wt% was observed in the previous studies [65]. The decrease in tensile strength mainly attributed to developed stress concentration sites due to addition of capsules and lower interfacial adhesion between capsules and base epoxy. The decrease in tensile modulus is due to addition of low modulus PMMA shell capsules into comparatively high modulus epoxy matrix. Capsules pull out from the base epoxy phenomenon and PMMA shell thickness also can be ascribed to reduction in tensile strength and tensile modulus.

Table 4.5 Tensile strength of (LY556+HY951), (CY230+HY951) capsules reinforced epoxy

Capsules wt%	**LY556+HY951**		**CY230+HY951**	
	Tensile strength (MPa)	**reduction in Tensile strength (%)**	**Tensile strength (MPa)**	**reduction in Tensile strength (%)**
0	32.16	--	32.16	--
2.5	26.35	18.06	26.45	17.75
5	22.29	30.69	23.55	26.77
7.5	20.52	36.19	21.77	32.30
10	15.42	52.05	19.92	38.05

Table 4.6 Tensile modulus of (LY556+HY951), (CY230+HY951) capsules reinforced epoxy

Capsules wt%	**LY556+HY951**		**CY230+HY951**	
	Tensile modulus (GPa)	**reduction in Tensile modulus (%)**	**Tensile modulus (GPa)**	**reduction in Tensile modulus (%)**
0	1.05	--	1.05	--
2.5	0.97	7.61	1.03	1.90
5	0.82	21.90	0.98	6.66
7.5	0.78	25.71	0.95	9.52
10	0.77	26.67	0.93	11.42

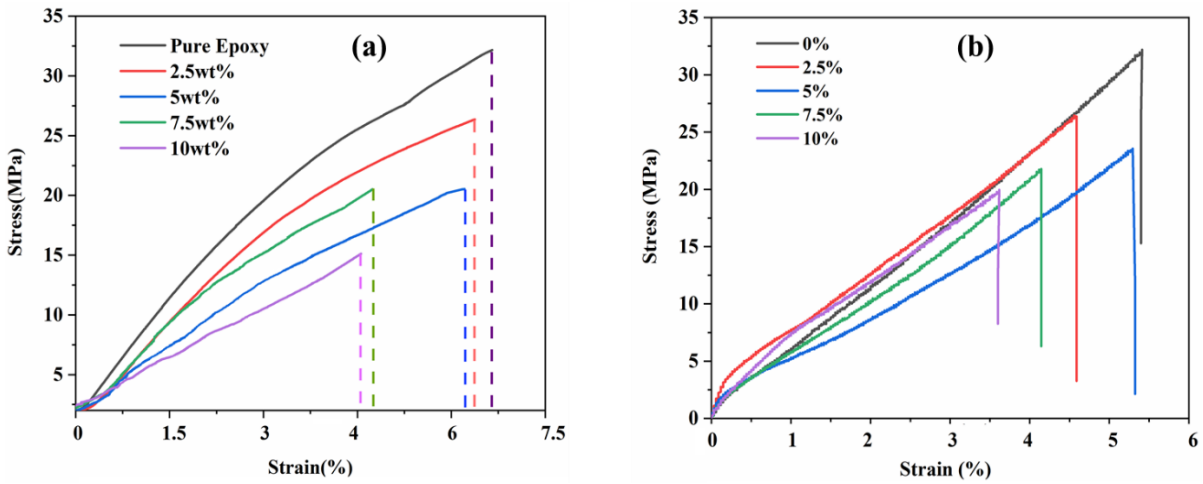

Figure 4.12 Typical stress-strain curves of (a) LY556+HY951 capsules (b) CY230+HY951 capsules reinforced epoxy composite

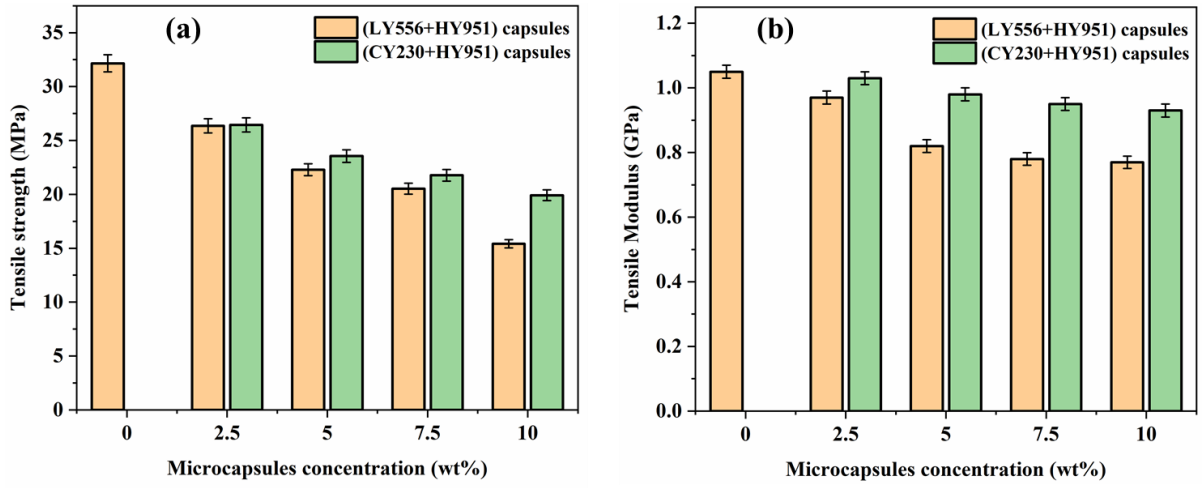

Figure 4.13 Effect of capsules type & wt% on the (a) Tensile strength (b) Tensile modulus of epoxy composite

4.4.5 Qualitative self-healing assessment of capsules reinforced epoxy composite

It is well understood that the capsules ability to deliver healing agent to the crack surface affects the self-healing performance of the system. In order to verify the developed microcapsules ability to rupture, flowability behavior and self-healing capability, an artificial crack was created on the (LY556+HY951) capsules, (CY230+HY951) capsules reinforced epoxy composite. It can be noticed from Figure 4.14(a) and Figure 4.15(a) that the microcapsules present in the crack path were ruptured and released the healing agent into the crack surface. Thus, it is evidenced that as prepared microcapsules were capable to rupture and release healing

agent into the crack plane. The cracked surfaces were kept in contact and allowed to self-heal at room temperature for 24 hrs and then examined under 3D optical microscope for healed cracks. Figure 4.14(b) and Figure 4.15(b) represent the healed cracks in the respective epoxy composites. Since the developed microcapsules had comparable core content, shell thickness and good flowability as microcapsules reported in the previous studies [66], it is confirmed that the developed capsules can have applications in the self-healing composites.

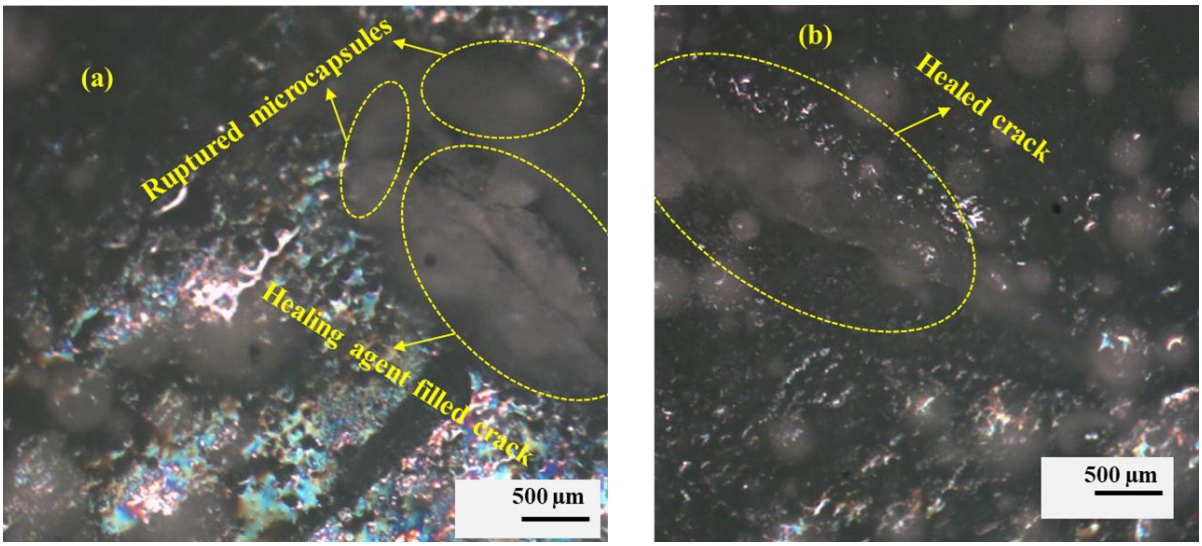

Figure 4.14 3D microscope images of LY556+HY951 capsules incorporated epoxy composite (a) microcapsules rupture and healing agent release (b) healed crack

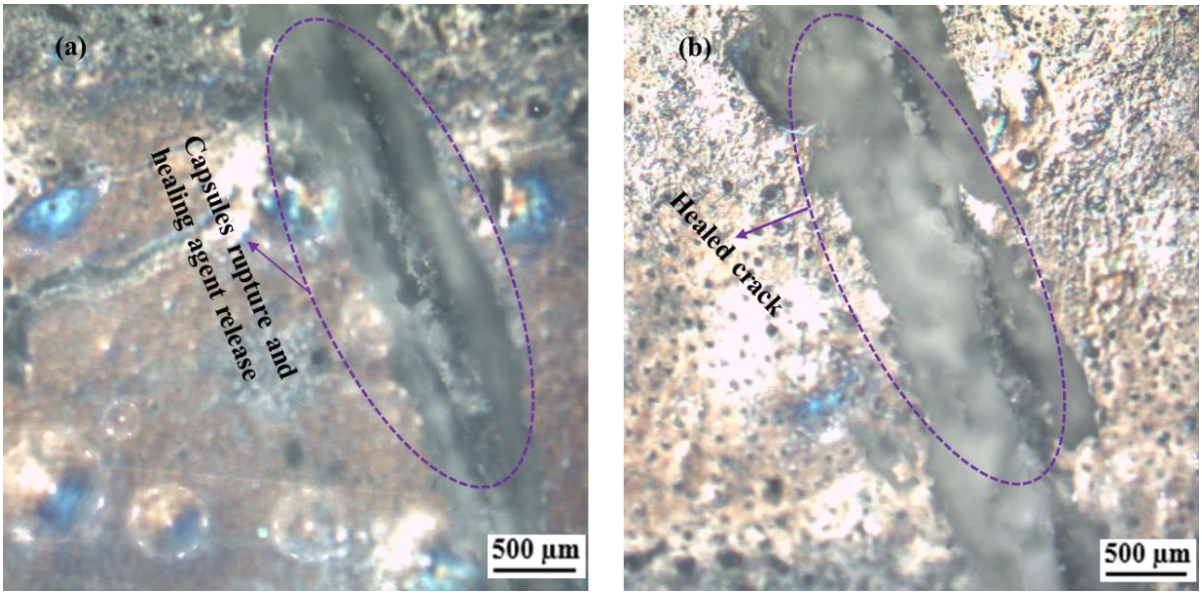

Figure 4.15 3D microscope images of CY230+HY951 microcapsules incorporated epoxy composite (a) ruptured microcapsules (b) healed crack

4.4.6 Quantitative self-healing assessment of capsules reinforced epoxy composite

As discussed in the section 4.3.2.2, quantitative self-healing performance of the system is measured by evaluating the healed specimen ability to recover its original fracture toughness. Quantitative self-healing performance usually expressed in terms of healing efficiency and is defined as the ratio of mode I fracture toughness of healed specimen to virgin specimen. In order to examine the influence of microcapsules type and their concentration on the fracture toughness of composite, (LY556+HY951) capsules reinforced, (CY230+HY951) capsules reinforced TDCB specimens were fabricated and tested for mode I fracture toughness.

Figure 4.16 demonstrates the representative load- displacement graphs of pure epoxy, 7.5 wt% (CY230+HY951) capsules, 7.5 wt% (LY556+HY951) capsules reinforced TDCB epoxy specimens. Mode I fracture test load-displacement graphs of 2.5 wt% - 10 wt% (LY556+HY951) capsules reinforced virgin and healed composites are as shown in Figure 4.17. It is observed that pure epoxy, both types of capsules incorporated composites were failed in brittle fracture mode and showed rough fracture surface. At lower displacement values, both virgin and healed samples showed gentle slope and also resisted more loads than the pure epoxy. In healed samples due to increased crack resistance, crack tear away from the healed surface and thus require additional energy to fracture. The stick-slip phenomenon and increased displacement of healed sample can be ascribed to requirement of extra energy during fracture[65].

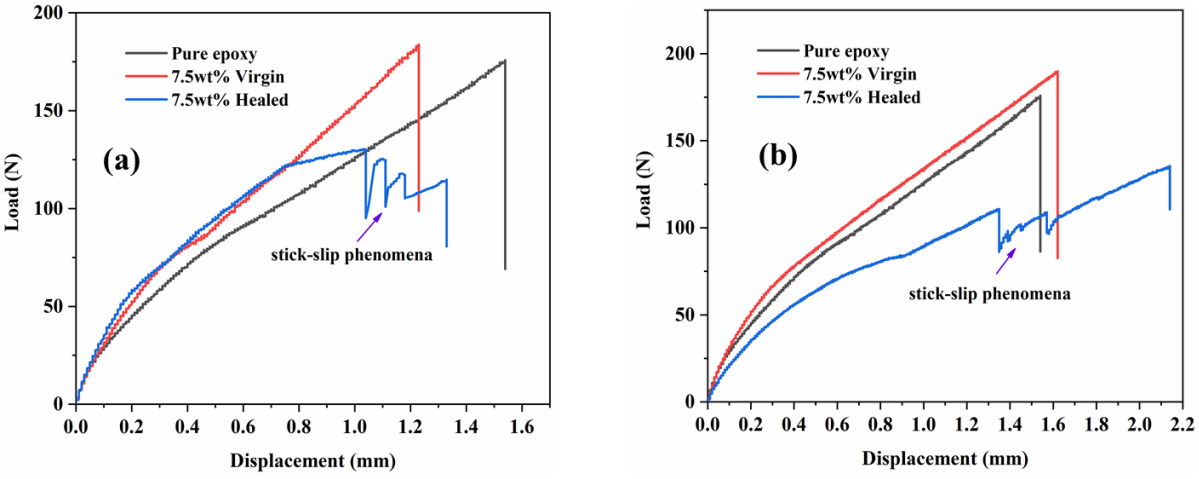

Figure 4.16 Mode I fracture load- displacement graphs of (a) LY556+HY951 capsules reinforced epoxy composites (b) CY230 +HY951 capsules reinforced epoxy composites

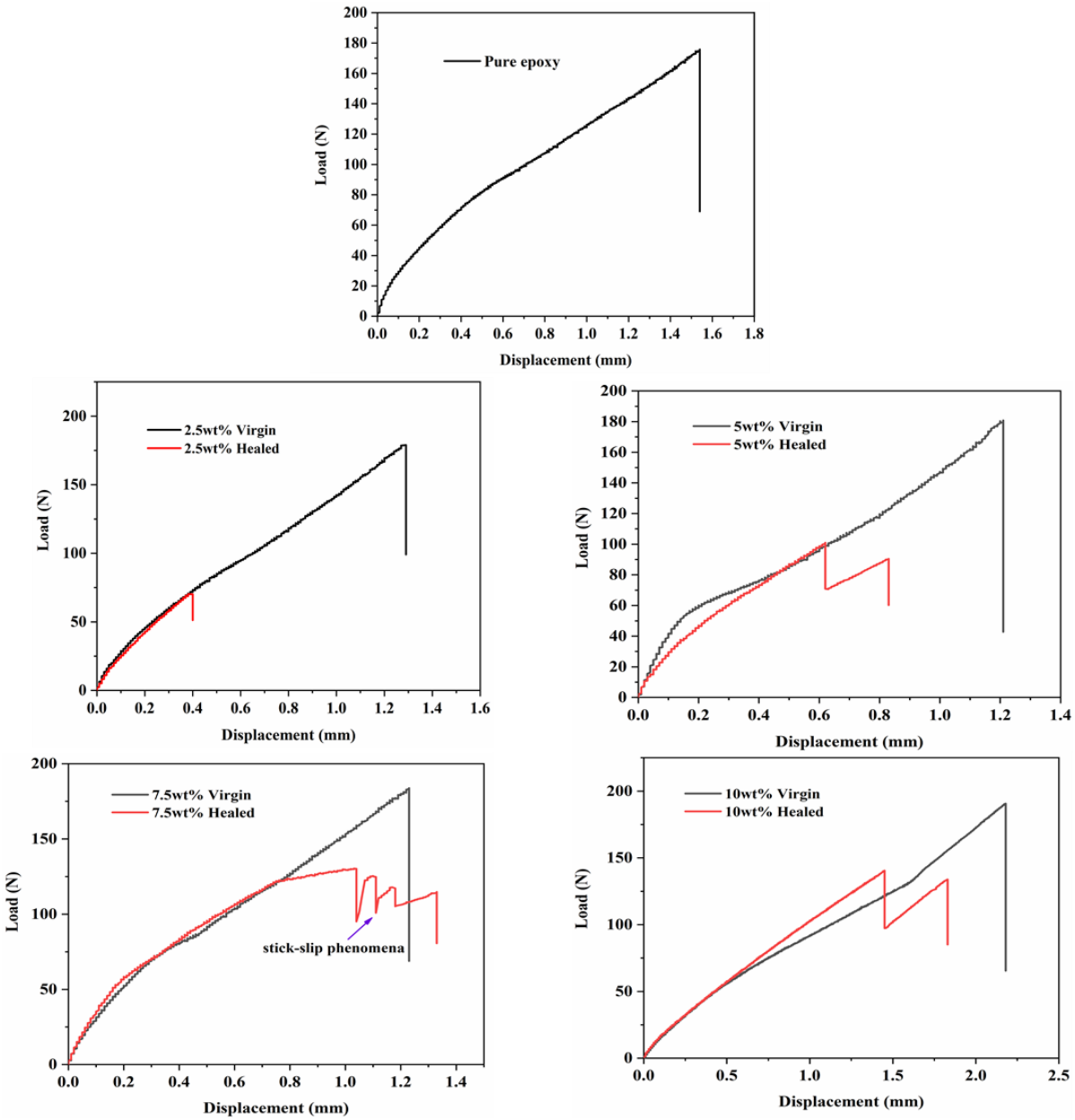

Figure 4.17 Typical Load- displacement curves of (LY556+HY951) capsules reinforced epoxy composites obtained from TDCB samples fracture test

Figure 4.18(a) shows the effect of microcapsules type and their concentration on the fracture toughness of capsules reinforced virgin and healed epoxy composite. It can be noted from the Table 4.7 and Table 4.8 that the fracture toughness of pure epoxy increased from 1.970 MPam$^{1/2}$ to 2.135 MPam$^{1/2}$ and from 1.970 MPam$^{1/2}$ to 2.170 MPam$^{1/2}$ with the addition of 10 wt% (LY556+HY951) capsules and 10 wt% (CY230+HY951) capsules respectively. From the results it is observed that the fracture toughness of healed specimens increases with the increase in capsules concentration from 2.5 wt% to 10 wt%. The fracture toughness of the healed samples was calculated by considering the average peak load. Few previous

studies[63,65] also observed similar increasing trend of fracture toughness with the increase in capsules concentration. The increase in fracture toughness due to addition of capsules can be attributed crack pinning toughening mechanism. Generally, in particles reinforced epoxy composites, crack pinning by filler materials contribute to increased toughness [89]. Similarly, in the current study also crack pinning around the PMMA capsules causes increased crack resistance and as a result increase in fracture toughness of the composite can be observed. CY230+HY951 capsules reinforced healed samples and virgin samples showed higher fracture toughness than the other combination samples. This increment phenomenon is due to increased number of healed zones and increased crack resistance during crack path. Hence, from this analysis it is suggested that lower viscosity epoxy capsules combination is better to get good fracture toughness properties.

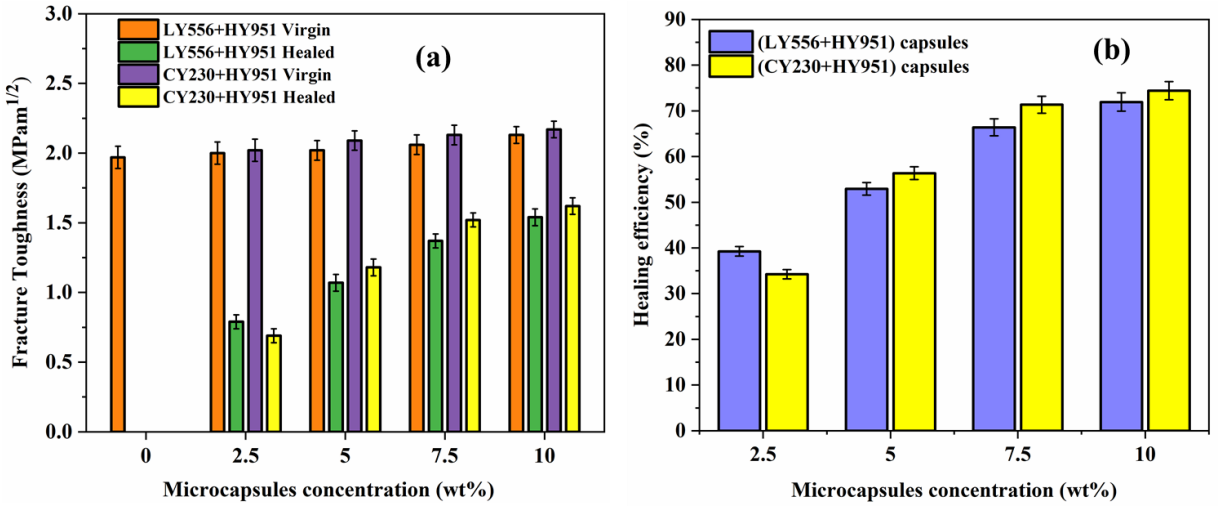

Figure 4.18 Effect of capsules type & wt% on the (a) fracture toughness (b) healing efficiency

Table 4.7 Fracture toughness and healing efficiency of LY556+HY951 capsules incorporated epoxy samples

Capsules (wt%)	Virgin peak load (N)	Healed avg. Peak load (N)	Virgin fracture toughness, K_{IC} ($MPam^{1/2}$)	Healed fracture toughness, K_{IC} ($MPam^{1/2}$)	Healing efficiency (%)
0	175.85	---	1.970	--	--
2.5	178.90	70.25	2.004	0.787	39.26
5	180.80	95.70	2.025	1.072	52.93
7.5	183.85	122.04	2.059	1.367	66.38
10	190.65	137.16	2.135	1.536	71.94

Table 4.8 Fracture toughness and healing efficiency of CY230+HY951 capsules incorporated epoxy samples

Capsules (wt%)	Virgin peak load (N)	Healed avg. Peak load (N)	Virgin fracture toughness, K_{IC} ($MPam^{1/2}$)	Healed fracture toughness, K_{IC} ($MPam^{1/2}$)	Healing efficiency (%)
0	175.85	---	1.970	--	--
2.5	180.30	61.72	2.019	0.691	34.23
5	186.20	104.96	2.085	1.176	56.36
7.5	189.90	135.50	2.127	1.518	71.35
10	193.75	144.18	2.170	1.615	74.41

To examine the influence of epoxy resin capsules viscosity and their concentration on the self-healing efficiency, same type of hardener microcapsules were used in LY556+HY951 combination and CY230+HY951 combination. Figure 4.18(b) indicates the influence of capsules concentration on the of self-healing efficiency of epoxy composite. It is noted from the results that the healing efficiency is proportional to the capsules concentration and increases with the increase in capsules wt% content. The maximum healing efficiency of epoxy composite with the LY556+HY951 capsules combination is measured as 71.94% and with the CY230+HY951 capsules combination measured as 74.41%. The increase in self-healing efficiency with the increase in capsules wt% is due to release of stoichiometric quantity of healing agent from the broken capsules and the curing reaction between them. From the results it is understood that 7.5 wt% capsules content is sufficient to recover 66.38% virgin load in LY556+HY951 capsules combination and 71.35% virgin load in CY230+HY951 capsules combination. With the increase in capsules content from 7.5 wt% to 10 wt%, LY556+HY951 capsules combination showed 7.72% improvement in self-healing efficiency and 24.85% decrease in tensile strength whereas CY230+HY951 capsules combination showed 4.11% improvement in self-healing efficiency and 8.49% decrease in tensile strength. With the increase in capsules content, even though healing efficiency increases at the same time the % reduction in the mechanical properties also increases. Hence, an optimum capsules content should satisfy both the mechanical properties and the self-healing efficiency. Since CY230+HY951 capsules combination showed less percentage reduction in the mechanical properties and 71.35% healing efficiency at 7.5 wt%, this combination and 7.5 wt% capsules concentration are recommended as an ideal parameters to fabricate capsules incorporated self-healing epoxy composite. Finally, from this study it is concluded that the less viscous epoxy

resin capsules combination shows better self-healing performance than the other type of combination.

4.4.7 Fracture surface investigation of self-healing epoxy composites

In order to understand the self-healing performance in detail, fractured surface of 7.5 wt% LY556+HY951 capsules reinforced and CY230+HY951 capsules incorporated epoxy composites were analysed under SEM and shown in Figure 4.19 and Figure 4.20 respectively. It is understood from the fractography that the fractured surface is rough throughout the crack plane. Presence of crack tail elucidates the crack pinning mechanism, which is the main reason for the increase in fracture toughness of the epoxy composite. During the crack propagation, capsules rupture and supplies healing agent to the crack plane. Number of ruptured micro capsules and released healing agent can be observed from Figure 4.19 and Figure 4.20. Even though capsules were uniformly distributed throughout the composite, for few cracked regions healant was not supplied. This phenomenon can be attributed to pull out of the capsules from the base epoxy. Thus, capsules pull out also causes for decreased self-healing performance and thus for decreased self-healing efficiency. During the crack propagation, sometimes crack is forced to change its path and thus require additional energy for fracture. This phenomenon is known as crack path deflection and can be noticed in Figure 4.19 and Figure 4.20. Thus, from the fractography it is confirmed that presence of crack pinning, crack path deflection and microcracking mechanisms in both types of capsules combinations are the main reasons for the increase in fracture toughness and healing efficiency with the increase in capsules wt%.

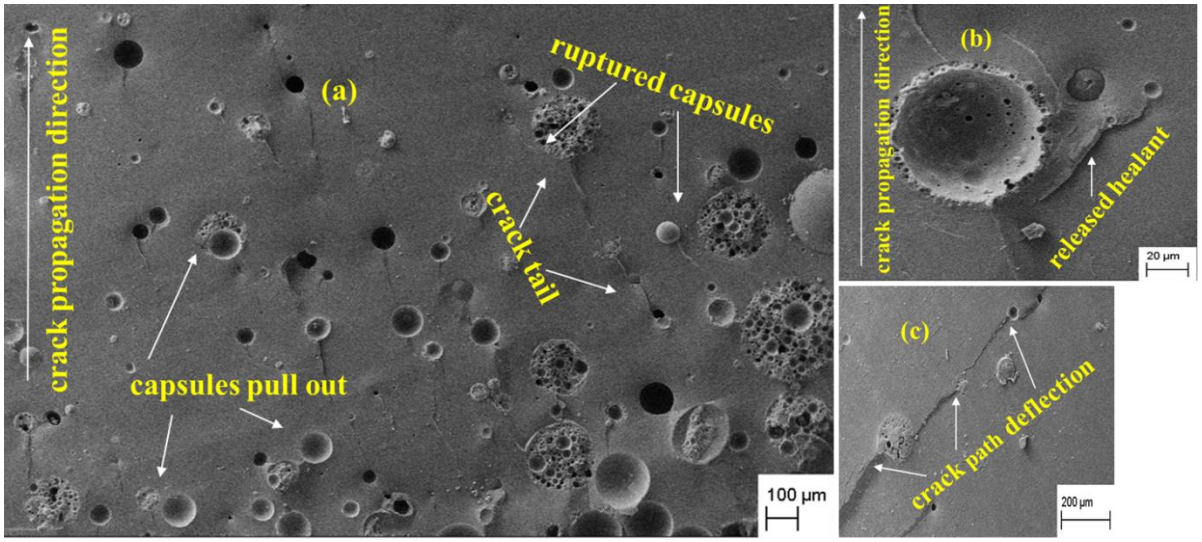

Figure 4.19: Fracture surface images of 7.5 wt% LY556+HY951 capsules reinforced epoxy composite (a) capsules distribution (b) released healant (c) crack path deflection

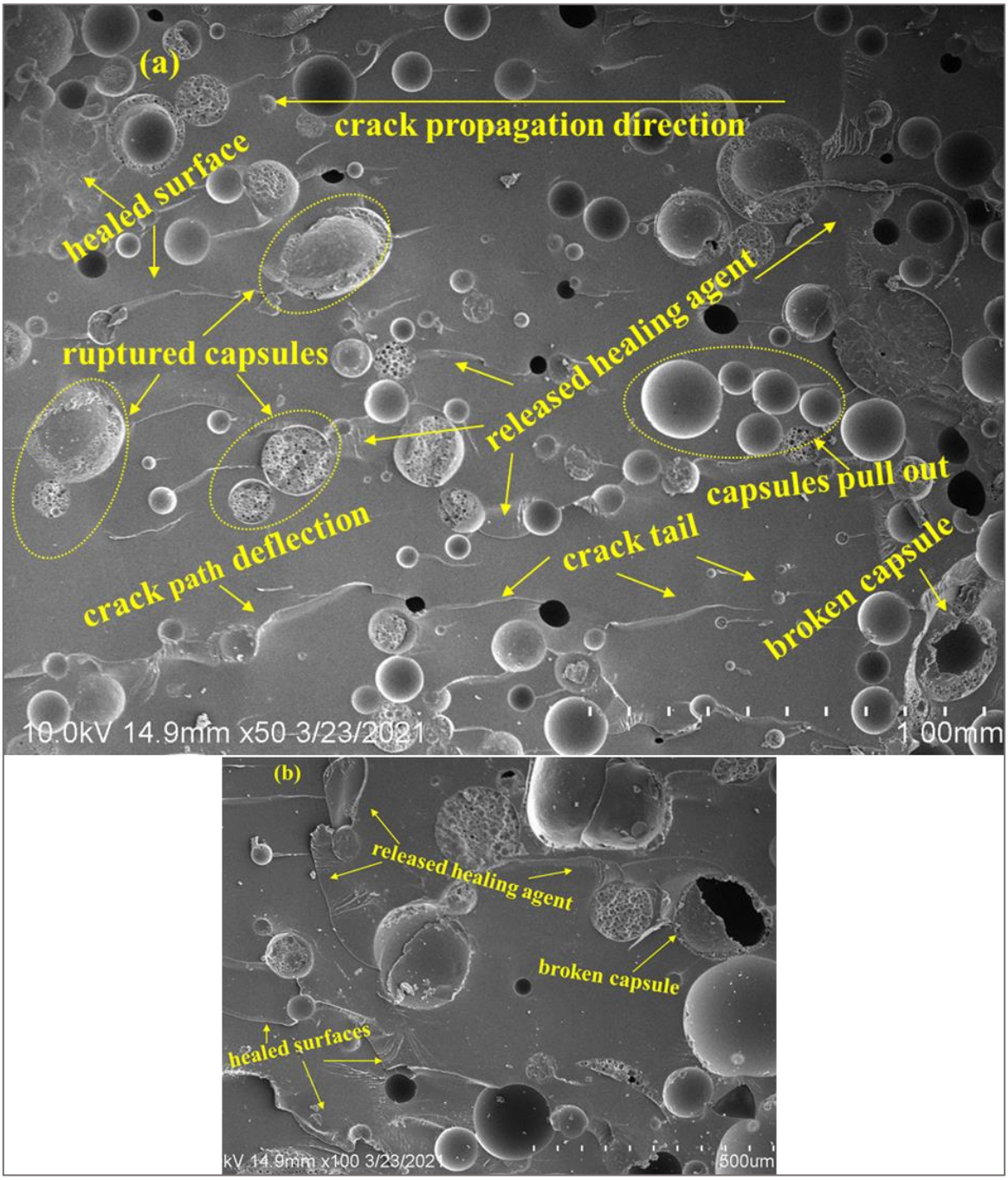

Figure 4.20 Fracture surface images of 7.5 wt% CY230+HY951 capsules reinforced epoxy composite (a) ruptured capsules and released healant (b) healed surfaces

4.5 Conclusions

(LY556+HY951) capsules reinforced and (CY230+HY951) capsules reinforced self-healing epoxy composites were fabricated and evaluated for mechanical performance and healing efficiency. The effect of epoxy microcapsules core material viscosity on the tensile strength and self-healing performance of composite was investigated. Following conclusions can be inferred from the current study.

- DTA analysis confirmed that the addition of capsules to pure epoxy does not affect its curing process appreciably. TGA analysis confirmed that the capsules reinforced epoxy composite can have applications up to 200˚C without any mass loss.
- Presence of major peaks of both epoxy and hardener microcapsules in the FTIR spectrum of capsules reinforced epoxy composite confirmed the addition of both capsules into composite.
- Tensile strength, Charpy impact strength of capsules reinforced epoxy composite decreased and flexural strength initially increased and then decreased with the increase in capsules concentration.
- With the addition of 7.5 wt% of LY556+HY951 capsules, tensile strength, flexural strength and Charpy impact strength of pure epoxy decreased from 32.16 MPa to 20.52 MPa, 64.09 MPa to 31.12 MPa and 22.54 kJ/m^2 to 13.72 kJ/m^2 respectively.
- Effect of epoxy microcapsules core material viscosity on the tensile strength of capsules reinforced composite was investigated and found that the tensile strength of pure epoxy decreased from 32.16 MPa to 15.42 MPa and from 32.16 MPa to 19.92 MPa with the addition of 10 wt% LY556+HY951 capsules and CY230+HY951 capsules respectively.
- Healed epoxy composites fracture toughness increased from 0.78 MPam$^{1/2}$ to 1.53 MPam$^{1/2}$ and from 0.69 MPam$^{1/2}$ to 1.61 MPam$^{1/2}$ with the increase in LY556+HY951 capsules, CY230+HY951 capsules content from 2.5 wt% to 10 wt% respectively.
- Healing efficiency of epoxy composite increased from 39.26% to 71.94% and from 34.23% to 74.41% with the increase in LY556+HY951 capsules, CY230+HY951 capsules concentration from 2.5 wt% to 10 wt% respectively.
- CY230+HY951 capsules combination showed better mechanical properties and self-healing performance than the LY556+HY951 capsules combination.
- 2:1 c/s ratio CY230 epoxy capsules, 4:1 c/s ratio HY951 hardener capsules, 1:1 capsules weight ratio, 7.5 wt% of CY230+HY951 microcapsules concentration and room temperature curing for 24 hrs were suggested as an ideal process parameters to fabricate dual capsules reinforced self-healing epoxy composite.

Chapter 5

Self-healing performance and damping characterization of capsules reinforced CFRP composite

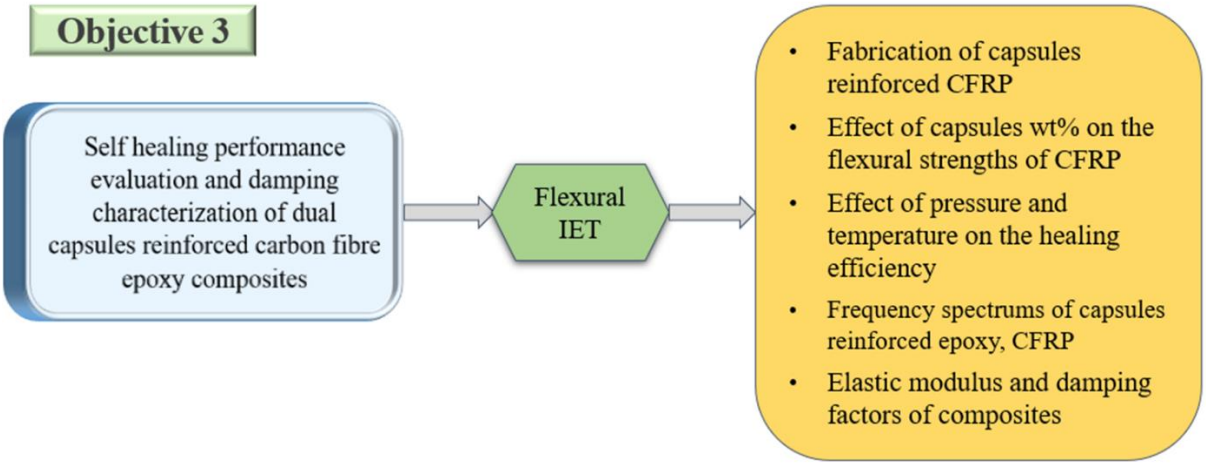

This chapter deals with the fabrication and self-healing performance evaluation of dual capsules reinforced carbon fibre epoxy composites and investigates the effect of initial damages and microcapsules concentration on the flexural strength of composite. Effect of healing temperature and pressure on the healing efficiency of composite are assessed based on the recovery in flexural strength. Finally, damping characterization of dual capsules reinforced CFRP composite is investigated and healing efficiency is assessed based on dynamic elastic properties recovery.

5.1 Introduction

To avoid premature failure of the component, selected materials in the designing of structural components should withstand harsh environmental conditions and offer good mechanical properties under various loading conditions. Composite materials such as CFRP and GFRP possess multi directional load bearing capacity, good corrosion resistance and better mechanical properties. Because of structural advantages such as light weight, tailorable properties and design flexibilities, composite materials have been replacing most of the conventional materials in the applications such as aircraft frames, wings and engine components. However, composite materials experience deterioration, damage and failure due to impact loads such as bird strikes and lightning strikes. In general, the damage begins at microscopic level in the form of micro voids and then extends to microcracking, interfacial fracture and finally leads to catastrophic failure of the component. But, due to anisotropic nature of the composites detection and repair of these damages at microscopic level is a challenging task. Though few repair strategies are available they can't be employed because of their inefficiency for invisible damages. Hence to address these challenges and to offer a promising solution few authors [39,108,132] employed self-healing technology in the composite structures. These self-healing materials provide autonomic detection, repair of the micro cracks and thus restores the functionality and extends the service life of the component.

To fabricate the epoxy based polymer composites with inbuilt self-healing capability different self-healing systems such as intrinsic and extrinsic approaches were investigated. Intrinsic approaches achieve self-healing through inherent reversibility of covalent bonds and extrinsic approaches achieve through encapsulation of healing agents in microcontainers, hollow glass fibres or microvascular networks. Shabani et al. [133] implemented the intrinsic self-healing system to investigate the healing of micro cracks in the glass fibre/epoxy cross ply laminate. Initial damages were created using tensile test and healing efficiency was evaluated

based on the recovery of flexural strength and flexural modulus. Williams et al. [134] utilized the hollow glass fibres approach to verify the self-healing functionality in the carbon fibre/epoxy laminates. Quasi static impact loads were applied to create the initial damages and self-healing performance was evaluated by calculating the recovery in four point bend flexural strength.

One of the most progressive, commercializable and successful approach is capsule based self-healing approach. In this approach healing occurs through the curing reaction between released healing agents i.e., reaction between polymerizable monomer and corresponding curing agent. Different fabrication techniques such hand layup [103,106] and vacuum assisted resin infusion [95,135] were investigated to fabricate fibre reinforced self-healing epoxy composites. Due to simplicity in fabrication and ease of integration of microcapsules with matrix material, hand layup technique is most commonly employed in the applications. Yuan et al. [106] fabricated epoxy-mercaptan microcapsules embedded woven glass fibre/epoxy composites using hand layup technique and created initial damages using low velocity impact loads. They studied the recovery in damage area as a function of capsules size, concentration, applied impact energy and evaluated the healing efficiency based on the recovery in compressive strength after impact and reported the max efficiency of 86%.

Investigation on self-healing of frequently induced damages such as matrix micro cracking and fibre-matrix debonding(delamination) are necessary for the successful implementation of fibre reinforced self-healing polymer composites in the structural applications. Ebrahimnezhad et al. [96] explored the self-healing of matrix micro cracking and delamination damages in the glass fibre/epoxy composites by employing diluted epoxy encapsulated urea formaldehyde microcapsules and imidazole catalyst in the epoxy matrix. Quasi static indentation test was used to create initial damages and self-healing was evaluated based on the recovery of tensile strength and interlaminar shear strength. Few researchers used compression after impact (CAI) [136], tensile test [109], flexural test [108] and Interlaminar fracture tests [102] to assess the recovery in aforesaid damages and thus to evaluate the self-healing performance of fibre reinforced composites.

Though few studies available on the self-healing of CFRP composites none of the studies employed epoxy resin, amine hardener encapsulated dual microcapsules system to evaluate matrix micro cracking and delamination damage recovery. Effect of microcapsules concentration on the flexural properties and self-healing performance was not investigated.

None of the studies reported the effect of elevated temperature and external pressures on the healing behavior of matrix cracking and delamination damages.

High specific strength and stiffness made composites to find applications as aircraft structures and automotive body components. But during service conditions these components experience vibrations and hence to employ self-healing composites in these applications it is important to understand the damping behavior and evaluate the self-healing performance based on stiffness recovery. But most of the available literature focused on the recovery in mechanical strength rather than the recovery in stiffness (dynamic elastic properties). No literature was reported on the dual capsules reinforced CFRP composites to evaluate healing efficiency based on stiffness recovery. In an attempt to address above mentioned challenges and to investigate dual capsules reinforced CFRP composite present study is carried out.

5.2 Materials and Methods

Materials and procedures used to fabricate dual capsules reinforced CFRP composites are discussed in this section.

5.2.1 Materials

CY230 epoxy resin encapsulated and HY951 amine hardener encapsulated PMMA microcapsules were used as healing materials and synthesized as discussed in the chapter 3. CY230 and HY951 microcapsules with respective average diameter of 67.64 μm and 63.31 μm were used in this study. LY556 epoxy resin of density 1.16 g/cc and HY951 hardener of density 0.98 g/cc were used to fabricate polymer matrix and obtained from Huntsman corporation, Mumbai. Plain weave bi-directional carbon fibre of 200 GSM with density of 1.8 g/cc used as reinforcement and obtained from Composites Tomorrow, Vadodara, India.

5.2.2 Fabrication of dual capsules reinforced carbon fibre/epoxy composite

CY230 epoxy capsules and HY951 hardener capsules reinforced self-healing CFRP composite was fabricated by considering 50:50 wt% of matrix and carbon fibre and capsules wt% of 5, 10 and 15. Hand layup technique and 12 layers of 200 GSM bi-directional plain weave carbon fibres were used to prepare laminates. The detailed fabrication procedure is as follows.

- Required number of carbon fibre layers were calculated and cut into the desired dimensions. Prior to cutting, edges of the carbon fibre were glued with masking tape and required dimensions were marked on it. Gluing the masking tape to fibre edges helps to avoid peeling of fibres during cutting.

- Required amount of matrix and microcapsules were calculated and measured accurately using weighing balance. Optimum weight ratio of 1:1 was considered to calculate the required mass of microcapsules.
- Calculated amount of microcapsules were added to epoxy at 40˚C and rotated for 20 min at 400 rpm to ensure uniform distribution of microcapsules in the epoxy.
- The mix was allowed to degas for 5 min using vacuum desiccator to remove entrapped air bubbles. Later, to this mix hardener equals to 10 wt% of epoxy was added and rotated for 5 min using mechanical stirrer and again degassed for 3 min.
- Wooden mould of dimensions 180 X 165 X 3.2 mm^3 was prepared and wax applied OHP sheet was kept on the surface of the mould for easy removal of composite after curing.
- Dual capsules reinforced epoxy was poured on the OHP sheet and uniformly distributed throughout the mould using roller. Carbon fibre was laid on top of the mix and again poured the mix on the fibre and uniformly distributed. Same process was repeated till the completion of number of layers.
- On the top layer of carbon fibre only pure epoxy was applied and one more wax applied OHP sheet was kept on top of it and applied few dead weights to ensure proper bonding.
- Neat CFRP composites (composite without any microcapsules) were also synthesized in the similar way as capsules reinforced CFRP but without any microcapsules addition.
- Both neat CFRP and capsules reinforced CFRP composites were cured at room temperature for 48 hrs followed by post curing at 80°C for 4 hrs.
- Cured laminate was cut into required flexural specimen dimensions (80 X 12 X 3.2 mm^3) using scroll saw and as per ASTM D790 standard.

5.2.3 Calculations of number of carbon fibre layers required

To fabricate laminate with desired thickness, required number of layers can be calculated using rule of mixture of composites. According to this rule, volume of the laminate is equal to the sum of its individual constituents volume.

Volume of the composite = Volume of fibre + Volume of matrix Eq.5.1

Thus, $$Volume\ fraction of\ \ fibre\,(V_f) = \frac{Volume of\ \ fibre}{Total\ volume} = \frac{\frac{W_f}{\rho_f}}{\frac{W_f}{\rho_f} + \frac{W_m}{\rho_m}}$$ Eq.5.2

$$Volume\ fraction of\ matrix\,(V_m) = \frac{Volume of\ \ matrix}{Total\ volume} = \frac{\frac{W_m}{\rho_m}}{\frac{W_f}{\rho_f} + \frac{W_m}{\rho_m}}$$ Eq.5.3

Where W_m - weight fraction of matrix; W_f - weight fraction of fibre; ρ_m - density of matrix and ρ_f - density of fiber

By substituting the W_m = 0.5, W_f = 0.5, ρ_m = 1.16 g/cc and ρ_f = 1.8 g/cc in Eq.5.2 and Eq.5.3

We will get, volume fraction of fibre (V_f) = 0.3857 and volume fraction of matrix (V_m) = 0.6142

$$Density of\ composite(\rho_C) = \rho_f V_f + \rho_m V_m$$ Eq.5.4

By substituting V_f and V_m values in Eq.5.4, we will get ρ_c = 1.391g/cc

By considering mould dimensions as 180 X 165 X 3.2 mm^3;Volume of the composite = 95.04cc

Weight of composite = ρ_c X V_c = 132.2 g

Weight of matrix = 0.5 X 132.2 = 66.1 g

Weight of fibre = 66.1 g

Mass of each carbon layer = 5.45 g

No of layers required = 66.1/5.45 = 12.12~**12**

W_m = 0.5, W_f = 0.5 were considered such that more number of capsules can be incorporated in the matrix and thus can get better healing efficiencies. As per Hoa S V [137] maximum volume fraction of fibre that can be employed in the hand layup technique to get optimum properties is around 40%. Since the calculated values lied within the range, the selected values W_m =0.5 and W_f =0.5 are justified.

The calculations used to determine required mass of each microcapsule type are as follows.

Weight of matrix = 70 g (66+4 g extra for losses)

Weight of epoxy = 0.91 X 70 = 63.7 g

Weight of hardener = 6.3 g

For 5 wt% capsules, required mass of **each** capsule type = (63.7 X (5/100))/2 = 1.59 g

Thus, for other wt% capsules also required mass was calculated and can be found in Table 5.1

Table 5.1 Required mass of each capsule to fabricate self-healing CFRP composite

capsules wt%	required mass of each capsule (g)
5	1.59
10	3.18
15	4.77

Since area under inspection and the damage volumes considered are higher than the damage volumes considered in the capsules reinforced epoxy composite study, twice the capsules wt% is considered in this study.

Though increasing the capsules wt% increases the healing ability; at the same time epoxy matrix viscosity also increases and thus cannot completely wet the carbon fibres. Hence in this study capsules wt% was restricted to 15 wt% to ensure proper wetting of fibres with epoxy matrix.

5.2.4 Fabrication of capsules reinforced composites for damping assessment

Table 5.2 indicates the list of composites used to evaluate the damping characterization of self-healing composites. 7.5 wt% capsules reinforced epoxy composites were fabricated as discussed in the section 4.2.2 and 15 wt% capsules reinforced CFRP composites were fabricated as discussed in the section 5.2.2. V indicates virgin samples; D indicates damaged samples and H indicates healed samples. Damaged samples were fabricated by applying 70% peak load on the virgin samples and the same samples were allowed to self-heal to prepare healed samples.

Table 5.2 List of self-healing composites used to assess damping characterization

Composite type	Composite dimensions (L X b X t) in mm	Mass (g)
Pure Epoxy	60 X 12 X 2.6	2.17±0.11
(7.5 wt% + epoxy) V	60 X 12 X 2.6	2.13±0.13
(7.5 wt% + epoxy) D	60 X 12 X 2.6	2.04±0.12
(7.5 wt% + epoxy) H	60 X 12 X 2.6	2.08±0.11
Pure CFRP	60 X 12 X 2.6	2.57±0.15
(15 wt% + CFRP) V	60 X 12 X 2.6	2.48±0.13
(15 wt% + CFRP) D	60 X 12 X 2.6	2.41±0.12
(15 wt% + CFRP) H	60 X 12 X 2.6	2.44±0.14

5.3 Mechanical, self-healing performance evaluation and damping behavior analysis

This section deals with the mechanical test used to assess the effect of microcapsules concentration on the flexural strength and self-healing performance of CFRP composite. The techniques used to evaluate the damping behavior of capsules reinforced epoxy, CFRP composites are discussed.

5.3.1 Mechanical performance evaluation

In order to study the mechanical behavior of capsules reinforced CFRP composite and neat CFRP composite, three point bending test was conducted by employing AE30kN UTM. The flexural dimensions used were 80 X 12 X 3.2 mm^3 and 56 mm span, 1 kN load cell and 2 mm/min speed rate were applied during testing. Effect of initial damages, microcapsules concentration and healing conditions on the flexural strength of composite were evaluated. For each result, three identical samples were tested and average was considered for reporting. Flexural strength and flexural strain were calculated according to Eq.5.5 and Eq.5.6 respectively.

$$Flexural\ strength = \frac{3PL}{2bd^2} \qquad \text{Eq.5.5}$$

$$Flexural\ strain = \frac{6\delta d}{L^2} \qquad \text{Eq.5.6}$$

Where P - applied Load in N; L - Span distance in mm; b - width of the specimen; d - thickness of the specimen; δ - displacement in mm

5.3.2 Self-healing performance evaluation

To assess the self-healing performance of capsules reinforced CFRP composite, first, commonly generated damages such as matrix microcracking and delamination should be introduced into the composite. For this purpose, neat CFRP composite with same dimensions as capsules reinforced CFRP was tested till failure and noted the damage loads corresponding to matrix microcracking and delamination. Later, same damage loads were applied on the capsules reinforced CFRP composite and allowed to self-heal under different healing conditions. AE30kN UTM and three point bending setup were used to induce the damages in the composite. Figure 5.1 shows the load-displacement graph obtained from flexural test and represents the damage loads corresponding to matrix cracking, delamination and fibre rupture of the composite.

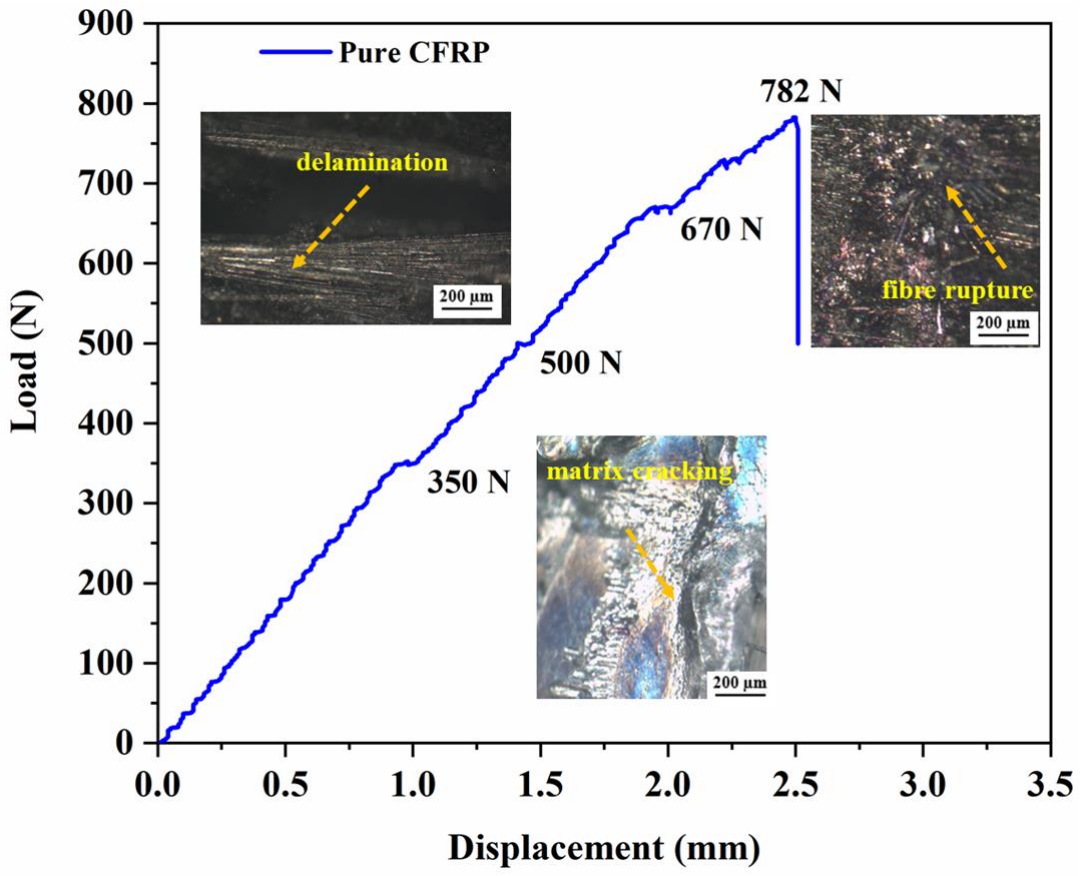

Figure 5.1 Representative damage loads of CFRP composite

From the load-displacement graph it can be observed that composite had elastic behavior up to certain extent and then showed a dip in the load which indicates induce of some form of damage. In order to understand the type of damage induced in the composite at different applied loads, composite was examined under optical microscope and analysed. From the observation, it was understood that 350 N applied load induced micro cracking in matrix and further loading caused delamination and fibre rupture damages in the composite. At 500 N applied load delamination was initiated and propagated further and finally fibre rupture occurred at 782 N. Normally, capsules based healing approach heals the damages by increasing the adhesion between fibre and matrix and thus may not be effective to heal fibre rupture which is a severe damage. Hence only matrix microcracking and delamination damages were considered in the present study.

Figure 5.2(a) shows the schematic representation of self-healing assessment procedure followed in the current study to evaluate CFRP composites. As discussed in the section 5.2.2, capsules reinforced CFRP composites were fabricated and cut into flexural specimens as per ASTM D790. Matrix microcracking and delamination damages were induced by applying 350N and 500 N loads. The damaged specimens were allowed to heal under different healing conditions and retested under same conditions to investigate recovery in flexural strength and thus to assess self-healing performance of the composite. Figure 5.2(b) represents the matrix microcracking healing in CFRP composite. The induced damage triggers the rupture of microcapsules and releases the healing agents into the crack plane. The curing reaction between released healants polymerizes the crack plane and thus cures the damage.

For investigating self-healing behavior of CFRP composite, three types of flexural samples i.e., virgin (samples without any damage), damaged (samples subjected to respective damage) and healed (samples healed for respective damages) were considered. For each type atleast three samples were tested and average results were reported in the study. Healing efficiency (η) of the composite was assessed based on the flexural strength recovery and calculated using Eq.5.7.

$$\eta = \frac{\sigma_{healed} - \sigma_{damaged}}{\sigma_{virgin} - \sigma_{damaged}} \qquad \text{Eq.5.7}$$

Where σ_{healed} represents flexural strength of healed specimen; $\sigma_{damaged}$ represents flexural strength of damaged samples and σ_{virgin} represents virgin sample flexural strength.

To find out $\sigma_{damaged}$, first, respective damage was induced in the sample by applying load corresponds to matrix cracking or delamination and then again tested till failure. To find out σ_{healed}, samples with respective damages were allowed to self-heal under different conditions and then again retested under same loading conditions till failure.

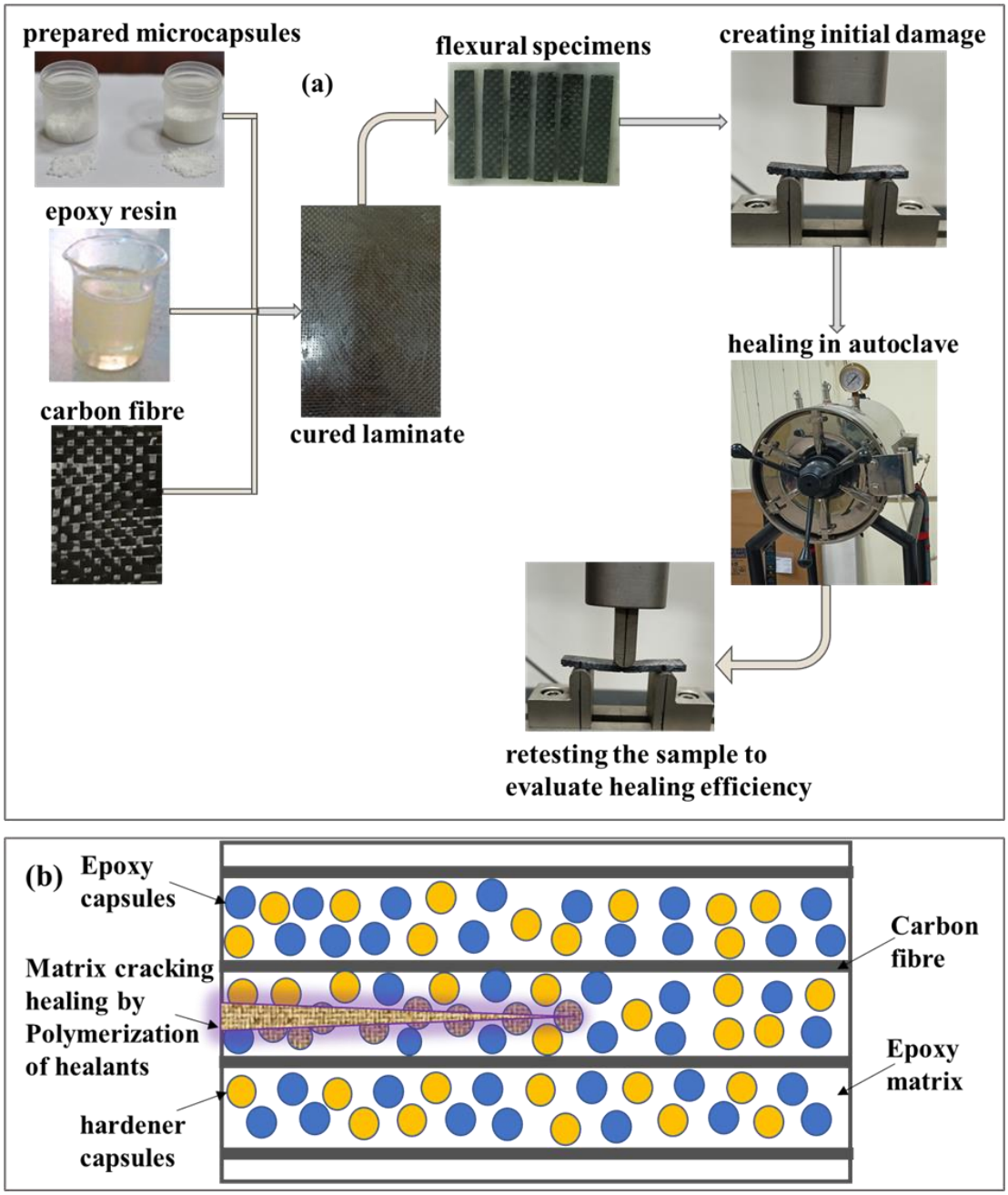

Figure 5.2 Schematic representation of (a) self-healing assessment procedure (b) matrix micro cracking healing in CFRP composite

Damaged samples were kept in Indfurr Autoclave (specifications: max. temperature: 200˚C, max. pressure: 60 PSI, Inert gas: Argon) and allowed to heal at different pressure and

temperatures. Effect of microcapsules concentration, healing temperature and healing pressure on the healing efficiency of 5, 10 and 15 wt% capsules reinforced CFRP composite were assessed based on the flexural strength recovery and using Eq.5.7.

5.3.3 Damping characterization

During service conditions composite structures experience vibrations and hence the damping characterization of self-healing composites is necessary and important to understand. In order to study the damping behavior of self-healing composites, Impulse excitation technique (IET) and flexural vibration mode is considered.

Basically, IET is an Impulse based non-destructive technique used to measure dynamic elastic properties of the material according to ASTM E 1876. IET uses resonant frequency to calculate the elastic modulus of the specimen and thus can also be used to characterize the damping behavior of the specimen. Figure 5.3 shows the schematic and experimental setup used in the present study. In this test setup, an impulse tool (excitation unit) was used to excite and induce the vibrations in the test specimen. A microphone senses these vibration signals and then passes to data acquisition system which finally passes to RFDA software. After reaching predefined convergence criterion, the software provides resonant frequency and amplitude decay constant of the measured vibrations. By using Eq.5.8 and Eq.5.10, dynamic elastic modulus and damping factor of the specimen can be evaluated. The distance between specimen supports, excitation location and microphone location were defined in accordance with sample dimensions and the flexural vibration configuration recommended by ASTM standard and shown in Figure 5.3 (c).

$$dynamic\ Elastic\ modulus(E) = 0.9465\frac{m\ {f_f}^2}{b}\left(\frac{L^3}{t^3}\right)T_1 \qquad \text{Eq.5.8}$$

For specimens with $L/t > 20$, T_1 can be calculated using

$$T_1 = \left[1.000 + 6.585\left(\frac{t}{L}\right)^2\right] \qquad \text{Eq.5.9}$$

$$damping\ \ factor\ \ (Q^{-1}) = \frac{K}{\pi\ f_f} \qquad \text{Eq.5.10}$$

Where m - mass of the specimen in g; b - width of the specimen in mm; t - thickness of the specimen in mm; L - Length of the specimen in mm; f_f - resonant frequency in Hz; T_1 - correction factor for flexural mode; Q^{-1} - damping factor; k - exponential decay parameter

relation between damping factor and damping ratio (ζ) can be given by $Q^{-1} = 2\zeta$. Eq.5.11

Damping factor or damping ratio describes how vibration signals of the system decay after the disturbance and is a measure of reduction in vibration signals due to energy absorption of the system. It also represents the internal friction of the specimen. Resonant frequency is an indirect indication of stiffness, mass and geometry of the specimen.

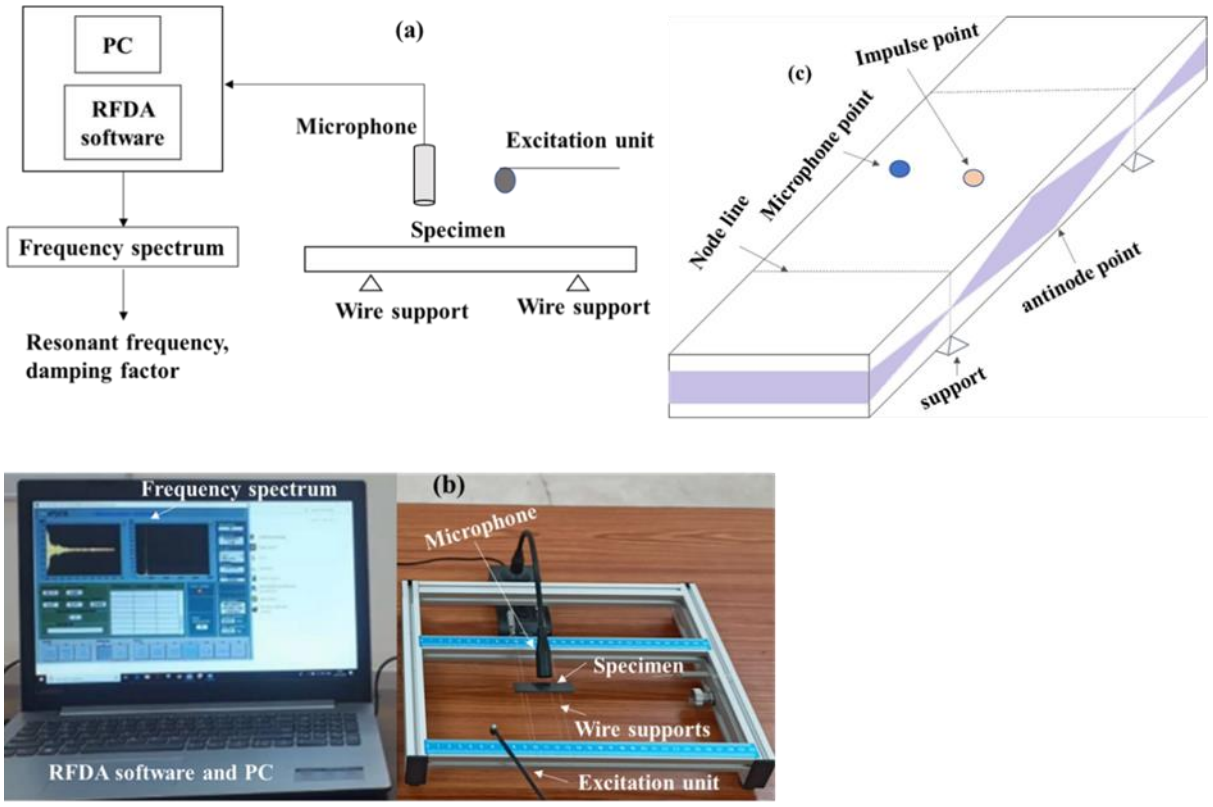

Figure 5.3 IET setup (a) schematic view (b) experimental setup (c) flexural vibration mode

To analyse the damping characteristics of capsules reinforced composite, two types of optimized composites i.e., 7.5 wt% capsules reinforced epoxy and 15 wt% capsules reinforced CFRP were considered. For each composite type, three types of samples virgin, damaged and healed samples were considered. Damaged samples were prepared by applying 70% of peak loads on the virgin samples. The same damaged samples were allowed to self-heal at 80°C for 4 hrs followed by room temperature healing for 24 hrs. For each sample type, three specimens were tested and the average results were reported.

5.3.4 Self-healing efficiency based on stiffness recovery

To assess structural integrity of the components stiffness is one of the important parameters to consider and hence in this study an attempt is made to evaluate the self-healing performance based on stiffness recovery. Static tests such as tensile and flexural tests provides elastic

modulus based on local strain values and hence can be called as local elastic modulus but to understand component stiffness behavior, a technique which provides the overall elastic modulus of the specimen is required. Since IET test satisfies this condition, the elastic modulus (which indirectly represents stiffness of the component) values obtained through IET test were considered to assess the self-healing performance of the composite.

Based on the obtained elastic modulus values, the healing efficiency(η) of the composite was calculated using Equation 5.12.

$$\eta = \frac{E_{Healed} - E_{Damaged}}{E_{Virgin} - E_{Damaged}} \qquad \text{Eq.5.12}$$

Where E_{Healed} - elastic modulus of the healed specimen; $E_{Damaged}$ - elastic modulus of the damaged specimen; E_{Virgin} - elastic modulus of the virgin specimen.

5.4 Results and Discussion

Effect of different healing conditions and microcapsules concentration on the self-healing efficiency of capsules reinforced CFRP composite are discussed in this section. Damping characterization and healing performance based on elastic properties recovery also discussed.

5.4.1 Effect of capsules wt% on the flexural strength of CFRP composite

To have structural applications developed composites should possess good mechanical properties and good self-healing performance. During service conditions, composite structures subject to flexural loads and hence it is important to understand the effect of capsules addition on the flexural strength of the composite. It can be noticed from the Figure 5.4(a) that pure CFRP composite had flexural strength of 534.87 MPa and with the increase in capsules concentration flexural strength of the composite decreased. With the addition of 5, 10 and 15 wt% capsules to pure CFRP, its flexural strength decreased from 534.87 MPa to 524.21, 516.83 and 495.77 MPa respectively. Flexural strength of the pure CFRP decreased by 1.99%, 3.37% and 7.31% with the addition of 5, 10 and 15 wt% microcapsules respectively. The decrease in flexural strength can be mainly attributed to two factors, increase in matrix viscosity and agglomeration. Mostly, with the increase in capsules wt% viscosity of the epoxy matrix increases and as a result micro voids, bubbles formed during fabrication may not be removed completely which in turn causes for reduction in flexural strength. Increased epoxy matrix viscosity also causes for reduction in the chances of complete wetting of the fibers and thus

can reduce the strength of the composite [103]. Agglomeration of capsules causes for stress concentration effect and thus can reduce the flexural strength of the composite [138].

To induce damages such as matrix microcracking and delamination, 350 N and 500 N respectively were applied on the composite and investigated for the effect of initial damages and capsules concentration on the flexural strength of the composite. Table 5.3 indicates the flexural strengths of matrix microcracked and delaminated capsules reinforced CFRP composites. D- matrix cracking represents samples subjected to 350 N damage load and then tested to flexural strength. Similarly, D- Delamination represents sample subjected to 500 N damage load and then tested to flexural strength. It is observed from the results that by applying the damage force of 350 N on the 5 wt% capsules reinforced composite, flexural strength of the composite reduced from 524.21 MPa to 410.25 MPa. This implies that the composite lost 21.73% of its initial flexural strength due to matrix cracking damage. Similarly, by applying the delamination damage load i.e., 500 N on the 5 wt% composite, its flexural strength reduced to 370.47 MPa which indicates 29.32% reduction in its initial strength. Likewise, the flexural strength of 10 wt% capsules reinforced CFRP composite reduced by 23.95% and 32.32% by applying the damage load of 350 N and 500 N respectively. Effect of initial damages on the flexural strength of the composites and the % reduction in their initial flexural strengths due to apply of matrix cracking, delamination damage loads can be observed from Figure 5.4(b).

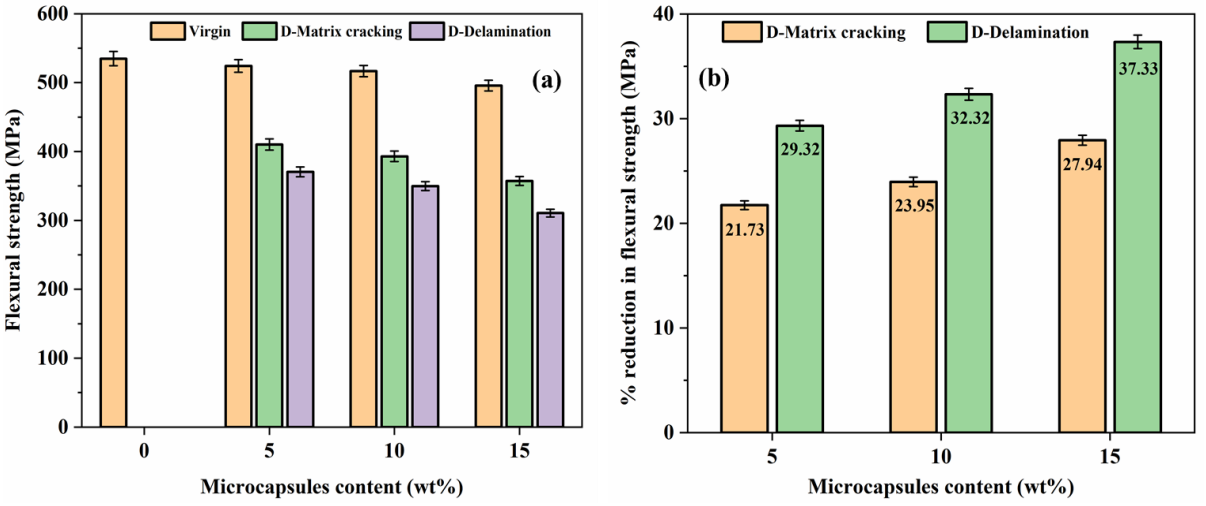

Figure 5.4 Effect of capsules wt% on the (a) flexural strength of virgin, damaged samples (b) % reduction of flexural strength in damaged samples

Table 5.3 Flexural strength of capsules reinforced CFRP composite

capsules wt%	Virgin Flexural strength (MPa)	D- Matrix cracking Strength (MPa)	D- Delamination Strength (MPa)
0	534.87	--	--
5	524.21	410.25	370.47
10	516.83	393.03	349.79
15	495.77	357.24	310.69

Since the microcapsules addition decreases the flexural strength of the composite, to create more damage volumes and thus to verify self-healing performance at worst conditions, damage loads which were obtained from the pure CFRP flexural test were considered to create matrix cracking and delamination in the capsules reinforced composites.

5.4.2 Effect of healing conditions on the flexural strength of self-healing CFRP composite

Figure 5.5 shows the stress-strain curves of 5 wt% capsules reinforced CFRP composite obtained from three point bending test. The damaged samples were kept in the autoclave and allowed to heal under various conditions like at room temperature (RT) for 48 hrs, at 80°C for 4 hrs followed by RT healing for 24 hrs, at 80˚C by applying 1 bar pressure for 4 hrs followed by RT healing for 24 hrs and at 80˚C by applying 2 bar pressure for 4 hrs followed by RT healing for 24 hrs. It can be noticed from the stress-strain curves that all the healed samples had greater stress-strain values than the damaged samples. This phenomenon indicates that the damages were healed and as a result developed increased crack resistance during retesting. Figure 5.5(c) indicates that the flexural strength of matrix cracking damaged sample increased from 410.25 MPa to 460.57 MPa after healing at RT for 48hrs. Similarly, after healing at 80˚C, (80˚C + 1 bar) and (80˚C + 2 bar) healing conditions, flexural strength of the composite increased from 410.25 MPa to 462.04 MPa, 464.87 MPa and 467.81 MPa respectively. For delamination damaged samples also similar kind of increasing trend was observed. The

flexural strength of the delamination damaged sample increased from 370.47 MPa to 441.66 MPa after healing at (80˚C + 2 bar) for 4hrs followed by healing at RT for 24hrs. Table 5.4 illustrates the effect of healing conditions on the flexural strength of 5 wt% capsules reinforced CFRP composite induced with matrix cracking and delamination damages. From the results it can be concluded that the healing at elevated temperature and external pressures increases the recovered flexural strength of the damaged samples.

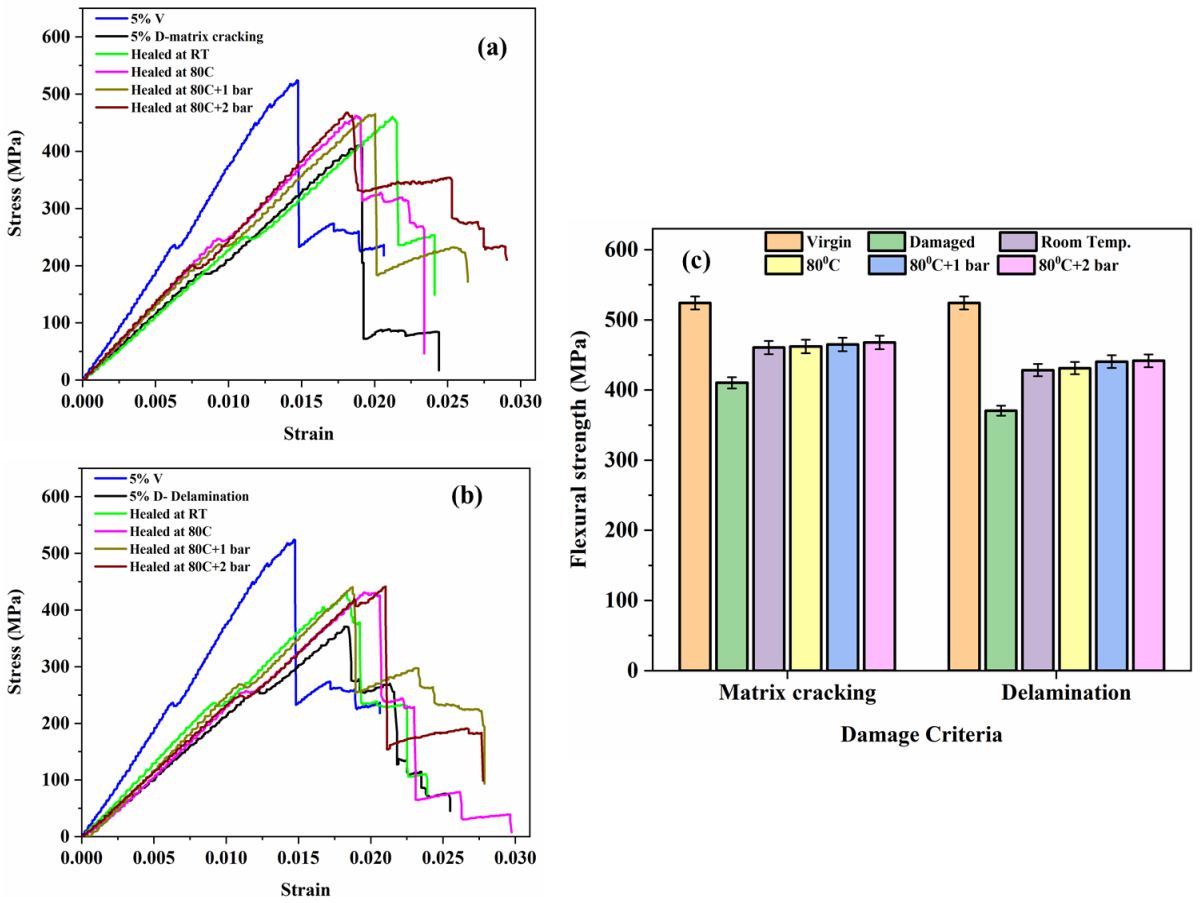

Figure 5.5 5 wt% capsules reinforced CFRP composite (a) stress - strain curves of samples healed for matrix cracking damage (b) stress - strain curves of samples healed for delamination damage (c) flexural strength of virgin, damaged and healed samples

In the stress-strain curves, 5% V indicates flexural strength of 5 wt% capsules reinforced virgin composite and can be noted as 524.21 MPa. 5% D-matrix cracking and 5% D-delamination represents flexural strength of matrix cracking damage induced and delamination damage induced 5 wt% capsules reinforced composite respectively.

Table 5.4 Flexural strength of 5 wt% capsules reinforced healed specimens

Healing condition	Healed samples flexural strength (MPa)	
	Matrix cracking	Delamination
RT	460.57	428.4
80°C	462.04	431.24
80°C + 1 bar	464.87	440.47
80°C + 2 bar	467.81	441.66

Figure 5.6 and Figure 5.7 represents the stress-strain curves of 10 wt% capsules and 15 wt% capsules reinforced CFRP composites obtained at different healing conditions. In both the cases all the healed samples showed greater stress-strain values than the damaged samples which confirm the successful healing of respective damages. It can be observed that the flexural strength of matrix cracking, delamination damage induced 10 wt% capsules reinforced composite increased from 393.03 MPa to 455.47 MPa and 349.79 MPa to 418.42 MPa respectively after healing at RT for 48 hrs. Compared to matrix cracking healed sample, delamination healed sample showed less flexural strength. This phenomenon can be attributed to incomplete filling of damaged surface due to requirement of more healing agent and time to heal delamination damage. With the increase in healing temperature from RT to 80˚C, flexural strength of matrix cracking healed 10 wt% capsules reinforced composite increased from 455.47 MPa to 461.32 MPa. This can be ascribed to at elevated temperatures viscosity of healing agent reduces and consequently more healing agent will be supplied to the crack plane to quickly heal the damaged surface and thus to get better flexural strength. Table 5.5 and Table 5.6 represents flexural strength of 10 wt% and 15 wt% capsules reinforced healed composites. Both matrix cracking, delamination damages healed samples showed higher flexural strengths at elevated temperature and external pressure conditions than the room temperature and without pressure healing conditions. Hence from the study it can be recommended that elevated temperature and pressures are ideal conditions to heal the composites.

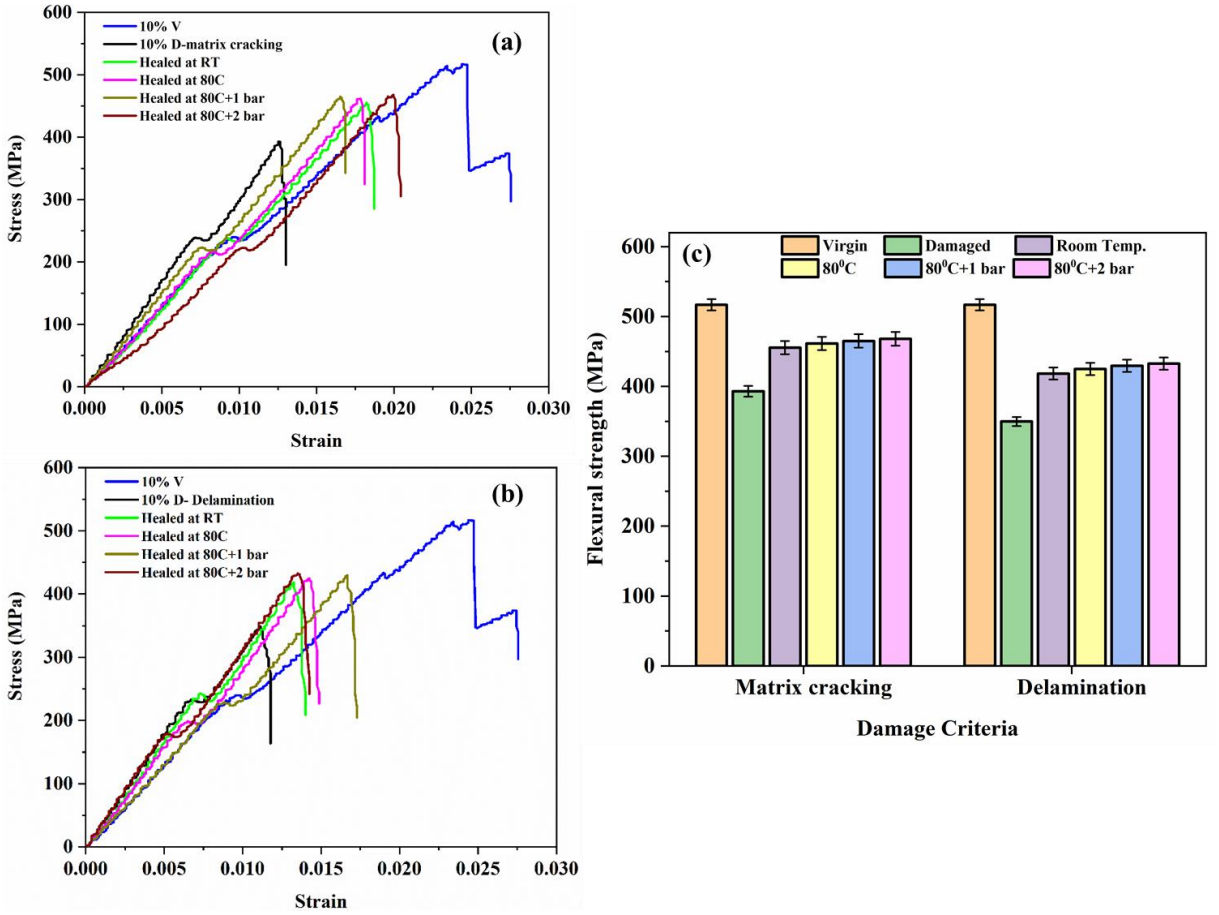

Figure 5.6 10 wt% capsules reinforced CFRP composite (a) stress - strain curves of samples healed for matrix cracking damage (b) stress - strain curves of samples healed for delamination damage (c) flexural strength of virgin, damaged and healed samples

Table 5.5 Flexural strength of 10 wt% capsules reinforced healed specimens

Healing condition	Healed samples flexural strength (MPa)	
	Matrix cracking	Delamination
RT	455.47	418.42
80°C	461.32	424.92
80°C+ 1 bar	465.01	429.46
80°C+ 2 bar	468.09	432.57

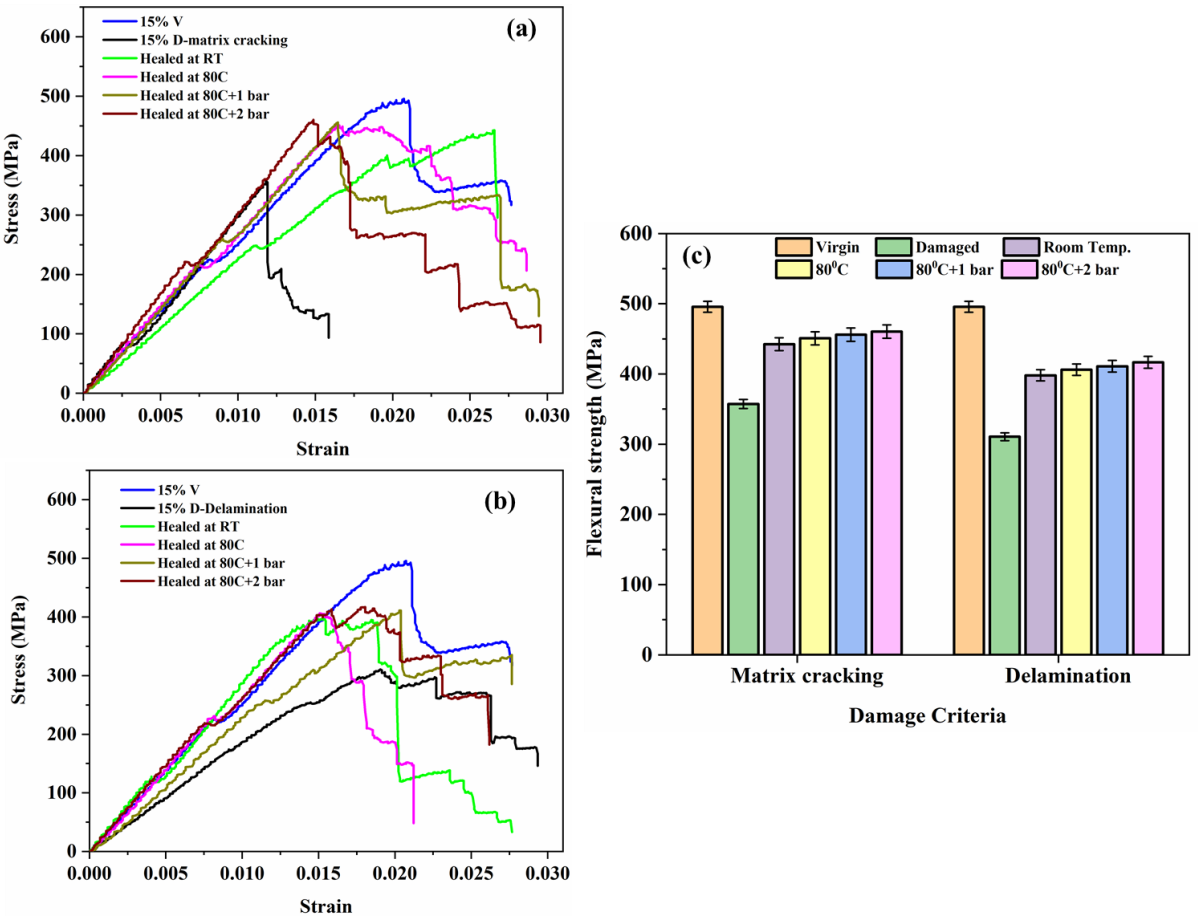

Figure 5.7 15 wt% capsules reinforced CFRP composite (a) stress - strain curves of samples healed for matrix cracking damage (b) stress - strain curves of samples healed for delamination damage (c) flexural strength of virgin, damaged and healed samples

Table 5.6: Flexural strength of 15 wt% capsules reinforced healed specimens

Healing condition	**Healed samples flexural strength (MPa)**	
	Matrix cracking	**Delamination**
RT	442.49	398.05
80°C	450.82	406.05
80°C+ 1 bar	456.02	411.04
80°C+ 2 bar	460.43	416.75

5.4.3 Fracture surface investigation of self-healing CFRP composite

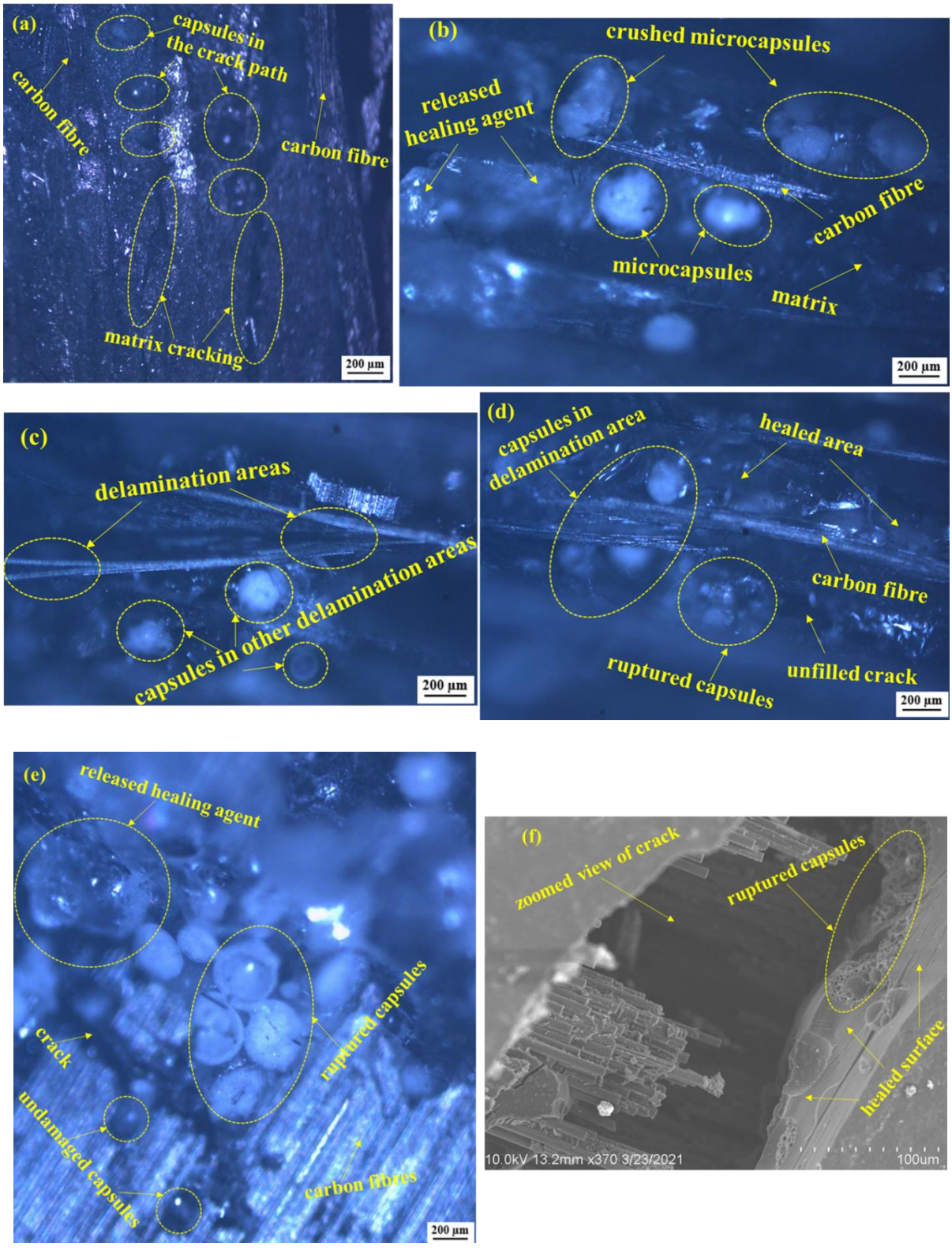

Figure 5.8 Fracture surface of 15 wt% capsules reinforced self-healing CFRP composite (a) after 350 N damage force applied (b) after matrix cracking healing (c) after 500N damage force applied (d) after matrix cracking healing (e) OM image - top view (f) SEM - top view

In order to visualize the matrix cracking and delamination damages induced in the composite and to verify the developed microcapsules ability to rupture, cracked surfaces were examined under 3D optical microscope and SEM. Matrix cracking and delamination damages induced in the composite due to apply of 350 N and 500 N can be observed from the Figure 5.8(a),(c) respectively. The damaged samples were kept intact using C- clamps and allowed to self-heal at 80˚C using Autoclave. The healed samples were re-examined after 48 hrs of healing period and found that the developed capsules were able to rupture and supply healing agent to the damaged surfaces. Healed surfaces, ruptured microcapsules and released healing agent can be observed in the Figure 5.8. It can be noticed from Figure 5.8(d) that few unfilled cracks were present in the delamination damage recovery. Thus, less flexural strength regain in delamination damage healed samples can be attributed to incomplete filling of crack surfaces. The crack path, interactions among carbon fibre, microcapsules and matrix surfaces can be clearly understood from Figure 5.8(e) and (f).

5.4.4 Effect of temperature on the self-healing efficiency of CFRP composite

In order to study the influence of elevated temperatures on the healing efficiency, capsules reinforced CFRP composites were induced with damages and allowed to self-heal at RT, 80˚C and assessed for healing efficiency according to Eq.5.7. According to Ghazali et al. [95] temperature range of 70˚C – 100°C is preferred for faster curing reaction between epoxy and hardener and hence 80˚C was selected to investigate the effect of elevated temperature on the healing efficiency.

It is observed that the healing efficiency increased for both matrix cracking and delamination damage recoveries with the increase in temperature from RT to 80˚C. This phenomenon can be mainly attributed to reduced viscosity of healing agents and faster curing reaction between released stoichiometric amount of healing agents. Since the developed microcapsules had average size in the range of 60 μm they can be easily dispersed into the fibre rich regions and thus can heal the damages effectively. It can be noticed from Table 5.7 that due to healing at elevated temperature the healing efficiency of 10 wt% capsules reinforced composite increased from 50.43% to 55.16% and 41.08% to 44.97% for matrix cracking and delamination damage recoveries respectively. Since delamination damage is a severe damage sometimes rupture and breakage of fibres may happen during loading and thus less healing efficiencies of delamination damage recoveries can be attributed to unfilled cracks and healing agents inability to heal ruptured and broken carbon fibres [139]. By increasing the capsule wt%

this reduction in healing efficiencies can be addressed and the same can be evident from Figure 5.9. For matrix cracking, delamination damage recovery, healing efficiency of 15 wt% capsules reinforced composite increased from 61.53% to 67.55% and 47.20% to 51.52% with the increase in healing temperature from RT to 80˚C. For same wt% capsules and same damage type, higher healing efficiencies were obtained at elevated temperature and hence 80˚C is considered as the healing temperature in the further study.

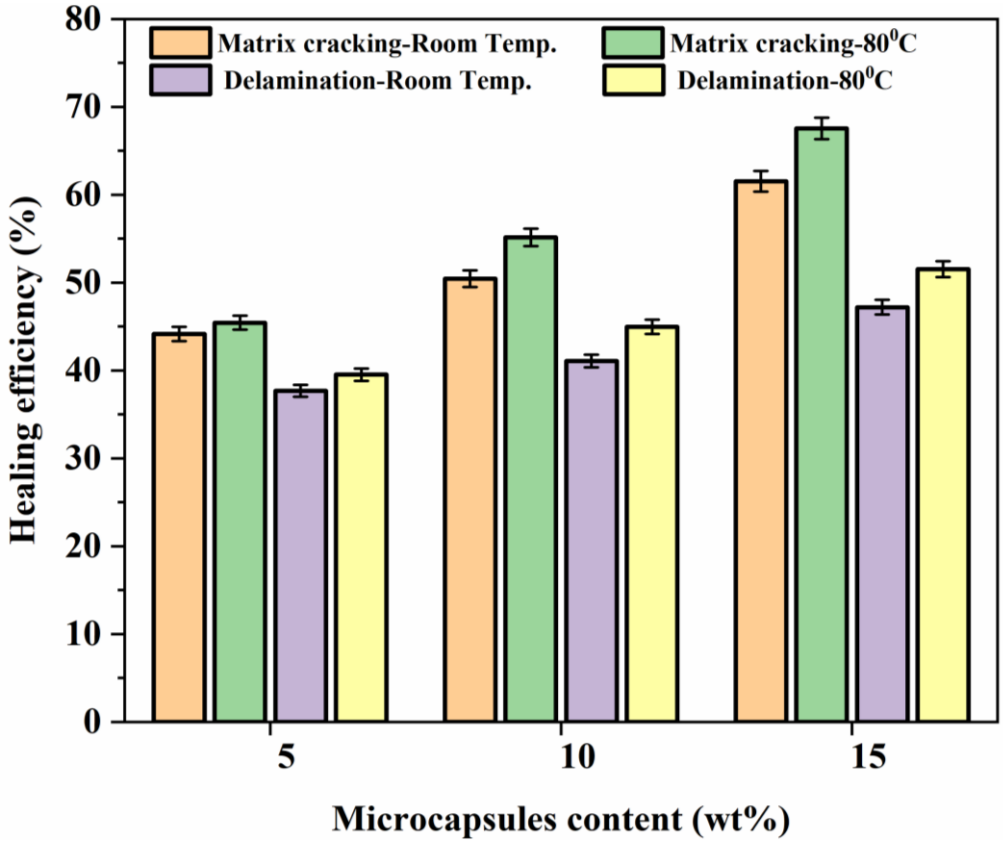

Figure 5.9 Effect of temperature on the self-healing efficiency of CFRP composite

Table 5.7 Healing efficiency of capsules reinforced CFRP composite at RT and 80˚C

capsules wt%	matrix cracking		delamination	
	RT	80˚C	RT	80˚C
5	44.15	45.44	37.68	39.52
10	50.43	55.16	41.08	44.97
15	61.53	67.55	47.20	51.52

5.4.5 Effect of pressure on the self-healing efficiency of CFRP composite

In order to verify the effect of pressure on the healing efficiency of composite, 1 bar and 2 bar pressures were applied at 80˚C and evaluated for healing performance enhancement. Figure 5.10(a) proves that for matrix cracking damage recovery, healing efficiency of 15 wt% capsules reinforced composite increases from 67.55% to 71.30% and to 74.48% by applying a healing pressure of 1 bar and 2 bar respectively. The assistance of external pressure can reduce the crack width during healing and thus requires less healing agent to heal the crack compared to healing condition without external pressure [135]. Table 5.8 shows the effect of healing pressure on the self-healing efficiency of 5, 10 and 15 wt% capsules reinforced CFRP composites. It is observed that for both matrix cracking recovery and delamination recovery, healing efficiency increased with the increase in capsules concentration and with the aid of external pressure. Maximum healing efficiencies were obtained at 15 wt% capsules concentration, 80˚C + 2 bar healing condition and shown in Figure 5.10(b). It can be noted from the results that the maximum healing efficiency obtained for matrix cracking recovery is 74.48% and for delamination recovery is 57.30%. But with the increase in healing pressure from 1 bar to 2 bar, in most of the cases, the increase in healing efficiency is restricted to < 5%. Hence, 1 bar pressure is suggested as an ideal pressure to heal the composites. Compared to cracking, delamination damages are severe damages and hence to heal those damages and to achieve good healing efficiencies applying external pressure is necessary. Finally, from this study it can be recommended that 15 wt% capsules concentration and 80˚C + 1 bar healing conditions are ideal to fabricate capsules reinforced CFRP composite.

Table 5.8 Effect of healing pressure on the self-healing efficiency of CFRP composite

Pressure	**Matrix cracking**			**Delamination**		
	5%	**10%**	**15%**	**5%**	**10%**	**15%**
0	45.44	55.16	67.55	39.52	44.97	51.52
1	47.92	58.14	71.3	45.53	47.69	54.21
2	50.5	60.63	74.48	46.03	49.55	57.30

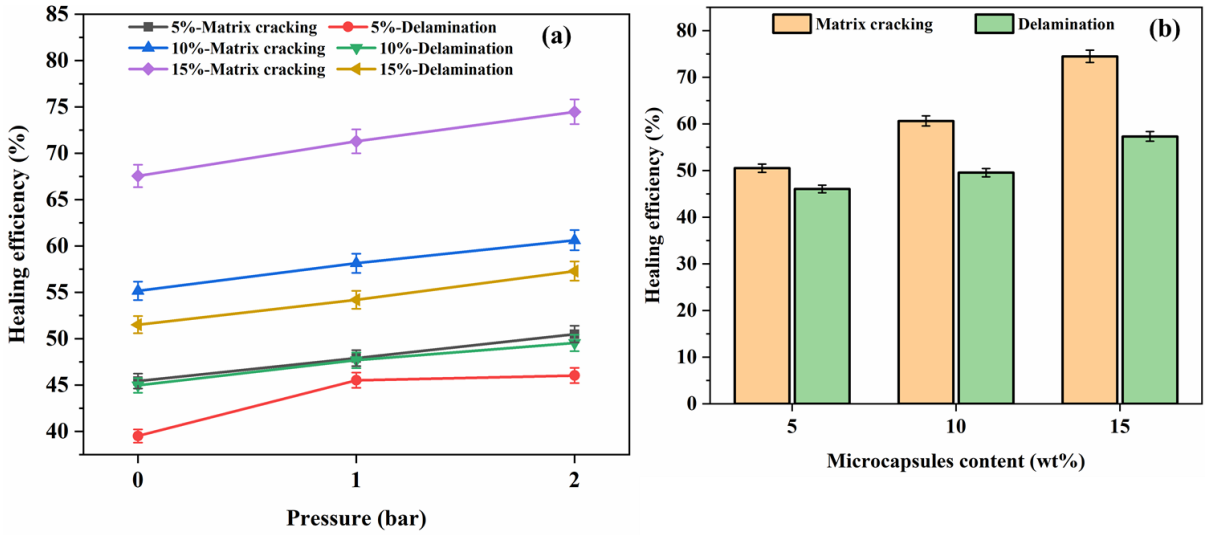

Figure 5.10 Effect of healing conditions on the self-healing efficiency of capsules reinforced CFRP composite (a) pressure (b) microcapsules concentration

5.4.6 Microstructural investigation of self-healing CFRP composite

In order to understand the mechanisms of self-healing behavior, fracture surfaces of 15 wt% capsules reinforced CFRP composite were examined under microscope and shown in Figure 5.11. The mechanisms such as crack pinning, crack path deflection and microcapsules rupture were observed. Generally crack pinning mechanism blocks the crack path and thus helps to retard the failure of the component. Sometimes crack is forced to change its path due to presence of filler materials such as microcapsules and thus requires additional energy for fracture. This phenomenon also helps to retard the failure and can be observed in the Figure 5.11. Crack, during its propagation either deflects the capsule or ruptures it. The former case causes for crack path deflection and the latter case causes for microcapsule rupture. Whenever microcapsules subject to rupture healing agent will be released from the capsules and heals the damage by polymerization reaction between released healants. Number of ruptured microcapsules, released healing agent and healed surfaces can be observed in the Figure 5.11. Capsules pull out, a mechanism which indicates the weaker interfacial adhesion between matrix and microcapsules was not observed in the fracture surface of composite and hence it can be concluded that the developed capsules had good bonding with matrix material. The adhesion bonding among carbon fibres, microcapsules and epoxy matrix can be observed in the Figure 5.11.Thus from the study it is understood that crack pinning, crack path deflection and microcapsules rupture are the mechanisms behind the self-healing performance of the capsules reinforced CFRP composite.

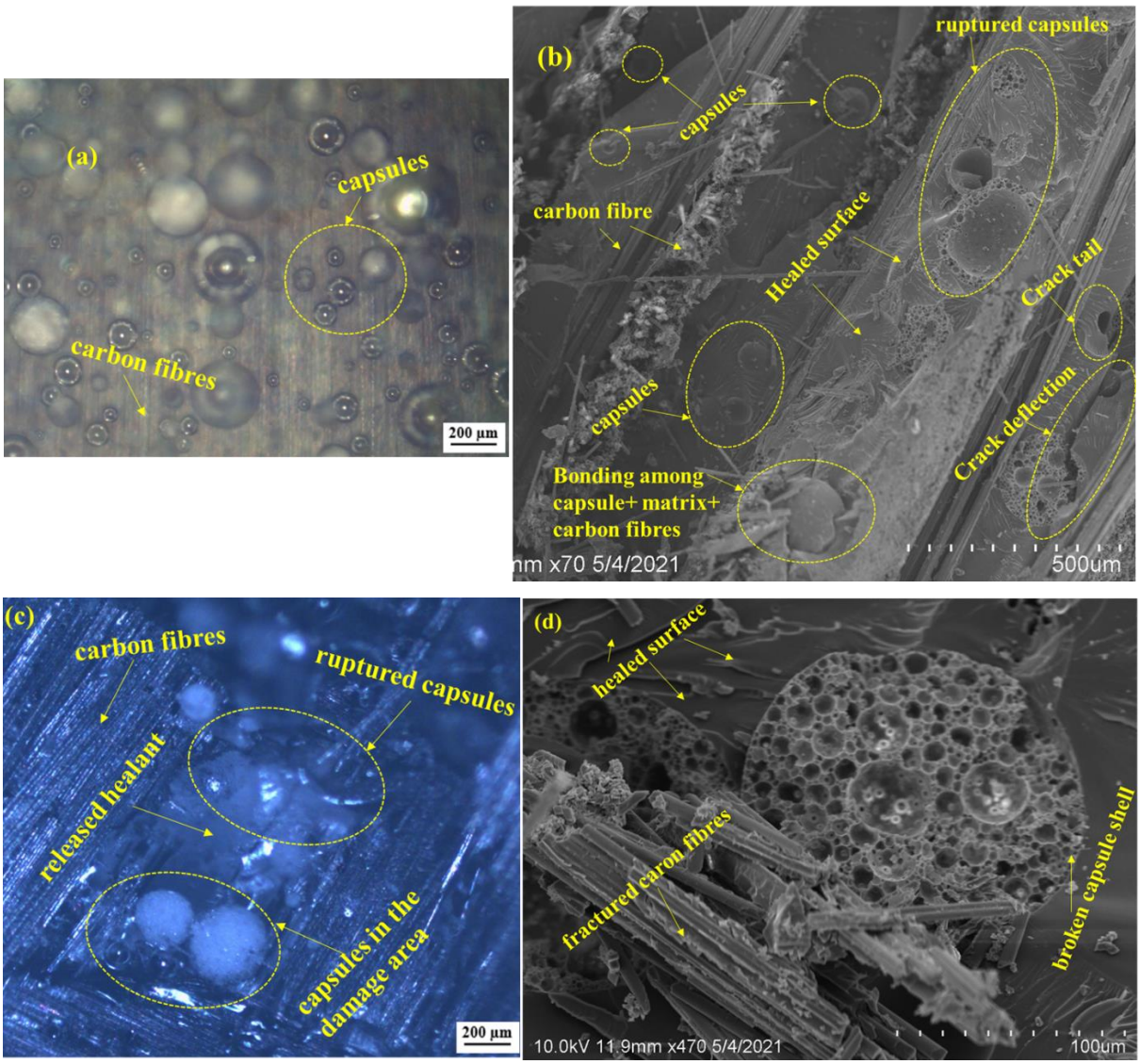

Figure 5.11 Micrographs of 15 wt% capsules reinforced CFRP composite (a) microcapsules distribution on top of carbon fibre (b) fractured surface side view - SEM image (c) fractured surface side view - OM image (d) healed surfaces

5.4.7 Damping characterization of pure epoxy and pure CFRP

As IET technique provides elastic modulus as a function resonant frequency, by validating the elastic modulus results, reliability of the IET test results can be verified. Thus, to verify the reliability of the results obtained through IET, elastic modulus of pure epoxy and pure CFRP composite obtained through IET test and standard flexural test were compared. It can be observed from the Table 5.9 that the results obtained through IET test were in the same range as results obtained through flexural test and well within the acceptable limits. Hence, the elastic modulus and damping factors obtained through IET test for capsules reinforced self-healing CFRP composites were considered for further analysis.

The little difference between the results obtained from two different techniques can be attributed to strain rate effect and intrinsic inhomogeneity of the composite materials. Moreover, the elastic modulus obtained through IET test represents overall elastic modulus and the elastic modulus obtained through flexural test depends on the local strain effect and hence represents local elastic modulus.

Table 5.9 Elastic modulus of pure epoxy and CFRP obtained through IET and flexural test

Composite type	Elastic modulus (GPa)	
	Through IET	Through flexural test
Pure Epoxy	3.97	3.26
Pure CFRP	48.15	45.18

5.4.8 Damping characterization of dual capsules reinforced epoxy/CFRP composite

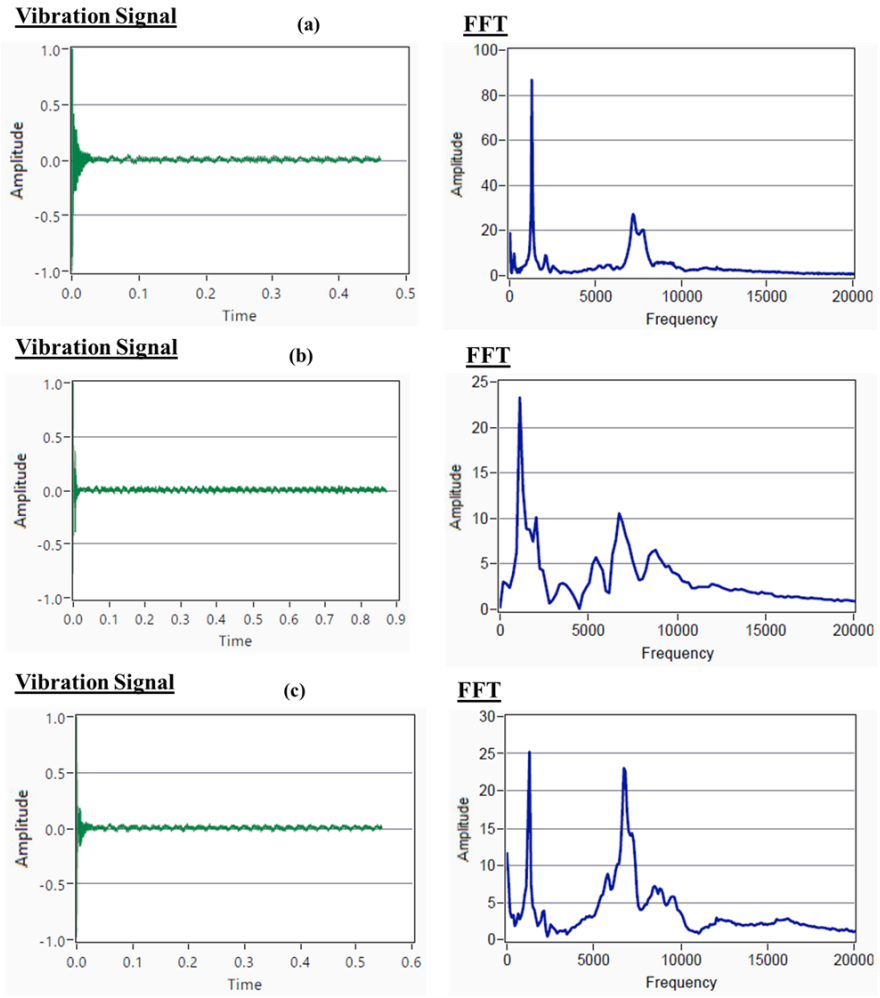

Figure 5.12 Time domain and frequency domain spectrums of capsules reinforced epoxy composite (a) virgin (b) damaged (c) healed

Figure 5.12 and Figure 5.13 shows the vibration signals and the respective frequency spectrums of capsules reinforced virgin, damaged and healed epoxy/CFRP composite. It can be observed from the results that the resonant frequency of pure epoxy and pure CFRP decreases with the addition of microcapsules. This can be attributed to increased dissipation of vibrational energy due to addition of capsules. It is noted that the resonant frequency of the damage induced composite is lower than the resonant frequency of the capsules reinforced both virgin and healed composites. Same trend was observed for both epoxy and CFRP composites and can be attributed to microcracks present in the damaged composite.

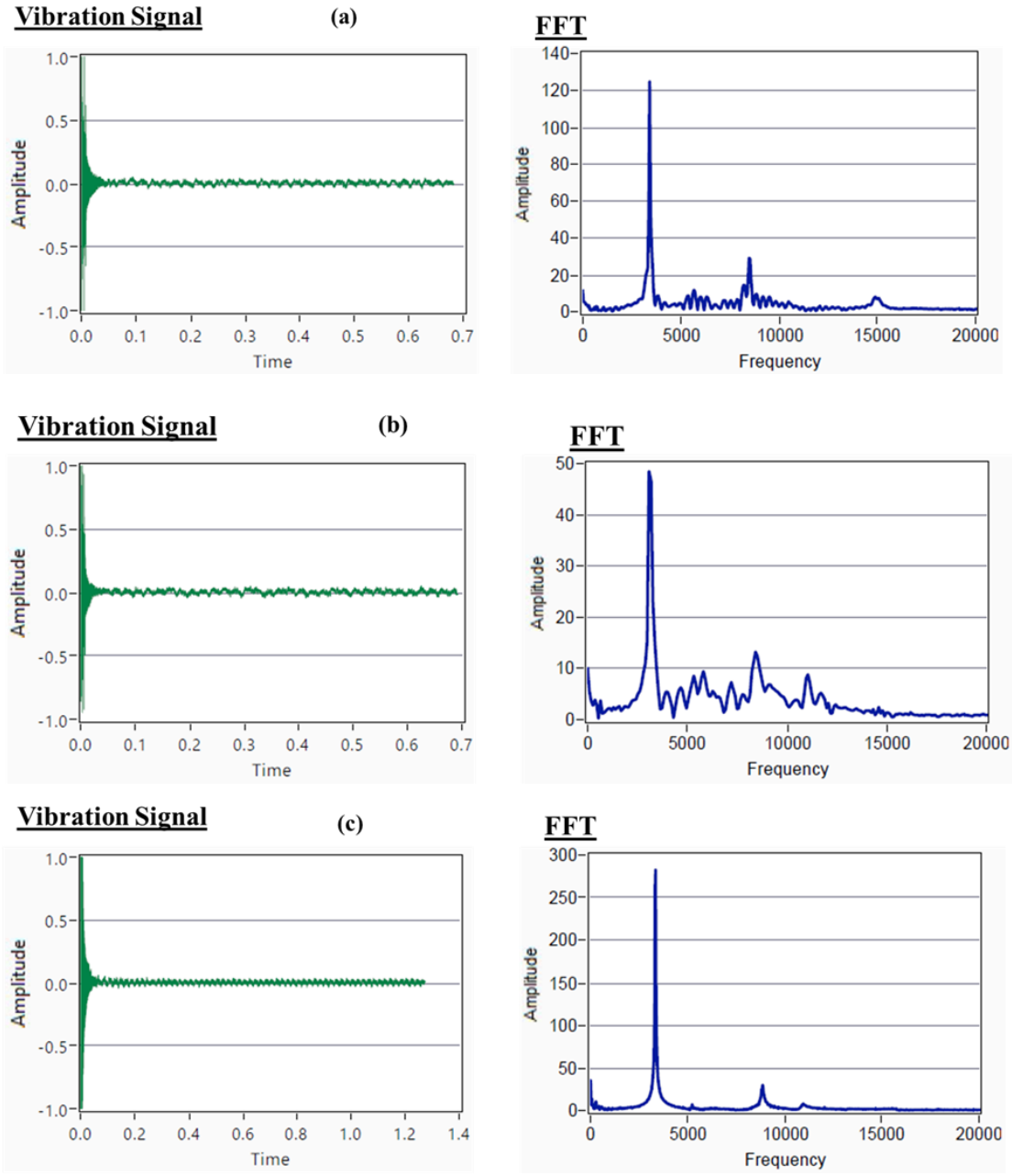

Figure 5.13 Time domain and frequency domain spectrums of capsules reinforced CFRP composite (a) virgin (b) damaged (c) healed

Elastic modulus and damping factor of the composite were calculated by employing Eq.5.8 and Eq.5.10 in the respective frequency domain signals of the composites. Figure 5.14 shows the damping factor of capsules reinforced epoxy and CFRP composites. It can be observed from the results that the addition of capsules increases the damping factor of both types of composites. Damping factor of pure epoxy increased from 0.0148 to 0.0231 and pure CFRP increased from 0.0029 to 0.0105 with the addition of optimized 7.5 wt% and 15 wt% capsules respectively. The addition of capsules into epoxy increases the energy absorption capacity of the composite and hence the increase in damping factor can be noticed. In addition to capsules wt%, the damping factor also influences by the viscoelastic nature of the epoxy and the interfacial bonding between microcapsules and matrix. Compared to virgin samples, the damping factor of damaged samples increased in both types of composites and can be ascribed to micro cracks generated during damage creation. Generally, defects such as micro voids, dislocations and various interfaces propagate or subject to slippage during vibrations and thereby helps in dissipating vibration energy [140,141]. Thus, the increase in damping factor of damaged samples can be attributed to dissipation of vibration energy at defects. In both the composites, healed samples had less damping factor than the damaged samples and can be attributed to recovered microcracks during the healing process. As natural frequency of pure CFRP is higher than the natural frequency of pure epoxy, the less damping factor of pure CFRP compared to pure epoxy can be attributed to CFRP's natural frequency. Resonant frequency and damping factors of both types of composites can be observed from Table 5.10.

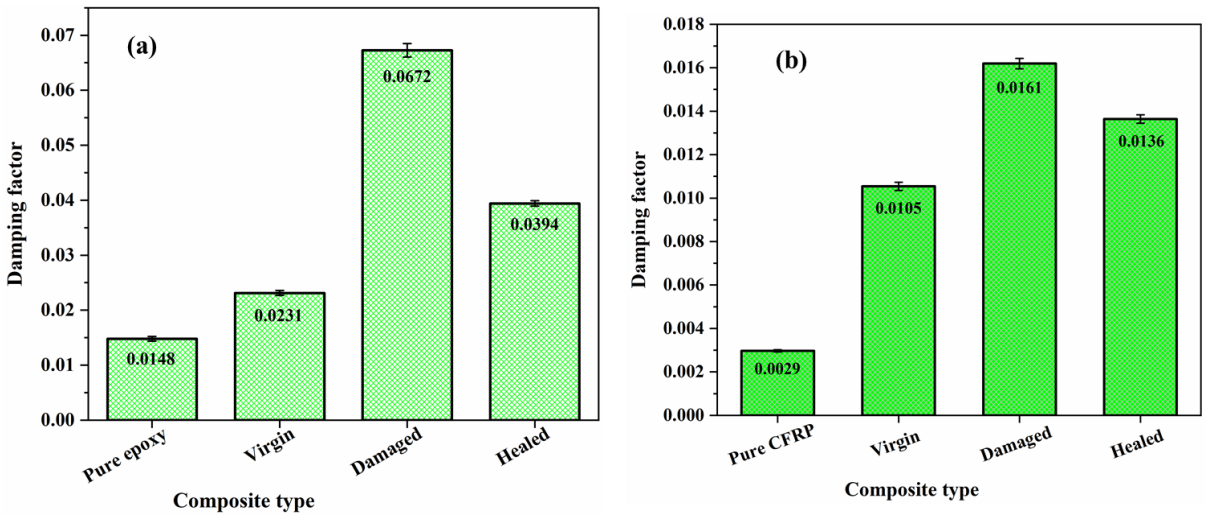

Figure 5.14 Damping factors of (a) capsules reinforced epoxy (b) capsules reinforced CFRP

Table 5.10 Resonant frequency and damping factor of capsules reinforced epoxy/CFRP

Composite type	Resonant frequency (Hz)	Damping factor	E (GPa)
Pure Epoxy	1360.65	0.0148±0.0004	3.97±0.07
(7.5 wt% + epoxy) V	1318.55	0.0231±0.0004	3.42±0.06
(7.5 wt% + epoxy) D	1192.29	0.0672±0.0012	2.74±0.05
(7.5 wt% + epoxy) H	1272.43	0.0394±0.0005	3.23±0.06
Pure CFRP	4248.15	0.0029±0.0001	48.15±0.84
(15 wt% + CFRP) V	3413.08	0.0105±0.0001	24.84±0.43
(15 wt% + CFRP) D	3135.37	0.0161±0.0002	20.54±0.35
(15 wt% + CFRP) H	3365.89	0.0136±0.0001	22.85±0.38

5.4.9 Self-healing efficiency evaluation of dual capsules reinforced epoxy/CFRP composite

Figure 5.15 shows the effect of microcapsules addition on the elastic modulus of pure epoxy and pure CFRP. With the addition of capsules, the elastic modulus of both pure epoxy and pure CFRP decreased and can be mainly attributed to incorporation of low modulus (2.68GPa) PMMA capsules into high modulus (3.3GPa) epoxy matrix. Interfacial bonding and the interactions between microcapsules and matrix also affects the elastic modulus of the composite. It can be observed from the Figure 5.15 that the elastic modulus of the capsules reinforced virgin epoxy decreased from 3.42 GPa to 2.74 GPa and capsules reinforced virgin CFRP decreased from 24.84 GPa to 20.54 GPa respectively. This decrement can be attributed to loss of stiffness due to induced damage. After self-healing at 80˚C, the elastic modulus of the damaged epoxy composite and damaged CFRP composite increased to 3.23 GPa and 22.85 GPa respectively. The increase in elastic modulus of the healed composites can be attributed to recovered microcracks during healing. Due to higher flexural stiffness of the carbon fibres, Pure CFRP had higher elastic modulus than the pure epoxy.

Self-healing efficiency of capsules reinforced epoxy/CFRP composites based on elastic modulus (which indirectly represents stiffness) recovery were calculated using Eq.5.12 and shown in Figure 5.15(c). It was observed that capsules reinforced epoxy and CFRP composites

had healing efficiencies of 72.05% and 53.72% respectively. In order to validate the results, healing efficiencies obtained through stiffness recovery were compared with healing efficiencies obtained through static tests such as mode I fracture test and flexural test and shown in Figure 5.15(c). It can be observed from the results that the healing efficiencies obtained through IET test (72.05% and 53.72%) were comparable to healing efficiencies obtained through mode I fracture test (71.35%) and flexural test (51.52%). Hence, it can be concluded from the study that the IET approach can be used to evaluate the healing performance of the composites based on stiffness recovery. The difference in healing efficiencies obtained through two different approaches can be attributed to difference in healing efficiency evaluation criteria, their corresponding properties and testing procedures.

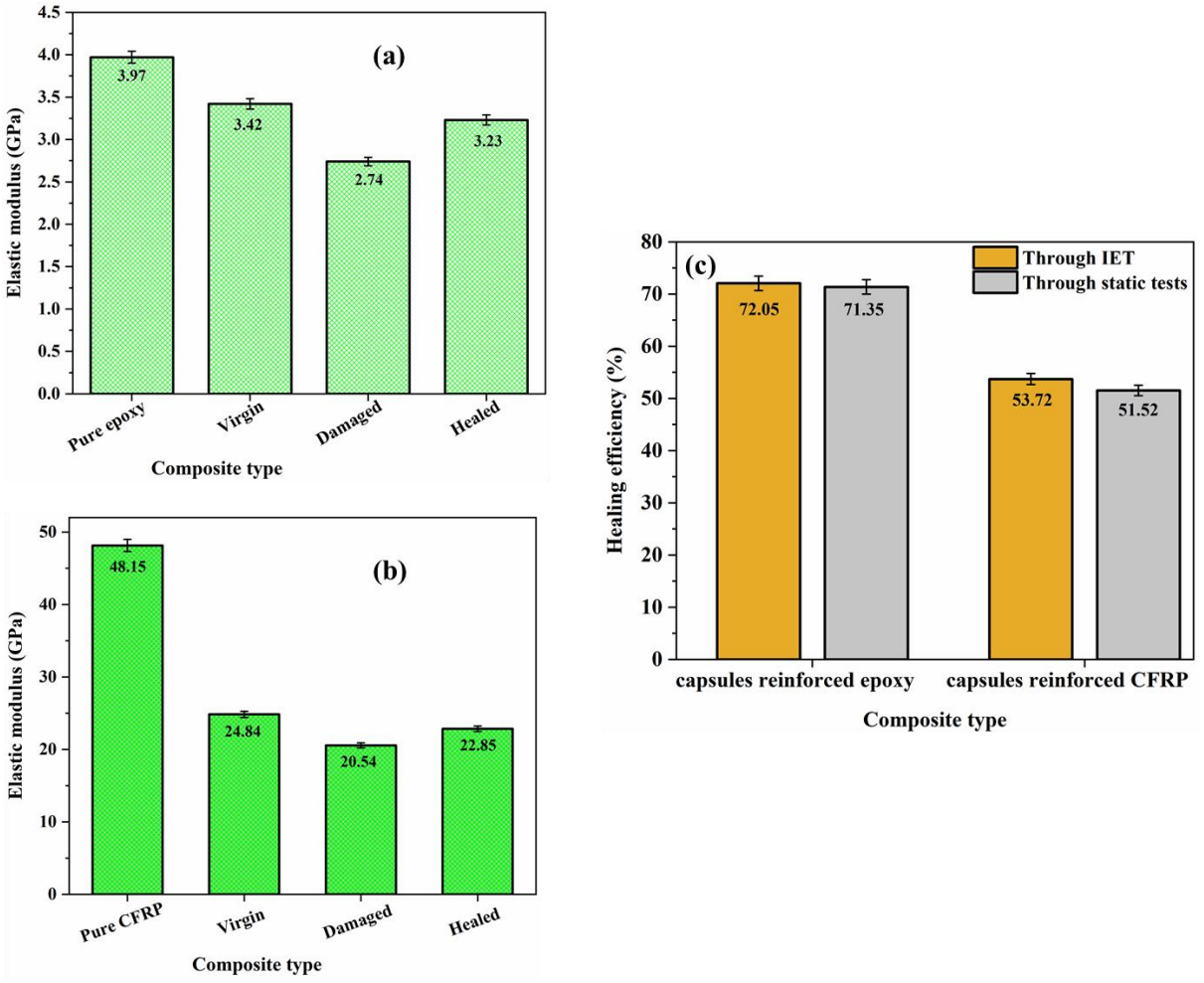

Figure 5.15 Elastic modulus of (a) capsules reinforced epoxy (b) capsules reinforced CFRP (c) healing efficiency of capsules reinforced epoxy and CFRP composite

5.5 Conclusions

Epoxy resin, amine hardener encapsulated capsules reinforced CFRP composites were fabricated and evaluated for damping characterization and self-healing performance. Effect of initial damages induced, microcapsules concentration, healing temperature and healing pressure were investigated to optimize the healing performance. self-healing efficiency was evaluated based on the flexural strength regain and stiffness recovery. The following conclusions can be drawn from the study.

- Effect of microcapsules concentration on the flexural strength of CFRP composite was investigated by reinforcing the capsules at 5, 10 and 15 wt% and found that flexural strength of CFRP decreases from 534.87 MPa to 495.77 MPa with the addition of 15 wt% microcapsules.
- Matrix cracking, delamination damages were induced in the self-healing composite and the flexural strength recovery was investigated at different healing conditions.
- Healing efficiency of CFRP composite increases with the increase in capsules concentration and found to be optimum at 15 wt%
- Effect of healing temperature on the self-healing efficiency of the composite was investigated and found that for 15 wt% capsules addition, healing efficiency increased from 61.53% to 67.55% with the increase in healing temperature from RT to 80˚C.
- Healing efficiency of 15 wt% capsules reinforced CFRP increased from 67.55% to 71.30% and from 51.52% to 54.21% for matrix cracking, delamination damages recovery respectively by healing at (80˚C + 1 bar) healing condition.
- 15 wt% of capsules concentration and (80˚C + 1 bar) healing condition were recommended to fabricate capsules reinforced CFRP composite.
- Microstructural investigation of fractured surface of CFRP composite showed fracture mechanisms such as crack pinning, crack path deflection and microcapsules rupture.
- Damping characterization of capsules reinforced epoxy, capsules reinforced CFRP were investigated using Impulse excitation technique (IET) and found that the damping factor of pure epoxy, CFRP increases with the reinforcement of microcapsules.

- Compared to capsules reinforced virgin composite, the damping factor of damaged and healed composites increased and can be attributed to increased dislocations and increased surface area respectively.
- Self-healing efficiency of the capsules reinforced epoxy, capsules reinforced CFRP composite was assessed based on stiffness recovery using IET technique and found to be 72.05% and 53.72% respectively.
- Healing efficiencies obtained through IET technique were comparable and well within the acceptable limits to healing efficiencies obtained through mode I fracture test and flexural test. Hence IET approach can be used to evaluate the healing performance of the composites based on stiffness recovery.

Chapter 6

Numerical studies on microcapsules mechanical strength and stress distribution at mode I fracture crack front

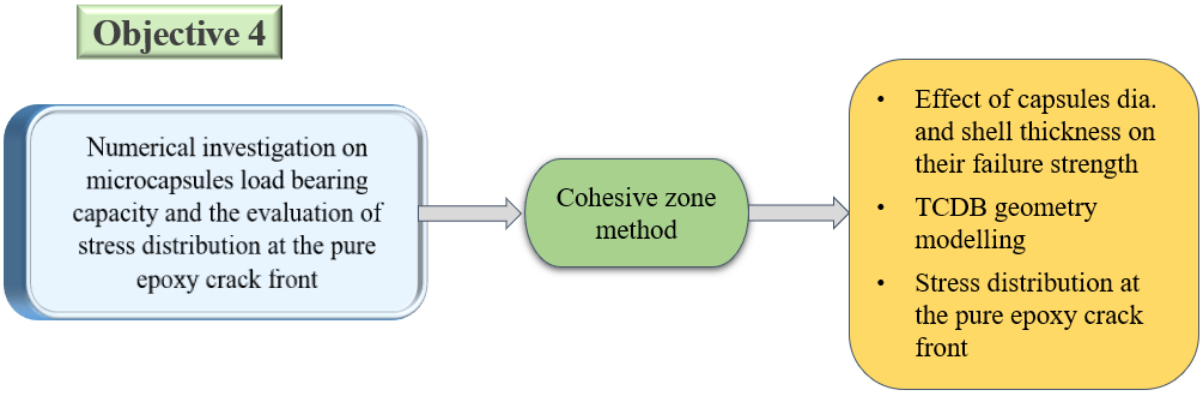

This chapter deals with the modelling of PMMA microcapsules, effect of microcapsule diameter and shell thickness on their mechanical strength. Crack propagation pattern in TDCB specimen during mode I fracture test and the stresses generated at the epoxy matrix crack front are discussed.

6.1 Introduction

Eventually polymer composites develop cracks during their service life and thus may not fulfil their intended functionality if the crack is not revamped. The invisible microcracks which are not possible to repair can be addressed through a bio inspired technology such as capsules based self-healing approach. In this approach, healing agent encapsulated microcapsules will be embedded into epoxy matrix and then allowed to cure either at room temperature or at elevated temperatures. Whenever the crack intercepts the microcapsules, they subject to rupture and releases the liquid healing agent into the crack surfaces by capillary action and then polymerizes the crack by reacting with either catalyst or another liquid healing agent.

An optimal combination of microcapsule average diameter and shell thickness are crucial to guarantee the mechanical triggering and repair of the damaged component. Capsules with high shell thickness will not rupture easily and thus prevents the release of healing agent. Conversely, if the shell thickness is too thin, the healing agent may be lost in the matrix during the mixing of microcapsules with matrix material. Thus, indirectly the shell thickness of microcapsule decides the amount of healing agent available to repair the crack. In addition, mechanical properties of the microcapsules such as failure strength, hardness and elastic modulus depends on the type of shell material and its thickness. Hence, in order to have better self-healing performance, it is important to investigate the effect of shell material and its thickness on the failure strength of the microcapsules. Experimental techniques such as micromanipulation, micropipette aspiration, tweezers, Atomic Force Microscope (AFM) and nanoindentations were available to evaluate the failure strength and elastic modulus of the single microcapsule [83,142].

Microcapsules with different core material and shell material were experimented to evaluate their failure strength. Sun et al. [143] investigated the mechanical strength of microcapsules synthesized with different shell materials such as urea formaldehyde, melamine formaldehyde and gelatin using micromanipulation technique and concluded that the rupturing force required to break the capsules is dependent on the diameter of the capsules. Few researchers [86,144,145] investigated the force-displacement profiles of the microcapsules by

compressing them till failure and evaluated the mechanical strength of the capsules. Ahangaran et al. [146] calculated the hardness and elastic modulus of epoxy encapsulated and mercaptan encapsulated PMMA microcapsules using nano indentation technique. They concluded that the elastic modulus and hardness are highly dependent on the average molecular weight of the PMMA and the core material that is encapsulated.

In addition to above mentioned techniques, few researchers [147–149] used XFEM technique to estimate the mechanical strength of the microcapsules. Mercade et al. [85] studied the stress-strain behaviour of core-shell microcapsules using FEM and micromanipulation compression techniques. Elastic-perfectly plastic deformations with and without strain hardening effect were studied and the failure stress, failure strain of melamine formaldehyde microcapsules were estimated. Few authors [86,150,151] verified the experimental mechanical properties of the perfume oil encapsulated single PMMA microcapsule, DCPD encapsulated single urea formaldehyde capsule using FEM. Microcapsules with different shell thickness to radius ratio were investigated and concluded that thin shell microcapsules have clear bursting point whereas thick shell capsules did not have any clear bursting point. In few numerical studies, cohesive zone crack model [152] and Hertz model [86] were employed to simulate the load-displacement profiles of the different self-healing materials.

Though it is important to know the failure strength of the developed microcapsules, very few studies [86,146] discussed the failure strength of PMMA microcapsules. Stresses developed in the matrix material and the failure strength of the microcapsules are important to design the self-healing system. Hence, in this study an attempt is made to investigate the effect of microcapsules diameter and shell thickness on its failure strength. In FEM, different combinations of materials and loads which are difficult to measure through experiments can be modelled and evaluated. Hence in this study FEM is chosen to estimate the strength of PMMA microcapsules.

Several experimental and numerical studies [63,66,153,154] evaluated the self-healing performance of epoxy systems based on fracture toughness recovery using TDCB specimens. To design self-healing system, it is important to understand how crack propagates in the TDCB specimen during mode I fracture test. Hence, in this study an attempt is made to investigate crack propagation and the stresses developed at the crack front.

6.2 Methodology

Procedure followed to develop model, material properties, boundary conditions and meshing techniques used in the analysis are discussed in this section.

6.2.1 Development of Model

PMMA microcapsules and pure epoxy TDCB specimens were modelled using Abaqus V 6.13 software. Microcapsules of diameter 100, 200, 300 µm and shell thickness of 5, 8, 10 µm were modelled. TDCB geometry discussed in the section 4.3.2.2 is modelled with same dimensions.

Modelling of TDCB geometry divided into three steps. (i) modelling of upper and lower parts. (ii) modelling of cohesive layer.(iii) assembly of cohesive layer to upper and lower parts. As shown in Figure 6.1, TDCB geometry had symmetry w.r.t to XZ plane hence only upper part was modelled and lower part was obtained by mirroring the upper part. In order to study crack propagation, a cohesive layer of thickness 0.2 mm was considered .Surface to point contact was used to assemble cohesive layer with upper and lower parts.

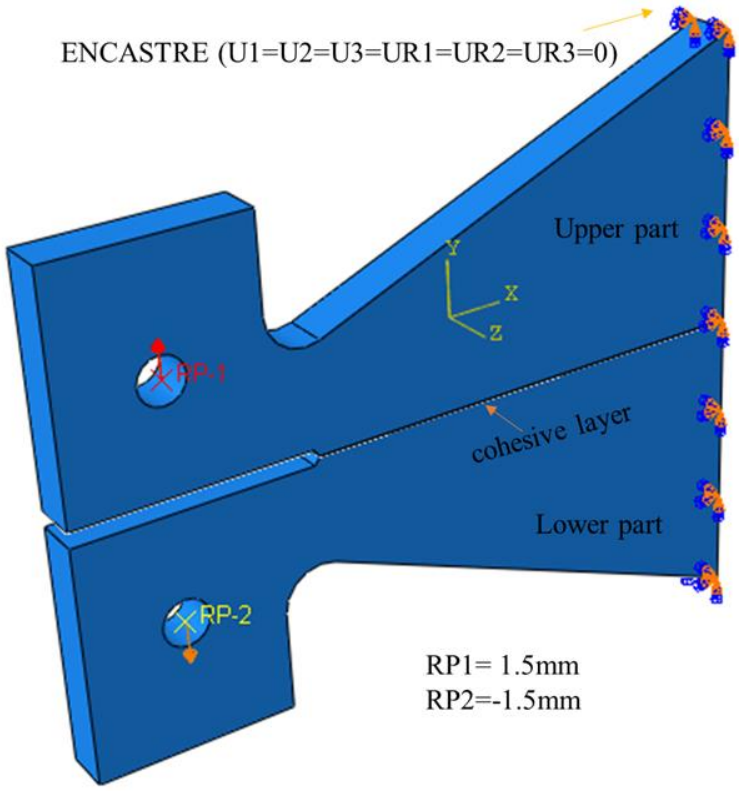

Figure 6.1 TDCB geometry model and boundary conditions

6.2.2 Assumptions

- Microcapsules are homogeneous materials and exhibit elastic deformation behaviour for small deformation (< 15% of total deformation) ranges.

- The bending resistance of the microcapsules on the failure strength was neglected.
- The effect of shape of capsule on its failure strength was neglected.
- The core material's influence in determining the strength of the microcapsule was neglected
- Pure epoxy behaves as isotropic and linear elastic material

6.2.3 Material properties and boundary conditions

Table 6.1 and Table 6.2 indicates the material properties used during simulation of microcapsules and TDCB specimen respectively.

Table 6.1 Material properties of microcapsules used in the study

Criteria	Remarks
Element Type	Hexagonal solid elements (C3D8R element)
Model	Hertzian plastic model
Element size	4.1µm
capsule size	Diameter: 100-300 µm Shell thickness : 5, 8, 10 µm
Elastic modulus (GPa)	2.68
Poisson's ratio (µ)	0.32

Table 6.2 Material properties of pure epoxy used in the TDCB specimen simulation

Component	Criteria	Remarks
TDCB assembly	Element Type	Hexagonal elements (C3D8R solid element)
	Element size	0.1 mm
	Model	cohesive zone model (CZM), Mode independent analysis
Cohesive zone	Fracture energy (G_{IC})	1.176 mJ
	Normal strength	0.3 MPa
	Stiffness (E_{nn})	$1e^{6}$
Pure epoxy	Elastic modulus (GPa)	3.3
	Poisson's ratio (µ)	0.35
	Density (tonne/mm^3)	$1.16e^{-9}$

Same material was considered for cohesive surface, upper and lower parts. Fracture energy was calculated from mode I fracture stress intensity factor using Eq.4.5. Normal cohesive strength and stiffness were calculated as discussed in the Masood et al. [155] study. Pure epoxy properties were taken from standard data sheet.

In experimental techniques such as micromanipulation and nano indentation, microcapsule glued to glass surface and then subject to point loads to evaluate its failure strength. In order to reproduce real time boundary conditions in the simulation, microcapsule bottom surface (point of contact) was restrained in all the directions and point load was applied on the top surface. In the nano indentation of PMMA microcapsules, applied loads were in the range of 5 mN to 14 mN [86,146,156]. Hence, in the present study also same loads were applied on the microcapsules with different diameters and thickness to evaluate their failure strength. Microcapsule shell material modelled as linear elastic solid that yields upon compression. Hertz contact model was used to calculate the compressive displacement of the microcapsules during loading. Young's modulus is independent of capsules diameter [157] and capsule shell thickness [86]. Hence in the current study, same elastic modulus was used for capsules with different diameter and shell thickness.

During mode I fracture test, upper part hole and lower part hole of TDCB specimen will be held in the UTM fixtures and pulled such that crack opening occurs along the centre line of the specimen. Hence, in the simulation centre nodes of the upper and lower part hole were marked with reference point (RP) and connected to respective hole inner surfaces via beam constraints. The other end edge of the specimen was constrained in all the directions. The inner surfaces of the holes were considered as non-rigid surfaces to minimize the computational time. As discussed in the section 4.4.6, for pure epoxy, maximum displacement obtained at failure was 1.5 mm. Hence to validate the simulation model same displacement was applied at the upper and lower part hole. The boundary conditions used in the TDCB geometry simulation can be observed from Figure 6.1.

6.2.4 Meshing

The mesh domain was divided into small elements using hexahedral mesh cells. Since the hexahedral meshing ensures the reliability of results and high accuracy, it is chosen as the required mesh cell in the present study. C3D8R hexagonal solid elements were considered for meshing of microcapsules. Different element sizes were investigated by employing automatic meshing technique and found optimized mesh independent results at element size of 4.1 μm.

For TDCB specimen also automatic meshing technique and C3D8R type hexagonal solid elements were considered. For all the three parts i.e., upper part, lower part and cohesive surface same element type was considered. 0.1 mm mesh size was applied and ensured smooth flow of elements between the components. The mesh near the edge of the crack tip and along the cohesive surface was refined to ensure obtained results were independent of mesh size. The elemental quality and connectivity among the elements of modelled microcapsules and TDCB specimen can be observed from Figure 6.2.

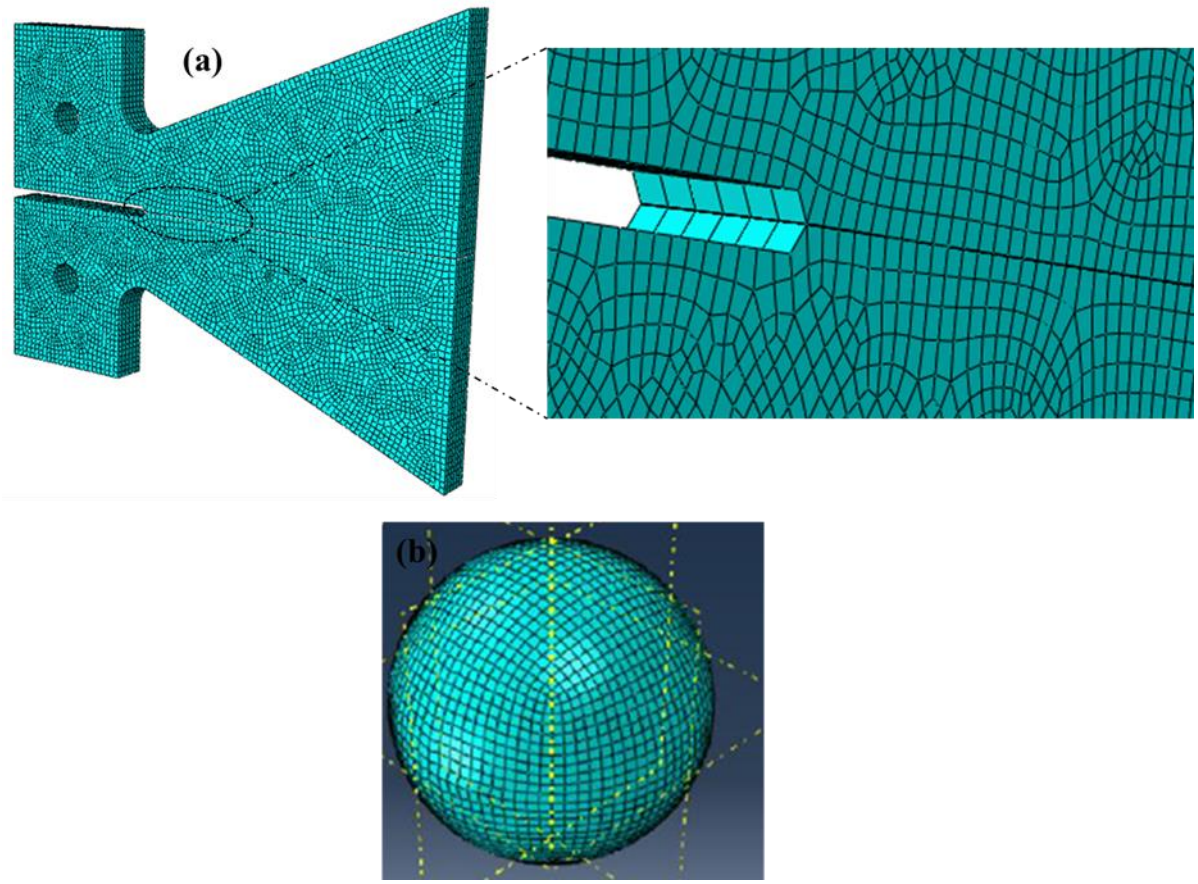

Figure 6.2 Meshing of (a) TDCB specimen (b) PMMA microcapsule

3D nonlinear static analysis and XFEM- cohesive zone damage model were employed to study the quasi static crack propagation in the TDCB specimen. An initial pre crack was defined at the junction of tip of the side groove and cohesive surface. Similar to experimental conditions, vertical displacements were applied and then analysed the crack advancement along the cohesive surface. Whenever the cohesive tensile stress exceeds the critical stress crack advances through element and component fails finally whenever the strain energy exceeds the critical strain energy. In the cohesive zone, crack propagation was modelled using linear Traction-Separation law. Reaction force at the upper hole was studied as a function of vertical

displacement and compared with experimental results for model verification. Finally, the stress distribution and deformation at the crack tip were computed.

6.2.5 Hertz Model

Hertz contact model is used to evaluate the elastic properties and compressive displacements of the microcapsules. According to this model, elastic modulus of the microcapsule can be estimated using

$$F = \frac{4E\sqrt{R}}{3(1-\nu_p{}^2)}\delta^{\frac{3}{2}} \qquad \text{Eq.6.1}$$

Where E - Elastic modulus of microcapsule; R-radius of capsule; F - applied force; *v* - Poisson's ratio; δ - half of the total compressive displacement

Assumptions used in the Hertz model are

- Strains are small and within the elastic limit
- Microcapsule is considered as elastic half space i.e., actual area of contact is less than the radius of the capsule
- Surfaces are continuous and non-conforming and
- The mating bodies are in frictionless contact

6.2.6 Cohesive Zone Model Theory

Cohesive zone model employs Traction-Separation law to investigate the crack propagation in polymer specimens. It relates traction and separation at cohesive surface and studies crack initiation and propagation. According to Park et al. [158], effective separation ($\overline{\Delta}$) at an interface can be given by $\overline{\Delta} = \sqrt{\Delta_n{}^2 + \Delta_t{}^2}$ Eq.6.2

Where Δ_n, Δ_t represents normal and tangential separations.

When effective separation ($\overline{\Delta}$) < effective critical separation ($\overline{\Delta_c}$) then the normal Traction (T_n) and tangential Traction (T_t) are given by

$$T_n = K_p\ \Delta_n \qquad \text{Eq.6.3}$$

$$T_t = K_p\ \Delta_t \qquad \text{Eq.6.4}$$

Where K_p represents penalty stiffness.

During the loading, whenever the effective separation ($\overline{\Delta}$) equals to effective critical separation ($\overline{\Delta_c}$), crack initiates at the interface. Ratio between normal and tangential cohesive strengths and penalty stiffness decides the effective critical separation and thus the crack propagation criterion. When normal cohesive strength (σ_{max}) and tangential cohesive strength (τ_{max}) becomes equal effective critical separation can be define as

$$\overline{\Delta_c} = \frac{\sigma_{\max}}{K_p} \qquad \text{Eq.6.5}$$

During further loading, whenever a criterion occurs such that $\overline{\Delta_c} < \overline{\Delta} < \overline{\Delta_f}$, crack propagates further and normal, tangential tractions can be re written as

$$T_n = (1-d)\, K_p\, \Delta_n \qquad \text{Eq.6.6}$$

$$T_t = (1-d)\, K_p\, \Delta_t \qquad \text{Eq.6.7}$$

Where $\overline{\Delta_f}$ represents effective complete failure criterion and d- damage variable

To address the damage variable two types of damage models i.e., linear and exponential models are available. To investigate fracture toughness as a function of mode of damage there are few mixed mode models such as B-K model are available. Present study deals with Mode I fracture only, hence mode independent model is considered to investigate the crack propagation.

6.3 Results and Discussion

This section deals with the validation of models, effect of microcapsule diameter and shell thickness on their mechanical strength and stress distribution at mode I fracture crack front.

6.3.1 Validation of the models

Simulation results of the current study are compared with experimental results to validate the accuracy of the model. Figure 6.3 shows the comparison of both TDCB model and microcapsule model with their respective experimental results. As discussed in the section 4.4.6, the maximum peak load obtained during mode I fracture test for pure epoxy was 175.85N and from the numerical study it is observed that the maximum peak load is 185.08 N. Since the variation in the results is less than 5%, the TDCB model can be used for further study. Similarly, for a applied load of 14 mN, numerical results of 10 µm shell thickness microcapsule with different average sizes were compared with experimental results of Pan et al. [86]. Compressive strength of experimented and simulated microcapsules results were comparable

and within the limits, hence from this study it can be concluded that the PMMA microcapsules model can be used for further study.

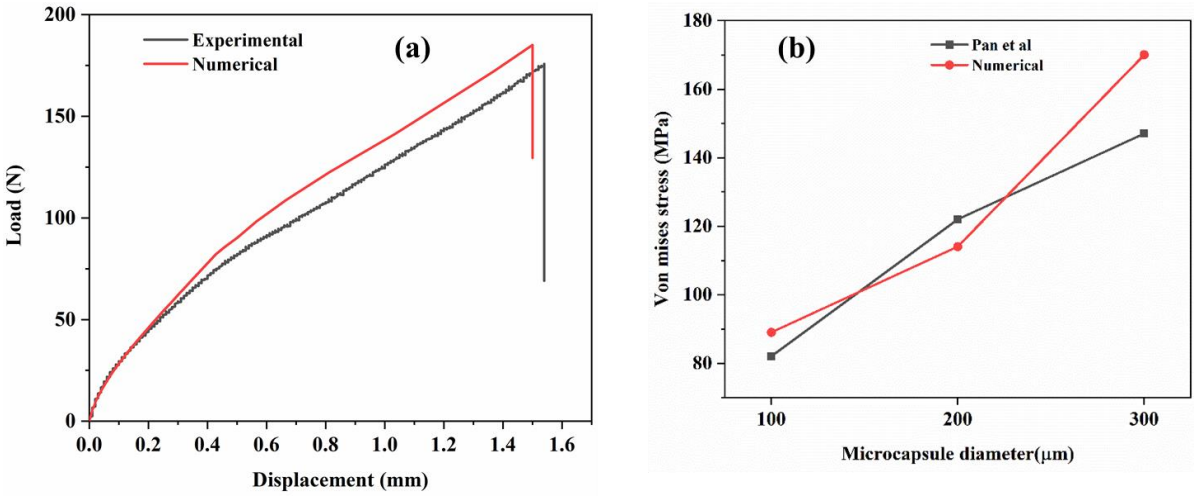

Figure 6.3 Validation of (a) TDCB model (b) PMMA microcapsules model

6.3.2 Effect of microcapsule diameter on its mechanical strength

In practical, it is difficult to synthesize capsules with fixed diameter and generally they will be synthesized in narrow size distribution. Hence to study the strength of microcapsules, three microcapsules with average diameter of 100 μm, 200 μm and 300 μm were modelled. The shell thickness of all the three microcapsules was considered as 5 μm. The strength of the microcapsule is evaluated by applying a constant load of 5 mN on all three microcapsules. It can be noticed from the Figure 6.4 that the von mises stress developed in the microcapsules is decreased with the increase in capsule diameter. Whenever same load applied on the capsules with same thickness but different diameters, the area of contact and the resisting force offered by smaller diameter capsule (100 μm capsule) are less than the other diameter capsules. Hence higher von mises stress develops in the smaller diameter capsules. With the increase in diameter, area of contact and the resistance to external loads increases and hence smaller von mises stress can be observed. As the stresses developed in the larger diameter capsule are lesser than other two diameter capsules, it can be concluded that larger diameter capsules require comparatively higher forces to rupture. Thus, this study suggests selection of required diameter capsules for designing of the self-healing system and concludes that smaller diameter capsules break easily than the larger diameter capsules.

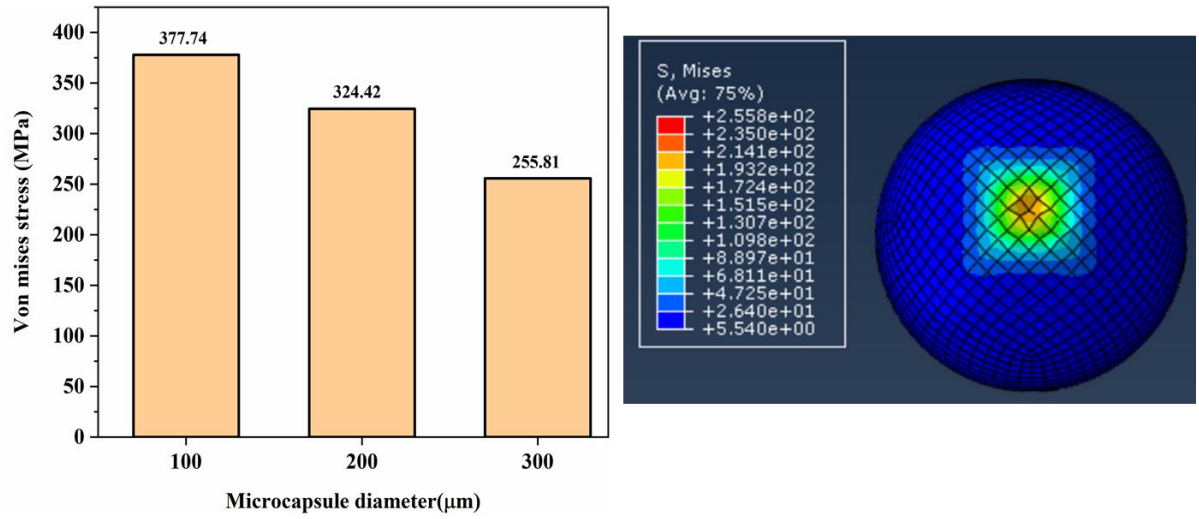

Figure 6.4 Effect of microcapsule diameter on its mechanical strength

6.3.3 Effect of microcapsule shell thickness on its mechanical strength

In order to investigate the effect of shell thickness on the mechanical strength of microcapsule, as discussed in the section 6.2.3, three point loads 5 mN, 10 mN and 14 mN were applied on the capsules with different shell thickness. Mechanical strength of the microcapsules with 100, 200, 300 μm diameter and shell thickness of 5, 8, 10 μm were investigated by applying above mentioned point loads. Figure 6.5 shows the effect of shell thickness on the mechanical strength of microcapsule. It can be noticed from the results that the von mises stress developed in the microcapsule decreased with the increase in capsule shell thickness. With the increase in shell thickness, resistance to deformation increase and hence less von mises stress can be noticed. From the experimental results it was reported that the compressive strength of 8 μm average shell thickness PMMA microcapsule is 124 MPa [86,159]. It can be observed from Figure 6.5 that the von mises stress developed in the 100 μm diameter capsule with 8 μm shell thickness is 126 MPa. Whenever, von mises stress developed in the capsule exceeds its compressive strength, capsule subject to rupture. Since von mises stress developed in the 100 μm diameter capsule is just more than its compressive strength, it can be concluded that the applied load is just sufficient to initiate the rupture of the microcapsule.

With the above mentioned capsule diameter, shell thickness and applied point loads nine different capsules were modelled and investigated for stress-strain profiles during compression. Table 6.3 indicates the specifications of the different microcapsules used in the study. Figure 6.6 shows the stress-strain profiles of the different microcapsules. It can be observed from the graphs that the deformation in the capsules is in μm range and most of the

capsules had linear stress-strain profiles. Microcapsules having comparable specifications also shown similar stress- strain profiles during mechanical strength evaluation using nanoindentation technique [34]. Effect of shell thickness and the maximum von mises stress developed in each microcapsule can be understood from the given stress-strain profiles.

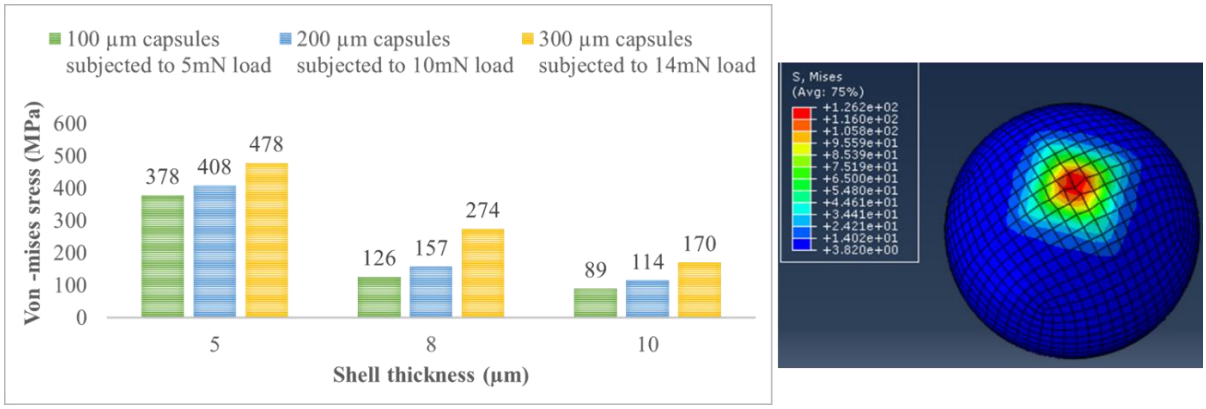

Figure 6.5 Effect of shell thickness on the mechanical strength of microcapsule

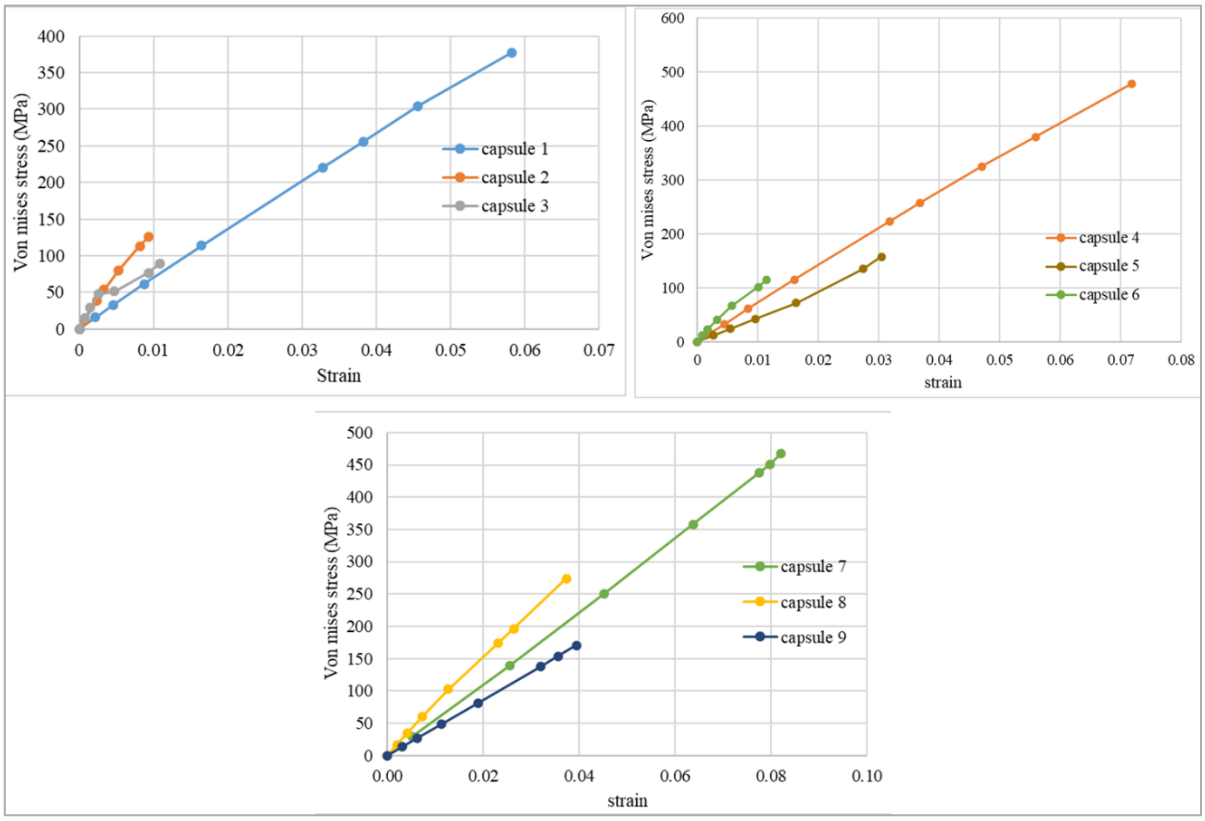

Figure 6.6 Effect of shell thickness on the mechanical strength of microcapsule

Table 6.3 Specifications of different microcapsules

Capsule number	Diameter of the capsule (μm)	Thickness of the capsule (μm)	Applied Load (mN)
1	100	5	5
2	100	8	5
3	100	10	5
4	200	5	10
5	200	8	10
6	200	10	10
7	300	5	14
8	300	8	14
9	300	10	14

6.3.4 Stress distribution at the crack front

As discussed in the cohesive zone model theory when the tensile stress reaches the critical stress crack initiates and propagates further with the increase in applied load. It was noted from the experimental results that pure epoxy had brittle fracture and hence in the stress distribution simulation results principal stress is considered. Figure 6.7 shows the crack propagation along the cohesive zone. It can be confirmed from the results that TDCB geometry facilitates the crack propagation along the centre line of the component. It is observed from the results that the maximum stress was developed at the crack tip and observed as 28 MPa.

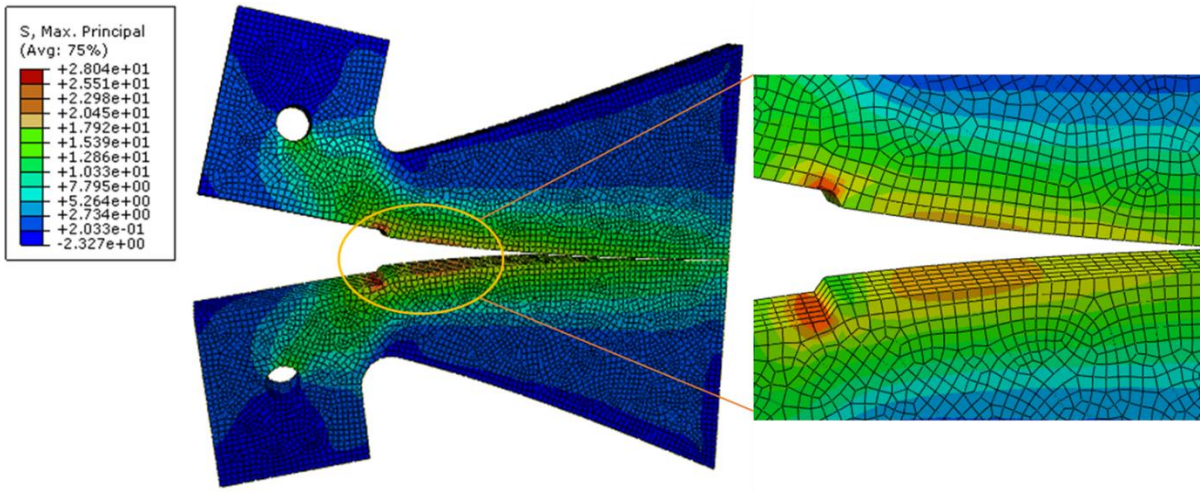

Figure 6.7 stress distribution at the crack front

6.4 Conclusions

PMMA microcapsules with different diameter and shell thickness were modelled and evaluated for their mechanical strength. TDCB geometry was modelled and investigated for stress distribution at the crack front. Following are the some of the conclusions that can be drawn from the current study.

- For the same applied loads and shell thickness, smaller diameter capsule break easily than the larger diameter capsule.
- With the increase in shell thickness von mises stress developed in the capsule decreases. Maximum von mises stress developed in the microcapsule with 100 μm diameter and 8 μm shell thickness is observed as 126 MPa.
- Microcapsules shows linear stress- strain profiles during deformation.
- Microcapsules rupture criteria was evaluated by comparing the compressive yield strength of the capsule and von mises stress developed in the capsule.
- TDCB geometry was modelled for pure epoxy and compared with load-displacement experimental results to calculate the stress distribution at the crack front.
- The maximum principal stress observed at the crack front is 28 MPa.

Chapter 7

Conclusions and Future scope

7.1 Conclusions

The main objective of the work comprised of fabricating the CFRP composites with inbuilt self-healing functionality and thus to re-establish the structural integrity. To achieve this, two separate healing agents i.e., epoxy resin, amine hardener encapsulated PMMA microcapsules were developed using oil in water solvent evaporation method and investigated for optimum parameters. Dual microcapsule self-healing system was selected to verify the self-healing functionality in the base epoxy matrix. Effect of microcapsule type and concentration on the mechanical and self-healing performance of the base epoxy were investigated. Separately optimized dual microcapsules were integrated with CFRP composite and evaluated for flexural strength, damping characterization and self-healing efficiency. Effect of induced damage on the flexural strength and healing efficiency of dual capsules reinforced CFRP composite was studied. Numerical studies were conducted on the load bearing capacity of the single microcapsule and the stresses developed at the crack front. The following are some of the conclusions that can be drawn from the results of the current study.

- HY951 hardener capsules synthesized with SDS surfactant have better properties than the capsules synthesized with PVA surfactant and hence SDS surfactant is suggested as an ideal surfactant to synthesize hardener microcapsules.
- Optimized process parameters to synthesize amine hardener microcapsules are 40°C processing temperature, 4:1 core to shell ratio, 500 rpm, ratio of oil phase to water phase in between 1:7 to 1:9 and 5 wt% SDS surfactant concentration.
- Optimized process parameters to synthesize epoxy resin microcapsules are 40˚C processing temperature, 400 rpm, 5 wt% SDS surfactant concentration and 1:1 core to shell ratio for LY556 capsules and 2:1 for CY230 capsules.
- The average capsule size of the LY556 epoxy,CY230 epoxy and HY951 hardener microcapsules synthesized at optimum conditions were measured as 61.58 µm, 67.64 µm and 63.31 µm respectively.
- SEM, FTIR, ^{1}H NMR and TGA analyses confirmed the successful encapsulation of LY556 epoxy resin, CY230 epoxy resin and HY951 hardener in the PMMA.
- With the addition of 7.5 wt% of LY556+HY951 capsules, tensile strength, flexural strength and Charpy impact strength of pure epoxy decreased from 32.16 MPa to 20.52 MPa, 64.09 MPa to 31.12 MPa and 22.54 kJ/m^2 to 13.72 kJ/m^2 respectively.

- Healing efficiency of epoxy composite increased from 39.26% to 71.94% and from 34.23% to 74.41% with the increase in LY556+HY951 capsules, CY230+HY951 capsules concentration from 2.5 wt% to 10 wt% respectively.
- CY230+HY951 capsules combination showed better mechanical properties and self-healing performance than the LY556+HY951 capsules combination.
- 2:1 c/s ratio CY230 epoxy capsules, 4:1 c/s ratio HY951 hardener capsules, 1:1 capsules weight ratio, 7.5 wt% of CY230+HY951 microcapsules concentration and room temperature curing for 24 hrs were suggested as an ideal process parameters to fabricate dual capsules reinforced self-healing epoxy composite.
- 15 wt% of capsules concentration and (80˚C + 1 bar) healing condition were recommended to fabricate capsules reinforced CFRP composite.
- Healing efficiency of 15 wt% capsules reinforced CFRP increased from 67.55% to 71.30% and from 51.52% to 54.21% for matrix cracking, delamination damages recovery respectively by healing at (80˚C + 1 bar) healing condition.
- Compared to capsules reinforced virgin composite, the damping factor of damaged and healed composites increased and can be attributed to increased dislocations and increased surface area respectively.
- Self-healing efficiency of the capsules reinforced epoxy, capsules reinforced CFRP composite was assessed based on stiffness recovery using IET technique and found to be 72.05% and 53.72% respectively.
- Healing efficiencies obtained through IET technique were comparable and well within the acceptable limits to healing efficiencies obtained through mode I fracture test and flexural test. Hence IET approach can be used to evaluate the healing performance of the composites based on stiffness recovery.
- For the same applied loads and shell thickness, smaller diameter capsule break easily than the larger diameter capsule.
- With the increase in shell thickness von mises stress developed in the capsule decreases. Maximum von mises stress developed in the microcapsule with 100 μm diameter and 8 μm shell thickness is observed as 126 MPa.
- The maximum principal stress observed at the crack front is 28 MPa.

7.2 Future scope

Though preliminary concerns related to fabrication and assessment of self-healing functionality in polymer composites addressed in the current study, still there is a lot of scope to work on many other aspects. Following are some of the aspects that can be considered for future study.

- Nano size epoxy, hardener microcapsules can be developed using ultrasonic probe sonicator and may be investigated to reduce % decrease in mechanical properties of the capsules reinforced epoxy.
- In the present study developed microcapsules are used to address structural integrity. However, developed micro/nano capsules can be employed in other applications such as smart adhesive systems.
- Micromechanical properties of the developed capsules can be investigated. Micro CT and ultrasonic characterization techniques can be used to characterize the capsules reinforced epoxy.
- Dual capsule reinforced CFRP composite can be evaluated for self-healing performance in different fracture modes based on fracture toughness recovery.
- Capsules reinforced epoxy and CFRP composites can be modelled and evaluated for optimum capsules wt%, healing conditions and maximum healing efficiency at different environmental conditions.

References

[1] Blaiszik B., Kramer SLB, Olugebefola SC, Moore JS, Sottos NR, White SR. Self-Healing Polymers and Polymer Composites. Annu Rev Mater Res 2010;40:179–211. https://doi.org/10.1002/9781118082720.

[2] Kahar NNFNMN, Osman AF, Alosime E, Arsat N, Azman NAM, Syamsir A, et al. The versatility of polymeric materials as self-healing agents for various types of applications: A review. Polymers (Basel) 2021;13:1–34. https://doi.org/10.3390/polym13081194.

[3] Xu Y, Li Y, Chen Q, Fu L, Tao L, Wei Y. Injectable and self-healing chitosan hydrogel based on imine bonds: Design and therapeutic applications. Int J Mol Sci 2018;19. https://doi.org/10.3390/ijms19082198.

[4] Grandview research. Self-healing Materials Market Size, Share & Trends Analysis report by product, by technology, by application and segment forecast 2019:GVR-1-68038-829-9.

[5] Dubey R, Shami TC, Rao KUB. Microencapsulation Technology and Applications. Def Sci J 2009;59:82–95.

[6] Dursun T, Soutis C. Recent developments in advanced aircraft aluminium alloys. Mater Des 2014;56:862–71. https://doi.org/10.1016/j.matdes.2013.12.002.

[7] Zhang X, Chen Y, Hu J. Recent advances in the development of aerospace materials. Prog Aerosp Sci 2018;97:22–34. https://doi.org/10.1016/j.paerosci.2018.01.001.

[8] Campbell FC. Structural Composite Materials. ASM International; 2010. https://doi.org/10.31399/asm.tb.scm.9781627083140.

[9] Gharghabi P, Lee J, Mazzola MS, Lacy TE. Development of an experimental setup to analyze carbon/epoxy composite subjected to current impulses. Proc Am Soc Compos - 31st Tech Conf ASC 2016.

[10] Diamanti K, Soutis C. Structural health monitoring techniques for aircraft composite structures. Prog Aerosp Sci 2010;46:342–52.

[11] Zhao X, Gao H, Zhang G, Ayhan B, Yan F, Kwan C, et al. Active health monitoring of an aircraft wing with embedded piezoelectric sensor/actuator network: I. Defect detection, localization and growth monitoring. Smart Mater Struct 2007;16:1208–17.

[12] Sharif-Khodaei Z, Aliabadi MH. Assessment of delay-and-sum algorithms for damage detection in aluminium and composite plates. Smart Mater Struct 2014;23. https://doi.org/10.1088/0964-1726/23/7/075007.

[13] Tong Z, Zhentai Z, Rui Z. A dynamic welding heat source model in pulsed current gas tungsten arc welding. J Mater Process Technol 2013;213:2329–38.

[14] Shams SS, El-Hajjar RF. Overlay patch repair of scratch damage in carbon fiber/epoxy laminated composites. Compos Part A Appl Sci Manuf 2013;49:148–56. https://doi.org/10.1016/j.compositesa.2013.03.005.

[15] Klinge S, Bartels A, Steinmann P. The multiscale approach to the curing of polymers incorporating viscous and shrinkage effects. Int J Solids Struct 2012;49:3883–900. https://doi.org/10.1016/j.ijsolstr.2012.08.016.

[16] Dong Yang Wu, Sam Meure DS. Self-healing polymeric materials: A review of recent developments. Prog Polym Sci 2008;33:479–522.

[17] Yuan YC, Rong MZ, Zhang MQ. Preparation and characterization of microencapsulated polythiol. Polymer (Guildf) 2008;49:2531–41.

[18] Kessler MR, Sottos NR, White SR. Self-healing structural composite materials. Compos Part A Appl Sci Manuf 2003;34:743–53.

[19] Pang JWC, Bond IP. A hollow fibre reinforced polymer composite encompassing self-healing and enhanced damage visibility. Compos Sci Technol 2005;65:1791–9. https://doi.org/10.1016/j.compscitech.2005.03.008.

[20] Trask RS, Bond IP. Biomimetic self-healing of advanced composite structures using hollow glass fibres. Smart Mater Struct 2006;15:704–10. https://doi.org/10.1088/0964-1726/15/3/005.

[21] Toohey KS, Sottos NR, Lewis JA, Moore JS, White SR. Self-healing materials with microvascular networks. Nat Mater 2007;6:581–5. https://doi.org/10.1038/nmat1934.

[22] Williams HR, Trask RS, Knights AC, Williams ER, Bond IP. Biomimetic reliability strategies for self-healing vascular networks in engineering materials. J R Soc Interface 2008;5:735–47. https://doi.org/10.1098/rsif.2007.1251.

[23] Billiet S, Hillewaere XKD, Teixeira RFA, Du Prez FE. Chemistry of crosslinking

processes for self-healing polymers. Macromol Rapid Commun 2013;34:290–309. https://doi.org/10.1002/marc.201200689.

[24] Garcia SJ. Effect of polymer architecture on the intrinsic self- healing character of polymers. Eur Polym J 2014;53:118–25.

[25] Yamaguchi M, Ono S, Okamoto K. Interdiffusion of dangling chains in weak gel and its application to self-repairing material. Mater Sci Eng B Solid-State Mater Adv Technol 2009;162:189–94. https://doi.org/10.1016/j.mseb.2009.04.006.

[26] Montarnal D, Tournilhac F, Hidalgo M, Couturier JL, Leibler L. Versatile one-pot synthesis of supramolecular plastics and self-healing rubbers. J Am Chem Soc 2009;131:7966–7. https://doi.org/10.1021/ja903080c.

[27] Varley RJ, van der Zwaag S. Towards an understanding of thermally activated self-healing of an ionomer system during ballistic penetration. Acta Mater 2008;56:5737–50. https://doi.org/10.1016/j.actamat.2008.08.008.

[28] Varley RJ, Van der Zwaag S. Development of a quasi-static test method to investigate the origin of self-healing in ionomers under ballistic conditions. Polym Test 2008;27:11–9. https://doi.org/10.1016/j.polymertesting.2007.07.013.

[29] White, Scott R, Sottos, N. R, Geubelle, P. H, Moore, Jeffrey S, Kessler, M. R, Sriram, S. R, et al. Autonomic healing of polymer composites. Nature 2001;409:794–7. https://doi.org/10.1038/35057232.

[30] Brown EN, Kessler MR, Sottos NR, White SR. In situ poly(urea-formaldehyde) microencapsulation of dicyclopentadiene. J Microencapsul 2003;20:719–30. https://doi.org/10.1080/0265204031000154160.

[31] Liu X, Sheng X, Lee JK, Kessler MR. Synthesis and characterization of melamine- urea-formaldehyde microcapsules containing ENB-based self-healing agents. Macromol Mater Eng 2009;294:389–95. https://doi.org/10.1002/mame.200900015.

[32] Jinglei Y, Keller MW, Moore JS, White SR, Sottos NR. Microencapsulation of isocyanates for self-healing polymers. Macromolecules 2008;41:9650–5.

[33] Cho SH, Andersson HM, White SR, Sottos NR, Braun P V. Polydiniethylsiloxane-based self-healing materials. Adv Mater 2006;18:997–1000.

[34] Su JF, Wang XY, Dong H. Micromechanical properties of melamine-formaldehyde microcapsules by nanoindentation: Effect of size and shell thickness. Mater Lett 2012;89:1–4. https://doi.org/10.1016/j.matlet.2012.08.072.

[35] Ollier RP, Penoff ME, Alvarez VA. Microencapsulation of epoxy resins : Optimization of synthesis conditions. Colloids Surfaces A Physicochem Eng Asp 2016;511:27–38. https://doi.org/10.1016/j.colsurfa.2016.09.081.

[36] Caruso MM, Delafuente DA, Ho V, Sottos NR, Moore JS WS. Solvent-promoted self-healing epoxy materials. Macromolecules 2007;40(25):8830–32.

[37] Mauldin TC, Kessler MR. Self-healing polymers and composites. Int Mater Rev 2010;55:317–46. https://doi.org/10.1179/095066010X12646898728408.

[38] Dry CM. Three designs for the internal release of sealants, adhesives, and waterproofing chemicals into concrete to reduce permeability. Cem Concr Res 2000;30:1969–77. https://doi.org/10.1016/S0008-8846(00)00415-4.

[39] Trask RS, Williams GJ, Bond IP. Bioinspired self-healing of advanced composite structures using hollow glass fibres. J R Soc Interface 2007;4:363–71.

[40] Banshiwal JK, Tripati DN. Self-Healing Polymer Composites for Structural Application. Funct. Mater., IntechOpen; 2019, p. 1–22.

[41] Yuan YC, Yin T, Rong MZ, Zhang MQ. Self healing in polymers and polymer composites. Concepts, realization and outlook: A review. Express Polym Lett 2008;2:238–50. https://doi.org/10.3144/expresspolymlett.2008.29.

[42] Toohey KS, Sottos NR, White SR. Characterization of microvascular-based self-healing coatings. Exp Mech 2009;49:707–17. https://doi.org/10.1007/s11340-008-9176-7.

[43] Hansen CJ, Wu W, Toohey KS, Sottos NR, White SR, Lewis JA. Self-healing materials with interpenetrating microvascular networks. Adv Mater 2009;21:4143–7. https://doi.org/10.1002/adma.200900588.

[44] Patrick JF, Hart KR, Krull BP, Diesendruck CE, Moore JS, White SR, et al. Continuous self-healing life cycle in vascularized structural composites. Adv Mater 2014;26:4302–8. https://doi.org/10.1002/adma.201400248.

[45] Diesendruck CE, Sottos NR, Moore JS, White SR. Biomimetic Self-Healing. Angew

Chemie - Int Ed 2015;54:10428–47. https://doi.org/10.1002/anie.201500484.

[46] Zhang P, Li G. Advances in healing-on-demand polymers and polymer composites. vol. 57. Elsevier Ltd; 2016. https://doi.org/10.1016/j.progpolymsci.2015.11.005.

[47] Chen X, Dam MA, Ono K, Mal A, Shen H, Nutt SR, et al. A thermally re-mendable cross-linked polymeric material. Science 2002;295:1698–702.

[48] Zhong N, Post W. Self-repair of structural and functional composites with intrinsically self-healing polymer matrices: A review. Compos Part A Appl Sci Manuf 2015;69:226–39. https://doi.org/10.1016/j.compositesa.2014.11.028.

[49] Cordier P, Tournilhac F, Soulié-Ziakovic C, Leibler L. Self-healing and thermoreversible rubber from supramolecular assembly. Nature 2008;451:977–80. https://doi.org/10.1038/nature06669.

[50] Liu YL, Chuo TW. Self-healing polymers based on thermally reversible Diels-Alder chemistry. Polym Chem 2013;4:2194–205. https://doi.org/10.1039/c2py20957h.

[51] Fortunato G, Tatsi E, Rigatelli B, Turri S, Griffini G. Highly Transparent and Colorless Self-Healing Polyacrylate Coatings Based on Diels–Alder Chemistry. Macromol Mater Eng 2020;305:1–6. https://doi.org/10.1002/mame.201900652.

[52] Scheiner M, Dickens TJ, Okoli O. Progress towards self-healing polymers for composite structural applications. Polymer (Guildf) 2016;83:260–82.

[53] Park JS, Darlington T, Starr AF, Takahashi K, Riendeau J, Thomas Hahn H. Multiple healing effect of thermally activated self-healing composites based on Diels-Alder reaction. Compos Sci Technol 2010;70:2154–9.

[54] Yang Y, Ding X, Urban MW. Chemical and physical aspects of self-healing materials. Prog Polym Sci 2015;49–50. https://doi.org/10.1016/j.progpolymsci.2015.06.001.

[55] Guadagno L, Vertuccio L, Naddeo C, Calabrese E, Barra G, Raimondo M, et al. Self-healing epoxy nanocomposites via reversible hydrogen bonding. Compos Part B Eng 2019;157:1–13. https://doi.org/10.1016/j.compositesb.2018.08.082.

[56] Burattini S, Greenland BW, Merino DH, Weng W, Seppala J, Colquhoun HM, et al. A healable supramolecular polymer blend based on aromatic π-π Stacking and hydrogen-bonding interactions. J Am Chem Soc 2010;132:12051–8.

[57] Wool RP, O'Connor KM. A theory of crack healing in polymers. J Appl Phys 1981;52:5953–63. https://doi.org/10.1063/1.328526.

[58] Kim YH, Wool RP. A Theory of Healing at a Polymer Polymer Interface. Macromolecules 1983;16:1115–20. https://doi.org/10.1021/ma00241a013.

[59] Brown EN, Sottos NR, White SR. Fracture testing of a self-healing polymer composite. Exp Mech 2002;42:372–9. https://doi.org/10.1177/001448502321548193.

[60] Coope TS, Mayer UFJ, Wass DF, Trask RS, Bond IP. Self-healing of an epoxy resin using scandium(III) triflate as a catalytic curing agent. Adv Funct Mater 2011;21:4624–31. https://doi.org/10.1002/adfm.201101660.

[61] Kamphaus JM, Rule JD, Moore JS, Sottos NR, White SR. A new self-healing epoxy with tungsten (VI) chloride catalyst. J R Soc Interface 2008;5:95–103. https://doi.org/10.1098/rsif.2007.1071.

[62] Wang Y, Pham D, Ji C, Harkin-jones E. Self-healing composites : a review. Cogent Eng 2015;2:1075686. https://doi.org/10.1080/23311916.2015.1075686.

[63] Jin H, Mangun CL, Stradley DS, Moore JS, Sottos NR, White SR. Self-healing thermoset using encapsulated epoxy-amine healing chemistry. Polymer (Guildf) 2012;53:581–7. https://doi.org/10.1016/j.polymer.2011.12.005.

[64] Li Q, Siddaramaiah, Kim NH, Hui D, Lee JH. Effects of dual component microcapsules of resin and curing agent on the self-healing efficiency of epoxy. Compos Part B Eng 2013;55:79–85. https://doi.org/10.1016/j.compositesb.2013.06.006.

[65] Yan CY, Min ZR, Ming QZ, Chen J, Gui CY, Xue ML. Self-healing polymeric materials using epoxy/mercaptan as the healant. Macromolecules 2008;41:5197–202. https://doi.org/10.1021/ma800028d.

[66] Ahangaran F, Hayaty M, Navarchian AH, Pei Y, Picchioni F. Development of self-healing epoxy composites via incorporation of microencapsulated epoxy and mercaptan in poly(methyl methacrylate) shell. Polym Test 2019;73:395–403.

[67] McGinity J, O'Donnell P. Preparation of microspheres by the solvent evaporation technique. Adv Drug Deliv Rev 1997;28:25–42. https://doi.org/10.1016/S0169-409X(97)00049-5.

[68] Li M, Rouaud O, Poncelet D. Microencapsulation by solvent evaporation: State of the art for process engineering approaches. Int J Pharm 2008;363:26–39.

[69] Zhao Y, Fickert J, Landfester K, Crespy D. Encapsulation of self-healing agents in polymer nanocapsules. Small 2012;8:2954–8. https://doi.org/10.1002/smll.201200530.

[70] Blaiszik BJ, Sottos NR, White SR. Nanocapsules for self-healing materials. Compos Sci Technol 2008;68:978–86. https://doi.org/10.1016/j.compscitech.2007.07.021.

[71] Loxley A, Vincent B. Preparation of Poly(methylmethacrylate) Microcapsules with Liquid Cores. J Colloid Interface Sci 1998;208:49–62.

[72] Yuan L, Gu A, Liang G. Preparation and properties of poly(urea-formaldehyde) microcapsules filled with epoxy resins. Mater Chem Phys 2008;110:417–25. https://doi.org/10.1016/j.matchemphys.2008.02.035.

[73] Zhang T, Zhang M, Tong X-M, Feng C, Jian-Hui Q. Optimal preparation and characterization of poly (urea-formaldehyde) microcapsules. J Appl Polym Sci 2010;115:2162–9. https://doi.org/10.1002/app.

[74] Ullah H, Azizli KAM, Man ZB, Che Ismail MB, Khan MI. The potential of microencapsulated self-healing materials for microcracks recovery in self-healing composite systems: A review. Polym Rev 2016;56:429–85.

[75] Ahangaran F, Hayaty M, Navarchian AH. Morphological study of Polymethyl methacrylate microcapsules filled with self-healing agents. Appl Surf Sci 2017;399:721–31. https://doi.org/10.1016/j.apsusc.2016.12.116.

[76] Li W, Jiang Z, Yang Z, Zhao N, Yuan W. Self-healing efficiency of cementitious materials containing microcapsules filled with healing adhesive: Mechanical restoration and healing process monitored by water absorption. PLoS One 2013;8:1–18. https://doi.org/10.1371/journal.pone.0081616.

[77] Araya-Hermosilla R, Broekhuis AA, Picchioni F. Reversible polymer networks containing covalent and hydrogen bonding interactions. Eur Polym J 2014;50:127–34. https://doi.org/10.1016/j.eurpolymj.2013.10.014.

[78] García SJ, Fischer HR, White PA, Mardel J, González-García Y, Mol JMC, et al. Self-healing anticorrosive organic coating based on an encapsulated water reactive silyl ester: Synthesis and proof of concept. Prog Org Coatings 2011;70:142–9.

[79] Zhu DY, Rong MZ, Zhang MQ. Preparation and characterization of multilayered microcapsule-like microreactor for self-healing polymers. Polymer (Guildf) 2013;54:4227–36. https://doi.org/10.1016/j.polymer.2013.06.014.

[80] Zhang H, Yang J. Development of self-healing polymers via amine-epoxy chemistry: I. Properties of healing agent carriers and the modelling of a two-part self-healing system. Smart Mater Struct 2014;23. https://doi.org/10.1088/0964-1726/23/6/065003.

[81] Brancart J, Scheltjens G, Muselle T, Van Mele B, Terryn H, Van Assche G. Atomic force microscopy-based study of self-healing coatings based on reversible polymer network systems. J Intell Mater Syst Struct 2014;25:40–6.

[82] In CW, Holland RB, Kim JY, Kurtis KE, Kahn LF, Jacobs LJ. Monitoring and evaluation of self-healing in concrete using diffuse ultrasound. NDT E Int 2013;57:36–44. https://doi.org/10.1016/j.ndteint.2013.03.005.

[83] Liu M. Understanding the Mechanical Strength of Microcapsules and Their Adhesion on Fabric Surfaces. PhD Thesis; 2010.

[84] Nguyen VB, Wang CX, Thomas CR, Zhang Z. Mechanical properties of single alginate microspheres determined by microcompression and finite element modelling. Chem Eng Sci 2009;64:821–9. https://doi.org/10.1016/j.ces.2008.10.050.

[85] Mercade´-Prieto R, Allen R, Zhang Z, York D, Preece JA, Goodwin TE. Failure of Elastic-Plastic Core – Shell Microcapsules under Compression. Am Inst Chem Eng J 2011;00. https://doi.org/10.1002/aic.12804.

[86] Pan X, Mercadé-Prieto R, York D, Preece JA, Zhang Z. Structure and Mechanical Properties of Consumer-Friendly PMMA Microcapsules. Ind Eng Chem Res 2013;52:11253–65. https://doi.org/10.1021/ie303451s.

[87] Brown EN, White SR, Sottos NR. Microcapsule induced toughening in a self-healing polymer composite. J Mater Sci 2004;39:1703–10.

[88] Yin T, Rong MZ, Zhang MQ, Yang GC. Self-healing epoxy composites - Preparation and effect of the healant consisting of microencapsulated epoxy and latent curing agent. Compos Sci Technol 2007;67:201–12.

[89] Tripathi M, Rahamtullah J, Kumar D, Rajagopal C, Kumar Roy P. Influence of microcapsule shell material on the mechanical behavior of epoxy composites for self-

healing applications. J Appl Polym Sci 2014;131:1–9.

[90] Kosarli M, Bekas DG, Tsirka K, Baltzis D, Vaimakis-Tsogkas D, Orfanidis S, et al. Microcapsule-based self-healing materials: Healing efficiency and toughness reduction vs. capsule size. Compos Part B Eng 2019;171:78–86.

[91] Caruso MM, Blaiszik BJ, White SR, Sottos NR, Moore JS. Full recovery of fracture toughness using a nontoxic solvent-based self-healing system. Adv Funct Mater 2008;18:1898–904. https://doi.org/10.1002/adfm.200800300.

[92] Zhang L, Dong X, Chen H. Study on the effects of the self-healing microcapsules on the tensile properties of polymer composite. Adv Mater Res 2011;299–300:460–5. https://doi.org/10.4028/www.scientific.net/AMR.299-300.460.

[93] Coppola AM, Thakre PR, Sottos NR, White SR. Tensile properties and damage evolution in vascular 3D woven glass/epoxy composites. Compos Part A Appl Sci Manuf 2014;59:9–17. https://doi.org/10.1016/j.compositesa.2013.12.006.

[94] Barbero EJ, Ford KJ. Characterization of self-healing fiber-reinforced polymer-matrix composite with distributed damage. J Adv Mater 2007;39:20–7.

[95] Ghazali H, Ye L, Zhang MQ. Interlaminar fracture of CF/EP composite containing a dual-component microencapsulated self-healant. Compos Part A Appl Sci Manuf 2016;82. https://doi.org/10.1016/j.compositesa.2015.12.012.

[96] Ebrahimnezhad-Khaljiri H, Eslami-Farsani R. The tensile properties and interlaminar shear strength of microcapsules-glass fibers/epoxy self- healable composites. Eng Fract Mech 2020;230.

[97] Xiao DS, Yuan YC, Rong MZ, Zhang MQ. A facile strategy for preparing self-healing polymer composites by incorporation of cationic catalyst-loaded vegetable fibers. Adv Funct Mater 2009;19:2289–96. https://doi.org/10.1002/adfm.200801827.

[98] Rule JD, Brown EN, Sottos NR, White SR, Moore JS. Wax-protected catalyst microspheres for efficient self-healing materials. Adv Mater 2005;17:205–8. https://doi.org/10.1002/adma.200400607.

[99] Rule JD, Sottos NR, White SR. Effect of microcapsule size on the performance of self-healing polymers. Polymer (Guildf) 2007;48:3520–9.

[100] Jin H, Miller GM, Sottos NR, White SR. Fracture and fatigue response of a self-healing epoxy adhesive. Polymer (Guildf) 2011;52:1628–34.

[101] Kessler MR, Sottos NR, White SR. Self-healing structural composite materials. Compos Part A Appl Sci Manuf 2003;34:743–53.

[102] Manfredi E, Cohades A, Richard I, Michaud V. Assessment of solvent capsule-based healing for woven E-glass fibre-reinforced polymers. Smart Mater Struct 2015;24. https://doi.org/10.1088/0964-1726/24/1/015019.

[103] Yin T, Zhou L, Rong MZ, Zhang MQ. Self-healing woven glass fabric/epoxy composites with the healant consisting of micro-encapsulated epoxy and latent curing agent. Smart Mater Struct 2008;17. https://doi.org/10.1088/0964-1726/17/01/015019.

[104] Kessler MR, White SR. Self-activated healing of delamination damage in woven composites. Compos Part A Appl Sci Manuf 2001;32:683–99.

[105] P.A.Bolimowski, Boczkowska A. Autonomous self-healing based on epoxy resin-imidazole chemistry in carbon fiber-reinforced polymer composites. J Appl Polym Sci 2018;136.

[106] Yuan YC, Ye Y, Rong MZ, Chen H, Wu J, Zhang MQ, et al. Self-healing of low-velocity impact damage in glass fabric/epoxy composites using an epoxy-mercaptan healing agent. Smart Mater Struct 2011;20. https://doi.org/10.1088/0964-1726/20/1/015024.

[107] Blaiszik BJ, Baginska M, White SR, Sottos NR. Autonomic recovery of fiber/matrix interfacial bond strength in a model composite. Adv Funct Mater 2010;20:3547–54. https://doi.org/10.1002/adfm.201000798.

[108] Ebrahimnezhad-Khaljiri H, Eslami-Farsani R. Experimental investigation of flexural properties of glass fiber–epoxy self-healable composite structures containing capsulated epoxy healing agent and $NiCl_2$ (imidazole)$_4$ catalyst. J Ind Text 2019;0:1–18. https://doi.org/10.1177/1528083719892923.

[109] Sanada K, Yasuda I, Shindo Y. Transverse tensile strength of unidirectional fibre-reinforced polymers and self-healing of interfacial debonding. Plast Rubber Compos 2006;35:67–72. https://doi.org/10.1179/174328906X79914.

[110] McIlroy DA, Blaiszik BJ, Caruso MM, White SR, Moore JS, Sottos NR. Microencapsulation of a reactive liquid-phase amine for self-healing Epoxy composites.

Macromolecules 2010;43:1855–9. https://doi.org/10.1021/ma902251n.

[111] Ahangaran F, Navarchian AH, Picchioni F. Material encapsulation in poly(methyl methacrylate) shell: A review. J Appl Polym Sci 2019;48039:1–21.

[112] Ebrahimnezhad-Khaljiri H, Eslami-Farsani R, Arbab Chirani S. Microcapsulated epoxy resin with nanosilica-urea formaldehyde composite shell. J Appl Polym Sci 2020;137:1–13. https://doi.org/10.1002/app.48580.

[113] Kim DM, Yu HC, Yang HI, Cho YJ, Lee KM, Chung CM. Microcapsule-type self-healing protective coating for cementitious composites with secondary crack preventing ability. Materials (Basel) 2017;10. https://doi.org/10.3390/ma10020114.

[114] Sharma S, Choudhary V. Parametric study for epoxy loaded PMMA microcapsules using Taguchi and ANOVA methods. Express Polym Lett 2017;11:1023–36. https://doi.org/10.3144/expresspolymlett.2017.96.

[115] S. Torza and S. G.Mason. Three-Phase Interactions In Shear and Electrical Fields. J Colloid Interface Sci, 1970;33:67–83. https://doi.org/10.1016/0021-9797(70)90073-1.

[116] Li Q, Mishra AK, Kim NH, Kuila T, Lau KT, Lee JH. Effects of processing conditions of poly(methylmethacrylate) encapsulated liquid curing agent on the properties of self-healing composites. Compos Part B Eng 2013;49:6–15.

[117] Khan NI, Halder S, Goyat MS. Effect of epoxy resin and hardener containing microcapsules on healing efficiency of epoxy adhesive based metal joints. Mater Chem Phys 2016;171:267–75. https://doi.org/10.1016/j.matchemphys.2016.01.017.

[118] Khan NI, Halder S, Goyat MS. Influence of dual-component microcapsules on self-healing efficiency and performance of metal-epoxy composite-lap joints. J Adhes 2017;93:949–63. https://doi.org/10.1080/00218464.2016.1193806.

[119] Petrie EM. Epoxy Adhesive Formulations. McGraw-Hill Companiess, Inc. USA; 2006. https://doi.org/10.1036/0071455442.

[120] Hsieh TH, Kinloch AJ, Masania K, Taylor AC, Sprenger S. The mechanisms and mechanics of the toughening of epoxy polymers modified with silica nanoparticles. Polymer (Guildf) 2010;51:6284–94. https://doi.org/10.1016/j.polymer.2010.10.048.

[121] Ma J, Mo M-S, Du X-S, Dai S-R, Luck I. Study of Epoxy Toughened by In Situ Formed

Rubber Nanoparticles. J Appl Polym Sci 2008;110:304–12. https://doi.org/10.1002/app.

[122] Giannotti MI, Galante MJ, Oyanguren PA, Vallo CI. Role of intrinsic flaws upon flexural behaviour of a thermoplastic modified epoxy resin. Polym Test 2003;22:429–37. https://doi.org/10.1016/S0142-9418(02)00124-1.

[123] Bekas DG, Tsirka K, Baltzis D, Paipetis AS. Self-healing materials: A review of advances in materials, evaluation, characterization and monitoring techniques. Compos Part B Eng 2016. https://doi.org/10.1016/j.compositesb.2015.09.057.

[124] Jin H, Mangun CL, Griffin AS, Moore JS, Sottos NR, White SR. Thermally stable autonomic healing in epoxy using a dual-microcapsule system. Adv Mater 2014;26:282–7. https://doi.org/10.1002/adma.201303179.

[125] Yuan YC, Rong MZ, Zhang MQ, Yang GC. Study of factors related to performance improvement of self-healing epoxy based on dual encapsulated healant. Polymer (Guildf) 2009;50:5771–81. https://doi.org/10.1016/j.polymer.2009.10.019.

[126] Zhang H, Wang P, Yang J. Self-healing epoxy via epoxy-amine chemistry in dual hollow glass bubbles. Compos Sci Technol 2014;94:23–9.

[127] Brown EN. Use of the tapered double-cantilever beam geometry for fracture toughness measurements and its application to the quantification of self-healing. J Strain Anal Eng Des 2011;46:167–86. https://doi.org/10.1177/0309324710396018.

[128] Tsangouri E, Aggelis D, Hemelrijck D Van. Quantifying thermoset polymers healing efficiency: A systematic review of mechanical testing. Prog Polym Sci 2015;49–50:154–74.

[129] Guadagno L, Raimondo M, Naddeo C, Longo P, Mariconda A, Binder WH. Healing efficiency and dynamic mechanical properties of self-healing epoxy systems. Smart Mater Struct 2014;23. https://doi.org/10.1088/0964-1726/23/4/045001.

[130] Brown EN, Sottos NR, White SR. Fracture testing of a self-healing polymer composite. Exp Mech 2002;42:372–9. https://doi.org/10.1007/bf02412141.

[131] Xiao DS, Yuan YC, Rong MZ, Zhang MQ. Self-healing epoxy based on cationic chain polymerization. Polymer (Guildf) 2009;50:2967–75.

[132] Mohammadi MA, Eslami-Farsani R, Ebrahimnezhad-Khaljiri H. Experimental

investigation of the healing properties of the microvascular channels-based self-healing glass fibers/epoxy composites containing the three-part healant. Polym Test 2020;91. https://doi.org/10.1016/j.polymertesting.2020.106862.

[133] P. Shabani, M.M.Shokrieh, Saeedi A. A novel model to simulate the formation and healing of cracks in self healing cross-ply composites under flexural loading. Compos Struct 2020;235:111750.

[134] Williams G, Trask R, Bond I. A self-healing carbon fibre reinforced polymer for aerospace applications. Compos Part A Appl Sci Manuf 2007;38:1525–32. https://doi.org/10.1016/j.compositesa.2007.01.013.

[135] Yin T, Rong MZ, Wu J, Chen H, Zhang MQ. Healing of impact damage in woven glass fabric reinforced epoxy composites. Compos Part A Appl Sci Manuf 2008;39:1479–87. https://doi.org/10.1016/j.compositesa.2008.05.010.

[136] Patel AJ, Sottos NR, Wetzel ED, White SR. Autonomic healing of low-velocity impact damage in fiber-reinforced composites. Compos Part A Appl Sci Manuf 2010;41:360–8. https://doi.org/10.1016/j.compositesa.2009.11.002.

[137] Hoa S Van. Principles of the manufacturing of composite materials. 2009. https://doi.org/10.2307/3000.

[138] Bolimowski PA, Bond IP, Wass DF. Robust synthesis of epoxy resin-filled microcapsules for application to self-healing materials Subject Areas : Author for correspondence : Philos Trans R Soc a-Mathematical Phys Eng Sci 2016;374. https://doi.org/10.1098/rsta.2015.0083.

[139] Friedrich K, Breuer U. Multifunctionality of Polymer Composites: Challenges and New Solutions. Elsevier Inc.; 2015. https://doi.org/10.1016/C2013-0-13006-1.

[140] Fronk TH, Akula VMK, Fugal SR. Passive Damping of Laminated Composite Materials with Engineered Defects. Smart Struct. Mater. 2002 Damping Isol., vol. 4697, SPIE Press; 2002, p. 43–50. https://doi.org/10.1117/12.472679.

[141] Chung DDL. Review: Materials for vibration damping. J Mater Sci 2001;36:5733–7. https://doi.org/10.1023/A:1012999616049.

[142] Neubauer MP, Poehlmann M, Fery A. Microcapsule mechanics: From stability to function. Adv Colloid Interface Sci 2014;207:65–80.

[143] Sun G, Zhang Z. Mechanical strength of microcapsules made of different wall materials. Int J Pharm 2002;242:307–11. https://doi.org/10.1016/S0378-5173(02)00193-X.

[144] Hu J, Chen HQ, Zhang Z. Mechanical properties of melamine formaldehyde microcapsules for self-healing materials. Mater Chem Phys 2009;118:63–70. https://doi.org/10.1016/j.matchemphys.2009.07.004.

[145] Dubreuil F, Elsner N, Fery A. Elastic properties of polyelectrolyte capsules studied by atomic-force microscopy and RICM. Eur Phys J E 2003;12:215–21.

[146] Ahangaran F, Hayaty M, Navarchian AH, Picchioni F. Micromechanical assessment of PMMA microcapsules containing epoxy and mercaptan as self-healing agents. Polym Test 2017;64:330–6. https://doi.org/10.1016/j.polymertesting.2017.10.014.

[147] Gilabert FA, D.Garoz, Paepegem WV. Macro and Micro- modelling of crack propagation in encapsulation based self healing materials:Application of XFEM and cohesive surface techniques. Mater Des 2017;130:459–78.

[148] Chen C, Ji H, Wang H. Damage Properties Simulations of Self-Healing Composites. J Nanosci Nanotechnol 2013;13:6679–86. https://doi.org/10.1166/jnn.2013.7780.

[149] Thao TDP. Quasi-brittle self-healing materials: Numerical modelling and applications in civil Engineering. PhD Thesis, National University of Singapore; 2011.

[150] Ahmed A, Sanada K, Fanni M, El-Moneim AA. A practical methodology for modeling and verification of self-healing microcapsules-based composites elasticity. Compos Struct 2018;184:1092–8.

[151] Ahmed A, Sanada K. Micromechanical modeling and experimental verification of self-healing microcapsules-based composites. Mech Mater 2019;131:84–92.

[152] Ponnusami SA, Krishnasamy J, Turteltaub S, Zwaag S van der. A cohesive-zone crack healing model for self-healing materials. Int J Solids Struct 2018;134:249–63.

[153] Gómez DG, Gilabert FA, Tsangouri E, Hemelrijck D Van, Hillewaere XKD, Du Prez FE, et al. In-depth numerical analysis of the TDCB specimen for characterization of self-healing polymers. Int J Solids Struct 2015;64–65:145–54.

[154] Minoo D. Shokrian, Shelesh-Nezhad K, Najjar R. Toughening effect of nanocomposite-wall microcapsules on the fracture behavior of epoxy. Polymer 2019;168:104–15.

[155] Masood SN, Singh AK, Viswamurthy SR. Simulation & validation of delamination growth in CFRP specimens under mixed mode loading using cohesive elements. INCCOM-14, Hyderabad,Jan22-23, 2016.

[156] Lee J, Zhang M, Bhattacharyya D, Yuan YC, Jayaraman K, Mai YW. Micromechanical behavior of self-healing epoxy and hardener-loaded microcapsules by nanoindentation. Mater Lett 2012;76:62–5. https://doi.org/10.1016/j.matlet.2012.02.052.

[157] Keller MW, Sottos NR. Mechanical properties of microcapsules used in a self-healing polymer. Exp Mech 2006;46:725–33. https://doi.org/10.1007/s11340-006-9659-3.

[158] Park K, Choi H, Paulino GH. Assessment of cohesive traction-separation relationships in ABAQUS: A comparative study. Mech Res Commun 2016;78:71–8.

[159] Bangs Laboratories. Material Properties of Polystyrene and Poly(methyl methacrylate) (PMMA) Microspheres. Tech support doc 0021; 2015; 1-2.

List of Publications

a) International Journals

1. Raj Kumar Pittala, B Satish Ben, B Avinash Ben, Self-healing performance assessment of epoxy resin and amine hardener encapsulated polymethyl methacrylate microcapsules reinforced epoxy composite, Journal of applied polymer science, Vol 138, Issue 23, 2021. **(SCI) IF:3.12**

2. Raj Kumar Pittala, Satish Ben B, Avinash Ben B, Effect of epoxy resin healing agent viscosity on the self-healing performance of capsules reinforced polymer composite, Journal of polymer research, Vol 28, Article no 102, 2021. **(SCI) IF:3.09**

3. Raj Kumar Pittala, B Satish Ben, Synthesis and characterization of amine hardener filled microcapsules for self-healing composite applications, Materials Research Express, Vol.6, Issue 11, 2019. **(SCI) IF:1.62**

4. Raj Kumar Pittala, Satish Ben B, Syam Kumar Chokka, Niranjan Prasad, Numerical investigation into effect of self-healing composite microcapsules thickness and diameter on their failure strength, World Journal of Engineering, Vol 18, Issue 3, pp.373-378, 2020. **(ESCI & Scopus)**

5. Raj Kumar Pittala, G Dhanaraju, B Satish Ben, B Avinash Ben, Damping behaviour and self-healing performance evaluation of microcapsules reinforced epoxy composites by Impulse Excitation technique, Journal of Reinforced Plastics and Composites, **(Accepted) (SCI) IF: 3.71**

6. Raj Kumar Pittala, G Dhanaraju, B Satish Ben, B Avinash Ben, Self-healing of matrix cracking and delamination damage assessment in microcapsules reinforced carbon fibre epoxy composite under flexural loading, Composite Structures,**(Under revision)**

b) International conferences

1. Raj Kumar Pittala, B Satish Ben, Synthesis of amine hardener filled microcapsules for self-healing applications, ICAFMD, Feb 26-28, 2019, NIT Warangal

2. Raj Kumar Pittala, Satish Ben B, Syam Kumar Chokka, Niranjan Prasad, Numerical investigation into failure assessment of self-healing composite microcapsules, ICAM^{5}, 25th-27th Sept. 2019, NIT Warangal